

**NASA CONTRACTOR  
REPORT**



**NASA CR-2**



**NASA CR-2552**

**APPROXIMATION CONCEPTS FOR  
EFFICIENT STRUCTURAL SYNTHESIS**

**LOAN COPY: RETURN TO  
AFWL TECHNICAL LIBRARY  
KIRTLAND AFB, N. M.**

*Lucien A. Schmit, Jr., and Hirokazu Minra*

*Prepared by*  
**UNIVERSITY OF CALIFORNIA, LOS ANGELES**  
**Los Angeles, Calif. 90024**  
*for Langley Research Center*



**NATIONAL AERONAUTICS AND SPACE ADMINISTRATION • WASHINGTON, D. C. • MARCH 1976**



0061233

1. Report No. NASA CR-2552		2. Government Accession No.	
4. Title and Subtitle APPROXIMATION CONCEPTS FOR EFFICIENT STRUCTURAL SYNTHESIS		5. Report Date March 1976	
		6. Performing Organization Code	
7. Author(s) Lucien A. Schmit, Jr. and Hirokazu Miura		8. Performing Organization Report No.	
9. Performing Organization Name and Address University of California, Los Angeles Los Angeles, CA 90024		10. Work Unit No. 506-17-21-01	
		11. Contract or Grant No. NGR-05-007-337	
12. Sponsoring Agency Name and Address National Aeronautics and Space Administration Washington, D. C. 20546		13. Type of Report and Period Covered Contractor Report	
		14. Sponsoring Agency Code	
15. Supplementary Notes Technical Monitor: W. Jefferson Stroud, Structures and Dynamics Division, NASA Langley Research Center, Hampton, Virginia 23665 Topical Report			
16. Abstract In summary, it is shown that efficient structural synthesis capabilities can be created by using approximation concepts to mesh finite element structural analysis methods with nonlinear mathematical programming techniques. First, the history of the application of mathematical programming techniques to structural design optimization problems is reviewed. Then, several rather general approximation concepts are described. There follows a description of the technical foundations of the ACCESS 1 computer program, which implements several approximation concepts. Finally, a substantial collection of structural design problems involving truss and idealized wing structures is presented. It is concluded that since the basic ideas employed in creating the ACCESS 1 program are rather general, its successful development supports the contention that the introduction of approximation concepts will lead to the emergence of a new generation of practical and efficient, large scale, structural synthesis capabilities in which finite element analysis methods and mathematical programming algorithms will play a central role.			
17. Key Words (Suggested by Author(s)) Structural synthesis Structural optimization Minimum mass design Mathematical programming		18. Distribution Statement Unclassified - Unlimited  STAR category 39	
19. Security Classif. (of this report) Unclassified	20. Security Classif. (of this page) Unclassified	21. No. of Pages 311	22. Price* \$9.25



## PREFACE

This report presents some results of a continuing research program on Approximation Concepts in Structural Synthesis. The development of the ACCESS 1 computer program was initiated in May 1973 and preliminary results were first obtained in November 1973. Operational versions of the ACCESS 1 program were delivered to the NASA Langley Research Center in May 1974. During the last year this program has been further exercised on a variety of problems.

The research effort reported herein was carried out in the Department of Mechanics and Structures at UCLA. Dr. Hirokazu Miura carried primary responsibility for the development of ACCESS 1 and Professor Lucien A. Schmit, Jr. served as the principal investigator. This manuscript was prepared by the Reports Group in the School of Engineering and Applied Science at UCLA.

The authors want to take this opportunity to express their gratitude to Dr. G. N. Vanderplaats of NASA Ames Research Center for his cooperation in making available the CONMIN optimization program as well as several valuable subroutines used in the analysis portion of ACCESS 1.



CONTENTS

LIST OF FIGURES . . . . .	ix
LIST OF TABLES . . . . .	xi
NOMENCLATURE . . . . .	xvii
SUMMARY . . . . .	1
1. HISTORICAL BACKGROUND. . . . .	3
1.1 Early Work . . . . .	3
1.2 The Decade from 1960-1970. . . . .	4
1.2.1 Special Purpose Applications. . . . .	5
1.2.2 General Purpose Applications. . . . .	8
1.3 Consolidation and Assessment Period. . . . .	10
1.4 Design Oriented Structural Analysis. . . . .	15
1.5 Recent Special Purpose Applications. . . . .	19
1.6 Recent General Purpose Applications. . . . .	23
2. APPROXIMATION CONCEPTS -- THE KEY TO CONSTRUCTING TRACTABLE STRUCTURAL SYNTHESIS FORMULATIONS. . . . .	27
2.1 Introduction . . . . .	27
2.2 Statement of Structural Synthesis Problem. . . . .	28
2.3 Reducing the Number of Design Variables. . . . .	29
2.3.1 Design Variable Linking . . . . .	29
2.3.2 Reduced Basis Concept for Design. . . . .	31
2.3.3 Two Step Reduction in the Number of Independent Design Variables. . . . .	32
2.4 Reducing the Number of Constraints . . . . .	34
2.4.1 Regionalization . . . . .	35
2.4.2 "Throw Away" Concept. . . . .	37
2.4.3 Two Step Reduction in the Number of Constraints . . . . .	40

CONTENTS (Cont'd)

2.5	Reducing the Number of Detailed Structural Analyses. . . .	42
2.5.1	Iterative Methods . . . . .	43
2.5.2	Reduced Basis Concept for Analysis. . . . .	44
2.5.3	Explicit Approximations . . . . .	46
2.5.4	Combining Approximate Analysis Methods. . . . .	51
2.6	Summary — A Tractable Formulation. . . . .	51
3.	A NEW STRUCTURAL SYNTHESIS CAPABILITY. . . . .	53
3.1	Introduction . . . . .	53
3.2	Scope and Limitations. . . . .	55
3.3	Description of ACCESS 1 . . . . .	58
3.3.1	Formulation . . . . .	58
3.3.2	Organization. . . . .	64
3.3.3	Input Data Required . . . . .	68
3.3.4	Function of Preprocessor. . . . .	71
3.3.5	Design Process Control. . . . .	73
3.3.6	Approximate Problem Generator . . . . .	76
3.3.6.1	Displacement evaluation. . . . .	76
3.3.6.2	Constraint evaluation and deletion . . . .	78
3.3.6.3	Explicit approximation of retained constraints . . . . .	80
3.3.7	Optimization Algorithms . . . . .	88
3.3.7.1	CONMIN . . . . .	90
3.3.7.2	NEWSUMT. . . . .	93
4.	EXAMPLE APPLICATIONS OF ACCESS 1 . . . . .	99
4.1	Introduction . . . . .	99

## CONTENTS (Cont'd)

4.2	Truss Structures . . . . .	99
4.2.1	Planar Ten Bar Truss (Problems 1-4). . . . .	100
4.2.1.1	Stress limits only, single load condition (Problems 1 and 2). . . . .	100
4.2.1.2	Stress and displacement limits, single load condition (Problems 3 and 4). . . . .	103
4.2.2	Twenty Five Bar Space Truss. . . . .	107
4.2.3	Seventy Two Bar Space Truss (Problem 6). . . . .	110
4.2.4	Truss Idealization of Wing Carry Through Structure (Problem 7). . . . .	112
4.3	Idealized Wing Structures . . . . .	117
4.3.1	Eighteen Element Wing Box Beam (Problem 8) . . . . .	117
4.3.1.1	Detailed Problem Statement. . . . .	118
4.3.1.2	Results and Discussion. . . . .	119
4.3.2	Swept Wing Example (Problem 9) . . . . .	122
4.3.2.1	Detailed Problem Statement. . . . .	123
4.3.2.2	Results and Discussion. . . . .	124
4.3.3	Delta Wing Example (Problem 10). . . . .	128
4.3.3.1	Detailed Problem Statement. . . . .	128
4.3.3.2	Results and Discussion. . . . .	130
4.3.4	Additional Data on Example Problems. . . . .	134
5.	CONCLUSIONS AND RECOMMENDATIONS . . . . .	139
Appendix A	— Finite Elements Employed . . . . .	145
A.1	Truss Element with Uniform Cross Sectional Area . . . . .	147
A.2	Constant Strain Triangular Element (CST). . . . .	150
A.3	Symmetric Shear Panel Element (SSP) . . . . .	153

CONTENTS (Cont'd)

Appendix B — Relationship Between "Throw Away" Concept and Detailed Implementation. . . . .	159
Appendix C — Derivation of Pseudo Load Vector Formula . . . . .	161
REFERENCES . . . . .	163
FIGURES . . . . .	169
TABLES . . . . .	205

## LIST OF FIGURES

### Figures

1.	Design Variable Linking. Simple Example. . . . .	169
2.	Throw Away Followed by Regionalization. . . . .	170
3.	Regionalization Followed by Throw Away. . . . .	171
4.	ACCESS 1 Basic Organization . . . . .	172
5.	Finite Element Model for Eighteen Element Wing Box (Model 1). . . . .	173
6.	Compact Vector Form of System Stiffness Matrix [K] Used to Reduce Storage Requirements for ACCESS 1 . . . . .	174
7.	Truncation Boundary Value (TBV) versus Truncation Factor (TRF). . . . .	175
8.	Interior Penalty Function (Fiacco and McCormick, Ref. 79) . . .	176
9.	Extended Interior Penalty Function (Kavlie and Moe, Ref. 75) . . . . .	177
10.	Planar Ten Bar Cantilever Truss . . . . .	178
11.	Iteration Histories for Problem 3, Planar Ten Bar Cantilever Truss. . . . .	179
12.	Iteration Histories for Problem 4, Planar Ten Bar Cantilever Truss. . . . .	180
13.	25 Bar Space Truss. . . . .	181
14.	Iteration Histories for Problem 5, 25 Bar Space Truss . . . . .	182
15.	72 Bar Space Truss. . . . .	183
16.	Iteration Histories for Problem 6, 72 Bar Space Truss . . . . .	184
17.	Truss Idealization of Wing Carry Through Structure. . . . .	185
18.	Iteration Histories for Problem 7 Wing Carry-Through Structure Truss Model (From Ref. 83). . . . .	186
19.	Eighteen Element Wing Box (Model 2) . . . . .	187
20.	Iteration History for Problem 8, 18 Element Wing Box . . . . .	188

## LIST OF FIGURES (Cont'd)

### Figures

21.	Finite Element Model for Swept Wing Example (Problem 9) . . . . .	189
22.	Final Skin Panel Thickness Distribution. 150(130) Element Swept Wing . . . . .	190
23.	Final Web Thickness Distribution for Swept Wing Example. Cases Without Spar Caps . . . . .	191
24.	Final Web Thickness Distribution for Swept Wing Example Cases with Spar Caps. . . . .	192
25.	Critical Constraints for Final Designs 150(130)-Element Swept Wing. . . . .	193
26.	Iteration Histories for Problem 9 150, (130) Element Swept Wing . . . . .	194
27.	Delta Wing Example (Problem 10). . . . .	195
28.	Alternate Linking Arrangements for the Skin (CST Elements) of Delta Wing Examples (Problem 10). . . . .	196
29.	Alternate Linking Arrangements for the Webs (SSP Elements) of Delta Wing Examples (Problem 10). . . . .	197
30.	Final Skin Panel Thickness Distributions for Four Delta Wing Examples (Problem 10) . . . . .	198
31.	Final Web Thickness Distribution for Two Delta Wing Examples (Problem 10) . . . . .	199
32.	Critical Constraints for Final Designs of Delta Wing Examples; Problems 10A, 10B and 10C . . . . .	200
33.	Critical Constraints for Final Designs of Delta Wing Examples; Problems 10D and 10E . . . . .	201
34.	Iteration History for Delta Wing Examples; Problems 10A - 10E . . . . .	202
35.	Weight versus Elapsed CPU Time for Delta Wing Example Problem 10C, CST Design Variables, 12 SSP Design Variables . . . . .	203

## LIST OF TABLES

1.	ACCESS 1 Main Storage Requirements . . . . .	205
2.	Nodal Coordinates for 18 Element Wing Box Example . . . . .	206
3.	TRUSS Element Descriptions for 18 Element Wing Box Example . . . . .	207
4.	CST Element Descriptions (Model 1) for 18 Element Wing Box Example . . . . .	208
5.	SSP Element Descriptions for 18 Element Wing Box Example . . . . .	209
6.	TRUSS Element Material Properties for 18 Element Wing Box Example . . . . .	210
7.	CST Element Material Properties for 18 Element Wing Box Example . . . . .	211
8.	SSP Element Material Properties for 18 Element Wing Box Example . . . . .	212
9.	Displacement Boundary Conditions for 18 Element Wing Box Example . . . . .	213
10.	Load Condition Data for 18 Element Wing Box Example . . . . .	214
11.	Displacement Constraints for 18 Element Wing Box Example . . . . .	215
12.	Truncation Factors for Delta Wing Example . . . . .	216
13.	Nodal Coordinates for Planar Ten Bar Cantilever Truss . . . . .	217
14.	TRUSS Element Descriptions for Planar Ten Bar Cantilever Truss . . . . .	218
15.	Displacement Boundary Conditions for Planar Ten Bar Cantilever Truss . . . . .	219
16.	Load Condition Data (Problems 1A, 1B, 1C, 1D, 3) for Planar Ten Bar Cantilever Truss . . . . .	219
17.	TRUSS Element Material Properties for Planar Ten Bar Cantilever Truss . . . . .	220

LIST OF TABLES (Cont'd)

18.	Final Designs for Problems 1A, 1B, 1C, 1D Planar Ten Bar Cantilever Truss . . . . .	221
19.	Comparison of Minimum Weights Achieved and Number of Analysis Required . . . . .	222
20.	Final Designs for Problems 1A', 1B', 1C', 1D' for Planar Ten Bar Cantilever Truss . . . . .	223
21.	Load Condition Data (Problems 2 and 4) for Planar Ten Bar Cantilever Truss . . . . .	224
22.	Final Designs for Problem 2 for Planar Ten Bar Cantilever Truss . . . . .	225
23.	Displacement Constraints for Planar Ten Bar Cantilever Truss . . . . .	226
24.	Final Designs for Problem 3 Planar Ten Bar Cantilever Truss . . . . .	227
25.	Iteration History Data for Problem 3 Planar Ten Bar Cantilever Truss . . . . .	228
26.	Final Designs for Problem 4 Planar Ten Bar Cantilever Truss . . . . .	229
27.	Iteration History Data for Problem 4 Planar Ten Bar Cantilever Truss . . . . .	230
28.	Nodal Coordinates for Twenty Five Bar Space Truss . . . . .	231
29.	TRUSS Element Descriptions for Twenty Five Bar Space Truss . . . . .	232
30.	Displacement Boundary Conditions for Twenty Five Bar Space Truss . . . . .	233
31.	Load Condition Data for Twenty Five Bar Space Truss . . . . .	233
32.	Element Material Properties for Twenty Five Bar Space Truss . . . . .	234
33.	Final Designs for Problem 5 Twenty Five Bar Space Truss . . . . .	235
34.	Iteration History Data for Problem 5 Twenty Five Bar Space Truss . . . . .	236

LIST OF TABLES (Cont'd)

35.	Nodal Coordinates for Seventy Two Bar Space Truss . . . . .	237
36.	Truss Element Descriptions for Seventy Two Bar Space Truss . . . . .	238
37.	Displacement Boundary Conditions for Seventy Two Bar Space Truss . . . . .	240
38.	Load Condition Data for Seventy Two Bar Space Truss . . . . .	240
39.	Element Material Properties for Seventy Two Bar Space Truss . . . . .	241
40.	Final Designs for Problem 6 Seventy Two Bar Space Truss . . . . .	242
41.	Iteration History Data for Problem 6 Seventy Two Bar Space Truss . . . . .	243
42.	Nodal Coordinates for Sixty Three Bar Truss Wing Carry through Structure . . . . .	244
43.	Truss Element Descriptions for Sixty Three Bar Truss Wing Carry through Structure . . . . .	245
44.	Displacement Boundary Conditions for Sixty Three Bar Truss Wing Carry through Structure . . . . .	247
45.	Load Condition Data for Sixty Three Bar Truss Wing Carry through Structure . . . . .	247
46.	Final Designs for Sixty Three Bar Truss Wing Carry through Structure . . . . .	248
47.	Iteration History Data for Problem 7 Sixty Three Bar Wing Carry through Structure. . . . .	250
48.	CST Element Descriptions (Model 2) for 18 Element Wing Box Example . . . . .	251
49.	Final Designs for Problem 8, 18 Element Wing Box Example . . . . .	252
50.	Iteration History Data for Problem 8, 18 Element Wing Box Example . . . . .	253
51.	Nodal Coordinates for 150 (130) Element Swept Wing . . . . .	254

LIST OF TABLES (Cont'd)

52.	Truss Element Description for 150 (130) Element Swept Wing . . . . .	255
53.	CST Element Description for 150 (130) Element Swept Wing . . . . .	256
54.	SSP Element Description for 150 (130) Element Swept Wing . . . . .	259
55.	Displacement Boundary Conditions for 150 (130) Element Swept Wing . . . . .	262
56.	Element Material Properties for 150 (130) Element Swept Wing . . . . .	263
57.	Load Condition Data for 150 (130) Element Swept Wing . . . . .	264
58.	Final Designs for Problem 9 150 (130) Element Swept Wing . . . . .	265
59.	Iteration History for Problem 9 150 (130) Element Swept Wing . . . . .	266
60.	Nodal Coordinates for 133 Element Delta Wing . . . . .	267
61.	CST Element Description for 133 Element Delta Wing . . . . .	268
62.	SSP Element Description for 133 Element Delta Wing . . . . .	270
63.	Displacement Boundary Conditions for 133 Element Delta Wing . . . . .	272
64.	Load Condition Data for 133 Element Delta Wing . . . . .	272
65.	Element Material Properties for 133 Element Delta Wing . . . . .	273
66.	Displacement Constraint Data for 133 Element Delta Wing . . . . .	274
67.	Final Designs for 133 Element Delta Wing . . . . .	275
68.	Iteration History for 133 Element Delta Wing . . . . .	277

LIST OF TABLES (Cont'd)

69.	Nodal Coordinates (in SI units) for 150(130) Element Swept Wing. . . . .	278
70.	Load Condition Data (in SI units) for 150(130) Element Swept Wing. . . . .	279
71.	Final Designs (in SI units) for 150(130) Element Swept Wing. . . . .	280
72.	Iteration History (in SI units) for 150(130) Element Swept Wing. . . . .	281
73.	Nodal Coordinates (in SI units) for 133 Element Delta Wing . . . . .	282
74.	Displacement Constraints (in SI units) for 133 Element Delta Wing . . . . .	283
75.	Final Designs (in SI unit) for 133 Element Delta Wing . . . . .	284
76.	Iteration History for Problem 10 (in SI unit) 133 Element Delta Wing . . . . .	286
77.	Initial Weights of All Example Problems. . . . .	287
78.	CPU Times for Truss Examples . . . . .	288
79.	CPU Times for Wing Examples. . . . .	289



## NOMENCLATURE

Symbol	Definition	First Appearance
$A_i, \vec{A}, A_i^{(L)}, A_i^{(U)}$	cross sectional areas of truss elements	
B	number of basis vectors	Eq. (2.6)
[B]	response transformation matrix	Eq. (2.21)
$B_T, B_C, B_S$	sets of integers identifying reciprocal linked variables	
C	total number of linked variables	Eq. (2.3)
$C_x, C_y, C_z$	constant terms	Eqs. (2.37 ~ 40)
$C_b$	constant in the weight equation	Eqs. (3.23, 24)
$[\vec{C}], \vec{C}_j$	partial inverse of the system stiffness matrix [K]	Eq. (3.45)
$c_a$	reduction ratio of the penalty multiplier $r_a$	Eq. (3.65)
$D_i, \vec{D}, D_i^{(L)}, D_i^{(U)}$	sizing variable for the i-th finite element	Eqs. (2.1 ~ 4)
[ $\mathcal{D}$ ]	diagonal matrix	Eq. (3.31)
d	move distance variable in the direction $\vec{S}_m$	Eq. (3.69)
$E_\ell$	modulus of elasticity for elements in configuration/material group $\ell$	
$\vec{e}_{B+1}, \vec{e}_b$	normalized form of the displacement vector $\vec{u}$ and the first derivative of $u$	Eqs. (2.26 ~ 28)
$\vec{e}_j$	vector with J elements all of which are zero except for the j-th element which has unit value	Eq. (3.45)
$F^{(P)}(\vec{\alpha}), F_e^{(P)}(\vec{\alpha})$	sum of all participating penalty or extended penalty terms during the p-th stage of design process	Eqs. (3.63, 64)
$TV_{bk}$	total number of retained $\vec{V}_{bk}$ vectors	Sec. 3.3.6.2

$g_q(\vec{D})$	the q-th constraint function in terms of $\vec{D}$	Eq. (2.1)
$\tilde{H}_q^{(p)}(\vec{\alpha})$	extended interior penalty function	Eq. (3.66)
$h_q(\vec{\alpha}), h_q(\vec{\delta}), h_q(\vec{y})$	q-th constraint function	
$\tilde{h}_q(\vec{\alpha}), \tilde{h}_q(\vec{\delta})$	explicit approximate representation for the q-th constraint function	
$h_q^-(\vec{\alpha}), h_q^-(\vec{\delta})$	equal to $-h_q(\vec{\alpha}), -h_q(\vec{\delta})$ , respectively	Eq. (3.34)
I	total number of finite elements in analysis model	Eq. (2.4)
$I_T, I_C, I_S$	total number of finite elements in TRUSS, CST and SSP categories	Eq. (3.6~9)
J	number of unknown analysis variables arising from the structural idealization	
$J_r$	reduced number of independent analysis variables	
$J_u$	the set of integers identifying the constrained displacement degrees of freedom	Eq. (3.3)
$J'$	set of integers identifying the displacement degrees of freedom defining the values of the retained constraints	
[K]	system stiffness matrix	
K	total number of load conditions	
$K_x$	constant	Eq. (2.39)
$[k_i]$	element stiffness matrix in the reference coordinate system	
$[\tilde{k}_i]$	element stiffness matrix in the local element coordinate system	
$[L], \vec{L}_c, L_{ic}$	linking matrix made up of C columns $\vec{L}_c$ and $I \times C$ elements $L_{ic}$	Eqs. (2.3, 4)

$[L]$	decomposed lower triangular matrix	
$l_i$	length of the $i$ -th truss element	Eq. (3.9)
$M(\vec{D})$	objective function in terms of $\vec{D}$	Eq. (2.2)
$\vec{P}_k$	load vector for the $k$ -th static load condition	
$Q$	total number of constraints	Eq. (2.1)
$Q_R^{(p)}$	total number of constraints to be retained during the $p$ -th stage of design process	Eq. (2.41)
$Q_b, Q_s$	total number of behavior and the side constraints, respectively	Eqs. (3.27, 28)
$[R], \vec{R}_b, R_{cb}$	basis reduction matrix made up of $B$ column vectors $\vec{R}_b$	Eqs. (2.6, 7)
$R_q(\vec{\delta})$	$q$ -th response ratio as a function of $\vec{\delta}$	Eq. (2.13)
$R$	mean radius of tubular member	Eq. (4.1)
$r_a$	penalty multiplier in the interior penalty function formulation	Eq. (3.63)
$S_i$	surface area of CST element $i$	Eq. (3.9)
$\vec{S}_m$	normalized direction vector	Eq. (3.73)
$s_i$	surface area of SSP element $i$	Eq. (3.9)
$[T]$	matrix made up of $B$ column vector $\vec{T}_b$	Eqs. (2.8, 9)
$\vec{T}_b$	the $b$ -th independent prelinked basis vector	Eqs. (2.8, 9)
$T_{ib}, T_{ib}^{(r)}$	element of $\vec{T}_b$ and its reciprocal	Eqs. (2.8, 9)
TRF	truncation factor	Eq. (3.35)
TBV	truncation boundary value	Eq. (3.35)

$\vec{t}, t_i, t_i^{(L)}, t_i^{(U)}$	membrane thickness of CST elements	
$\vec{u}_k, u_{jk}, u_j^{(L)}, u_j^{(U)}$	displacement response vector for the k-th load condition and its j-th component	Eq. (2.17)
$\vec{u}_{ik}(\vec{D})$	vector of displacements associated with the i-th finite element in the k-th load condition	Eq. (3.43)
$\vec{u}_v$	displacement response basis vector	Eq. (2.21)
$\vec{u}_j, \vec{u}_{jk}$	explicit approximation of the displacement degrees of freedom	Eq. (2.21)
$u_a$	upper limit radius for spherical displacement constraint	Eq. (2.33)
$u_x, u_y, u_z$	scalar displacement components at a particular node	
$\vec{u}_x, \vec{u}_y, \vec{u}_z$	explicit approximation of the displacement components $u_x, u_y, u_z$	
$\vec{v}_{bk}$	pseudo load vector	Eq. (3.42)
$\vec{v}, v_v$	generalized displacement degrees of freedom after basis reduction in analysis variable space	Eq. (2.21)
$W(\vec{\alpha}), W(\vec{\delta})$	objective function in terms of $\vec{\alpha}, \vec{\delta}$	Eqs. (2.11) (3.26)
$\vec{Y}$	vector of selected response quantities such as stresses or displacements	Eq. (2.32)
$Y_q(\vec{Z}), Y_q(\vec{\delta})$	q-th response quantity of interest	Eq. (2.12)
$Y_q^{(-)}, Y_q^{(+)}$	lower and upper limits on $Y_q(\vec{\delta})$	
$\vec{Y}_q(\vec{Z})$	explicit approximation for the q-th response quantity	Eq. (2.34)
$\vec{Z}, \vec{Z}_p$	vector of intermediate design variables corresponding to the design $\vec{\delta}$ or $\vec{\delta}_p$	
$Z_b, Z_{pb}$	component of $\vec{Z}$ or $\vec{Z}_p$	

$\vec{\alpha}, \alpha_b, \alpha_b^{(L)}, \alpha_b^{(U)}$	reciprocal of the independent design variable after linking	Eqs. (3.12, 13)
$\vec{\alpha}_m$	the m-th design in the a-th unconstrained minimization	
$\beta_i$	reciprocal of the sizing variable for element i	Eq. (3.13)
$\vec{\gamma}, \gamma_c, \gamma_c^{(L)}, \gamma_c^{(U)}$	independent design variable after linking	Eqs. (2.3 - 7)
$\vec{\delta}, \delta_b$	independent design variable after linking and/or basis reduction	Eqs. (2.6 - 9)
$\epsilon$	small constant transition parameter in extended penalty function definition	p. 84 Eq. (3.66)
$\theta$	push off factor in the method of feasible directions	
$[\Lambda_i]$	coordinate transformation matrix for the i-th finite element	Eq. (3.30)
$\nu_\ell$	Poisson's ratio	
$\Pi$	total potential energy	Eq. (2.22)
$\tilde{\Pi}$	approximation of $\Pi$	Eq. (2.23)
$\rho_\ell, \rho_i$	specific weight	
$\sigma_{ik}$	axial stress in truss element i under load condition k	
$\sigma_{xik}, \sigma_{yik}$	normal stress component in the i-th CST or SSP element under load condition k	
$\sigma_{a_i}, \sigma_{a_\ell}$	allowable Von Mises equivalent stress	
$\sigma_i^{(L)}, \sigma_i^{(U)}$	lower or upper bound on the axial stress in truss element i	
$\sigma_{eik}$	Von Mises equivalent stress in element i under load condition k	
$\tilde{\sigma}_{eik}(\vec{\alpha})$	explicit approximation of $\sigma_{eik}$ as a function of $\vec{\alpha}$	

$\vec{\tau}, \tau_i, \tau_i^{(L)}, \tau_i^{(U)}$	thickness of symmetric shear panel (SSP) element	
$\phi^{(p)}(\vec{\alpha}, r_a), \phi_e^{(p)}(\vec{\alpha}, r_a)$	sum of objective function and penalty function formulation during the p-th stage of the iterative design process.	Eq. (3.63, 67)
$\tilde{\phi}_e^{(p)}(\vec{\alpha}, r_a)$	explicit approximation of $\phi_e^{(p)}(\vec{\alpha}, r_a)$	Eq. (3.70)
<b>Subscripts</b>		
a :	$u_a$	allowable limit
	$r_a, c_a$	sequence number of unconstrained minimization for the interior penalty function formulation
B :		total number of independent design variables after linking and/or basis reduction
b :	$\vec{R}_b, \delta_b$	index for independent design variables after linking and/or basis reduction
b(i):	$\delta_{b(i)} \alpha_{b(i)}$	independent design variable number associated with the i-th finite element
C :		total number of independent design variables after linking
	$I_C$	quantity associated with CST elements
c :	$\gamma_c$	index for independent design variables after linking
e :	$\sigma_{eik}$	Von Mises equivalent stress
	$\phi_e^{(p)}, F_e^{(p)}$	indication of using extended penalty
I :		total number of finite elements in analysis model
i :	$D_i, A_i$	index for finite elements

j	: $u_{jk}$	index for the independent displacement degrees of freedom in the finite element model	
k	: $\vec{u}_k, \vec{P}_k$	index for independent static load conditions	
l		index for configuration groups	
l(i)		configuration group number associated with the i-th finite element	
m	: $\vec{\alpha}_m, \vec{S}_m$	index for one dimensional minimization steps	Eq. (3.69)
P	: $u_p, v_p, w_p$	identifier for P node of the finite element	Eq. (3.51)
p	: $\vec{\delta}_p$	index for the stages in the iterative design procedure	Eq. (2.27)
Q		Identifier for Q node of the finite element	
q	: $g_q(\vec{D})$	index for the constraint functions	Eq. (2.1)
R	:	identifier for R node of the finite element	
S	: $I_S$	quantity associated with SSP element	
s	: $I_s$	quantity associated with side constraints	Eq. (3.28)
T	: $I_T$	quantity associated with truss elements	
u	: $J_u$	quantity associated with displacement variables	Eq. (3.3)
x	: $\sigma_{xik}$	x-component of the quantity	
y	: $\sigma_{yik}$	y-component of the quantity	
z	: $\sigma_{zik}$	z-component of the quantity	
v	: $v_v, \vec{u}_v$	index for the reduced number of independent generalized displacement degrees of freedom	Eq. (2.21)

### Superscript

L	: $D_i^{(L)}$	lower bound of the associated quantity	
p	: $Q_R^{(p)}$	index for the stages of the iterative design process	
r	: $T_{ib(i)}^{(r)}$	reciprocal of the associated quantity	Eq. (3.12)
T	: $[\mathcal{L}]^T$	transpose of a matrix	
U	: $D_i^{(U)}$	upper bound of the associated quantity	
-	: $h^-(\vec{q})$	negative of the function	Eq. (3.34)

### Special Symbols

$\delta$	: $\delta \tilde{\Pi}, \delta \vec{v}$	variation of the associated quantity
$\in$		"is an element of a set"
$\Delta$		small perturbation of the associated quantity
[ ]		matrix quantity
L ]		column vector presented horizontally
$\rightarrow$	: $\vec{u}, \vec{D}$	vector quantity
$\nabla$		gradient operator
$\sim$	: $\vec{u}, \tilde{\Pi}$	explicit approximation of the associated quantity

## SUMMARY

It is shown that efficient structural synthesis capabilities can be created by using approximation concepts to mesh finite element structural analysis methods with nonlinear mathematical programming techniques. The philosophically attractive generality inherent to the mathematical programming formulation of structural design optimization problems is retained and excellent efficiency is achieved by replacing the design optimization problem with a sequence of small explicit approximate problems, that preserve the essential features of the primary design problem. At the outset, the short but lively history of the application of mathematical programming techniques to structural design optimization problems is reviewed.

In Section 2 several rather general approximation concepts are described. Basically these concepts provide mechanisms by which the primary mathematical programming statement of a structural design problem, involving large numbers of design variables and many implicit constraint functions, can be replaced by a sequence of approximate problems involving relatively small numbers of design variables and a substantially reduced number of constraints that are all explicit functions of the design variables.

Section 3 describes the technical foundations of the ACCESS 1 computer program. This program implements several of the approximation concepts described in Section 2. The overall efficiency of the ACCESS 1 program is achieved through the carefully coordinated use of: (1) design variable linking; (2) dynamically updated constraint deletion; (3) high quality explicit approximations for retained constraints; (4) a finite element analysis organized with the design optimization task in mind; and (5) a selective sensitivity scheme in which only those partial derivatives needed, to construct explicit approximations of retained constraints, are evaluated.

Section 4 presents results for a substantial collection of truss and idealized wing structures. Since differences due to idealization and modeling details can be virtually eliminated for truss structures, these examples are compared with some previously reported optimum design results. On the other hand, in the idealized wing examples emphasis is placed on examining the influence of finite element modeling and design variable linking on the minimum weight designs attainable.

Based on the numerical results reported it is concluded that, for structural synthesis problems of modest but useful size, approximation concepts usually make it possible to obtain a practical near optimum design within 5 to 10 analyses. When measured by the number of conventional analyses required to obtain a candidate optimum design, ACCESS 1 is found to be competitive with recursive redesign techniques based on fully stressed design and discretized optimality criteria concepts. Finally, it is argued that since the basic ideas employed in creating the ACCESS 1 program are rather general, its successful development supports the contention that the introduction of approximation concepts will lead to the emergence of a new generation of practical and efficient, large scale, structural synthesis capabilities in which finite element analysis methods and mathematical programming algorithms will play a central role.

## 1. HISTORICAL BACKGROUND

### 1.1 Early Work

The application of mathematical programming techniques to structural design optimization problems has a relatively short but lively history. Prior to 1958 research in this area was built on the plastic design philosophy. Briefly stated, this approach seeks to minimize the weight while precluding plastic collapse of the structure when it is subjected to overload conditions obtained by scaling up service load conditions. Within the context of the plastic design philosophy a significant class of structural optimization problems can be formulated as linear programs. The early applications of linear programming techniques to the minimum weight design of planar frames based on the theory of plastic collapse (such as Refs. 1,2 and 3) did not consider multiple or alternative loading conditions. Subsequently, the need for dealing with alternative loading conditions in the plastic design context was recognized and dealt with successfully (see for example Refs. 4,5 and 6). The early applications of mathematical programming methods to optimum structural design took the form of linear programs because they were formulated within the simplifying context of the plastic collapse design philosophy.

As early as 1955 (see Ref. 7) it was recognized that a more general class of structural design optimization problems could be viewed as nonlinear mathematical programming problems. While Ref. 7 did not consider multiple loading conditions, the fundamental importance of inequality constraints in properly stating structural design optimization problems was clearly recognized. The influence of Ref. 7 was probably limited by the fact that the mathematical problem was treated in classical form using Lagrange multipliers and slack variables. The resulting large number of unknowns and the apparent need to

find all the solutions of the governing set of nonlinear simultaneous equations were discouraging when bigger problems were contemplated.

What has been characterized as a "period of triumph and tragedy for the technology of structural optimization"\* was ushered in by Ref. 8, where the coupling together of finite element structural analysis and nonlinear mathematical programming techniques to generate automated methods for structural optimization was first suggested. Working within the elastic design philosophy it was shown that the minimum weight design of elastic statically indeterminate structures could be cast as a nonlinear mathematical programming problem in design variable space. The formulation set forth in Ref. 8 considered a multiplicity of distinct loading conditions and a variety of inequality constraints, including stress, displacement and member size limitations. Since the design optimization problem treated in Ref. 8 had the form of a nonlinear programming problem, it followed that the optimum design did not necessarily lie at a vertex in the design space. Therefore, it was pointed out in Ref. 8 that, contrary to the commonly held viewpoint, the minimum weight design for a statically indeterminate structure is not necessarily one in which each member is fully stressed in at least one load condition. The algorithm used to generate solutions for several simple three bar truss examples in Ref. 8 was a rather primitive feasible directions type method, that was called the method of alternate steps.

## 1.2 The Decade from 1960-1970

During the decade from 1960-1970 the structural synthesis concept (i.e. the rational formulation and numerical application of mathematical programming methods to the quantifiable portion of the structural design process) developed

---

\* See Ref. 32.

along two main lines, namely: (1) special purpose applications to fundamental and recurring problems involving a broad range of complex failure modes and loading environments; and (2) general purpose applications based on finite element structural analyses considering static stress, displacement, and member size constraints under a multiplicity of distinct loading conditions.

### 1.2.1 Special Purpose Applications

Some examples of structural synthesis capabilities reported during the 1960's that fall into the first category are now cited and briefly discussed. In 1963 an automated minimum weight design capability for rectangular simply supported waffle plates subject to multiple loading conditions was reported in Ref. 9. In this seven design variable problem various buckling and combined stress failure modes were guarded against and the existence of relative minima associated with distinct design subconcepts was revealed.

In 1965 the first effort to apply a mathematical programming approach to optimum design while taking aeroelastic constraints into account was reported in Ref. 10. A highly idealized double wedge wing was studied considering a plausible mix of constraints restricting flutter Mach number, static aeroelastic displacements, combined stress, and angle of attack. The objective function to be minimized was taken as the total energy required to drive the wing through a sequence of several flight conditions and the option to impose a maximum wing weight constraint was included.

The minimum weight design of stiffened cylindrical shells represents a recurring problem of fundamental importance in aerospace applications. In 1968 the first application of mathematical programming methods to this important problem was reported in Ref 11. Later the same year a structural synthesis capability for the minimum weight design of stiffened cylindrical

shells, representative of the state-of-the-art (circa 1968), was presented in Ref. 12. The problem was formulated using the Fiacco-McCormick interior penalty function and numerical results were obtained by executing a sequence of unconstrained minimizations using the Davidon-Fletcher-Powell variable metric algorithm. The constraint repulsion characteristic of this formulation made it possible to employ approximate buckling analyses during major portions of the design procedure. In a sense, this feature was a philosophical precursor of the currently emerging approximation concepts approach in structural synthesis. In 1969 an extension of this capability to the minimum weight design of barrel shells was reported in Ref. 13. As an illustration of the important role structural synthesis capabilities can play in evaluating design concepts, the following quotation from Ref. 13 is cited: "For shells designed to support axial compressive loads, the results show that important weight savings can be provided by slight meridional curvature. For the particular shell examined herein, the maximum weight saving is about 30%. The large increases (factors of 5 to 9 in strength) recently attributed to barreling cannot be directly translated into weight savings when comparisons are made between minimum-weight designs. Yielding becomes an important failure constraint at lower loads for barreled shells than for cylindrical shells."

A mathematical programming approach has also been applied to the minimum weight optimum design of stiffened fiber composite cylindrical shells (see Refs. 14 and 15). The design variables include the depth and width of the hat stiffeners, the stiffener spacings, the fiber volume content, and the ply orientation angles. Multiple load conditions are treated and each load condition is described in terms of a combination of axial, radial, and torsional load. It is pointed out that the weight objective function is

independent of the ply angles and it is shown that alternative optima are common for this type of structure (i.e. the set of design variable values that gives the minimum weight is not unique).

In 1968 an application of the mathematical programming approach to the automated optimum design of an ablating thermostructural panel was reported in Ref. 16. Analysis of a trial design involved a one-dimensional nonlinear transient thermal analysis, to predict the temperature distribution, followed by a stress analysis that employed temperature dependent material properties. The design variables were the initial ablator thickness, the sandwich structure thicknesses (skins and core), the insulation thickness and the panel planform dimensions. Two alternative objectives were considered, namely: (1) minimization of the weight per unit area of surface protected, subject to a constraint on the maximum depth of the shield; and (2) minimization of the total shield depth, subject to a constraint on the maximum weight per unit surface area protected. The loading environment was described by time dependent heat flux and dynamic pressure inputs. The optimization problem was formulated using an extension of the Fiacco-McCormick penalty function technique which accommodates parametric inequality constraints.

In 1969 an application of the mathematical programming approach to the minimum weight optimum design of planar truss-frame structures subject to dynamic loads was reported in Ref. 17. Inequality constraints were placed on the maximum dynamic displacements and stresses and the natural frequencies of the structure could be excluded from certain bands. The limited class of structures and the use of shock spectral analysis notwithstanding, this work probably represents the most comprehensive structural optimization investigation carried out in the dynamic response regime prior to 1970.

Reference 18 (1970) reports on a minimum weight structural optimization capability for a rather general class of laminated fiber composite plate type structure. The design variables considered include lamina thicknesses as well as orientation angles and a wide variety of strength and elastic stability failure modes were guarded against. A direct Rayleigh-Ritz analysis for anisotropic plates was used as the principal analysis tool. The most extensive problem formulated in Ref. 18 involved 21 design variables, 45 distinct failure modes and 3 independent loading conditions. This work was influenced significantly by Ref. 12 in the sense that it: (1) made use of some simple approximation concepts in the failure mode analysis and (2) employed a modified version of optimization program given in Ref. 12.

#### 1.2.2 General Purpose Applications

Attention is now focused on some examples of structural synthesis capabilities reported during the 1960's that clearly fall into the second category, namely they represent general purpose programs based on finite element structural analysis methods and mathematical programming techniques. The first major efforts to apply mathematical programming techniques to the design of complex structural systems represented by finite element models were reported in Refs. 19,20, and 21. The optimum design capability reported in Ref. 21 considers static stress and displacement limits as well as multiple load conditions and minimum member sizes. Structural analyses are carried out using the well known finite element displacement method and the element repertoire includes bars and shear panels as well as triangular and quadrilateral plane stress membrane elements. The initial phase of the design optimization procedure employs the stress ratio procedure. This is followed by a second phase which applies a special type of feasible direction method

called the "optimum vector" method. The partial derivatives of response quantities, such as displacements and stresses used by the mathematical programming algorithm, are determined from analytic expressions and the use of finite difference techniques is avoided. The program does not employ design variable linking and hence each finite element in the analysis model has one design variable associated with it. The largest example reported in Ref. 21 involved 152 finite elements, 135 displacement degrees of freedom and 2 distinct load conditions. Guarding against violation of stress and displacement limitations, a reduction of the idealized structural weight from 119 lbs. to 73 lbs. was achieved in approximately 2 hours of IBM 7094 run time.

A second major effort to apply mathematical programming techniques to the design of complicated structural systems represented by finite element models was reported in Refs. 22 and 23. In this work special emphasis was placed on least weight design of stressed-skin structures with holes and cut-outs. The minimum weight optimum design capability reported in Ref. 23 considers stress, displacement and member size constraints and multiple loading conditions are taken into account. Structural analyses are executed using an efficient finite element displacement method module and the available finite element library contains a rod, a plane stress triangle, three variations of four node plane stress plates, and two "beam-like" elements. The optimization algorithm used is a feasible directions method based on Zoutendijk's algorithm. In Ref. 23 partial derivatives of response quantities with respect to design variables are computed using analytic expressions obtained by implicit differentiation of the governing equilibrium equations, thus avoiding the use of a first order finite difference procedure employed in the earlier work reported in Ref. 22. It should be noted that a special type of partial design

variable linking is also provided for, and therefore the number of independent design variables is significantly smaller than the number of finite elements in the structural analysis model. The importance of reducing the number of structural analyses and the number of partial derivative calculations was recognized in Ref. 23 and several devices aimed at improving overall efficiency of the design optimization procedure were introduced. In particular, various techniques were employed for improving the efficiency of the one dimensional searches, thus reducing the number of structural analyses. Furthermore, partial derivatives were only recalculated when the design moved outside of a user defined hypersphere. The capability reported in Ref. 23 permits the use of up to 100 design variables and 700 displacement degrees of freedoms. The largest example reported in Ref. 23 involves 600 finite elements, 300 nodes and 5 load conditions. These results were obtained with a less efficient antecedant of the program described in Ref. 23 and while the run time is not reported it is thought to be substantial (of the order of 3.5 hours on a CDC 6600 according to Section 8.3.3 of Ref. 24).

### 1.3 Consolidation and Assessment Period

The rapid development of the structural synthesis concept during the 1960's stimulated a great deal of interest in structural engineering applications of mathematical programming techniques. By around 1970 these developments had become extensive and a period of consolidation and assessment, characterized by state-of-the-art review papers and educational endeavors, ensued. For example Ref. 25 contains an overview of the progress reported during the 1960's and Ref. 24 presents a comprehensive and detailed description of the state-of-the-art in structural design applications of mathematical programming techniques as of 1970. A growing awareness of the potentialities

in this field was also enhanced by educational endeavors such as the AIAA Professional Studies short course on structural synthesis given in April 1970 (see Ref. 26) and the publication of an excellent text book in 1971 on algorithmic tools for engineering design optimization (Ref. 27).

Nevertheless, by 1970 it had become apparent that, while two first generation general purpose structural synthesis capabilities had emerged (see Refs. 21 and 23) practical application of mathematical programming methods to structural design optimization was lagging far behind the prevailing level of structural analysis capability. It is only natural to ask, why the apparent high promise of these new design tools had not been more fully realized in practice by 1970? There are many possible explanations, however, it is suggested here that the following are amongst the more important and plausible responses:

- (1) Because of the easy availability of fully developed finite element structural analysis capabilities there was a tendency to treat analysis and optimization modules as two black boxes, tie them together, and let the optimization procedure drive the analysis routine through an excessively large number of complete highly refined analyses;
- (2) It had not yet been widely recognized that structural analysis for design optimization is a task with special characteristics that are dictated by the objective of generating, with minimum effort, estimates of critical and near critical behavior adequate to rationally guide design modification;

- (3) There was some tendency in practice to divert development effort toward automation of more traditional and familiar recursive redesign procedures based on fully stressed design concepts and discretized optimality criteria (see for example Refs. 28,29,30, and 31).

In any event, by 1971 it had become clear that the then available optimization capabilities that combined finite elements structural analysis with mathematical programming techniques required inordinately long run times to solve optimization problems of only modest proportions (or as a harsher critic put it they were hopelessly inefficient). Indeed, in Ref. 32 it was suggested that the mathematical programming approach to structural optimization was little more than "an interesting research toy." Furthermore, it was stated that "there appeared little immediate prospect for the development of more efficient non-linear programming algorithms to overcome the economic barriers to widespread operational usage on real structures."

It seemed to some investigators that an insurmountable efficiency barrier had been encountered in the application of mathematical programming techniques to structural design optimization problems. This led them to expend renewed effort on the implementation of redesign procedures based on fully stressed design concepts and discretized optimality criteria. For example Ref. 33 reports on the ASOP (Automated Structural Optimization Program) computer program, developed for the minimum weight design of large practical structures. The iterative design procedure employed consists of a stress ratio algorithm (alternate stress ratio resizing and scaling to the critical constraint) followed by a numerical search phase which provides a mechanism for handling displacement constraints. The largest example problem

reported in Ref. 33 involves 890 finite elements, 1171 degrees of freedom and four distinct loading conditions. Ignoring deflection constraints and using the stress ratio algorithm a reasonable design of significantly lower weight was obtained after 9 resizing cycles. In Ref. 34 a design procedure based on the combined use of stress ratio and optimality criteria concepts was reported. For stress constrained design problems members were resized in proportion to the ratio of actual stress to the allowable stress. For displacement constraints an optimality criteria based resizing procedure was employed. The method reported in Ref. 34 was applied to several standard truss type test problems as well as an 18 element wing box beam structure. In most instances satisfactory results were obtained in less than ten iterations. The design optimization procedure presented in Ref. 35 is based on a generalized energy criteria and its theoretical basis is similar to the method presented in 34 with the exception of some details involved in coping with multiple constraints. A resizing formula involving element energies and their "target energies" is used for dealing with multiple constraints. Stress critical members are resized by the stress ratio technique and these sizes are then treated as minimum member sizes during resizing by the energy criteria. Results for several practical example problems are also reported in Ref. 35. In Ref. 36 a unified optimality criteria method, for structural systems discretized into finite elements, was described for both stress and stiffness constraints. Optimality criteria and recursive redesign rules were presented for stress, displacement, buckling and frequency constraints. Results for several large example problems are reported in Ref. 36.

Since around 1970 a major development activity in automated interdisciplinary aerospace vehicle design has been underway (see for example Refs. 37-43). A thoughtful review and assessment of this activity will be found in

Ref. 43. The structural optimization modules in these emerging large scale capabilities have by and large been based upon the combined use of fully stressed design methods and mathematical optimization methods (see Refs. 37 and 40). The general approach followed is well characterized by the mixed method described in Ref. 40, which reflects the widely held current viewpoint that while mathematical programming methods are at present well suited to component optimization, they are not computationally competitive for dealing with large structural systems of practical importance. Thus in Ref. 40 a fully stressed design method was used to obtain a gross overall distribution of material while the detailed design of rings and stiffened panels (fuselage components) was carried out using mathematical programming techniques.

The application of design procedures, based on stress ratio and optimality criteria methods, to large finite element structural systems has been a necessary expedient because of the absence of computationally efficient alternatives. It is however widely recognized that design procedures based on optimality criteria, and fully stressed design concepts can only be shown to yield optimum designs under rather restrictive special conditions. When these methods are employed a criterion related to the structural behavior is derived on the premise that when a design satisfying the criterion is found the objective function automatically takes on an optimum value. On the other hand design procedures based on the application of mathematical programming techniques to structural design are quite general and the orderly logic of this approach remains philosophically attractive. No assumptions are made at the outset as to how many and which design constraints will in fact become critical at the optimum design. Indeed, it appears that the principal objection to the mathematical programming approach has been the rapid increase in computational

effort with problem size (i.e. computational inefficiency for problems of practical importance).

#### 1.4 Design Oriented Structural Analysis

The continuing active development of structural design procedures for structural systems represented by finite element assemblages has stimulated interest in the area of design oriented structural analysis methods (see for example Refs. 44-52). These papers reflect a growing realization that analysis for design optimization is a task with special characteristics. For example, as pointed out in Ref. 44, the structural analysis task associated with design optimization requires behavior prediction for many structures of somewhat similar form. Until recently the dominant objective of finite element structural analysis procedures has been accurate prediction of structural behavior given an arbitrary design. However, in the structural design context, the objective of structural analysis should be to generate, with minimum effort, an estimate of the critical and potentially critical response quantities adequate to guide the design modification sequence. Developments in design oriented structural analysis have tended to fall into three categories: 1) sensitivity analysis techniques, (2) basis reduction in analysis variable space, and (3) reexamination of how finite element methods are organized, focusing on how to improve their organization so that they lend themselves better to the design optimization task. For example Ref. 45 falls into the first category and it presents an effective method for obtaining the rates of change of response quantities with respect to design variables when the governing analysis equations form a set of linear simultaneous equations. Reference 46 presents methods for obtaining the rates of change of response quantities with respect to design variables when the governing analysis is an eigenproblem of the

form  $Ax = \lambda Bx$  (where  $A$  and  $B$  are real symmetric matrices and  $B$  is positive definite). The methods presented in Ref. 46 are therefore applicable to structural design problems involving buckling, frequency, and dynamic response constraints. The original motivation for this type of sensitivity analysis, which yields partial derivative information (rates of change of response quantities with respect to design variables) resided in the fact that the more powerful mathematical programming algorithms required constraint gradients. However, it has since become apparent that the results of such sensitivity analyses can be used in various ways. First, as previously noted, they can be used to provide constraint gradient information within optimization algorithms. Second, they can be used to set up approximate analyses using first order Taylor series expansions. Third, they can be used as a guide to the designer working in a man-machine interactive mode, where only the structural analysis and the associated sensitivity analysis is executed by the computer. In the context of automated structural design optimization, it now appears that the most important use of these sensitivity analyses is in the construction of approximate analyses based on Taylor series expansions. With respect to static structural analysis, based on the finite element displacement method, the generation of approximate analyses using Taylor series expansions was outlined in Section 9 of Ref. 26. The ability of first-order Taylor series approximations to predict static stress and displacement response with relatively small errors even for large design modifications has been substantiated by the investigation reported in Ref. 47.

Turning to the second category of developments in design oriented structural analysis, namely basis reduction in analysis variable space, attention is focused on Refs. 44 and 48. The basic idea of constructing an

approximate analysis solution using a few well chosen basis vectors can be applied in a variety of ways. It is common practice in dynamic analysis to express displacement response in terms of a reduced set of generalized coordinates and normal mode vectors. In the case of static structural analysis the reduced basis approach can be employed in conjunction with either the force (see Ref. 44) or the displacement (see Ref. 48) method of analysis. If a set of  $r$  independent analysis vectors is available ( $r < n$ , where  $n$  is the number of unknown analysis variables arising from the structural idealization and discretization) from previously analyzed designs, then the vector of analysis variables can be approximated as a linear combination of these  $r$  known vectors. The undetermined participation coefficients for each of the  $r$  known vectors become the unknowns of the approximate analysis. Substituting the approximate representation into an appropriate energy formulation and taking the stationary condition leads to a set of  $r$  simultaneous equations that can be solved for the participation coefficients. The results reported in Refs. 44 and 48 demonstrated the potential of reduced basis approximations in static structural analysis. In Ref. 49 an improved reduced basis technique is reported. The basis employed has  $(r+1)$  normalized vectors, where  $r$  is taken equal to the number of independent design variables. Working within the context of the displacement method, the base vectors are taken to be the displacement solution vector for the original design and the first derivatives of this vector with respect to each of the  $r$  independent design variables. However, it should be noted that while the reduced basis approach to approximate static structural analysis decreases the number of unknowns, the resulting matrices are densely populated. Furthermore, this approach does not yield an explicit approximation for the response quantities in terms of the design variables.

More recently (see Ref. 50) methods of approximate structural analysis, using Taylor series expansions and the modified reduced basis method of Ref. 49, have been studied in the context of the mixed methods of structural analysis where forces and displacements are treated simultaneously as the basic response quantities. In Ref. 51 an approximate analysis technique, based on first order Taylor series expansions, is presented for truss structures where the design variables include joint coordinates prior to deformation. The approximate analysis method is developed in the context of the mixed method of structural analysis with joint displacements and modified member forces taken as the basic unknowns of the structural analysis.

The third category of design oriented structural analysis development reexamines the organization of finite element methods of structural analysis seeking improved analysis efficiency in the context of iterative automated design procedures. The work reported in Ref. 52 is representative of this sort of investigation and it provides a means of determining the natural frequencies and mode shapes of a modified design without having to perform a complete reanalysis. A set of stiffness parameters and a set of inertia parameters are defined so that the system stiffness matrix and the system mass matrix can be formed as linear combinations of invariant matrices that can be computed once and stored. In general these design parameters can be nonlinear (but explicit) functions of the structural design variables. The complete system stiffness and mass matrices are reduced by static condensation and an eigensolution is obtained for the reduced system. The dimensions of the eigenproblem are then further reduced using the first  $r$  normal modes leading to the generalized stiffness and mass matrices. These generalized stiffness and mass matrices are expanded into a first order Taylor series form in terms

of the design parameters. The generalized stiffness and mass matrices are then generated for any perturbation of the design variables by using these Taylor series expansions and the eigenanalysis of the modified structure involves small matrices of dimensions  $r \times r$ . It should be noted that the foregoing method, set forth in Ref. 52, assumes that the eigenvectors, obtained from the eigensolution executed after static condensation, are invariant with respect to design modifications. Also the method does not lead to an explicit approximation for frequencies and normal modes, since analysis of a modified design requires solution of an eigenproblem involving matrices of dimension  $r \times r$ . It should be noted that in Ref. 53 special attention is given to organizing the assembly of the system stiffness matrix so as to facilitate efficient reassembly for modified designs. Attention is limited to structures where the elements stiffness matrices are linearly dependent on the design variables. Using design variable linking, the system stiffness matrix is assembled by summing the invariant part and the contributions to the system stiffness matrix from the group of elements linked to each independent design variable. Developments in the area of design oriented analysis will continue to have a profound effect on improving the efficiency of structural design optimization procedures.

### 1.5 Recent Special Purpose Applications

In the time period since 1970 both special and general purpose applications of mathematical programming methods to structural optimization have continued to appear in the literature. In the special purpose category there has been particular interest in dealing with flutter constraints (see Refs. 54 through 59) and fiber composite structures (see Refs. 60 through 64).

In Ref. 54 equations for finding the partial derivatives of the flutter velocity of an aircraft structure with respect to sizing type design variables were derived and a numerical design procedure was developed for seeking a minimum mass design subject to a specified flutter velocity constraint. The design procedure employed utilizes two gradient search methods and a gradient projection technique. The optimization procedure was applied to the design of a wing box beam with twelve independent design variables.

In Ref. 55 an automated design optimization program (SWIFT) was reported which considers static strength and flutter constraints using a mathematical programming formulation. The wing was treated as a sandwich plate with preassigned planform and depth distribution. The skins were assumed to be isotropic and their thickness distribution was optimized. The thickness distribution was represented by a series of assumed polynomials with the participation coefficients taken as the design variables. The optimization algorithm employed in Ref. 55 is a SUMT interior penalty function formulation used in conjunction with a Davidon-Fletcher-Powell unconstrained minimization routine. An important point made in Ref. 55 is that optimum designs obtained by considering strength and flutter constraints concurrently can be significantly lighter than designs obtained by initially considering strength constraints only and then scaling up the design to prevent flutter.

In Ref. 56 an automated procedure for preliminary design optimization of lifting surface type structures was reported. In this study an equivalent plate representation of the wing structure (including transverse shear deformation) was employed and the design variables included planform descriptors (leading and trailing edge sweep-angle, root chord, and wing semi-span), wing depth distribution and skin thickness distribution. The objective function

was taken to be a function of the structural weight and the aerodynamic drag. A wide variety of behavior constraints (including static stress, static displacement, natural frequency, flutter, root angle of attack and gross lift) and side constraints (including constraints on planform shape, wing area, tip chord dimension, wing depth, and skin gage) under various flight conditions (including alternative fuel mass distributions) were considered. Second order piston theory, in which the wing depth distribution is taken into account, was used to predict both steady and unsteady pressure distributions on the wing surfaces. The optimization algorithm employed in Ref. 56 was Zoutendijk's method of feasible directions. The preliminary design optimization study reported in Ref. 56 represents one of the most ambitious efforts in this area to date. However, it must be noted that relatively large numbers of analyses and rather long run times were required to obtain final designs. A companion development to that reported in Ref. 56 was reported in Ref. 57. A multi-web delta wing was modeled using three types of finite elements (shear panels, bars and membrane triangles) and weight minimization was taken to be the objective of the optimization procedure. The design variables are thicknesses and cross sectional areas and design variable linking was employed. The design requirements included restrictions on the strength, stability, frequency and flutter characteristics of the structure in each of several flight conditions. The optimization problem is formulated using an interior penalty function formulation and the sequence of unconstrained minimizations is carried out using the Davidon-Fletcher-Powell algorithm. Results for several example problems were reported in Ref. 57, however the amount of run time required to obtain final design was rather long (approximately 100 minutes on a UNIVAC 1108). A concise summary of Refs. 56 and 57 will be found in

Ref. 58. In Ref. 59 a numerical procedure (based on Zoutendijk's method of feasible directions) for minimum weight sizing of aircraft structural components, subject to a specified lower bound on flutter speed, was presented. The method was devised to utilize the most general and accurate of current analytic flutter predictions so that substructures of arbitrary aerodynamic and structural complexity can be optimized. Results for two example problems were reported in Ref. 59; namely, a two variable subsonic wing example and a relatively large supersonic delta wing example.

While considerable progress has been recently reported in applying mathematical programming methods to the design of fiber composite laminates (see Refs. 60 and 61) and structural components (see Refs. 62 and 63) less attention has been focused on optimum structural design with fiber composite materials at the structural systems level (see Ref. 64). The structural optimization procedure reported in Ref. 64 deals with the design of fiber composite structures subject to static strength and aeroelastic constraints including flutter. The basic structural idealization is an equivalent plate representation (neglecting transverse shear deformation) and a direct Rayleigh-Ritz assumed displacement approach is employed to carry out the structural analyses. The design variables considered include lamina orientation angles, lamina thickness distributions, and the magnitude of prelocated balance masses. Behavior constraints taken into account include static stress, strain and displacement limitations as well as aeroelastic constraints which prevent divergence and flutter. Lower limits can be specified for the layer thicknesses and the fundamental frequency. While weight is taken as the primary objective function, options are provided to treat other objective functions either instead of or in combination with weight. The optimization problem dealt with in Ref. 64 is formulated using an interior penalty function formulation.

## 1.6 Recent General Purpose Applications

Attention is now directed to recently reported applications of mathematical programming techniques to finite element based structural design problems. In Ref. 65 a minimum weight optimum design capability was reported which employs a sequence of linear program approach known as the move limit method. Static stress, displacement and member size constraints are included and attention is given to organizing the analysis so that the system stiffness matrix can be formed from invariant matrices associated with unit values of the independent design variables. This capability includes triangular membrane elements in which the strains and thickness vary linearly and bar elements in which axial strain and cross sectional area vary linearly. A special form of design variable linking is optionally available since thicknesses (or cross sectional areas) of relevant adjacent elements can be set equal at finite element grid points. Results for several hole reinforcement problems, similar to those examined in Ref. 22, are presented. While Ref. 65 does not contain information on the number of structural analyses required to converge the procedure, the run times reported are long (between 5000 and 10,000 seconds on an ICL 1907 machine).

In Ref. 66 a design procedure combining finite element structural analysis and mathematical programming techniques is described and applied in the context of ship structures. Multiple load conditions are considered and stress, simple buckling and minimum size constraints are provided for. Both sizing and configuration variables are treated. Bar and quadrilateral plane stress elements are used in the finite element modeling. Design variable linking is used to reduce the number of design variables and a regionalization scheme is employed to reduce the number of stress constraints. Selection of

the stress constraints to be retained is carried out automatically by examining the stress states in all elements within a region, and selecting the maximum of each stress type to form the behavioral constraints for that region. The optimization algorithm employed is a sequence of linear programs approach using design variable move limits and selective constraint retention. The minimum weight design of an oil tanker transverse frame is presented in Ref. 66. This example problem involves 4 load conditions, 297 panel and bar elements, 352 displacement degrees of freedom, and 22 design variables. Starting from an infeasible initial design a weight reduction of 17.5% was obtained after seven iterations. The required run time is given as 59.45 CPU minutes on an IBM 360/67 computer.

An automated procedure for the design of wing structures to satisfy strength and flutter requirements was reported in Ref. 53. The computer program WIDOWAC was developed for design of minimum mass wing structures subject to flutter, strength and minimum gage constraints. The WIDOWAC program is based on finite element structural idealization and mathematical programming methods are used to carry out the optimization. The flutter constraint calculations employ second order piston theory aerodynamics.<sup>†</sup> This program is currently the most efficient finite element based mathematical programming type optimization capability which includes flutter, strength, and minimum gage constraints. The efficiency achieved by the WIDOWAC program is attributed to: (1) the use of iterative analysis methods to significantly reduce reanalysis effort compared with that required for the original analysis of the structure; (2) the use of linking to reduce the number of independent design variables; and (3) introduction of a modified Newton's method to carry out the unconstrained minimizations for the SUMT type interior penalty function

---

<sup>†</sup>The WIDOWAC program has recently been extended to include kernel function aerodynamics for subsonic conditions.

formulation. A representative example problem reported in Ref. 53 involved 1 load condition, 23 design variables, 156 displacement degrees of freedom, and 187 finite elements. Convergence for this example required 333 analyses and approximately 400 seconds of CPU time on a CDC 6600 computer.

Another finite element based mathematical programming type structural optimization capability is currently being developed by Vanderplaats. This effort is motivated by the view that traditional preliminary design methods are often inadequate, even at the conceptual design level, when investigating new and unusual aircraft configuration concepts. A computer program for structural analysis and design (SAD) has been developed which currently deals with static stress, displacement and member size constraints. The finite element library includes the following elements: truss, constant strain triangles, rectangular membrane, and symmetric shear panels. A CDC 7600 version of the SAD program can accommodate problems with up to: (a) 50 independent design variables, (b) 300 displacement degrees of freedom; (c) 5 load conditions and (d) 100 elements of each type. The optimization algorithm employed is a modification of Zoutendijk's method of feasible directions with improved numerical stability and the ability to deal efficiently with infeasible designs (Ref. 67). A modular optimization program implementing this improved feasible directions algorithm is documented in Ref. 68.

Before closing this review of the historical background it is appropriate to briefly cite four other works, because they are the immediate antecedents of the research results to be presented in this report. The reduced based concept in design space was set forth and initially explored in Refs. 69 and 70. The essential idea presented was to let the vector of design variables be expressed as a linear combination of design basis vectors. The

initial investigations reported in Refs. 69 and 70 were restricted to stress limited truss problems and basis vectors were obtained using stress ratio methods considering one load condition at a time. Thus the number of generalized design variables in any particular application was equal to the number of load conditions.

In Refs. 71 and 72 it was shown that a collection of approximation concepts could be used in concert to significantly improve structural synthesis efficiency. Truss structures subject to stress and displacement constraints under alternative loading conditions were considered. The optimization algorithm employed was an adaptation of the method of inscribed hyperspheres (see Ref. 73) and high efficiency was achieved by using approximation concepts including temporary deletion of noncritical constraints, design variable linking, and Taylor series expansions of constraint functions in terms of reciprocal design variables.

## 2. APPROXIMATION CONCEPTS — THE KEY TO CONSTRUCTING TRACTABLE STRUCTURAL SYNTHESIS FORMULATIONS

### 2.1 Introduction

While it is a time honored practice in structural engineering to employ a gradation of approximation levels in both analysis and design procedures relatively little attention has been given to the use of approximation concepts in the structural synthesis context.

There are various levels of approximation commonly employed in structural analysis. These are generally agreed to include idealization and discretization. In the context of finite element methods idealization refers to the element types (e.g., truss, beam, membrane, plate, etc.) used to model the structure and discretization refers to the number of elements employed. Once the judgment decisions at the idealization and discretization level have been made, the structural analysis problem has a definite mathematical form, and the number of basic analysis variables is fixed (e.g., in the finite element displacement method the number of independent displacement degrees of freedom is known).

It is also possible to identify various approximation levels associated with the formulation of the structural synthesis problem. It can be argued that deciding on the kind, number, and distribution of design variables, the load conditions, and the constraints to be considered during the synthesis is somewhat analogous to making judgments that lead to an idealized discretized analysis model. Selecting an objective function (i.e., the scalar quantity that is to be minimized or maximized) essentially completes the mathematical formulation of the structural synthesis problem.

It is to be understood that the approximation concepts considered herein are intended to apply to a structural design problem that has been previously given specific mathematical form with respect to analysis and synthesis.

Most of the previously reported applications of the mathematical programming approach to structural optimization have suffered from one or more of the following excesses: (a) too many independent design variables were considered; (b) too many behavior constraints were considered throughout the synthesis process; and (c) too many detailed structural analyses were carried out during the synthesis. It is to be understood that the phrase "too many" as used in the foregoing sentence means more than necessary to obtain a practical near optimum design. The approximation concepts approach to structural synthesis achieves high efficiency by alleviating these excesses while retaining an adequate representation of the essential features of the structural design optimization problem.

## 2.2 Statement of Structural Synthesis Problem

A rather general class of structural synthesis problems can be stated in standard form as follows: given the preassigned parameters and the load conditions find the vector of design variables  $\vec{D}$  such that

$$g_q(\vec{D}) \geq 0; \quad q = 1, 2, \dots, Q \quad (2.1)$$

and

$$M(\vec{D}) \rightarrow \text{Min.} \quad (2.2)$$

At this point it is assumed that  $\vec{D}$  contains one scalar component for each finite element in an idealized structural representation involving  $I$  finite elements. The number of inequality constraints  $Q$  is also large since the set of inequalities  $g_q(\vec{D}) \geq 0; \quad q = 1, 2, \dots, Q$  usually contains one "behavior" constraint for each failure mode (e.g., upper limit on deflection) in each

load condition as well as "side" constraints (e.g., upper and lower limits on the components of  $\vec{D}$ ) that reflect fabrication and analysis validity considerations. It should also be recognized that most of the behavior constraints  $g_q(\vec{D}) \geq 0$ ;  $q = 1, 2, \dots, Q$  are not explicit functions of the design variables  $\vec{D}$ . Rather, these constraints are usually implicit functions of  $\vec{D}$ , and their precise numerical evaluation, for a particular design  $\vec{D}$ , requires a complete structural analysis. Finally, it is noted that when the objective function  $M(\vec{D})$  is taken to be the weight of the idealized structure,  $M(\vec{D})$  is usually an explicit function of  $\vec{D}$ .

### 2.3 Reducing the Number of Design Variables

Usually it is neither necessary nor desirable for each finite element in the structural analysis model to have its own independent design variable. Two techniques for reducing the number of independent design variables are (1) design variable linking, and (2) the reduced basis concept. These techniques are described in the sequel.

#### 2.3.1 Design Variable Linking

Various linking approaches are available; all share the basic strategy that one or, at most, a few independent design variables  $\gamma_c$  control the size of all finite elements in that linking group. For example, a wing planform could be divided into segments with a single independent design variable specifying the thickness of all the cover panels within a segment. In another approach, used in Ref. 53, the independent design variables were taken to be the thickness of the cover panels at the vertices of each wing planform segment; the thickness of the cover panels within a segment were taken to be a linear variation across the segment.

In the approach used herein, the design variable linking fixes the relative sizes of some preselected group of finite elements. Each component

$D_i$  of the vector  $\vec{D}$  is made proportional to only one of the new independent design variables  $\gamma_c$ . Stated mathematically the linking is given by

$$\vec{D} = \sum_{c=1}^C \vec{L}_c \gamma_c = [L] \vec{\gamma} \quad (2.3)$$

or in scalar form.

$$D_i = \sum_{c=1}^C L_{ic} \gamma_c = L_{i1} \gamma_1 + L_{i2} \gamma_2 + \dots + L_{ic} \gamma_c; \quad i=1,2,\dots,I \quad (2.4)$$

where it is understood that  $C \leq I$ . Each row of the matrix  $[L]$  in Eq. (2.3) contains only one nonzero term, and the summation on the right hand side of Eq. (2.4) contains only one nonzero term. In each case, the nonzero term is positive.

The design variable linking idea is illustrated graphically by the simple example shown in Fig. 1. The dotted lines define the element linking groups and the numbers shown refer to the finite elements. Let design variable linking groups 1,2,3 and 4 contain elements (1,2), (6,7,9), (3,4,8), and (5), respectively.

Then for this simple example Eq. (2.3) has the specialized form.

$$\begin{Bmatrix} t_1 \\ t_2 \\ t_3 \\ t_4 \\ t_5 \\ t_6 \\ t_7 \\ t_8 \\ t_9 \end{Bmatrix} = \begin{bmatrix} 1 & 0 & 0 & 0 \\ 1 & 0 & 0 & 0 \\ 0 & 0 & 1 & 0 \\ 0 & 0 & 1 & 0 \\ 0 & 0 & 0 & 1 \\ 0 & 1 & 0 & 0 \\ 0 & 1 & 0 & 0 \\ 0 & 0 & 0.7 & 0 \\ 0 & 0.6 & 0 & 0 \end{bmatrix} \begin{Bmatrix} \gamma_1 \\ \gamma_2 \\ \gamma_3 \\ \gamma_4 \end{Bmatrix} \quad (2.5)$$

The nonzero entries in column 2 of the foregoing [L] matrix specify that finite elements 6 and 7 (in Fig. 1) have the same thickness ( $\gamma_2$ ) while element 9 has a thickness  $0.6 \gamma_2$ , where  $\gamma_2$  is one of the four independent design variables in the reduced set  $\vec{\gamma}$ . The nonzero entries in the remaining columns of the specialized [L] matrix in Eq. (2.5) are to be given similar physical interpretation.

Design variable linking makes it possible to reduce the number of independent design variables while at the same time imposing constraints that can make the final designs more realistic. Linking also facilitates the introduction of constraints reflecting symmetry considerations, designer insight based on prior experience, as well as fabrication and cost considerations associated with the number of parts to be assembled.

### 2.3.2 Reduced Basis Concept for Design

The reduced basis concept in design space provides a means for further reducing the number of design variables in the original problem statement. This important idea and its initial exploration was first set forth in Refs. 69 and 70. The vector of design variables after linking, namely  $\vec{\gamma}$ , can be expressed as a linear combination of B independent basis vectors  $\vec{R}_b$ , that is,

$$\vec{\gamma} = \sum_{b=1}^B \vec{R}_b \delta_b = [R] \vec{\delta} = \delta_1 \vec{R}_1 + \delta_2 \vec{R}_2 + \dots + \delta_B \vec{R}_B \quad (2.6)$$

or in scalar form,

$$\gamma_c = \sum_{b=1}^B R_{cb} \delta_b = R_{c1} \delta_1 + R_{c2} \delta_2 + \dots + R_{cB} \delta_B; \quad c=1,2,\dots,C \quad (2.7)$$

The independent basis vectors  $\vec{R}_b$  are assumed to be known; the participation coefficients  $\delta_b$ , which represent a further reduced set of generalized design variables, are the unknowns. If the basis vectors are thought of as a set of well chosen functions evaluated at specified mesh points, then the reduced basis concept in design variable space can be viewed as a designer's Ritz method.

Base vectors can be drawn from various sources including optimality criteria solutions, stress ratio solutions (see Ref. 74), lower and upper bound-type solutions, and designs based on engineering insight.

The reduced basis concept in design space opens the way to the development of hybrid methods of structural optimization. It is likely to have a major unifying influence leading to the coordinated use of stress ratio, optimality criteria, lower bound and general mathematical programming methods.

### 2.3.3 Two Step Reduction in the Number of Independent Design Variable

After substituting Eq. (2.6) into Eq. (2.3) the vector of design variables  $\vec{D}$  is given by

$$\vec{D} = [L] \vec{\gamma} = [L][R] \vec{\delta} = \sum_{b=1}^B \vec{T}_b \delta_b = [T] \vec{\delta} \quad (2.8)$$

or, in scalar form, by

$$D_i = \sum_{b=1}^B T_{ib} \delta_b = T_{i1} \delta_1 + T_{i2} \delta_2 + \dots + T_{iB} \delta_B; \quad i=1,2,\dots,I \quad (2.9)$$

in which  $\vec{\gamma}$  denotes the vector of independent design variables after linking and  $\vec{\delta}$  represents the vector of independent design variables after also employing the reduced basis concept. The matrix  $[T]$  equals  $[L][R]$ , and the  $\vec{T}_b$  may be thought of as prelinked basis vectors.

Equation (2.8) represents a combined transformation that will implement a reduction in the number of design variables due to design variable linking followed by an application of the reduced basis concept in design space. It is emphasized that the basis vectors  $\vec{T}_b$  can be formed directly by imposing the same prespecified linking on each of the basis vector generator programs, regardless of its source. If design variable linking is not employed, then  $[L]$  is an identity matrix,  $C = I$ , and  $[R] = [T]$ . On the other hand, if only

design variable linking is employed, then [R] is an identity matrix,  $C = B$ , and  $[L] = [T]$ .

If the set of basis vectors is well chosen, a good approximation to the optimum design will be obtained by solving the mathematical programming problem in the reduced ( $\vec{\delta}$ ) space. The solution obtained in the reduced space will always be a feasible upper bound solution (with respect to the objective function being minimized) of the original design problem. In the event that the subspace spanned by the basis vectors contains the actual optimum design, the upper bound solution will coincide with the actual optimum design (assuming the absence of relative minima).

It should be recognized that design variable linking may be viewed as an improvement of the original problem statement or as a special type of basis reduction, depending upon the underlying motivation. When design variable linking is used to impose symmetry requirements or to introduce fabrication and cost control considerations, then it sharpens the problem statement. Under these circumstances design variable linking restricts the search for an optimum design to the subspace in which the desired solution must reside. On the other hand, if design variable linking is based on designer insight, prior experience, or simply arbitrary decisions aimed primarily at reducing the number of independent design variables, then it represents a special type of basis reduction.

When the original mathematical programming problem stated in Eqs. (2.1) and (2.2) is restated in the  $\vec{\delta}$  subspace — that is, find  $\vec{\delta}$  such that

$$h_q(\vec{\delta}) \geq 0; \quad q = 1, 2, \dots, Q \quad (2.10)$$

and

$$W(\vec{\delta}) \rightarrow \text{Min} \quad (2.11)$$

then the number of independent design variables is substantially reduced. However, the number of constraints  $Q$  is still very large and most of the  $h_q(\vec{\delta})$  continue to be implicit functions of the design variables  $\vec{\delta}$ , requiring lengthy analysis computations.

#### 2.4 Reducing the Number of Constraints

The proper statement of structural synthesis problems often involves a large number of inequality constraints — both behavioral and side constraints. The large number of behavior constraints arises because it is usually necessary to guard against a wide variety of failure modes in each of several distinct loading conditions. Numerous side constraints are needed to introduce fabrication limitations and to restrict the search for an optimum design to the portion of the design space where the failure mode analyses adequately predict the structural behavior. The techniques suggested in this section for reducing the number of constraints are aimed at facilitating the computer implementation of traditional design practice. Basically it is recognized that during each stage of an iterative design process, only critical and potentially critical constraints need to be considered. The central idea is to temporarily ignore redundant and noncritical constraints that are not currently influencing the iterative design process significantly.

All the approximation concepts presented here in Chapter 2 are valuable in their own right and they can be used separately or in various combinations. For example, the constraint deletion techniques, to be described in this section, can be used separately or in conjunction with approximate analysis methods. Constraint deletion used by itself can usually reduce the overall computational effort, since gradient information need only be computed for the

constraints retained. However, reducing the number of constraints is much more effective when it is coupled with certain approximate structural analysis methods.

A general strategy for the combined use of constraint deletion techniques and approximate analysis methods may be outlined as follows. Carry out a complete structural analysis, after which a relatively small number of critical or potentially critical constraints are identified. These and only these constraints are retained and examined using an approximate analysis technique during a stage of the iterative design process. Each stage consists of the following steps:

- (1) Carry out a complete structural analysis.
- (2) Define the critical and potentially critical constraints.
- (3) Generate the information needed to construct approximate analyses.
- (4) Carry out a sequence of design modifications using the approximate analyses to examine only those constraints identified in (2) above.

Approximate analysis methods are discussed subsequently in Section 2.5.

#### 2.4.1 Regionalization

One approach to reducing the number of behavioral constraints has been called regionalization in Ref. 66. The essential idea can be conveniently explained in terms of static stress constraints. Let the finite element model of a structure be subdivided into several regions. Upon executing a complete structural analysis for each of several load conditions let attention be directed toward determining the most critical stress constraints within each region in each load condition. If the region contains various types of finite elements (e.g., bars, shear panels, constant strain triangles) it may

be desirable to retain one most critical stress constraint for each load condition and element type. The reduction of constraints by use of regionalization schemes hinges upon the assumption that the design changes made during a stage in the synthesis are not so drastic as to result in a shift of the critical constraint location within a region. If troublesome shifting does occur, it may be necessary to reduce the size of the regions.

An important specialization of the regionalization approach to reducing the number of stress constraints retained, is based on using design variable linking to define the regions. The idea is to simply let each group of finite elements controlled by a single independent design variable after linking constitute a region. If it is further assumed that each group of finite elements controlled by a single independent design variable contains elements of only one type (all bars or all shear panels or all constant strain triangles), then the number of stress constraints reduces to the product of the number of load conditions times the number of independent design variables after linking. This specialized form of the regionalization approach to constraint reduction (which is employed subsequently in Section 3) makes it unlikely that there will be a shift in the location of the critical stress constraints. This is because changes in the independent design variables lead primarily to redistributions of forces between regions rather than within regions. It may be noted in passing, that the location of the critical stress constraints would be completely invariant for the special case of a statically determinate structure.

The regionalization approach to reducing the number of response constraints can in principle be applied to other types of constraints. It may, for example, be anticipated that for each load condition the transverse

displacement distribution over a local planform region on a thin wing structure will not change shape during a stage of the iterative design process. Then, after executing a complete static structural analysis for each of several load conditions, it would be possible to identify the most critical transverse displacement constraint in the prespecified planform region for each load condition. Using this approach the number of transverse displacement constraints would reduce to the product of the number of planform regions times the number of load conditions.

#### 2.4.2 "Throw Away" Concept

Another way of reducing the number of constraints retained during any particular stage of an iterative redesign process can be colloquially referred to as the "throw away" concept. In this approach unimportant (redundant or very inactive) constraints are temporarily ignored. This technique, like several others described herein, is used extensively in conventional structural design practice. It is described here in terms of a structural synthesis problem involving multiple static load conditions with stress and displacement constraints. For any trial design  $\vec{\delta}$ , specified by the numerical values of the generalized design variables  $\delta_b$  after linking and/or basis reduction (see Eq. (2.7) and (2.9)), it is a straightforward matter to execute a finite element structural analysis which yields a complete set of displacement and stress results for K load conditions. Let  $Y_q(\vec{\delta})$  represent the  $q^{\text{th}}$  response quantity of interest. Limitations on the  $q^{\text{th}}$  response quantity can often be stated as follows

$$Y_q^{(-)} \leq Y_q(\vec{\delta}) \leq Y_q^{(+)} \quad (2.12)$$

where  $Y_q^{(-)} < 0$  represents the negative limit and  $Y_q^{(+)} > 0$  denotes the positive limit (e.g., the allowable compressive stress and the allowable tensile stress

in a truss member or the negative and positive deflection limits on a nodal displacement component). It is then useful to define a quantity called the response ratio as follows

$$R_q(\vec{\delta}) = \left\{ \begin{array}{ll} Y_q(\vec{\delta})/Y_q^{(+)} & \text{if } Y_q(\vec{\delta}) \geq 0 \\ Y_q(\vec{\delta})/Y_q^{(-)} & \text{if } Y_q(\vec{\delta}) < 0 \end{array} \right\} \quad (2.13)$$

As the response ratio approaches unity the associated behavior constraint becomes critical.. Response constraints can be expressed in terms of response ratios as follows:

$$h_q(\vec{\delta}) = 1 - R_q(\vec{\delta}) \geq 0 \quad (2.14)$$

It is usually advisable to treat the various types of constraints (e.g., stress, displacement, etc.) separately because it is often desirable to use distinct criteria for deleting different types of constraints. Suppose for example that a complete structural analysis provides the following stress and displacement results:

Stress Constraints			Displacement Constraints		
q	R <sub>q</sub>	h <sub>q</sub>	q	R <sub>q</sub>	h <sub>q</sub>
1	0.23	0.77	1	0.46	0.54
2	0.79	0.21	2	0.36	0.64
3	0.88	0.12	3	0.54	0.46
4	0.74	0.26	4	0.94	0.06
5	0.91	0.09	5	0.49	0.51
6	0.37	0.63	6	0.72	0.28
7	0.42	0.58			

According to the "throw away" concept, only those constraints that are critical or potentially critical are retained during a stage of the iterative design process. If it is decided to temporarily delete (a) those stress constraints

with response ratios less than 0.5 and (b) those displacement constraints with response ratios less than 0.70\*, then the following stress and displacement constraints are retained:

Stress Constraints			Displacement Constraints		
q	$R_q$	$h_q$	q	$R_q$	$h_q$
2	0.79	0.21	4	0.94	0.06
3	0.88	0.12	6	0.72	0.28
4	0.74	0.26			
5	0.91	0.09			

Various techniques can be used to decide upon cut-off values for the response ratios. Rather than the fixed values (0.5 and 0.7) used above, one may prefer to use a fractional value of the most critical constraint within a type (stress, displacement, etc.). It may also be useful to increase the response ratio cut-off values after completing each stage (up to some upper limit less than 1), since the set of critical and near critical constraints tends to stabilize as the iterative design process converges.

It is often desirable to arrange the constraints within each type in order of decreasing value of the response ratio. In Ref. 71 such an ordered list of response ratios was called a posture table. Posture tables are a convenient and useful form of output. Continuing with the example case, suppose that only those constraints with response ratios greater than 0.80 are to be printed out. The final reduced posture tables are

---

\* In many instances the redistribution of material during a stage in an iterative design process, has a more marked influence on the location of critical stress constraints than on the location of critical deflection constraints. Therefore, it is frequently reasonable to employ higher cut-off values for displacement constraints than for stress constraints.

Stress Constraints			Displacement Constraints		
q	$R_q$	$h_q$	q	$R_q$	$h_q$
5	0.91	0.09	4	0.94	0.06
3	0.88	0.12			

It should be noted that it is usually more efficient to first reduce the number of constraints using deletion criteria, and then prepare an ordered list of surviving constraints. Furthermore, since the primary purpose of posture tables is to facilitate output interpretation, it may be best to generate them after both regionalization and "throw away" have been used to reduce the number of constraints to be ordered.

#### 2.4.3 Two Step Reduction in the Number of Constraints

It should be recognized that regionalization and "throw away" can be used together to reduce the number of behavioral constraints retained during any particular stage of an iterative design procedure. When using both of these constraint reduction techniques the set of constraints retained is independent of the order in which these operations are carried out.

To illustrate this point consider the set of nine elements shown in Fig. 1. Assume that under a single load condition the equivalent stress response ratios  $R_i$ ,  $i = 1, 2, \dots, 9$  have the following values 0.80, 0.85, 1.00, 0.75, 0.40, 0.45, 0.80, 0.60 and 0.40, respectively. It is understood that the regions coincide with the four design variable linking groups depicted by dotted lines in Fig. 1 and specified by the specialized [L] matrix in Eq. 2.5. Reduction of the number of constraints applying "throw away" first and then regionalization is shown schematically in Fig. 2. It is seen that using a response ratio cut-off value of 0.5 leads to the deletion of three constraints and the subsequent application of regionalization eliminates three

additional constraints. On the other hand, Fig. 3 illustrates the application of regionalization followed by use of the "throw away" concept. Examining Fig. 3 it is observed that regionalization deletes five constraints and the subsequent application of "throw away" leads to the elimination of one additional constraint. After applying regionalization and "throw away," in either order the same three constraints are retained, namely  $R_2 = 0.85$ ,  $R_3 = 1.00$  and  $R_7 = 0.80$ .

The number of displacement constraints to be retained during a stage can also be reduced by using a two step process involving both regionalization and "throw away," applied in either order. However, in many instances the number of displacement constraints is reduced enough by applying only the "throw away" concept, using a relatively large response ratio cut-off value (e.g., 0.7).

Assuming that only design variable linking has been used to reduce the number of independent design variables, side constraints on the original set of design variables  $D_i$ , expressed as

$$D_i^{(L)} \leq D_i \leq D_i^{(U)} ; \quad i = 1, 2, \dots, I \quad (2.15)$$

can be reduced to

$$\gamma_c^{(L)} \leq \gamma_c \leq \gamma_c^{(U)} ; \quad c = 1, 2, \dots, C \quad (2.16)$$

in which  $C < I$ . For the case of simple design variable linking the minimum and maximum member size constraints for all members linked to a single variable  $\gamma_c$  are parallel, and, therefore, it is a straightforward matter to permanently eliminate all the redundant side constraints. This reduces the number of side constraints from  $2I$  to  $2C$ . It is also possible to envision a further reduction by applying the "throw away" technique to the  $2C$  surviving side constraints.

At this point it is clear that approximation concepts are available for drastically reducing both the number of design variables (through linking and basis reduction) and the number of inequality constraints (through regionalization and "throw away") needed to adequately represent the synthesis problem during each stage of an iterative design process. Still, the remaining constraints could require many lengthy analysis computations. Therefore, attention is now directed to various methods of approximate structural analysis.

## 2.5 Reducing the Number of Detailed Structural Analyses

The function of an approximate structural analysis is to rapidly estimate the behavioral response of modified designs during a stage in an iterative design process. Approximate analyses are generally constructed using (a) information obtained during the detailed analysis carried out at the beginning of a stage and (b) special information needed to set up the approximate analysis (e.g., partial derivatives of response quantities with respect to design variables). When an approximate analysis method is used on conjunction with constraint reduction techniques (see Section 2.4) attention can be focused on constructing approximations for only those constraints that survive the deletion process.

Three basic types of approximate analysis will be discussed; namely, iterative techniques, reduced basis methods and the construction of explicit approximations. The explicit approximation methods lead to algebraic expressions for the surviving constraints as functions of the independent design variables and therefore they are particularly powerful in the optimization context. While the three approaches to approximate structural analysis to be discussed are rather general, it will be useful to explain them here using illustrations based on static structural analysis in the displacement method context.

### 2.5.1 Iterative Methods

Iterative methods of structural analysis are characterized by the fact that they can make effective use of information available from previously expended analysis effort and the convergence criteria can be varied to control the quality of the approximation. For example consider the linear static structural analysis problem

$$[K] \vec{u}_k = \vec{P}_k \quad (2.17)$$

where  $[K]$  is the system stiffness matrix, and  $\vec{u}_k$  represents the displacement response under load condition  $\vec{P}_k$  (for simplicity assume that  $\vec{P}_k$  is independent of the design variables). Let it be understood that Eq. (2.17) has been solved for  $\vec{u}_k$  and assume the results of the  $[\mathcal{L}] [\mathcal{D}] [\mathcal{L}]^T$  decomposition of  $[K]$  are saved. When the design is changed the governing analysis equation becomes

$$[K + \Delta K] (\vec{u}_k + \Delta \vec{u}_k) = \vec{P}_k \quad (2.18)$$

Then rearranging terms Eq. (2.18) can be written as

$$[K] (\vec{u}_k + \Delta \vec{u}_k) = \vec{P}_k - [\Delta K] (\vec{u}_k + \Delta \vec{u}_k) \quad (2.19)$$

which suggests the iterative analysis scheme

$$[K] (\vec{u}_k + \Delta \vec{u}_k)_{s+1} = \vec{P}_k - [\Delta K] (\vec{u}_k + \Delta \vec{u}_k)_s \quad (2.20)$$

with  $(\vec{u}_k + \Delta \vec{u}_k)_1 = \vec{u}_k$  the solution obtained from Eq. (2.17). It may be noted in passing, that the first cycle using Eq. (2.20) corresponds to the so-called "dummy load method," which is often used when dealing with arbitrary but small changes in the design variables. It is interesting to note that the linear displacement method of structural analysis used in the structural synthesis capability reported in Ref. 22 employed successive over relaxation. More recently, in Ref. 53 iterative methods were used to update vibration modes and

solutions of the flutter determinant. In summary then, iterative methods which may not be appropriate for a single analysis, because they must start with a good estimate of the solution, become more attractive when several analyses are to be executed in the course of a design optimization procedure.

### 2.5.2 Reduced Basis Concept for Analysis

Another approach to improving overall design optimization efficiency via the use of approximate analyses will be referred to as the reduced basis approach in analysis variable space. The number of analysis unknowns (e.g., displacement degrees of freedom or redundants) required to adequately predict behavior, for the purpose of guiding a stage in an iterative design process, is frequently less than the number arising from the idealization and discretization decisions. In dynamic structural analysis it is common practice to use static condensation and normal modes to achieve a two step reduction in the number of independent displacement degrees of freedom. It should be noted that both of these ideas have been employed to facilitate rapid reanalysis in Ref. 52.

The basic idea of constructing an approximate analysis solution using a linear combination of a few well chosen vectors can be applied in a variety of ways. For example, in the case of static structural analysis, the reduced basis approach can be employed in conjunction with either the force or the displacement method of analysis. If a set of  $J_r$  independent analysis vectors is available ( $J_r < J$  where  $J$  is the number of unknown analysis variables arising from the idealization and discretization), then the vector of analysis unknowns can be approximated as a linear combination of these  $J_r$  known vectors. The undetermined participation coefficients for each of the  $J_r$  known vectors become the unknowns of the approximate analysis. Substituting the approximate representation into an appropriate energy formulation and taking the stationary

condition leads to a set of  $J_r$  simultaneous equations that can be solved for the participation coefficients.

In the context of the finite element displacement method of structural analysis, the approximate displacement response can be represented by  $\vec{u}$ ; that is - let

$$\vec{u} \approx \vec{u} = \sum_{v=1}^{J_r} v_v \vec{u}_v = [B] \vec{v} \quad (2.21)$$

where the  $v_v$  are the participation coefficients, the  $\vec{u}_v$  denote the base vectors and  $[B]$  is a transformation matrix with columns corresponding to the  $\vec{u}_v$  vectors. The total potential energy is given by

$$\Pi = \frac{1}{2} \vec{u}^T [K] \vec{u} - \vec{u}^T \vec{P} \quad (2.22)$$

or expressed approximately in terms of  $\vec{v}$  (see Eq. (2.21)).

$$\Pi \approx \tilde{\Pi} = \frac{1}{2} \vec{v}^T [B]^T [K] [B] \vec{v} - \vec{v}^T [B]^T \vec{P} \quad (2.23)$$

Setting the stationary condition of  $\tilde{\Pi}$  with respect to the  $v_v$ ,  $v = 1, 2, \dots, J_r$  equal to zero yields

$$\delta \tilde{\Pi} = \delta \vec{v}^T \{ [B]^T [K] [B] \vec{v} - [B]^T \vec{P} \} = 0 \quad (2.24)$$

and this requires that

$$[B]^T [K] [B] \vec{v} = [B]^T \vec{P} \quad (2.25)$$

which represents a set of  $J_r$  simultaneous equations that can readily be solved for the  $v_v$ ;  $v = 1, 2, \dots, J_r$ . The potential of the reduced basis approach as a method of approximate static structural analysis has been demonstrated in Ref. 44 (force method context) and in Ref. 48 (displacement method context). More recently (Ref. 49) a modified reduced basis technique has been suggested in which the displacement response is approximated using a linear combination of  $(B+1)$  normalized base vectors as follows

$$\vec{u} \approx \vec{u} = v_{B+1} \vec{e}_{B+1} + \sum_{b=1}^B v_b \vec{e}_b \quad (2.26)$$

where

$$\vec{e}_{B+1} = \vec{u}(\vec{\delta}_p) / |\vec{u}(\vec{\delta}_p)| \quad (2.27)$$

represents the normalized form of the displacement solution for the design at the beginning of the  $p^{\text{th}}$  stage (i.e.  $\vec{\delta}_p$ ) and

$$\vec{e}_b = \frac{\partial \vec{u}}{\partial \delta_b}(\vec{\delta}_p) / \left| \frac{\partial \vec{u}}{\partial \delta_b}(\vec{\delta}_p) \right| \quad (2.28)$$

represents the normalized form of the first partial derivative of the displacement response  $\vec{u}$  with respect to the independent design variable  $\delta_b$  evaluated for the design  $\vec{\delta}_p$ . This modified reduced basis technique appears to be especially well suited to problems where the number of design variables has been reduced by design variable linking.

### 2.5.3 Explicit Approximations

The basic objective in this approach to approximate structural analysis is to obtain high quality algebraically explicit expressions for the behavioral constraints, that have survived the deletion process. These explicit approximations of the constraints retained, are used in place of the detailed analysis during a stage in the iterative design process.

Various techniques can be used to construct explicit constraint approximations. For example, in the structural synthesis of components, such as stiffened panels, it is often possible to represent various buckling constraints explicitly, except for the values of one (or more) coefficients that must be determined by using a more sophisticated (and computationally burdensome) stability analysis procedures. In this type of bilevel analysis procedure the algebraic form of the explicit constraints follow from a simplified

(level 1) analysis while certain key coefficients in these expressions are obtained from a more refined stability analysis (level 2) which is carried out only at the beginning of each stage in the iterative design process.

Another way of constructing explicit approximations of retained constraints is through the use of Taylor series expansions. For example consider a simple stress constraint of the following form

$$h_q(\vec{\delta}) = 1 - \frac{\sigma(\vec{\delta})}{\sigma_a} \geq 0. \quad (2.29)$$

Assuming the allowable stress  $\sigma_a$  is a given constant, an explicit approximation of this constraint can be constructed by expanding  $\sigma(\vec{\delta})$  in a first order Taylor series about the current trial design  $\vec{\delta}_p$ , that is

$$\sigma(\vec{\delta}) \approx \tilde{\sigma}^{(p)}(\vec{\delta}) = \sigma(\vec{\delta}_p) + \sum_{b=1}^B (\delta_b - \delta_{pb}) \frac{\partial \sigma}{\partial \delta_b}(\vec{\delta}_p) + \dots \quad (2.30)$$

Substituting the linear approximation for  $\sigma(\vec{\delta})$  given by Eq. 2.30 into Eq. 2.29 yields the following explicit approximation for the corresponding constraint, namely

$$h_q(\vec{\delta}) \approx \tilde{h}_q^{(p)}(\vec{\delta}) = 1 - \frac{1}{\sigma_a} \left\{ \sigma(\vec{\delta}_p) + \sum_{b=1}^B (\delta_b - \delta_{pb}) \frac{\partial \sigma}{\partial \delta_b}(\vec{\delta}_p) \right\} \quad (2.31)$$

The construction of first order Taylor series approximations requires the evaluation of first partial derivatives [e.g.  $\frac{\partial \sigma}{\partial \delta_b}(\vec{\delta})$ ]. It is also possible to construct more accurate approximations by retaining quadratic and/or higher order terms in Taylor series expansions. However, the computational burden of evaluating the higher derivatives needed to construct such expressions is substantial.

In order to improve the quality of explicit approximations, while maintaining good computational efficiency, it is important to bring available

insight regarding structural behavior to bear. This can often be done by carefully selecting response quantities ( $\vec{Y}$ ) and intermediate design variables ( $\vec{Z}$ ). Consider a behavioral constraint

$$h_q(\vec{Y}) \geq 0 \quad (2.32)$$

and assume that it is an explicit function of several response quantities ( $\vec{Y}$ ). For example, the requirement that the displacement at a node point remain within a sphere of given radius  $u_a$  would be expressed as

$$h_q(\vec{Y}) = u_a^2 - u_x^2 - u_y^2 - u_z^2 \geq 0 \quad (2.33)$$

where  $u_x$ ,  $u_y$  and  $u_z$  are in this instance the pertinent response quantities.

Now let it be understood that each of the response quantities  $Y_q$  is to be expanded in a Taylor series as function of some well chosen intermediate variables ( $\vec{Z}$ ) that are explicitly related to the independent design variables  $\vec{\delta}$ . Expanding  $Y_q$  as a function of  $\vec{Z}$  about the point  $\vec{Z}_p$  corresponding to the current design  $\vec{\delta}_p$  gives

$$\begin{aligned} Y_q(\vec{Z}) \approx \tilde{Y}_q(\vec{Z}) &= Y_q(\vec{Z}_p) + (\vec{Z} - \vec{Z}_p)^T \nabla Y_q(\vec{Z}_p) \\ &+ \frac{1}{2} (\vec{Z} - \vec{Z}_p) \left[ \frac{\partial^2 Y_q}{\partial Z_i \partial Z_j}(\vec{Z}_p) \right] (\vec{Z} - \vec{Z}_p) + \dots \end{aligned} \quad (2.34)$$

It is important to give careful consideration to the selection of intermediate variables  $\vec{Z}$ . In many situations of practical importance it should be possible to select the  $Z_b(\vec{\delta})$ ;  $b = 1, 2, \dots, B$  such that a high quality approximation will be obtained, even when only the linear term in Eq. (2.34) is retained. For example, it is easily shown that for statically determinate structures idealized by bar, shear panel, and constant strain triangular membrane elements both the stress and the displacement response are strictly linear in variables

that are the reciprocals of the usual sizing design variables (i.e., bar cross sectional areas, shear panel and membrane thicknesses). This suggests that for moderately indeterminate structures in this class, the quality of linear approximations for both stress and displacement response will be enhanced by using reciprocal variables, that is by letting

$$Z_b = 1/\delta_b ; \quad b = 1, 2, \dots, B \quad (2.35)$$

Assume for the purpose of illustration that the spherical displacement constraint represented by Eq. (2.33) applies at a node point on a structure that can be idealized using bar, shear panel and constant strain membrane triangles. Further assume that only sizing type design variables are considered. Then retaining only linear terms in Eq. (2.34) and using reciprocal design variables the response quantity  $u_x$  in Eq. (2.33) can be expressed approximately as

$$u_x(\vec{Z}) \approx \tilde{u}_x(\vec{Z}) = u_x(\vec{Z}_p) + \sum_{b=1}^B (Z_b - Z_{pb}) \frac{\partial u_x}{\partial Z_b}(\vec{Z}_p) \quad (2.36)$$

or replacing  $Z_b$  with  $1/\delta_b$  (see Eq. (2.35))

$$u_x(\vec{\delta}) \approx \tilde{u}_x(\vec{\delta}) = c_x + \sum_{b=1}^B \frac{K_{xb}}{\delta_b} \quad (2.37)$$

where

$$c_x = u_x(\vec{Z}_p) - \sum_{b=1}^B Z_{pb} \frac{\partial u_x}{\partial Z_b}(\vec{Z}_p) \quad (2.38)$$

and

$$K_x = \frac{\partial u_x}{\partial Z_b}(\vec{Z}_p) \quad (2.39)$$

It is apparent that explicit approximations corresponding to Eq. (2.37) can be obtained for  $u_y(\vec{\delta})$  and  $u_z(\vec{\delta})$ . Then upon substituting these explicit

approximations for  $u_x(\vec{\delta})$ ,  $u_y(\vec{\delta})$  and  $u_z(\vec{\delta})$  into Eq. (2.33) the following explicit approximation for the spherical displacement constraint is obtained

$$h_q(\vec{\delta}) \approx \tilde{h}_q(\vec{\delta}) = u_a^2 - \left( c_x + \sum_{b=1}^B \frac{K_{xb}}{\delta_b} \right)^2 - \left( c_y + \sum_{b=1}^B \frac{K_{yb}}{\delta_b} \right)^2 - \left( c_z + \sum_{b=1}^B \frac{K_{zb}}{\delta_b} \right)^2 \geq 0 \quad (2.40)$$

The foregoing discussion illustrates the flexibility of the explicit approximations approach to constructing algebraic expressions for the surviving inequality constraints, at any stage during an iterative design procedure. As described herein, the use of selected response quantities and intermediate design variables can often enhance the quality of the explicit approximations obtained.

It should be clearly recognized that the direct application of the Taylor series expansion technique to the constraint functions  $h_q(\vec{\delta})$  does not necessarily yield high quality explicit approximations. Frequently, it will be desirable to try and preserve the explicit nonlinearities that are apparent when the constraint functions are viewed as functions of the response quantities (e.g., see Eq. 2.33). Furthermore, the use of physical insight in selecting intermediate design variables (e.g., see Eq. 2.35) is generally worthwhile. It should also be noted that in some cases it will be desirable to carry out the optimization in  $\vec{Z}$  space rather than in  $\vec{\delta}$ . For example, if many or all of the approximate constraint functions can be expressed as linear functions of the  $\vec{Z}$  variables it may well prove attractive to express the objective function in terms of the variables  $\vec{Z}$  and then select an algorithm that takes advantage of the fact that most or all of the constraints considered during a particular stage have been made linear.

#### 2.5.4 Combining Approximate Analysis Methods

In principle it is possible to use various combinations of the three approaches to approximate analysis discussed. It is possible for example to envision the use of iterative methods in an analysis problem that has been simplified by employing reduced basis approximations in analysis variable space. This could then be followed by the generation of Taylor series approximations for the generalized displacement degrees of freedom that are the unknowns in the reduced basis analysis. It may be noted that the reduced basis method in analysis space examined in Ref. 49 (see Eqs. (2.26), (2.27) and (2.28)) may be viewed as a combined Taylor series-reduced basis method of approximate structural analysis.

#### 2.6 Summary — A Tractable Formulation

In any event it is evident at this juncture that a wide variety of approximation concepts exist and they can be innovatively employed to construct a sequence of tractable formulations, that adequately represent the essential features, of the class of structural design optimization problems stated by Eqs. (2.1) and (2.2).

In summary the basic problem, during each stage of the iterative design process, is made tractable by: (a) reducing the number of design variables through linking and/or basis reduction; (b) reducing the number of constraints via regionalization and "throw away", and (c) by constructing algebraically explicit approximations for the surviving constraints as functions of the design variables. The original mathematical programming problem (see Eq. (2.1) and (2.2)) has been reduced to a sequence of small and explicit problems of the form find  $\vec{\delta}$  such that

$$h_q(\vec{\delta}) \approx \tilde{h}_q^{(p)}(\vec{\delta}) \geq 0; \quad q \in Q_R^{(p)} \quad (2.41)$$

and

$$W(\vec{\delta}) \rightarrow \text{Min} \tag{2.42}$$

where it is understood that  $W(\vec{\delta})$  and the  $\tilde{h}_q^{(p)}(\vec{\delta})$  are explicit but not necessarily linear functions of the generalized design variables  $\vec{\delta}$ .

### 3. A NEW STRUCTURAL SYNTHESIS CAPABILITY

#### 3.1 Introduction

In this section, the technical foundations of the ACCESS\* 1 computer program are described. This program combines finite element and mathematical programming methods to form an efficient minimum weight optimum design capability for a significant class of structural synthesis problems. Attention is focused on two and three dimensional structural systems, made from isotropic materials that can be idealized using truss, triangular membrane and shear panel elements. Multiple static loading conditions are considered and stress, displacement and member size constraints are included.

Several of the approximation concepts described in Section 2 have been used in concert to develop this new capability. Design variable linking is employed to reduce the number of independent design variables. At each stage during the iterative design process the number of stress constraints is reduced by a specialized regionalization scheme, defined by finite element groups linked to the independent design variables. The number of stress constraints is further reduced using the "throw away" concept. The number of displacement constraints considered during each stage is reduced by temporarily deleting displacement constraints that are neither critical nor potentially critical. Strictly redundant side constraints are permanently deleted. The number of side constraints is reduced further by applying the "throw away" concept. First order Taylor series expansions of the displacement and stress response quantities, in terms of linked reciprocal variable, are used to construct explicit linear approximations of the surviving inequality constraints. The objective function expressed in terms of the linked reciprocal variables is nonlinear but explicit.

---

\* Approximation Concepts Code for Efficient Structural Synthesis

The finite element structural analysis is organized so as to take advantage of design variable linking and element configuration grouping, while at the same time facilitating the implementation of selective sensitivity analysis, discussed subsequently. If there are several finite elements of the same type (bars or shear panels or constant strain membrane triangles) having identical configuration and material properties, which may have different size (cross sectional area or thickness) and orientation in space, then these elements are said to belong to the same configuration group. The analysis is also organized so as to keep storage demands reasonable while at the same time facilitating the implementation of selective sensitivity analysis.

At the beginning of each stage of the synthesis a detailed structural analysis is carried out, and a complete set of structural response ratios is computed. This information is then used to identify the critical and potentially critical stress, displacement and side constraints to be retained during the upcoming stage of the design process. Explicit approximate representations are only generated for this reduced set of behavior constraints. These explicit approximations are constructed by expressing appropriate displacement and stress response quantities as linear functions of the linked reciprocal design variables using first order Taylor series expansions about the current design point. By using a reciprocal variable formulation the high quality of the first order Taylor series approximations for stress and displacement responses is assured. Only those partial derivatives needed to set up Taylor series approximations are evaluated — a feature called selective sensitivity analysis. It is noted that these partial derivatives are calculated directly with respect to the reduced set of design variables, which is more efficient than evaluating the partial derivatives with respect to the prelinked design variables and then applying the appropriate transformation.

The optimization phase of ACCESS 1 is modular. In current versions of ACCESS 1 optimization is carried out by either CONMIN (an optimization program package based on a modified feasible directions method, see Ref. 68) or NEWSUMT (a sequence of unconstrained minimizations technique based on an extended interior penalty function formulation (see Ref. 75) and a modified Newton method minimizer (see Ref. 53)).

### 3.2 Scope and Limitations

The structural synthesis capability to be described subsequently in Section 3.3 may be viewed as a pilot program aimed at demonstrating the feasibility of developing general purpose, large-scale, finite element structural synthesis capabilities that are practical and efficient. It is assumed that the topological form, the geometric configuration, and the structural materials to be employed are preassigned parameters. Attention is focused on two and three dimensional structural systems that can be idealized using the following three types of finite elements: truss elements of uniform cross sectional area (TRUSS), isotropic constant strain triangular membrane elements of uniform thickness (CST), and isotropic symmetric shear panel elements of uniform thickness (SSP).<sup>\*</sup> The basic assumptions and the resulting local stiffness matrices for these three finite element types are given in Appendix A for completeness. The physically significant design variables are understood to be the cross section areas of TRUSS elements and the thicknesses of CST and SSP elements. The number of independent design variables is reduced using design variable linking only. Design variable linking is limited to prespecified groups of finite elements that are all of the same type (e.g., all (TRUSS),

---

<sup>\*</sup>This type of element differs from the usual shear panel element in that it carries bending as well as shear loads. It is particularly useful for modeling midsurface symmetric thin wing structures because it permits uncoupling the wing inplane displacement response from the wing bending and twisting behavior.

all (CST), etc.). The given initial sizes are used to establish the fixed relative sizes for finite elements in a linked group. Finite element stiffness matrices for unit design variable values, expressed in the local coordinate system, are computed once and stored. In order to save storage space, element configuration groups are defined at the outset. Finite elements in a configuration group are of the same type, and they have (essentially)\* identical configuration and material properties. Then for unit values of the element sizing variables all elements in a configuration group have the same (unit) local stiffness matrix. Therefore it is only necessary to generate and store one (unit) local stiffness matrix for each configuration group.

Multiple distinct static loading conditions are considered. These loading conditions are taken to be independent of the design variables. Loadings that depend on the design variables (e.g., self-weight, temperature change, and static aeroelastic effects) are not treated herein. Each loading condition can include specified applied loads (expressed in the reference coordinate system) corresponding to each independent displacement degree of freedom. Uniform pressure distributions acting normal to the surface of CST elements may also be specified. These pressure loading are converted into work equivalent nodal loading expressed in the reference coordinate system.

Stress and displacement constraints are considered under each of several distinct static loading conditions. Separate upper and lower limits may be placed on each independent displacement component (expressed in the reference coordinate system). The limits on each displacement component are assumed to be the same for all loading conditions. Independent upper and lower axial

---

\* For thin wing applications CST elements having identical projections on the wing middle surface are assumed to be in the same configuration group.

stress limitations  $[\sigma_i^{(U)}, \sigma_i^{(L)}]$  may be specified for TRUSS elements. For CST and SSP elements an upper limit ( $\sigma_{ai}$ ) is placed on the Von Mises equivalent stress  $\sigma_{eik}$  defined by

$$\sigma_{eik} = \left( \sigma_{xik}^2 + \sigma_{yik}^2 - \sigma_{xik}\sigma_{yik} + 3\tau_{xyik}^2 \right)^{1/2} \leq \sigma_{ai} \quad (3.1)$$

where the subscript i refers to the element and the subscript k refers to the load condition. The limiting stress values ( $\sigma_{ai}$ ) are assumed to be the same for each loading condition and they are taken to be the same for all finite elements in an element configuration group. It should be noted that the SSP elements include a uniform shear stress as well as normal stress distributions of the form  $\sigma_x = cy$  and  $\sigma_y = 0$  where c is a constant. In addition to these behavioral constraints, minimum and maximum member sizes (cross sectional areas for TRUSS elements and thicknesses for CST and SSP elements) can be specified for each finite element.

The objective function is taken to be the total weight of the finite element idealization. For the limited class of finite elements included in ACCESS 1, the objective function is a linear in the regular sizing type design variables such as thicknesses and cross sectional areas of the finite elements. As noted earlier, however, it is found advantageous to formulate the optimization problem in terms of linked reciprocal design variables, hence the objective function becomes nonlinear but remains explicit.

There are six operational versions of the ACCESS 1 computer program and none of them employ secondary storage. The primary storage capacity required depends upon the optimizer chosen (CONMIN or NEWSUMT) and the sizes of the declared arrays in the program. The primary storage requirements for the six operational versions of ACCESS 1 are summarized in Table 1. The largest

problem that can currently be accommodated would involve 300 finite elements (100 of each type), 300 displacement degrees of freedom, 120 design variables and 5 distinct loading conditions. It is noted that the effective overlay of programs and arrays as well as the judicious use of auxiliary storage should permit future growth of maximum problem size.

### 3.3 Description of ACCESS 1

The ACCESS 1 computer program is a new type of structural synthesis capability based on the coordinated use of several approximation concepts drawn from those discussed in Section 2. The approximation concepts employed in creating the ACCESS 1 computer program are: (1) design variable linking, (2) temporary constraint deletion by regionalization and "throw away" and (3) construction of explicit approximations for retained constraint functions in terms of linked reciprocal design variables.

The description presented in this Section begins with a detailed formulation of the general class of problems treated (see Section 3.3.1). The formulation is then restated, casting it in terms of linked reciprocal design variables and normalized inequality constraints. The basic organization of the ACCESS 1 computer program is outlined (see Section 3.3.2) using the conceptual block diagram shown in Fig. 4. The input data required by ACCESS 1 are enumerated in Section 3.3.3. This is followed by descriptions of the four main parts of the ACCESS 1 program, they are: (1) the preprocessor (Section 3.3.4), (2) the design process control block, (Section 3.3.5), (3) the approximate problem generator, (Section 3.3.6) and (4) the optimization algorithm(s), (Section 3.3.7).

#### 3.3.1 Formulation

The basic structural synthesis problem dealt with by ACCESS 1 will now be formulated in detail. Let  $\vec{D}$  represent the original set of sizing variables.

It will be useful to give separate identity to the design variables for: TRUSS members  $\vec{A}$ , CST elements  $\vec{t}$ , and SSP elements  $\vec{\tau}$ . It is to be understood that  $\vec{D}$  represents all of the original design variables — the cross sectional areas  $\vec{A}$  and the thicknesses  $\vec{t}$  and  $\vec{\tau}$ . Let  $u_{jk}(\vec{D})$  denote the  $j^{\text{th}}$  displacement degree of freedom under the  $k^{\text{th}}$  loading condition. The upper and lower limits on  $u_{jk}(\vec{D})$  are represented by  $u_j^{(U)}$  and  $u_j^{(L)}$  respectively. Note that these limits are assumed to be the same for all  $K$  load conditions. Let  $\sigma_{ik}(\vec{D})$  denote the axial stress in the truss element  $i$  under load condition  $k$ . The upper and lower stress limits for truss element  $i$  are represented by  $\sigma_i^{(U)}$  and  $\sigma_i^{(L)}$  respectively. These stress limits are also assumed to be the same for all  $K$  load conditions. The Von Mises equivalent stress in either CST or SSP elements is represented by  $\sigma_{eik}(\vec{D})$  (see Eq. (3.1)) and the corresponding allowable stress  $\sigma_{ai}$  is also taken to be the same for all  $K$  load conditions. It is also understood that:  $A_i$  denotes the cross sectional area of truss member  $i$ ,  $t_i$  denotes the thickness of CST element  $i$ , and  $\tau_i$  represents the thickness of SSP element  $i$ . Furthermore, the superscripts (L) and (U) on  $A_i$ ,  $t_i$ , and  $\tau_i$  denote the minimum and maximum member size limitations. Finally, let  $I_T$ ,  $I_C$  or  $I_S$  denote the set of integers identifying respectively all TRUSS, CST or SSP elements making up the structural idealization. The basic structural synthesis problem dealt with by ACCESS 1 can be stated as follows:

Given the preassigned parameters and the load conditions;

Find

$$\vec{D}^T = [\vec{A}^T, \vec{t}^T, \vec{\tau}^T] \quad (3.2)$$

such that

$$u_j^{(L)} \leq u_{jk}(\vec{D}) \leq u_j^{(U)} ; j \in J_u ; k = 1, 2, \dots, K \quad (3.3)$$

$$\sigma_i^{(L)} \leq \sigma_{ik}(\vec{D}) \leq \sigma_i^{(U)} ; i \in I_T ; k = 1, 2, \dots, K \quad (3.4)$$

$$\sigma_{eik}^{(D)} \leq \sigma_{ai}; \quad i \in I_C \text{ and } I_S; \quad k = 1, 2, \dots, K \quad (3.5)$$

$$A_i^{(L)} \leq A_i \leq A_i^{(U)}; \quad i \in I_T \quad (3.6)$$

$$t_i^{(L)} \leq t_i \leq t_i^{(U)}; \quad i \in I_C \quad (3.7)$$

$$\tau_i^{(L)} \leq \tau_i \leq \tau_i^{(U)}; \quad i \in I_S \quad (3.8)$$

and the weight or objective function

$$\sum_{i \in I_T} \rho_i \ell_i A_i + \sum_{i \in I_C} \rho_i S_i t_i + \sum_{i \in I_S} \rho_i s_i \tau_i \quad (3.9)$$

is minimized, where it is understood that

- $J_u$  = the set of integers identifying the constrained independent displacement degrees of freedom,
- $K$  = the total number of load conditions,
- $\rho_i$  = the material weight density for the  $i^{\text{th}}$  finite element,
- $\ell_i$  = the length of truss element  $i$ ,
- $S_i$  = the surface area of CST element  $i$ , and
- $s_i$  = the surface area of SSP element  $i$ .

Before proceeding further, it will be useful to make a change of variables to a linked and normalized reciprocal variable formulation. As a point of departure, consider the most general change of variable discussed in Section 2.3.3 namely that represented by Eq. (2.9)

$$D_i = \sum_{b=1}^B T_{ib} \delta_b \quad (3.10)$$

Specializing this expression to the case where only design variable linking is employed to reduce the number of independent design variables gives

$$D_i = T_{ib(i)} \delta_{b(i)} \quad (3.11)$$

where the  $T_{ib(i)}$  are taken to be the values of  $D_i$  at the beginning of a particular stage in the design procedure and it is understood that the initial values of the  $\delta_{b(i)}$  for the stage are all 1.0. Note that the subscript  $b(i)$  denotes an integer element of a pointer vector  $\vec{b}$  which, given the value of  $i$  identifies the independent variable  $b$  to which the size of the finite element  $i$  is linked. To introduce the reciprocal variables, it is convenient to define the following notation:

$$\beta_i = \frac{1}{D_i} = \text{reciprocal of the sizing variable for element } i;$$

$$\alpha_{b(i)} = \frac{1}{\delta_{b(i)}} = \text{reciprocal of the } b^{\text{th}} \text{ independent variable after linking};$$

and

$$T_{ib(i)}^{(r)} = \frac{1}{T_{ib(i)}} = \text{the reciprocal of } D_i \text{ at the beginning of the current stage in the design procedure.}$$

With this notation Eq. (3.11) can be rewritten as

$$\frac{1}{\beta_i} = \frac{1}{T_{ib(i)}^{(r)}} \frac{1}{\alpha_{b(i)}} \quad (3.12)$$

which is equivalent to

$$\frac{1}{D_i} = \beta_i = T_{ib(i)}^{(r)} \alpha_{b(i)} \quad (3.13)$$

Introducing the change of variable represented by Eq. (3.13), at the beginning of each stage in the design procedure, reduces the number of variables via linking and introduces normalized reciprocal variables  $\vec{\alpha}$ . The term "normalized" is used here for the following reason. At the beginning of each stage, the  $T_{ib(i)}$  and  $\alpha_{b(i)}$  are redefined in such a way that the  $\alpha_{b(i)}$  are reinitialized to 1.0. This renormalization insures that all the variables  $\alpha_{b(i)}$  are of

the same order of magnitude which, in some cases, helps to reduce numerical problems in optimization algorithms. It should be recognized that while reciprocal design variables  $[\alpha_{b(1)}]$  are renormalized at the beginning of each stage, the design variable linking is invariant from stage to stage.

The basic problem statement embodied in Eq. (3.2) through (3.9) is now restated in terms of the linked reciprocal variables with the inequality constraints normalized as shown:

Find  $\vec{\alpha}$

such that

$$2[u_j^{(U)} - u_{jk}(\vec{\alpha})]/[u_j^{(U)} - u_j^{(L)}] \geq 0 \quad (3.14)$$

$$j \in J_U; \quad k=1,2,\dots,K$$

$$2[u_{jk}(\vec{\alpha}) - u_j^{(L)}]/[u_j^{(U)} - u_j^{(L)}] \geq 0 \quad (3.15)$$

$$j \in J_U; \quad k=1,2,\dots,K$$

$$2[\sigma_i^{(U)} - \sigma_{ik}(\vec{\alpha})]/[\sigma_i^{(U)} - \sigma_i^{(L)}] \geq 0 \quad (3.16)$$

$$i \in I_T; \quad k=1,2,\dots,K$$

$$2[\sigma_{ik}(\vec{\alpha}) - \sigma_i^{(L)}]/[\sigma_i^{(U)} - \sigma_i^{(L)}] \geq 0 \quad (3.17)$$

$$i \in I_T; \quad k=1,2,\dots,K$$

$$1 - (\sigma_{eik}(\vec{\alpha})/\sigma_{ia}) \geq 0; \quad i \in I_C \text{ and } I_S \quad k=1,2,\dots,K \quad (3.18)$$

$$1 - (\alpha_b/\alpha_b^{(U)}) \geq 0; \quad b=1,2,\dots,B \quad (3.19)$$

where

$$\alpha_b^{(U)} = \left\{ \begin{array}{l} \text{Min}_{i \in I_T} (T_{ib(i)} / A_i^{(L)}) ; \quad b \in B_T \\ \text{Min}_{i \in I_C} (T_{ib(i)} / t_i^{(L)}) ; \quad b \in B_C \\ \text{Min}_{i \in I_S} (T_{ib(i)} / \tau_i^{(L)}) ; \quad b \in B_S \end{array} \right\} \quad (3.20)$$

$$(\alpha_b^{(U)} / \alpha_b^{(L)}) - 1 \geq 0; \quad b=1,2,\dots,B \quad (3.21)$$

where

$$\alpha_b^{(L)} = \left\{ \begin{array}{l} \text{Max}_{i \in I_T} (T_{ib(i)} / A_i^{(U)}) ; \quad b \in B_T \\ \text{Max}_{i \in I_C} (T_{ib(i)} / t_i^{(U)}) ; \quad b \in B_C \\ \text{Max}_{i \in I_S} (T_{ib(i)} / \tau_i^{(U)}) ; \quad b \in B_S \end{array} \right\} \quad (3.22)$$

and

$$W(\vec{\alpha}) = \sum_{b \in B_T} \frac{C_b}{\alpha_b} + \sum_{b \in B_C} \frac{C_b}{\alpha_b} + \sum_{b \in B_S} \frac{C_b}{\alpha_b} \rightarrow \text{Min} . \quad (3.23)$$

Note that  $B_T$ ,  $B_C$  and  $B_S$  denote sets of integers identifying the linked reciprocal variables ( $\alpha_b$ ) that, respectively, control TRUSS, CST and SSP element sizes. Furthermore, the constants  $C_b$  in Eq. (3.23) are given by

$$C_b = \left\{ \begin{array}{l} \sum_{i, b(i)=b} \rho_i^{L_i} T_{ib(i)} ; \quad b \in B_T \\ \sum_{i, b(i)=b} \rho_i^{S_i} T_{ib(i)} ; \quad b \in B_C \\ \sum_{i, b(i)=b} \rho_i^{S_i} T_{ib(i)} ; \quad b \in B_S \end{array} \right\} . \quad (3.24)$$

Upon examination, it is apparent that the basic problem statement embodied in Eqs. (3.14) through (3.24) is of the general form, find  $\vec{\alpha}$  such that

$$h_q(\vec{\alpha}) \geq 0; \quad q = 1, 2, \dots, Q \quad (3.25)$$

and

$$W(\vec{\alpha}) \rightarrow \text{Min} \quad . \quad (3.26)$$

This form of the problem statement is similar to that given by Eq. (2.10) and Eq. (2.11) except for the use of linked reciprocal variables in Eqs. (3.25) and (3.26). The maximum number of constraints (Q) in Eq. (3.25) is given by the sum of the maximum number of behavior constraints  $Q_b$  and the maximum number of side constraints  $Q_s$ . From the detailed problem statement given by Eqs. (3.14) through (3.24) it is seen that

$$Q_b = 2 J_u K + 2 I_T K + (I_S + I_C) K \quad (3.27)$$

and it is emphasized that these constraints are implicit functions of the linked reciprocal design variables ( $\alpha_b$ ). The number of side constraints included in the problem statement given by Eqs. (3.14) through (3.24) is

$$Q_s = 2B. \quad (3.28)$$

in which B is the number of independent design variables after linking.

Note that the function of the definitions for  $\alpha_b^{(U)}$  and  $\alpha_b^{(L)}$  given by Eqs. (3.20) and (3.22) respectively, is to permanently eliminate strictly redundant side constraints. Design variable linking effectively reduces the number of side constraints in the problem statement from  $2(I_T + I_C + I_S)$  to  $2B$ .

### 3.3.2 Organization

Conventional finite element structural analysis programs can usually be viewed as having three main parts as follows:

- (a) input data processing,
- (b) structural analysis,
- (c) post processing and printout of results.

A structural analysis program that is to be integrated into a structural synthesis capability should be organized so as to facilitate efficient analysis of a sequence of modified designs. It should also be noted that in the design optimization context, structural analysis includes sensitivity analysis (i.e., calculation of partial derivatives of response quantities with respect to independent design variables). To achieve high overall efficiency it is useful to divide the structural analysis (part (b)) into two parts; the first part involving computations independent of the numerical values of the design variables and the second part containing computations involving the design variable values. In ACCESS 1 input data processing (a) and the first part of structural analysis (b) are contained in the "preprocessor" block of Fig. 4. The second part of the structural analysis (b) (i.e., the portion involving numerical values of the design variables) is in the "approximate problem generator" block.

The basic organization of the ACCESS 1 computer program is outlined in Fig. 4. The function of the "preprocessor" is to carry out those operations that need only be done once at the beginning of a given design problem. For example: (1) determining finite element dimensions and orientations relative to the reference coordinate system, (2) determining element stiffness matrices corresponding to unit values of the element sizing variables, and (3) constructing pointer vectors to control assembly of the system stiffness matrix. The "design process control" block in Fig. 4 interfaces with the "approximate problem generator" block and the "optimization algorithm" block.

A typical stage in the design process begins with the control block supplying a "trial design" to the "approximate problem generator" block. This trial design is subjected to a detailed finite element structural analysis

for all K load conditions. The results of this structural analysis are then used to evaluate all of the behavioral constraints. The number of stress constraints is reduced by using a regionalization scheme followed by application of the "throw away" concept (see Section 2.4.2). The number of displacement constraints and the 2B side constraints (see Eqs. (3.19) and (3.21)) are reduced using only a "throw away" technique. For critical and near critical constraints that survive the deletion process, explicit approximations are then constructed by employing first order Taylor series expansions of appropriate displacement degrees of freedom and stresses in terms of the linked reciprocal design variables.

The approximate but explicit representations for the set of constraints retained are passed back to the "design process control" block which appends the explicit objective function, normalizes the design variables and then gives this approximate, but tractable, mathematical programming problem to the "optimization algorithm" block. The design improvement process is now carried out by operating on the current approximate problem statement using either the CONMIN or the NEWSUMT optimization algorithm. The CONMIN optimizer (see Ref. 68) is based on a modified method of feasible directions (see Ref. 67) while the NEWSUMT optimizer is based on an extended interior penalty function (see Ref. 75) formulation used in conjunction with a modified Newton method minimizer (see Ref. 53). Either optimization algorithm can be used to generate an improved design or a near optimum solution of the approximate problem supplied by "design process control" for the current stage. After certain criteria are satisfied, the last design obtained by the optimization algorithm is passed back to the "design process control" block where it becomes the initial trial design for the next stage. This then completes a typical stage in the design

process. The overall, iterative, multistage design process is terminated by either a diminishing returns criterion with respect to weight reduction or an overriding termination criterion limiting the total number of stages.

Before turning to a more detailed discussion of the major parts of ACCESS 1 it is appropriate to point out a few key features of the program. First, it is emphasized that only one finite element structural analysis is executed per stage. In practice, the number of detailed finite element structural analyses carried out is always equal to one plus the total number of stages executed, since it is desirable to have a complete analysis of the final design obtained upon termination of the entire procedure. It should also be noted that only those partial derivatives required to construct explicit approximations of retained constraints need be computed. This is because constraint deletion is carried out prior to the construction of explicit approximations for the constraint functions. It is also important to recognize that none of the constraints included in the original problem statement (see Eqs. (3.14) through (3.24)) are permanently deleted (except for the strictly redundant side constraints, see Eqs. (3.20) and (3.22)). That is, in each stage, after completing the detailed finite element structural analysis, the constraints to be deleted are reestablished. This permits previously deleted constraints to reappear when appropriate, and it permits the dropping out of previously retained constraints. It should also be noted that both of the available optimization algorithm options can accommodate moderately infeasible starting points. Finally, it is observed that in practice the CONMIN option reduces the weight rapidly while tending to produce a sequence of near critical designs. On the other hand, the NEWSUMT option reduces the weight more gradually while tending to produce a sequence of noncritical designs that

"funnel down the middle" of the feasible region. More detailed descriptions of the various component parts of the ACCESS 1 program are offered in the sequel.

### 3.3.3 Input Data Required

In order to apply the ACCESS 1 computer program to a particular design optimization task it is necessary to prepare a set of data cards describing the problem at hand. While detailed data format instructions are not given here they will be found in Ref. 76. Nevertheless it will be useful to elaborate on the input data required.

Consider the 18 element wing box beam example drawn from Ref. 34, and shown in Fig. 5. The structure is symmetric with respect to the x-y plane. Note that there are no node numbers assigned in the middle surface of the box beam. This is due to the idealization employed which neglects inplane mid-surface displacements and assumes that the z displacements of the midsurface are the same as those of corresponding (x-y) locations on the upper surface. The ACCESS 1 program accommodates three kinds of finite elements, namely TRUSS elements (type 1), CST elements (type 2) and SSP elements (type 3). The idealization of the wing box shown in Fig. 5 involves 5 type 1 elements, 5 type 2 elements and 8 type 3 elements. Before proceeding any further it will be important to fix in mind the notions of design variable groups and configuration groups. If the design variables ( $D_i$ ) for each of several finite elements of the same type are linked to a single independent design variable ( $\delta_b$ ) (see Eq. (3.11)) then these elements belong to the  $b^{\text{th}}$  design variable group. If there are several finite elements of the same type having identical configuration and material properties, which may have different size (cross sectional area or thickness) and orientation in space, then these elements belong to the same configuration group ( $\ell$ ).

With the foregoing definitions in mind it is now a straightforward matter to set forth the data describing the example problem depicted in Fig. 5.

- (a) Job Description - provides for a two card identification of any particular problem (e.g. EIGHTEEN ELEMENT WING BOX DESIGN PROBLEM REF. AFFDL-TR-70-165).
- (b) Job Control Parameters - permits options from (0) minimum to (8) maximum controlling the amount of analysis information to be printed out after each intermediate design stage (e.g., 0 2 0)\* where the 2 in the middle is the print option indicator.
- (c) Basic Structural Descriptors - various integers describing the structural idealization and the number of loading conditions:
  - (1) number of nodes, number of spacial dimensions, number of boundary nodes, number of load conditions (e.g. 7 3 2 1).
  - (2) number of design variable linking groups for each element type (e.g. 5 3 8), indicating (5) independent design variables for the type 1 (TRUSS) elements, (3) independent design variables for the type 2 (CST) elements and (8) independent design variables for the type 3 (SSP) elements.
  - (3) number of configuration groups for each element type (e.g. 2 2 5), indicating (2) different configuration groups for the type 1 (TRUSS) elements, (2) different configuration groups for the type 2 (CST) elements, and (5) distinct configuration groups for the type 3 (SSP) elements.
  - (4) number of finite elements of each type (e.g. 5 5 8), indicating that the structure is represented by 5 truss elements (type 1), (5) CST elements (type 2) and (8) SSP elements (type 3).

---

\* The example numbers given conform with the detailed input format described in Ref. 76.

- (d) Node Numbers and their location with respect to a reference coordinate system (e.g. see Table 2).
- (e) Element Descriptions for all elements of all types:
- (1) TRUSS elements - member number, design variable linking group number, initial cross sectional area, upper limit on cross sectional area, lower limit on cross sectional area, configuration group number, P<sup>th</sup> node number, Q<sup>th</sup> node number, side constraint code\* for the element (e.g. see Table 3).
  - (2) CST elements - member number, design variable linking group number, initial thickness, upper limit on thickness, lower limit on thickness, configuration group number, P<sup>th</sup> node number, Q<sup>th</sup> node number, R<sup>th</sup> node number, and side constraint code for the element\* (e.g. see Table 4).
  - (3) SSP elements - member number, design variable linking group number, initial thickness, upper limit on thickness, lower limit on thickness, configuration group number, P<sup>th</sup> node number, Q<sup>th</sup> node number, and side constraint code for the element\* (e.g. see Table 5).
- (f) Material Properties for each configuration group for each element type
- (1) TRUSS elements - upper limit on axial stress, lower limit on axial stress, specific weight, modulus of elasticity (e.g. see Table 6).
  - (2) CST elements - upper limit on Von Mises equivalent stress, specific weight, modulus of elasticity, and Poissons ratio (e.g. see Table 7).

---

\*Side constraint code: -1 lower limit only; 0 nonnegativity only; +1 upper limit and nonnegativity; +2 upper and lower limits.

- (3) SSP elements - upper limit on Von Mises equivalent stress, specific weight, modulus of elasticity, and Poisson's ratio (e.g. see Table 8).
- (g) Displacement Boundary Conditions - boundary node number, boundary condition code for x, y and z displacement components, prescribed displacements if the corresponding boundary condition code is -1. Note that the boundary condition code is as follows: -1 denotes prescribed displacement; 0 denotes free, and +1 indicates a fixed condition. For the 18 element wing box example the displacement boundary conditions are given in Table 9.
- (h) Load Condition Data - for each load condition it is necessary to specify the number of nodes where loads are applied, as well as the node numbers and the applied force components in the x, y and z directions (e.g. see Table 10).
- (i) Displacement Constraints - number of displacements components constrained, node number, direction, constraint code, upper limit and lower limit. Let the x, y and z directions correspond to 1, 2 and 3, respectively. The displacement constraint code is as follows: -1 lower limit constraint only, 0 no constraint, 1 upper limit constraint only, 2 both upper and lower limit constraints. For the 18 element wing box example the displacement constraints are given in Table 11.

#### 3.3.4 Function of Preprocessor

Basically the "preprocessor" block (see Fig. 4) carries out calculations that need only be done once since they are independent of the numerical values of the design variables. The preprocessor performs the following computations

and stores the generated results as arrays in labeled COMMON BLOCKS that can be drawn on by the "approximate problem generator" block (see Fig. 4):

- (a) Read input data and print out input data.
- (b) Compute element data for:
  - (1) TRUSS elements - length, direction cosines of local coordinate axes relative to reference coordinates;
  - (2) CST elements - planform dimensions and direction cosines of local coordinate axes relative to reference coordinates;
  - (3) SSP elements - planform dimensions and direction cosines of local coordinate axes relative to reference coordinates.
- (c) Compute and store the local element stiffness matrix corresponding to a unit value of the element sizing variable for each configuration group associated with the TRUSS, CST and SSP element types.
- (d) Construct pointer vectors for (1) arranging the system stiffness matrix in compact vector form and (2) indicating boundary conditions corresponding to all displacement degrees of freedom.
- (e) Compute and store load vectors in the reference coordinate system for each independent load condition. Note that load vectors are independent of the design variables since body forces and thermal effects are not treated in ACCESS 1.
- (f) Identify and enumerate all possible constraints:
  - (1) side constraints - compute total number of side constraints and for each side constraint identify the associated element type and linking group.

- (2) stress constraints - compute total number of stress constraints per load condition and for each stress constraint identify the associated element type and element number.
- (3) displacement constraints - compute total number of displacement constraints per load condition and for each displacement constraint identify the associated node number and direction.

It should be noted that the associated element numbers (for side and stress constraints) and the associated node numbers (for displacement constraints) are assigned a negative sign for lower limit constraints and a positive sign for upper limit constraints.

After the preprocessing phase has been completed the program and local variables may be deleted from the main memory, if desired.

### 3.3.5 Design Process Control

The DPC (Design Process Control block) interfaces with the APG (Approximate Problem Generator block) and the OA (Optimization Algorithm block) as shown in Fig. 4. After the preprocessing phase has been completed the DPC is immediately activated. The primary functions carried out by the DPC can be outlined as follows:

- (1) Read optimizer control parameters;
- (2) Analyze the initial trial design (activate APG)<sup>†</sup>;
- (3) Set the initial values of the reduced set of design variables to unity (i.e., let  $\alpha_b^{(0)} = 1/\delta_b^{(0)} = 1$  for  $b = 1, 2, \dots, B$ , see Eq. (3.11));

---

<sup>†</sup>It is emphasized that APG includes structural analysis, constraint deletion and construction of explicit approximations for surviving constraints.

- (4) If the initial design is infeasible, scale the reduced set of reciprocal design variables uniformly so that the most critical approximate constraint is satisfied by a prespecified margin;
- (5) Using the approximate problem statement generated by APG (see step 2 or step 10) activate the OA which modifies the reduced set of reciprocal design variables ( $\alpha_b$ ) moving toward an optimum solution of the current approximate problem statement;
- (6) Update the element size design variables ( $D_i$ ) using the current scale factors ( $T_{ib(i)}$ ) and the values of the reduced set of reciprocal design variables obtained in step 5 (i.e. substitute  $\delta_{b(i)} = 1/\alpha_{b(i)}$  into Eq. (3.11));
- (7) Update the weight coefficients,  $C_b$ , appearing in Eq. (3.23) to reflect normalization of the reduced set of reciprocal design variables for the upcoming stage in the design process [i.e.  $C_b \leftarrow (C_b/\alpha_b)$ ];
- (8) Check convergence criteria and limit on maximum number of stages for the design procedure, if satisfied jump to step 13, otherwise continue to step 9;
- (9) Update linking table entries ( $T_{ib(i)}$ ) so that unit values of the reduced set of design variables ( $\delta_b = 1/\alpha_b = 1$ ) correspond to the current sizing design variables (see Eq. (3.11));
- (10) Analyze the current trial design (activate APG);
- (11) If the current design is infeasible scale the reduced set of reciprocal design variables uniformly so that the most critical approximate constraint is just satisfied;

- (12) Modify the truncation factor controlling the constraint deletion process and jump to step 5 (the dynamic truncation factor is discussed in Section 3.3.6.2);
- (13) Analyze the final design (activate APG);
- (14) If the final design is infeasible, scale the reduced set of reciprocal design variables uniformly so that the most critical approximate constraint is just satisfied;
- (15) Terminate the design procedure.

In the foregoing steps 1 through 4 may be viewed as an initialization phase, while steps 5 through 12 represent a stage in the iterative design procedure, and steps 13 through 15 constitute the termination phase. Note that in the design process outlined here, the APG and the OA are activated only once per design stage.

Although both optimizers (CONMIN and NEWSUMT) can accommodate infeasible starting points, the scaling steps (4 and 11) are inserted to reduce the burden on the optimizer by assuring that the initial design for each stage in the design process is at least feasible with respect to the approximate constraints. The improved design generated by the optimizer at each stage (see Fig. 4) is always feasible with respect to the approximate constraints, however, it may be in violation of the actual constraints. In the latter case, the infeasible design is scaled up to provide a feasible starting point for the upcoming stage. In most cases the improved designs generated by the optimizer are found to be feasible with respect to the actual constraints (particularly when the NEWSUMT algorithm is being used). Regardless of whether or not scale up occurs, the approximate problem statement for each upcoming stage is always generated using complete analysis results for the design available at the end of the previous stage. As a consequence, when scale up

occurs, the feasible starting point differs from the slightly infeasible design at which the approximate problem statement has been generated.

A final note of caution regarding scaling steps is appropriate. Rather unusual constraints such as upper limits on element sizes or positive lower limits on stresses or displacements may be imposed in ACCESS-1, but scaling will not work for constraints of this type. Therefore if constraints of this type (or thermal effects) are to be handled, the DPC must be modified to omit the scaling steps. In this event the built in capability of each optimizer to start from an infeasible initial design would be relied upon to bring the design into the feasible region with respect to the approximate constraints.

### 3.3.6 Approximate Problem Generator (APG)

Whenever the APG block (see Fig. 4) is activated by the DPC block, the sizing design variables for the current design are stored in the arrays where the initial element sizes were stored. Furthermore, all data generated by the preprocessor are available through labeled COMMON BLOCKS.

#### 3.3.6.1 Displacement evaluation

A finite element displacement method of structural analysis is built into ACCESS 1. To obtain the static displacement response of the structure under each of K load conditions it is necessary to set up and solve the following system of simultaneous equations

$$[K] \vec{u}_k = \vec{P}_k; \quad k = 1, 2, \dots, K \quad . \quad (3.29)$$

The system stiffness matrix [K] is assembled in compact vector form as illustrated in Fig. 6. The vector form of the system stiffness matrix is made up of elements from the first nonzero element through the diagonal element from each column of [K].

The assembly procedure for forming the system stiffness matrix  $[K]$  in compact vector form can be outlined as follows:

- (a) the configuration group number associated with the  $i^{\text{th}}$  finite element is identified as  $\ell(i)$ .
- (b) the local stiffness matrix  $[\tilde{k}_{\ell(i)}]$  (associated with unit value of the element sizing variable) is copied out and multiplied by the current size to form a local element stiffness matrix ( $[\tilde{k}_i] = D_i [\tilde{k}_{\ell(i)}]$ ). Since  $[\tilde{k}_i]$  is symmetric, only the upper triangle of  $[\tilde{k}_i]$  is stored in vector form.
- (c) The coordinate transformation matrix for the  $i^{\text{th}}$  finite element  $[\Lambda_i]$  is used to obtain the element stiffness matrix in the reference coordinate system. Since  $[\Lambda_i]$  is a relatively sparse matrix and its nonzero elements are easily computed the transformation

$$[k_i] = [\Lambda_i]^T [\tilde{k}_i] [\Lambda_i] \quad (3.30)$$

is not carried out as a matrix multiplication, and the elements of  $[k_i]$  are computed from explicit algebraic formulas.

- (d) The assembly subroutine identifies the position in the system stiffness matrix (expressed in compact vector form) where each element of  $[k_i]$  must be added in and then performs this addition.

The load vectors  $\vec{P}_k$ ;  $k = 1, 2, \dots, K$  previously generated by the preprocessor are copied into the locations where the displacement response vectors are to be stored.

The linear equation solver built into ACCESS 1 is based on the algorithm given in Ref. 77. The system stiffness matrix is decomposed into the product

of three matrices, namely

$$[K] = [L] [D] [L]^T \quad (3.31)$$

where  $[L]$  is a lower half triangular matrix and  $[D]$  is a diagonal matrix. After decomposition a sequence of back and forward substitutions for each  $\vec{P}_k$  leads to the corresponding displacement response vector  $\vec{u}_k$ . In ACCESS 1 the entire system stiffness matrix  $[K]$  (stored in compact vector form) and the complete set of load vectors  $\vec{P}_k$ ;  $k = 1, 2, \dots, K$  reside in the primary core storage simultaneously, and this characteristic constitutes an important restriction on the size of problem that can be handled by ACCESS 1.

### 3.3.6.2 Constraint evaluation and deletion

At the outset it should be recalled that during the preprocessing phase (see Section 3.3.4) all constraints that are to be evaluated have been identified, enumerated and subdivided into side, stress, and displacement constraints. Within the ACCESS 1 computer program the feasible region is defined as a set of points corresponding to nonpositive constraint function values. This is because the first version of ACCESS 1 was written with the CONMIN optimization package in mind. In CONMIN, constraints have nonpositive values in the feasible region. Therefore, in order to faithfully describe the constraint deletion procedures built into ACCESS 1 it will be convenient to rewrite the problem statement (summarized by Eq. (3.25) and Eq. (3.26)) as find  $\vec{\alpha}$  such that

$$h_q^-(\vec{\alpha}) \leq 0; \quad q = 1, 2, \dots, Q \quad (3.32)$$

and

$$W(\vec{\alpha}) \rightarrow \text{Min} \quad (3.33)$$

where it is understood that

$$h_q^-(\vec{\alpha}) = -h_q(\vec{\alpha}) \quad . \quad (3.34)$$

For each constraint type (i.e., stress, displacement, and side) the most critical constraint value is identified and the truncation boundary value (TBV) for deletion of unnecessary constraints is computed as follows

$$TBV = \{ \text{Max}_q [h_q^-(\vec{\alpha}) + c] \} TRF - c \quad (3.35)$$

where  $c$  is a preassigned constant taken as 1.2 for side constraints and 1.0 for stress and displacement constraints. It is to be understood that TRF is a truncation factor, with an initial value given as input data [typically  $(TRF)_1 = 0.1$ ], that is increased automatically in step 12 of the DPC [typically  $(TRF)_{p+1} = 1.2 (TRF)_p$ ] up to some maximum value denoted by TRFMAX (typically TRFMAX = 0.6). Since displacement constraints are found to be more stable than others (less sensitive to changes in the design variables) the TRF for displacement constraints is increased by 0.2 at each stage of the design process, that is  $TRF_{\text{displacement}} = TRF + 0.2$ . Table 12 gives a set of typical values for TRF and  $TRF_{\text{displacement}}$  for the first 8 stages of the design procedure followed in the delta wing example to be discussed in Section 4.3.3. The relationship between TBV and TRF given by Eq. (3.35) is illustrated in Fig. 7. For each type of constraint, all constraints whose values  $h_q^-(\vec{\alpha})$  are less than the current TBV are deleted from consideration during that design stage. The relationship between the detailed implementation of constraint deletion and the general "throw away" concept described in Section 2.4.2 is elucidated in Appendix B.

It should also be noted that essentially redundant stress constraints are deleted in ACCESS by implementing the regionalization concept in the following way. For each design variable linking group (b) for each loading condition (k) only the most critical stress constraint is considered by

ACCESS 1 at each stage during the design process. This immediately reduces the number of stress constraints from  $I \times K$  to  $B \times K$  constraints. From this reduced set of stress constraints only those for which

$$h_q^-(\vec{\alpha}) \geq TBV \quad (3.36)$$

are retained for the current design stage. The use of design variable linking groups to define regions makes shifting of the critical constraints during a design stage rather unlikely. This is because changes in the independent design variables will primarily cause force redistributions between regions rather than within design variable linking group regions. In this connection it may be helpful to recall that, for statically determinate structures, the location of the most critical constraint in each region for each load condition is independent of the set of values assigned to the design variables.

Constraints that survive the deletion process are treated as critical or potentially critical constraints and they are logged into a posture table that is a vector of pointers containing the label numbers of these constraints.

### 3.3.6.3 Explicit approximation of retained constraints

Since the objective function is simple and explicit in the exact form given by Eq. (3.23), no approximation is required. Furthermore the first and second partial derivatives of the objective function with respect to the linked reciprocal design variables  $\alpha_b$  are also easily obtained as

$$\frac{\partial W(\vec{\alpha})}{\partial \alpha_b} = -\frac{C_b}{\alpha_b^2} \quad ; \quad b = 1, 2, \dots, B \quad (3.37)$$

and

$$\frac{\partial^2 W(\vec{\alpha})}{\partial \alpha_b^2} = 2 \frac{C_b}{\alpha_b^3} \quad ; \quad b = 1, 2, \dots, B \quad (3.38)$$

On the other hand, the stress and displacement behavior constraints are complicated implicit functions of the independent design variables.

It is easily shown that for statically determinate structures idealized by TRUSS, CST and SSP finite elements, both the static stress and displacement response are strictly linear in reciprocal sizing design variables ( $\vec{\alpha}$ ). This suggests that for moderately indeterminate structures in this class the quality of both stress and displacement approximations will be enhanced by using reciprocal sizing variables ( $\vec{\alpha}$ ). Specifically, in ACCESS 1 first order Taylor series expansions are used to construct approximate representations for stress and displacement response quantities such as  $\sigma_{ik}(\vec{\alpha})$ ,  $\sigma_{eik}(\vec{\alpha})$  and  $u_{jk}(\vec{\alpha})$  (see Eqs. (3.14) through (3.18)).

The first order Taylor series approximation of the  $j^{\text{th}}$  displacement degree of freedom under the  $k^{\text{th}}$  load condition, based upon analysis of the current trial design  $\vec{\alpha}_p$  can be expressed as follows

$$u_{jk}(\vec{\alpha}) \approx \tilde{u}_{jk}(\vec{\alpha}) = u_{jk}(\vec{\alpha}_p) + (\vec{\alpha} - \vec{\alpha}_p)^T \nabla u_{jk}(\vec{\alpha}_p) \quad (3.39)$$

where  $\tilde{u}_{jk}(\vec{\alpha})$  represents the explicit approximation for the  $j^{\text{th}}$  displacement under the  $k^{\text{th}}$  load condition;  $u_{jk}(\vec{\alpha}_p)$  denotes the values of the  $j^{\text{th}}$  displacement under load condition  $k$  for the base point  $\vec{\alpha}_p$  of the current stage, and  $\nabla u_{jk}(\vec{\alpha}_p)$  stands for the gradient of the  $j^{\text{th}}$  displacement under load condition  $k$  evaluated at the same base point  $\vec{\alpha}_p$ . Note that the components of the

---

\* Designs for which complete structural analysis (and selective sensitivity analyses) are executed, in order to construct explicit approximations for an upcoming stage of the iterative design process, are called base point designs. In ACCESS 1 the base point design  $\vec{\alpha}_p$  for the  $p^{\text{th}}$  stage is always taken to be the last design obtained during the previous stage. When a base point design  $\vec{\alpha}_p$  is found to be infeasible with respect to the complete analysis, it is scaled up to give a feasible initial design for the upcoming  $p^{\text{th}}$  stage. Therefore, when scale up occurs the feasible initial design for the  $p^{\text{th}}$  stage differs from the slightly infeasible base point design  $\vec{\alpha}_p$ .

vector  $\nabla_{j_k}(\vec{\alpha}_p)$  are the partial derivatives  $\frac{\partial u_{jk}}{\partial \alpha_b}(\vec{\alpha}_p)$  for  $b = 1, 2, \dots, B$ , in which  $B$  is the total number of independent design variables after linking. An important new feature of the ACCESS 1 computer program is that only those partial derivatives needed to construct explicit approximations for constraints surviving the deletion process are evaluated. This feature is called selective sensitivity analysis. It should be noted that the necessary partial derivatives are obtained directly, i.e., without recourse to finite difference techniques.

For any particular trial design it is known that the stresses in a finite element can be readily determined if the displacement degrees of freedom are known. In ACCESS 1 subroutine SELDIS scans the set of stress and displacement constraints retained in a particular stage and identifies the subset of displacement degrees of freedom ( $j \in J'$ ) defining the values of the retained constraints. This scanning also determines which, if any, load conditions do not contribute any stress or displacement constraints to the retained set of constraints. Let  $K'$  denote the set of load conditions that contribute at least one stress or displacement constraint to the set of constraints retained after completing the deletion process described in Section 3.3.6.2.

In general, for linear static structural analysis problems governed by equilibrium equations of the form given in Eq. (3.29), implicit differentiation with respect to independent reciprocal design variables yields

$$\left[ \frac{\partial K}{\partial \alpha_b} \right] \vec{u}_k + [K] \frac{\partial \vec{u}_k}{\partial \alpha_b} = \frac{\partial \vec{F}_k}{\partial \alpha_b} ; \quad \begin{array}{l} b = 1, 2, \dots, B \\ k = 1, 2, \dots, K \end{array} \quad (3.40)$$

and

$$\frac{\partial \vec{P}_k}{\partial \alpha_b} = \vec{0}$$

when thermal effects and body forces (e.g. self-weight) are neglected as in ACCESS 1. Then Eq. (3.40) can be written as

$$[K] \frac{\partial \vec{u}_k}{\partial \alpha_b} = \vec{V}_{bk}; \quad \begin{matrix} b = 1, 2, \dots, B \\ k = 1, 2, \dots, K \end{matrix} \quad (3.41)$$

where the vectors

$$\vec{V}_{bk} = - \left[ \frac{\partial K}{\partial \alpha_b} \right] \vec{u}_k \quad (3.42)$$

are sometimes called pseudo load vectors. The selective sensitivity analysis concept implemented by the ACCESS 1 program involves the computation and storage of a set of vectors  $\vec{V}_{bk}$  for  $b = 1, 2, \dots, B$  and  $k \in K'$ . Note that  $[\partial K / \partial \alpha_b]$  in Eqs. (3.40) and (3.42) represents the partial derivative of the system stiffness matrix  $[K]$  with respect to the  $b^{\text{th}}$  independent reciprocal design variable after linking. In the ACCESS 1 program the matrices  $[\partial K / \partial \alpha_b]$  are neither computed nor stored. Instead of computing the  $\vec{V}_{bk}$  vectors from Eq. (3.42), they are determined directly from the local element stiffness matrices  $[\tilde{k}_{\ell(i)}]$  (associated with unit values of the element design variables) using the formula (see Appendix C for derivation)

$$\vec{V}_{bk} = - \sum_{i \in b} \frac{T_{ib(i)}}{\alpha_b(i)^2} [\Lambda_i]^T [\tilde{k}_{\ell(i)}] [\Lambda_i] \vec{u}_{ik} \quad \begin{matrix} b = 1, 2, \dots, B; \\ k \in K' \end{matrix} \quad (3.43)$$

where it is understood that  $\vec{u}_{ik}$  represents the displacement degrees of freedom (in the reference coordinate system) associated with the  $i^{\text{th}}$  finite element in the  $k^{\text{th}}$  load condition.

Using Eq. (3.41) a set of  $B \times K'$  vectors  $\vec{V}_{bk}$  is computed and stored. In general some of these pseudo load vectors will be null or trivially small. In ACCESS 1 the following scheme is employed to delete pseudo load vectors  $\vec{V}_{bk}$

of negligible importance. For load condition  $k$ , compute the absolute magnitude  $|\vec{V}_{bk}|$  for  $b = 1, 2, \dots, B$  and delete  $\vec{V}_{bk}$  from further consideration if

$$|\vec{V}_{bk}| \leq \epsilon \text{ Max}_b \{ |\vec{V}_{bk}| \} .$$

This deletion process is carried out separately for each load condition  $k \in K'$ . The result of the deletion process is to reduce the number of  $\vec{V}_{bk}$  vectors from  $B \times K'$  to  $TV_{bk}$ .

It is apparent that Eq. (3.41) provides a convenient means of computing the partial derivatives  $\frac{\partial u_{jk}}{\partial \alpha_b} (\vec{\alpha}_p)$  needed to construct explicit approximate representations for stress and displacement response quantities involved in the set of constraints surviving the deletion process described in Section 3.3.6.2. Since the decomposed form of the stiffness matrix (see Eq. (3.31)) is available (it was previously computed and stored in order to solve for the displacement vectors  $\vec{u}_k$ ) Eq. (3.41) may be rewritten as follows

$$[\mathcal{L}][\mathcal{D}][\mathcal{L}]^T \frac{\partial \vec{u}_k}{\partial \alpha_b} = \vec{V}_{bk} \quad . \quad (3.44)$$

Now, if the reduced number of  $\vec{V}_{bk}$  vectors, namely  $TV_{bk}$  is less than the number of displacement degrees of freedom in the subset defining the values of the retained constraints ( $J'$ ), then the partial derivatives desired are obtained by carrying out a sequence of back and forward substitutions for each  $\vec{V}_{bk}$  vector in the reduced set.

On the other hand if  $J' < TV_{bk}$  generation of a matrix  $[\tilde{C}]$ , called the partial inverse of  $[K]$  will require fewer back and forward substitutions than the foregoing procedure. Therefore, when  $J' < TV_{bk}$  the ACCESS 1 program branches and uses the following scheme to compute the desired partial derivatives. The matrix  $[\tilde{C}]$  is constructed in the following straightforward manner. Obtain a set of vectors  $\vec{C}_j$  by carrying out a sequence of back and

forward substitutions, for each of several right hand sides  $\vec{e}_j$ , operating on the following set of equations

$$[\mathcal{L}][\mathcal{D}][\mathcal{L}]^T \vec{C}_j = \vec{e}_j; \quad j \in J' \quad (3.45)$$

where  $\vec{e}_j$  is a vector with all zero elements except for a single element equal to unity corresponding to the  $j^{\text{th}}$  degree of freedom in the subset  $J'$ .

Now let the partial inverse matrix  $[\tilde{C}]$  be made up with the  $\vec{C}_j^T$  as its rows. Then it follows from Eq. (3.41) that

$$\frac{\partial \vec{u}_k}{\partial \alpha_b} = [K]^{-1} \vec{V}_{bk} \quad (3.46)$$

and the reduced set of partial derivatives required can be computed from

$$\frac{\partial \vec{u}_k}{\partial \alpha_b} = [\tilde{C}] \vec{V}_{bk} \quad (3.47)$$

which can be written in the scalar form

$$\frac{\partial u_{\ell k}}{\partial \alpha_b} = \sum_{j=1}^J \tilde{C}_{\ell j} v_{j b k} ; \quad \ell \in J', (b, k) \in TV_{bk}. \quad (3.48)$$

The scalar form given by Eq. (3.48) is particularly revealing, because it clearly shows that when the partial inverse branch of the ACCESS 1 program is followed [i.e., when  $J' < TV_{bk}$ ] only those partial derivatives needed are computed and stored.

With the necessary partial derivatives  $\left[ \frac{\partial u_{jk}}{\partial \alpha_b} (\vec{\alpha}_p); j \in J', k \in K' \text{ and } b \in B' \right]$  available in storage it is a straightforward matter to construct explicit approximations for the displacement and stress constraints retained after completing the deletion process described in Section 3.3.6.2. Examination of the stress and displacement constraints (Eqs. (3.14) through (3.18)) reveals that they are explicit functions of response quantities  $[u_{jk}(\vec{\alpha})]$ ,

$\sigma_{ik}(\vec{\alpha})$  and  $\sigma_{eik}(\vec{\alpha})$ ]. Explicit approximations of the displacement response quantities [i.e.,  $\tilde{u}_{jk}(\vec{\alpha})$ ] are available from Eq. (3.39).

For TRUSS elements the explicit approximations of the stresses  $\sigma_{ik}(\vec{\alpha})$  are given by

$$\sigma_{ik}(\vec{\alpha}) \approx \tilde{\sigma}_{ik}(\vec{\alpha}) = \sigma_{ik}(\vec{\alpha}_p) + (\vec{\alpha} - \vec{\alpha}_p)^T \nabla \sigma_{ik}(\vec{\alpha}_p) \quad (3.49)$$

where

$$\sigma_{ik}(\vec{\alpha}_p) = \underset{1 \times 1}{[D_i]} \underset{1 \times 2}{[B_i]} \underset{2 \times 6}{[\Lambda_i]} \underset{6 \times 1}{\vec{u}_{ik}(\vec{\alpha}_p)} \quad (3.50)$$

and for TRUSS elements  $[D_i]$ ,  $[B_i]$  and  $[\Lambda_i]$  are defined implicitly by Eqs. (A5), (A3) and (A4) of Appendix A. Furthermore, for TRUSS elements it is to be understood that

$$\vec{u}_{ik}^T = \left[ u_p, v_p, w_p, u_q, v_q, w_q \right] \quad (3.51)$$

where  $u_p, v_p, w_p$  and  $u_q, v_q, w_q$ , respectively denote the x,y,z displacement components of nodes P and Q with respect to the reference coordinate system (see Fig. A1 Appendix A). Since the matrices  $[D_i]$ ,  $[B_i]$  and  $[\Lambda_i]$  in Eq. (3.50) are independent of the reciprocal design variables after linking  $(\vec{\alpha})$ , the components of  $\nabla \sigma_{ik}(\vec{\alpha}_p)$  are given by

$$\frac{\partial \sigma_{ik}}{\partial \alpha_b}(\vec{\alpha}_p) = [D_i][B_i][\Lambda_i] \frac{\partial \vec{u}_{ik}}{\partial \alpha_b}(\vec{\alpha}_p) \quad (3.52)$$

For CST and SSP elements explicit approximations for the Von Mises equivalent stresses  $\sigma_{eik}(\vec{\alpha})$  are given by

$$\sigma_{eik}(\vec{\alpha}) \approx \tilde{\sigma}_{eik}(\vec{\alpha}) = \sigma_{eik}(\vec{\alpha}_p) + (\vec{\alpha} - \vec{\alpha}_p)^T \nabla \sigma_{eik}(\vec{\alpha}_p) \quad (3.53)$$

where the equivalent stress  $\sigma_{eik}$  is defined in terms of the stress components  $\sigma_{xik}, \sigma_{yik}$  and  $\tau_{xyik}$  by Eq. (3.1).

and the components of  $\nabla\sigma_{eik}(\vec{\alpha}_p)$  are given by

$$\frac{\partial\sigma_{eik}}{\partial\alpha_b}(\vec{\alpha}_p) = \frac{1}{2\sigma_{eik}} \left[ (2\sigma_{xik} - \sigma_{yik}), (2\sigma_{yik} - \sigma_{xik}), \right. \\ \left. 6\tau_{xyik} \right] \frac{\partial}{\partial\alpha_b} \begin{Bmatrix} \sigma_{xik} \\ \sigma_{yik} \\ \tau_{xyik} \end{Bmatrix} \quad (3.54)$$

For CST elements the appropriate stress-displacement relations are given by

$$\{\sigma_{ik}(\vec{\alpha}_p)\} = \begin{bmatrix} [D_i] & [B_i] & [\Lambda_i] \end{bmatrix} \vec{u}_{ik} \quad (3.55)$$

$\begin{matrix} 3 \times 3 & 3 \times 6 & 6 \times 9 & 9 \times 1 \end{matrix}$

where

$$\{\sigma_{ik}(\vec{\alpha}_p)\}^T = \left[ \sigma_{xik}, \sigma_{yik}, \sigma_{xyik} \right] \quad (3.56)$$

and

$$\vec{u}_{ik}^T = \left[ u_P, v_P, w_P, u_Q, v_Q, w_Q, u_R, v_R, w_R \right] \quad (3.57)$$

and it is understood that  $u_P, v_P, w_P, u_Q, v_Q, w_Q, u_R, v_R, w_R$  respectively denote the  $x, y, z$  displacement components of nodes P, Q and R with respect to the reference coordinate system (see Fig. A2 Appendix A). Furthermore, the matrices  $[D_i]$ ,  $[B_i]$  and  $[\Lambda_i]$  that appear in Eq. (3.55) are defined implicitly by Eqs. (A13), (A9) and (A10) of Appendix A.

For SSP elements the appropriate stress-displacement relations are given by

$$\{\sigma_{ik}(\vec{\alpha}_p)\} = \begin{bmatrix} [D_i] & [B_i] & [\Lambda_i] \end{bmatrix} \vec{u}_{ik} \quad (3.58)$$

$\begin{matrix} 3 \times 3 & 3 \times 4 & 4 \times 6 & 6 \times 1 \end{matrix}$

where  $\{\sigma_{ik}(\vec{\alpha}_p)\}$  is defined by Eq. (3.56) and  $\vec{u}_{ik}$  is defined by Eq. (3.51) with the understanding that the nodes P and Q are those shown in Fig. A3 of Appendix A. The matrices  $[D_i]$ ,  $[B_i]$  and  $[\Lambda_i]$  that appear in Eq. (3.58) are defined in Eqs. (A43), (A42) and (A48) of Appendix A.

For CST and SSP elements partial derivatives of the stress components, needed in Eq. 3.54, are given by expressions similar to Eq. 3.52 obtained by operating on Eq. 3.55 and 3.58 respectively.

At this juncture, all the information necessary to convert the basic problem statement, embodied in Eqs. (3.14) through (3.24), into an explicit approximate problem statement of the following form is available:

Find  $\vec{\alpha}$  such that

$$W(\vec{\alpha}) = \sum_{b=1}^B \frac{C_b}{\alpha_b} \rightarrow \text{Min} \quad (3.59)$$

and

$$h_q^-(\vec{\alpha}) \approx \hat{h}_q^-(\vec{\alpha}) = h_q^-(\vec{\alpha}_p) + (\vec{\alpha} - \vec{\alpha}_p)^T \nabla h_q^-(\vec{\alpha}_p) \leq 0; \quad q \in Q_R^{(p)} \quad (3.60)$$

where  $Q_R^{(p)}$  denotes the set of inequality constraints to be retained during the  $p^{\text{th}}$  stage of the iterative design procedure. This completes the discussion of the approximate problem generator block (see Fig. 4). It is emphasized in closing that the approximate problem statement which is passed through the design process control block to the optimization algorithm block, at each stage  $p$  in the design process (see Fig. 4), is relatively small and algebraically explicit.

### 3.3.7 Optimization Algorithms

Through the insightful use of approximation concepts the mathematical programming problem faced at each stage of the design procedure has been rendered small and explicit, yet still representative of the essential features of the structural design problem posed. As a result it is possible to employ any one of several well established nonlinear programming algorithms. The optimization algorithm block of ACCESS 1 (see Fig. 4) contains two options:

- (1) CONMIN - a modified feasible directions method due to Vanderplaats (see Ref. 68);
- (2) NEWSUMT - a sequence of unconstrained minimizations technique based on the Kavlie-Moe extended interior penalty function formulation (see Ref. 75) and a modified Newton method minimizer due to Haftka (see Ref. 53).

Before turning to a discussion of the CONMIN and NEWSUMT optimization algorithms it is appropriate, at this point, to say a word about two other optimization algorithms that could be added to the two options currently available. At each stage in the design procedure the approximate problem represented by Eqs. (3.59) and (3.60) involves only linear inequality constraints and a nonlinear but explicit objective function. In view of this, it would appear reasonable to consider using the well known gradient projection method of Rosen (see Ref. 78). A gradient projection option has not been implemented in the ACCESS 1 context because:

- (a) it was judged to be too specialized when looking ahead to including explicit but nonlinear constraint approximations  $\tilde{h}_q^{-1}(\vec{\alpha})$ ;
- (b) gradient projection does not tend to generate a sequence of noncritical designs "funneling down the middle" of the feasible region.

Another candidate optimization algorithm that was considered but not implemented as an option in ACCESS 1 is the method of inscribed hyperspheres (see Ref. 73). This method is a sequence of linear programs approach that tends to generate a set of noncritical feasible designs along an optimum trajectory. This characteristic facilitates the use of approximation concepts and the sequence

of LP's can be solved using existing computer programs. It should be noted that the method of inscribed hyperspheres was applied with considerable success in Ref. 72. A method of inscribed hyperspheres option has not been implemented in ACCESS 1 because:

- (a) the method requires linearization (not just explicit approximation) of both the inequality constraints  $[h_q^-(\vec{\alpha}) \leq 0]$  and the objective function  $[W(\vec{\alpha})]$ ;
- (b) in order to make the method work on truss problems it was found in Ref. 72 that tangent plane move limits, which could at least theoretically cut off the domain containing the optimum design, had to be used.

In the next section a brief discussion of the CONMIN optimization package is given. It may be noted that the CONMIN option was developed first because of the ready availability of this package. The NEWSUMT option was developed second and it tends to generate a sequence of designs that "funnels down the middle" of the feasible region. This represents a feature that is thought to be attractive in the context of approximation concepts and from an engineering point of view. It should be noted that most of the results presented in Section 4 of this report were obtained using the NEWSUMT option.

#### 3.3.7.1 CONMIN

CONMIN (a program for Constrained Function Minimization) is a general purpose program that has been widely used as a black box optimizer. It was written by G.N. Vanderplaats of NASA Ames and distributed through COSMIC. Relevant literature about the modified feasible directions method implemented by CONMIN will be found in Ref. 67 and further user oriented details are given in Ref. 68. The algorithm used is the method of feasible directions with the following modifications:

- (a) In the direction finding subproblem the push-off factors  $\theta_j$  are treated as functions of the constraint values (Ref. 67).
- (b) A special algorithm to search for a design in the feasible region, starting from an infeasible initial design is included (Ref. 67).
- (c) In the direction finding subproblem the Euclidian norm of the direction vector is constrained and the subproblem is reduced to a special form of quadratic program that is readily solved (Ref. 67).
- (d) For unconstrained minimization the conjugate gradient algorithm is employed (Ref. 68).
- (e) One dimensional minimization is carried out using a sequence of linear and quadratic approximations for the objective and constraint function variations, thus avoiding unnecessary function evaluations.
- (f) To alleviate the so called zig-zag behavior that feasible direction methods sometime exhibit (Ref. 27) constraint tolerances<sup>#</sup> are initially taken to be relatively large and then they are gradually decreased as the optimization algorithm converges.

CONMIN calls for the evaluation of objective and constraint functions as well as their gradient vectors (critical constraints only) at various points in the  $(\vec{\alpha})$  design space. In ACCESS 1 evaluation of these quantities is performed by subroutine TAYLOR which keeps all the information describing the current approximate problem statement available for calls from CONMIN. It

---

<sup>#</sup>In the feasible direction method a constraint is said to be critical if  $-\delta_q \leq h_q(\alpha) \leq 0$  where  $\delta_q$  is called the constraint tolerance.

should be noted that the gradients of the explicit approximate constraints  $(\vec{\nabla}_{\alpha} h_q(\vec{\alpha}); q \in Q_R^{(P)})$  retained at any stage in the design process are invariant over the design space. This is a consequence of the fact that in ACCESS 1 the explicit approximate constraint functions are constructed to be linear in the  $\alpha_b$ .

Qualitatively speaking, feasible direction methods tend to generate a sequence of designs on the constraint boundaries. For most structural design problems the optimum is found to reside on one or more constraint boundaries, hence it is reasonable to expect that a search along the constraint boundaries will often turn out to be efficient. It should also be noted that the special quadratic programming problems, used to solve for the useable-feasible directions are usually small. This is because the number of critical constraints is generally much smaller than the number of constraints included in the approximate problem statement.

In the ACCESS 1 context it should be kept in mind that at each stage during the iterative design procedure the optimization algorithm is being applied to a gradually improving approximate problem statement. Therefore it will probably be advisable to initially employ rather loose stage convergence criteria that are gradually tightened up as the multistage iterative design procedure outlined in Fig. 4 progresses.

Since the CONMIN package is well documented elsewhere (see Refs. 67 and 68) and in view of the fact that most of the results reported in Section 4 have been obtained using the NEWSUMT optimization algorithm, it seems appropriate to forego a more detailed description of CONMIN.

### 3.3.7.2 NEWSUMT

The NEWSUMT algorithm is a sequence of unconstrained minimization technique based on the extended interior penalty function formulation (see Ref. 75 and a modified Newton method (see Ref. 53) for carrying out the unconstrained minimizations. The explicit mathematical programming problem constructed by the approximate problem generator (see Fig 4), at each stage in the iterative design procedure, has the following form:

Find  $\vec{\alpha}$  such that

$$h_q(\vec{\alpha}) \approx \tilde{h}_q^{(p)}(\vec{\alpha}) \geq 0; \quad q \in Q_R^{(p)} \quad (3.61)$$

and

$$W(\vec{\alpha}) \rightarrow \text{Min} \quad . \quad (3.62)$$

Using the Fiacco-McCormick (see Ref. 79) interior penalty function formulation this problem is transformed into a sequence of unconstrained minimizations of the following form:

Let

$$\phi^{(p)}(\vec{\alpha}, r_a) = W(\vec{\alpha}) + r_a F^{(p)}(\vec{\alpha}) \quad (3.63)$$

where

$$F^{(p)}(\vec{\alpha}) = \sum_{q \in Q_R^{(p)}} [1/\tilde{h}_q^{(p)}(\vec{\alpha})] \quad (3.64)$$

and  $\phi^{(p)}$  is minimized with respect to  $\vec{\alpha}$  for a decreasing sequence of values

$$r_{a+1} = c_a r_a; \quad 0 < c_a < 1 \quad . \quad (3.65)$$

This well known SUMT type formulation is a stable and reliable algorithm and it has been extensively applied in the structural optimization context. This approach does however exhibit two shortcomings:

- (1) the method cannot use unconstrained minimization packages without special modification because the constraint repulsion type of penalty term (see  $F^{(p)}(\vec{\alpha})$  definition in Eq. (3.64)) is, strictly speaking, undefined in the infeasible (see Fig. 8) part of the positive design space;
- (2) the method usually requires more function evaluations than the method of feasible directions when using conventional unconstrained minimization algorithms such as the method of conjugate directions (see Ref. 80) or the variable metric method (see Ref. 81) of unconstrained minimization (with appropriate modifications in view of item (1) above).

The first of the foregoing shortcomings can be effectively eliminated by using the extended interior penalty function idea (see Ref. 75). In order to avoid the infinite discontinuity in  $1/\tilde{h}_q^{(p)}(\vec{\alpha})$  as  $\tilde{h}_q^{(p)}(\vec{\alpha})$  passes through zero, define the following modified penalty function:

$$\tilde{H}_q^{(p)}(\vec{\alpha}) = \left\{ \begin{array}{l} 1/\tilde{h}_q^{(p)}(\vec{\alpha}); \quad \tilde{h}_q^{(p)}(\vec{\alpha}) \geq \epsilon \\ [2\epsilon - \tilde{h}_q^{(p)}(\vec{\alpha})]/\epsilon^2; \quad \tilde{h}_q^{(p)}(\vec{\alpha}) < \epsilon \end{array} \right\} \quad (3.66)$$

The nature of the extended interior penalty function is illustrated in Fig. 9. It should be noted that  $\tilde{H}_q^{(p)}(\vec{\alpha})$  is continuous and has continuous first derivatives at the transition point defined by  $\tilde{h}_q^{(p)}(\vec{\alpha}) = \epsilon$ .

In ACCESS 1 the initial value of transition parameter  $\epsilon$  is given as an input parameter (typically  $\epsilon$  will have an initial value of 0.002) and it is then reduced at a rate which is a function of  $c_a$ .

Using the extended interior penalty function defined by Eq. (3.66), the SUMT formulation contained in Eqs. (3.63) through (3.65), can be cast in the alternative form:

Let

$$\phi_e^{(p)}(\vec{\alpha}, r_a) = W(\vec{\alpha}) + r_a F_e^{(p)}(\vec{\alpha}) \quad (3.67)$$

where

$$F_e^{(p)}(\vec{\alpha}) = \sum_{q \in Q_R^{(p)}} \tilde{H}_q^{(p)}(\vec{\alpha}) \quad (3.68)$$

and  $\phi_e^{(p)}$  is minimized with respect to  $\vec{\alpha}$  for a decreasing sequence of  $r_a$  values (see Eq. (3.65)). The functions  $\phi_e^{(p)}(\vec{\alpha}, r_a)$  are defined over the entire positive domain in  $\vec{\alpha}$  space, that is for all points such that  $\alpha_b > 0$ ;  $b = 1, 2, \dots, B$ . Negative values of the design variables ( $\alpha_b$ ) are avoided by drastically increasing the objective function values if one or more components of  $\vec{\alpha}$  become negative. The NEWSUMT algorithm has a built in move limit capability which restricts the design change relative to the design point at which the current approximate problem statement was generated. Whenever any component of the design vector  $\vec{\alpha}$  violates a move limit a new approximate problem is generated using a design point on the move limit boundary. In practice, this move limit capability has never actually been used because of the high accuracy of the explicit approximate analyses.

The second shortcoming of conventional SUMT type formulations is alleviated by reducing the number of function evaluations through the use of a modified Newton's method (Ref. 53) for unconstrained minimization. To minimize  $\phi_e^{(p)}(\vec{\alpha}, r_a)$  for a fixed value of  $r_a$ , it is necessary to perform a series of one dimensional minimizations each of which seeks the minimum value of  $\phi_e^{(p)}(\vec{\alpha}, r_a)$  along a line

$$\vec{\alpha} = \vec{\alpha}_m + d \vec{S}_m \quad (3.69)$$

where  $\vec{\alpha}_m$  is the current design,  $\vec{S}_m$  is a normalized direction vector and  $d$  is a scalar move distance variable. In the well known Newton procedure the

function to be minimized is replaced by a quadratic approximation based on a second order Taylor series expansion about the design point  $\vec{\alpha}_m$ , that is

$$\begin{aligned} \phi_e^{(p)}(\vec{\alpha}, r_a) &\approx \tilde{\phi}_e^{(p)}(\vec{\alpha}, r_a) = \phi_e^{(p)}(\vec{\alpha}_m, r_a) + (\vec{\alpha} - \vec{\alpha}_m)^T \nabla \phi_e^{(p)}(\vec{\alpha}_m, r_a) \\ &+ \frac{1}{2} (\vec{\alpha} - \vec{\alpha}_m)^T \left[ \frac{\partial^2 \phi_e^{(p)}}{\partial \alpha_b \partial \alpha_c}(\vec{\alpha}_m, r_a) \right] (\vec{\alpha} - \vec{\alpha}_m), \end{aligned} \quad (3.70)$$

where b and c are running indices for components of  $\vec{\alpha}$

Then the minimum of the quadratic approximation is obtained by taking the gradient of  $\tilde{\phi}_e^{(p)}(\vec{\alpha}, r_a)$ , setting it to zero

$$\begin{aligned} \nabla \phi_e^{(p)}(\vec{\alpha}, r_a) &= \nabla \phi_e^{(p)}(\vec{\alpha}_m, r_a) \\ &+ \left[ \frac{\partial^2 \phi_e^{(p)}}{\partial \alpha_b \partial \alpha_c}(\vec{\alpha}_m, r_a) \right] (\vec{\alpha} - \vec{\alpha}_m) = \vec{0} \end{aligned} \quad (3.71)$$

and solving for  $\vec{\alpha}$ , that is

$$\vec{\alpha} = \vec{\alpha}_m - \left[ \frac{\partial^2 \phi_e^{(p)}}{\partial \alpha_b \partial \alpha_c}(\vec{\alpha}_m, r_a) \right]^{-1} \nabla \phi_e^{(p)}(\vec{\alpha}_m, r_a). \quad (3.72)$$

The Newton method with line minimization (see Ref. 27) is obtained by comparing Eqs. (3.69) and (3.72) and letting the normalized direction vector  $\vec{s}_m$  be given by

$$\vec{s}_m = - \frac{\left[ \frac{\partial^2 \phi_e^{(p)}}{\partial \alpha_b \partial \alpha_c}(\vec{\alpha}_m, r_a) \right]^{-1} \nabla \phi_e^{(p)}(\vec{\alpha}_m, r_a)}{\left| \left[ \frac{\partial^2 \phi_e^{(p)}}{\partial \alpha_b \partial \alpha_c}(\vec{\alpha}_m, r_a) \right]^{-1} \nabla \phi_e^{(p)}(\vec{\alpha}_m, r_a) \right|}. \quad (3.73)$$

In Ref. 53 Haftka points out that when the Newton method with line minimization is applied to the unconstrained minimization of interior penalty function formulations, a good approximation of the matrix of second partial

derivatives  $\frac{\partial^2 \phi}{\partial \alpha_b \partial \alpha_c}(\vec{\alpha}_m, r_a)$  can often be obtained using only first derivatives. Referring to Eqs. (3.67), (3.68) and (3.66) it is easily shown that

$$\frac{\partial^2 \phi_e^{(p)}}{\partial \alpha_b \partial \alpha_c}(\vec{\alpha}, r_a) = \frac{\partial^2 W}{\partial \alpha_b \partial \alpha_c}(\vec{\alpha}) + r_a \sum_{q \in Q_R^{(p)}} \frac{\partial^2 \tilde{h}_q}{\partial \alpha_b \partial \alpha_c}(\vec{\alpha}) \quad (3.74)$$

and

$$\frac{\partial^2 \tilde{h}_q^{(p)}}{\partial \alpha_b \partial \alpha_c}(\vec{\alpha}) = \left\{ \begin{array}{l} \left[ 2 \frac{\partial \tilde{h}_q^{(p)}}{\partial \alpha_b}(\vec{\alpha}) \frac{\partial \tilde{h}_q^{(p)}}{\partial \alpha_c}(\vec{\alpha}) - \tilde{h}_q^{(p)}(\vec{\alpha}) \frac{\partial^2 \tilde{h}_q^{(p)}}{\partial \alpha_b \partial \alpha_c}(\vec{\alpha}) \right] / \left[ \tilde{h}_q^{(p)}(\vec{\alpha}) \right]^3 \\ - \frac{1}{\epsilon^2} \frac{\partial^2 \tilde{h}_q^{(p)}}{\partial \alpha_b \partial \alpha_c}(\vec{\alpha}) \quad ; \quad \tilde{h}_q^{(p)}(\vec{\alpha}) < \epsilon \end{array} \right\} \quad (3.75)$$

In Ref. 53 it is argued that for critical constraints  $\tilde{h}_q^{(p)}(\vec{\alpha})$  is small and therefore

$$2 \frac{\partial \tilde{h}_q^{(p)}}{\partial \alpha_b}(\vec{\alpha}) \frac{\partial \tilde{h}_q^{(p)}}{\partial \alpha_c}(\vec{\alpha}) \gg \tilde{h}_q^{(p)}(\vec{\alpha}) \frac{\partial^2 \tilde{h}_q^{(p)}}{\partial \alpha_b \partial \alpha_c}(\vec{\alpha}) \quad (3.76)$$

assuming  $\partial^2 \tilde{h}_q^{(p)} / \partial \alpha_b \partial \alpha_c$  is small. Furthermore, Ref. 53 points out that for noncritical constraints  $\tilde{h}_q^{(p)}(\vec{\alpha})$  is large and the entire righthand side of Eq. (3.75) is small since  $[\tilde{h}_q^{(p)}(\vec{\alpha})]^3$  appears in the denominator. Therefore, the contributions of noncritical constraints to the summation in Eq. 3.74 can be neglected, since they are small compared with the contributions from the critical and near critical constraints.

In the context of ACCESS 1 it is known that the  $\tilde{h}_q^{(p)}(\vec{\alpha})$  are all linear hence the  $\partial^2 \tilde{h}_q^{(p)} / \partial \alpha_b \partial \alpha_c$  vanish and the  $\partial \tilde{h}_q^{(p)} / \partial \alpha_b$  as well as the  $\partial \tilde{h}_q^{(p)} / \partial \alpha_c$  are invariant for the  $p^{\text{th}}$  approximate problem statement. It may also be

observed that  $[\partial^2 W / \partial \alpha_b \partial \alpha_c]$  is a diagonal matrix the elements of which are given explicitly by Eq. (3.38).

The optimization program NEWSUMT was written to implement the modified Newton method as an ACCESS 1 program option. Initially the scalar factor  $r_a$  is given a value such that  $\phi_e$  is equal to twice the value of the weight  $W$  (see Eq. (3.67)). The scalar  $r_a$  is decreased by a prespecified ratio ( $c_a$ ) every time minimization for the current value  $r_a$  is completed. The approximate problem statement is updated after a prespecified number of unconstrained minimizations ( $a'$ ). It is important to emphasize that ACCESS 1 permits the user to specify the cut factor ( $c_a$ ) and the number of unconstrained minimizations ( $a'$ ) to be executed prior to updating the approximate problem statement. Representative numbers for these control parameters are  $c_a = 0.3$  and  $a' = 2$ .

The one dimensional minimizations in NEWSUMT are carried out using the well known golden section method (see for example Ref. 82). This algorithm was adopted because of its inherently stable performance characteristics. One dimensional minimization convergence criteria are imposed on the sum of relative differences between the four function values involved at any step of the golden section search and on the interval size of the current search region. A maximum number of golden section iterations is also specified as input data.

## 4. EXAMPLE APPLICATIONS OF ACCESS 1

### 4.1 Introduction

In this chapter detailed results are presented for a substantial collection of sample problems. Unless otherwise noted, these designs have been generated by using a single precision NEWSUMT version of ACCESS 1 on the IBM 360/91 at UCLA. The truss examples presented in Section 4.2 are followed by results for several applications of ACCESS 1 to idealized wing structural configurations given in Section 4.3. The truss examples are separated out because they can be readily compared with previously reported results. In this regard truss structures offer an important advantage, since differences due to idealization and modeling details can be virtually eliminated. On the other hand, results for idealized wing structures, such as those given in Section 4.3, are easily influenced by differences in the finite element modeling. The wing box beam results presented in Section 4.3.1 are influenced by the shear web modeling employed. The swept-wing examples in Section 4.3.2 offer a comparison between optimum designs obtained by omitting and including spar cap bars in the idealization. The delta-wing examples in Section 4.3.3 illustrate the influence, on the minimum weight design attainable, of refining the design variable modeling (i.e., reducing the amount of design variable linking, hence increasing the number of independent design variables).

### 4.2 Truss Structures

There exists today a more or less standard set of truss problems for which solutions are available in the literature. In particular the planar ten bar truss problem, the 25 bar space truss problem, and the 72-bar space truss problems were set forth in Ref. 31. Solutions for these three

problems have also been given in Refs. 32, 34 and 72. In Ref. 83 the ten-bar truss problem is used to illustrate how the stress-ratio method, which seeks a fully-stressed design, can produce poor solutions for structures made up of members with markedly different allowable stresses. A truss idealization for the wing-carry-through-box of a heavy, swing-wing aircraft is also given in Ref. 83. This 63-bar truss problem is stated in detail in Ref. 83 and "competitive solutions by other methods" are invited. In Section 4.2.4 solutions obtained by ACCESS 1 are offered and compared with those given in Ref. 83.

#### 4.2.1 Planar Ten-Bar Truss (Problems 1-4)

In this section attention is focused on the planar ten bar cantilever truss shown in Fig. 10. The nodal coordinates describing the configuration are listed in Table 13. The truss element descriptions including initial cross sectional area, minimum member size, configuration group number, and nodal connectivity are listed in Table 14. Note that only lower limit side constraints ( $A_i^{(L)} = 0.100 \text{ in}^2$ ) are imposed on the member sizes and no design variable linking is specified. Therefore this design problem has ten independent design variables. The displacements at nodes 5 and 6 are set to zero, and it is then apparent that this planar problem involves eight independent displacement degrees of freedom. The displacement boundary conditions are specified in Table 15.

##### 4.2.1.1 Stress limits only, single load conditions (Problems 1 and 2)

In this subsection five example problems are discussed. The first four problems involve the previously described ten-bar truss subject to a single load condition consisting of 100 kip downward loads applied at nodes 4 and 2 (see Table 16). The truss element material properties for the first

of these four problems (Problem 1A) are given in Table 17. The subsequent set of three problems (Problems 1B, 1C and 1D) are the same as Problem 1A in all respects except that the allowable stresses in member 9 are modified to be  $\pm 30$  ksi,  $\pm 50$  ksi and  $\pm 70$  ksi, respectively. Results obtained using ACCESS 1 for Problem 1A, 1B, 1C and 1D are shown in Table 18 and they are essentially the same as the results obtained for this set of problems using the program reported in Ref. 72. As noted in Ref. 83 the results for Problems 1A and 1B can be duplicated using a fully-stressed design approach, while those for Problems 1C and 1D cannot. In Table 19 a comparison of the minimum weights achieved and the number of analyses required by three different optimum design methods is offered.

Examination of Table 19 indicates that the fully stressed design method fails on Problems 1C and 1D. It is also apparent that the ACCESS 1 results agree with those obtained using the method of inscribed hyperspheres (MIH) program reported in Ref. 72. The ACCESS 1 program is seen to be competitive and effective in obtaining correct solutions for this interesting set of stress limited single-load-condition problems. The set of active constraints for the final design given here for Problem 1A (see Table 18) includes minimum size constraints on members 2, 5, 6 and 10 as well as stress constraints in members 1, 3, 4, 7, 8 and 9. Note that the total number of critical constraints is equal to the number of independent design variables and each member is either stress critical or minimum size critical. For Problem 1B the set of active constraints is the same as that given above for Problem 1A except that the stress in member 10 is almost critical (i.e.  $\sigma_{10} = -29,870$ ). Examining the results in Table 18 reveals that the final designs obtained by ACCESS 1 for Problem 1C and 1D are identical. Furthermore, the set of active constraints does not involve either stress or minimum size

criticality of member 9. Indeed, since the stress constraint in member 9 is not critical at the final design obtained for Problem 1C, it follows that increasing the allowable stress for member 9 (e.g., from  $\pm 50,000$  to  $\pm 70,000$  lb/in<sup>2</sup>) should not influence the optimum design. The set of active constraints for the final design given for Problems 1C and 1D includes minimum size constraints on members 2, 5 and 6 as well as critical stress constraints in members 1,2,3,4,6,7,8 and 10. Note that the number of critical constraints is eleven, exceeding the number of independent design variables by one. It may be observed that in the final design for Problems 1C and 1D members 2 and 6 are fully stressed minimum size members while member 10 is fully stressed and as small as it can be consistent with equilibrium at node 1 (see Fig. 7). The results obtained by ACCESS 1 for Problems 1C and 1D recognize that members 6, 2 and 10 represent a less efficient load path than members 4 and 9 for transmitting the load applied at node 2 toward the supports. However, since the minimum size constraints prevent the elimination of members 2, 6 and 10 they are made as small as possible and fully stressed.

It is interesting to note that solutions for this set of problems with the minimum size constraints removed (i.e.,  $A_i \geq 0.1$  changed to  $A_i \geq 0$ ) can be readily obtained using the lower bound formulation given in Ref. 84. The method reported in Ref. 84 was used to obtain results from Problems 1A', 1B', 1C' and 1D' (i.e., Problems 1A, 1B, 1C and 1D with the minimum member size constraints removed). These results are given in Table 20 and they represent a set of four stable, statically determinant, fully-stressed designs with members 2, 5, 6 and 10 deleted. Comparing the results in Tables 18 and 20, it may be observed that as the allowable stress in member 9 is increased, the weight penalty associated with not being allowed to delete members increases.

A second stress-limited, single-load-condition example is now considered. This example, denoted Problem 2, is the same as Problem 1A except for the fact that a different loading condition is specified. Problem 2 is the ten bar planar truss depicted in Fig. 10 subject to the loading condition specified in Table 21 with allowable stress limits for all members given as  $\pm 25,000 \text{ lb/in}^2$  and minimum size limits set at  $A_i^{(L)} = 0.100 \text{ in}^2$ . Results obtained using both the CONMIN and the NEWSUMT versions of ACCESS 1 are shown in Table 22 along with the results reported for this problem in Refs. 31 and 72. The active constraints at the minimum-weight design are minimum member size for members 2, 5 and 10 while stress constraints are critical in members 1,3,4,6,7,8, and 9. Examination of Table 22 confirms that all four results are essentially the same for Problem 2. Note that while the CONMIN version of ACCESS 1 converges after only nine analyses, the final weight is 0.2% above the minimum weight, due to the fact that minimum size has not been achieved in members 2 and 10. It may also be observed that the number of analyses required to obtain the minimum weight using the NEWSUMT version of ACCESS 1 is the same as the number of analyses required to achieve this using the energy ratio recursive redesign procedure of Ref. 31. This may be viewed as particularly significant, since the energy ratio method is ideally suited to single load condition stress limited problems (with all members having the same allowable stress), while ACCESS 1 represents the implementation of a fundamentally more general approach.

#### 4.2.1.2 Stress and displacement limits, single load condition (Problems 3 and 4)

In this subsection two example problems involving the ten bar planar truss (see Fig. 10) under single loading conditions, but subject to stress, displacement and minimum member size constraints, are discussed. The first of

these two examples will be designated herein as Problem 3 and it is in fact the same as Problem 1A (see Section 4.2.1.1) except for the addition of vertical displacement limits equal to  $\pm 2.0$  inches at nodes 1 through 4 (see Fig. 10 and Table 23). In summary, Problem 3 involves the ten bar planar truss of Fig. 10 under the single loading condition given in Table 16, subject to the stress, displacement and minimum member limitations specified in Tables 17, 23 and 14, respectively (i.e.,  $\pm 25,000$  lbs/in<sup>2</sup>,  $\pm 2.0$  inches, and 0.100 in<sup>2</sup>). Results obtained using the NEWSUMT and CONMIN versions of ACCESS 1 are shown in Table 24 along with results reported in Refs. 72, 31, and 34.

For the designs obtained with ACCESS 1 and the design given in Ref. 72 the active constraints are the downward vertical deflections at nodes 1 and 2 as well as minimum member size constraints for members with cross sectional areas approaching 0.100 in<sup>2</sup> (i.e., members 2, 5 and 6 and 10). Examination of Table 24 reveals that while there are some small differences in material distribution all six results yield final weights that differ by less than 0.72%. It may also be observed that the number of analyses required to obtain a near optimum final design, using the NEWSUMT and CONMIN versions of ACCESS 1, is smaller than the number of analyses required to achieve comparable weights using the methods reported in Refs. 72, 31, and 34.

Iteration histories for the solutions given in Table 24 are presented in Table 25, and several histories are plotted in Fig. 11. Of the six iteration histories given in Table 25 the ACCESS 1 CONMIN history exhibits the strongest convergence and the ACCESS 1 NEWSUMT (Double Precision) history achieves the lowest weight. It should be noted that this problem has recently been studied further using various recursive redesign procedures based on stress

ratio and optimality criteria concepts (see Ref. 83). Since complete results including iteration histories are given in Ref. 83, it will suffice here to simply enumerate the final weights achieved and the number of analyses needed. Applying various recursive redesign procedures the following results for Problem 3 are reported in Ref. 83: namely 5112.13 lbs. in 18 analyses; 5192.57 lbs. in 24 analyses; 5092.19 in 40 analyses; 5409.52 lbs. in 23 analyses; 5064.27 lbs. in 37 analyses; 5063.99 lbs. in 46 analyses; 5077.40 lbs. in 21 analyses; and 5061.86 lbs. in 28 analyses. It is significant that the single precision NEWSUMT version of ACCESS 1 obtains a design that is within 1% of the lowest weight reported for this problem in only nine analyses. Furthermore, after twelve analyses the double precision NEWSUMT version of ACCESS 1 obtains a design that is within 0.3% of the lowest weight reported in Ref. 83.

The second example problem presented in this subsection will be designated as Problem 4 and it is the same as Problem 2 (see Section 4.2.1.1) except for the addition of vertical displacement limits equal to  $\pm 2.0$  inches at nodes 1 through 4 (see Fig. 10 and Table 23). In summary, Problem 4 deals with the ten bar planar truss shown in Fig. 10, subject to the single loading condition specified in Table 21, with the stress, displacement and minimum member limitations stipulated in Tables 17, 23 and 14, respectively (i.e.,  $\pm 25,000$  lbs/in<sup>2</sup>;  $\pm 2.0$  inches, and  $0.100$  in<sup>2</sup>). Design optimization results obtained for Problem 4 using the NEWSUMT and CONMIN versions of ACCESS 1 are presented in Table 26 along with results reported in Refs. 72 and 31. This problem is not dealt with in either Ref. 34 or Ref. 83.

For the designs obtained with ACCESS 1 and the design given in Ref. 72 the active constraints are the downward vertical deflection at node 2, tension stress constraints in members 5 and 6, as well as minimum member size constraints for members 2, 5 and 10. Examination of Table 26 reveals that all

three results obtained using various versions of ACCESS 1 are essentially the same. The material distributions found in Refs. 72 and 31 differ somewhat from that obtained using ACCESS 1. Note that the NEWSUMT version of ACCESS 1 obtains a final design weighing 4677 lbs in eleven analyses while the final result given in Ref. 31 has a weight of 4895.6 lbs after thirteen analyses. This result is 4.6% heavier than the lowest weight achieved using the NEWSUMT version of ACCESS 1. The CONMIN version of ACCESS 1 converges in nine analyses to a design that is 0.15% heavier than the lowest weight NEWSUMT design reported. The method of inscribed hyperspheres algorithm, used in Ref. 72, converges in 23 analyses to a design that is 0.32% heavier than the best weight obtained. It should be noted that the method reported in Ref. 72 represented a significant advance in efficiency over previously reported optimum design capabilities, based on combining finite element structural analysis and mathematical programming techniques. Nevertheless, it is apparent from the iteration history data presented herein (see Tables 25 and 27 as well as Figs. 11 and 12) that significant further efficiency improvement has been achieved during the development of ACCESS 1.

Iteration histories for the solutions given in Table 26 are presented in Table 27 and four of these histories are plotted in Fig. 12. Of the five histories given in Table 27 the ACCESS 1 CONMIN history exhibits the most rapid weight reduction while the ACCESS 1 NEWSUMT history achieves the lowest weight design. It is significant that all three ACCESS 1 solutions achieve a weight within 1% of the lowest weight reported for Problem 4 after only seven analyses.

Before closing this subsection it may be useful to explain why in Tables 24 and 26 the number of analyses needed is always one greater than the final

number of analyses indicated in the iteration histories (see Tables 25 and 27 or Figs. 11 and 12). The reason for this is that for all of the methods shown an extra analysis is always executed to insure that the final design given is acceptable. Whenever the extra analysis indicates any slight constraint violation, the final design is scaled up so that the results presented are always feasible. Finally, it may be noted that the slight weight increase on the CONMIN iteration history in Fig. 9 is due to a design scale up, which occurred when it was discovered that the design obtained using the 5th approximate problem statement was infeasible with respect to the actual constraints.

#### 4.2.2 Twenty-Five-Bar Space Truss (Problem 5)

Attention is now directed to the 25-bar space truss shown in Fig. 13. Special attention is called to the fact that member 1 joining nodes 1 and 2 is parallel to the x axis, since the drawings in Refs. 72, 31 and 34 are ambiguous. The nodal coordinates describing the layout of this much studied example problem are listed in Table 28. Herein, it will be assumed that this structure is to be symmetric with respect to both the x-z and the y-z planes in Fig. 13. This same assumption is made in Refs. 72 and 34. In Ref. 31 these symmetry conditions are not imposed, but the structure is subject to a set of six loading conditions that are reflections and rotations of the two load conditions used here (and in Refs. 72 and 34), such that the problems are equivalent. It may be noted in passing, that when all members are assumed to have the same initial size the designs generated at each iteration in Ref. 31, considering six load conditions, will be symmetric with respect to the x-z and the y-z planes in Fig. 13. The truss element descriptors including design variable linking group number, initial cross sectional area ( $A_i^{(0)} = 2.0 \text{ in}^2$ ), minimum member size ( $A_i^{(L)} = 0.01 \text{ in}^2$ ), configuration group number, and

and nodal connectivity are listed in Table 29. The side constraint code -1 in Table 29 indicates that only lower limit side constraints are imposed on member sizes and therefore no upper limit areas ( $A_i^{(U)}$ ) are given. It is observed that this example, which will be designated as Problem 5, has eight independent design variables after linking in order to impose symmetry. The displacements at nodes 7,8,9 and 10 are set to zero and it then becomes apparent that the displacement method analysis of this space truss involves eighteen independent displacement degrees of freedom. The displacement boundary conditions are specified in Table 30, where +1 denotes a fixed boundary condition. The two distinct loading conditions applied in Problem 5 are stipulated in Table 31. The material properties for each configuration group are given in Table 32. These include allowable stresses in tension ( $+40,000 \text{ lb/in}^2$ ) and compression (see Table 32) as well as the specific weight ( $0.1 \text{ lb/in}^3$ ) and the modulus of elasticity ( $10 \times 10^6 \text{ lb/in}^2$ ). In addition to the stress and minimum size constraints, displacement limits of  $\pm 0.35$  inches are imposed on nodes 1 through 6 in the x, y and z directions. In any event, Problem 5 has been stated here so that it is identical with the problem treated in Refs. 34 and 72. In summary, Problem 5 deals with the 25-bar space truss of Fig. 13 under the two distinct load conditions given in Table 31, subject to the stress and minimum member size limitations specified in Tables 32 and 29, respectively, as well as displacement limits of  $\pm 0.35$  inches on nodes 1 through 6 in the x, y and z directions.

The allowable compressive stresses given in Table 32 are identical with those given in Ref. 34 (Table III p. 62) and subsequently used in Ref. 72 for comparison purposes. It should be noted that the allowable compression

stresses used in Ref. 31 are the same as those given in Table 32 except that for configuration groups four and five  $\sigma_{\ell}^{(L)} = -2200 \text{ lb/in}^2$  while in configuration groups six and seven  $\sigma_{\ell}^{(L)} = -6016 \text{ lb/in}^2$ . It turns out that these discrepancies in the allowable compressive stresses used have only a small effect on the final designs obtained. This is due to the fact that the members (10, 11, 12 and 13) in configuration groups 4 and 5 are lightly loaded while the differences in the allowable compressive stresses used for the members in configuration groups 6 and 7 are not very large. It may be noted that a consistent set of compressive stress allowables can be calculated by adopting the procedure suggested on p. 73 of Ref. 21. Using the Euler buckling formula and assuming thin walled tubular members, with a maximum mean radius of two inches, leads to the following formula for the allowable compressive stress

$$\sigma_{cr} = -\frac{\pi^2 ER^2}{2\ell^2} = -\frac{\pi^2 \times 10^7 \times 2^2}{2\ell^2} \quad (4.1)$$

Substituting the appropriate member lengths into Eq. (4.1) yields the allowable compressive stresses given in Table 32, except that the entries for configuration groups 6 and 7 would be changed to  $-6016 \text{ lb/in}^2$ . If this change were made, configuration groups 6 and 7 would coalesce. Examination of Table 32 also reveals that configuration groups 1, 4 and 5 could be combined into a single configuration group.

Results obtained for Problem 5 using the NEWSUMT and CONMIN versions of ACCESS 1 are shown in Table 33 along with results reported in Refs. 72, 31 and 34. For the designs obtained with ACCESS 1 and the design given in Ref. 72 the active constraints are the y components of displacement at nodes 1 and 2 under both load conditions as well as the compressive stress in member 20 under load condition 2. All five final designs shown in Table 33 are nearly the same. The CONMIN result has a weight that is 0.61% higher than the lowest weight achieved, due primarily to the fact that the members in configuration groups 1, 4 and 5 have not fully converged to minimum size.

Iteration histories for the final designs given in Table 33 are listed in Table 34 and shown graphically in Fig. 14. In this instance the iteration history of Ref. 34 exhibits the most rapid weight reduction while ACCESS 1-NEWSUMT finds a design that is within 0.5% of the minimum weight design after only five analyses. Figure 14 reveals that the ACCESS 1 iteration histories are competitive with those obtained using recursive redesign procedures based on stress ratio and optimality criteria concepts (see Refs. 31 and 34). If attention is restricted to previously reported results based on combining finite element structural analysis with mathematical programming techniques, the efficiency gains that have been achieved with the introduction of approximation concepts, are seen to be dramatic. Specifically, for Problem 5 a weight of 552.9 pounds after 85 analyses was achieved using the program discussed in Ref. 23 (1971), a weight of 545.22 pounds after 14 analyses was reported in Ref. 72 (1974), while with ACCESS 1-NEWSUMT it has been possible to obtain a weight of 545.39 pounds after 7 analyses.

#### 4.2.3 Seventy-Two-Bar Space Truss (Problem 6)

In this section consideration is given to the 72-bar space truss shown in Fig. 15. The nodal coordinates describing the layout of this well studied example problem are specified in Table 35. The truss element descriptors including design variable linking group number, initial cross sectional area ( $A_1^{(0)} = 1.0 \text{ in}^2$ ), minimum member size ( $A_1^{(L)} = 0.1 \text{ in}^2$ ), configuration group number, and nodal connectivity are listed in Table 36. It is observed that this example, which will be designated as Problem 6, has sixteen independent design variables after linking. It is also interesting to note that this structure involves only four independent configuration group numbers, since all members are to have the same material properties and there

are only four distinct bar lengths. Therefore, Problem 6 as stated in Table 36, will require storage of only four local stiffness matrices (see Section 3.3.4). It should be noted that truss members can only be treated as belonging to the same configuration group when both their length and material properties are identical. The displacements at nodes 17,18,19 and 20 are set to zero and it is then apparent that the displacement method analysis of the truss depicted in Fig. 12 involves 64 independent displacement degrees of freedom. The displacement boundary conditions are specified in Table 37, where +1 denotes a fixed boundary condition. The two distinct loading conditions applied in Problem 6 are specified in Table 38. The material properties for each configuration group ( $\lambda$ ) are given in Table 39. These include the allowable stresses in tension and compression ( $\pm 25,000 \text{ lb/in}^2$ ), the specific weight ( $0.1 \text{ lb/in}^3$ ), and the modulus of elasticity ( $10 \times 10^6 \text{ lb/in}^2$ ). In addition to the stress and minimum size constraints, displacement limits of  $\pm 0.25$  inches are imposed on nodes 1 through 16 in the x,y and z directions.

Results for Problem 6, obtained using the NEWSUMT and CONMIN versions of ACCESS 1 are presented in Table 40 along with results reported in Refs. 72, 31, 34 and 83. For the designs obtained with ACCESS 1 the critical constraints are the compressive stress in members 1 through 4 under load condition two, the x and y displacements of node 1 under load condition 1 and the minimum member size requirements for the members of linking groups 7, 8, 11, 12, 15 and 16. Note that the members in planes parallel to the x-y base plane (see Fig. 15) become minimum size members, except for those in the top level plane. The final designs obtained using the NEWSUMT and CONMIN versions of ACCESS 1 are nearly the same while the previously reported material distributions differ somewhat from one another. The final designs reported in Refs. 72 and 34 exceed the lowest weight obtained with ACCESS 1 by 2.37% and

4.31%, respectively. It is also apparent that the weight and material distribution reported in Ref. 83 are almost the same as those obtained with ACCESS 1.

Iteration histories for the final designs given in Table 40 are listed in Table 41 and shown graphically in Fig. 16. The ACCESS 1 - CONMIN history and that reported in Ref. 83 exhibit rapid weight reduction in the first three iterations. It should be noted that the short iteration history reported in Ref. 83 was obtained by imposing small tolerances on the permissible weight increase. This type of convergence criteria would appear to implicitly assume that as soon as the method of Ref. 83 produces a weight increase further net weight reduction can not be achieved by continued iteration. On balance, it is clear from Table 41 and Fig. 16 that both the NEWSUMT and CONMIN versions of ACCESS 1 are competitive (measured in terms of the number of analyses needed to converge) with the automated redesign methods reported in Refs. 31, 34 and 83.

#### 4.2.4 Truss Idealization of Wing-Carry-Through Structure (Problem 7)

The example problem treated in this section, designated Problem 7 herein, was set forth in Ref. 83. The system considered represents a highly idealized truss element modeling (see Fig. 17) of the wing-carry-through box for a heavy, swing-wing aircraft. According to Ref. 83, "the loads are derived from a 2g condition of a half million pounds aircraft and from two assumed wing positions." Quoting further from Ref. 83, "The idealization is kept oversimplified to reduce the number of variables to a level that invites competitive solutions by other methods. Only bars are used in the modeling for the same reason. In any other candidate modeling there would be elements, e.g. shear panels, that are not unique in every program and the differences in the force displacement behavior would be aggravated during sizing iterations clouding

comparisons." In what follows the problem statement given in Ref. 83 is repeated for completeness, the invitation extended in Ref. 83 is accepted, and competitive solutions obtained with the ACCESS 1 program are presented and compared with those given in Ref. 83.

The truss idealization of the wing-carry-through structure shown schematically in Fig. 14 employs 63 truss elements and since design variable linking was not used in Ref. 83, the problem involves 63 independent design variables. The nodal coordinates describing the layout of this truss structure are specified in Table 42. The truss element descriptors including design variable linking group number (same as member number in this instance), initial cross sectional area ( $A_1^{(0)} = 20.0 \text{ in}^2$ ), minimum member size ( $A_1^{(L)} = 0.01 \text{ in}^2$ ), configuration group number, and nodal connectivity are listed in Table 43. The displacement at nodes 15, 16, 17, and 18 are set to zero and it is then apparent that the displacement method analysis of this 63 bar truss involves 42 independent displacement degrees of freedom. The displacement boundary conditions are specified in Table 44, where +1 denotes a fixed boundary condition. The two independent loading conditions applied in Problem 7 are specified in Table 45. The material properties (titanium alloy) are the same for all members. They include the allowable stresses in tension and compression ( $\pm 100,000 \text{ lb/in}^2$ ), the specific weight ( $0.16 \text{ lb/in}^3$ ), and the modulus of elasticity ( $16 \times 10^6 \text{ lb/in}^2$ ). The problem as stated was solved first without displacement constraints of any kind (i.e., Problem 7A Stress Constraints Only). Then the same problem was posed, except that the relative displacement of nodes 1 and 2 in the x direction (a measure of the rotation of the line 1-2 about a y axis in Fig. 14) was limited to 1.0 inch. Problem 7A with the addition of the foregoing relative displacement constraint is designated as Problem 7B. It should be noted that minor special modification of the standard ACCESS 1 program was required in order to handle the relative displacement constraint.

Results for Problems 7A and 7B obtained using the NEWSUMT version of ACCESS 1 are presented in Table 46 along with those reported in Ref. 83. Note that Problems 7A and 7B have been run twice using different control parameter values in the NEWSUMT version of ACCESS 1. In Table 46 the notation  $0.5 \times 2$  indicates that the cut factor  $c_a$  (see Eq. (3.65), Section 3.3.7.2) between unconstrained minimizations is set equal to 0.5 while 2 unconstrained minimizations are to be executed before updating the approximate problem statement. It is apparent from the results in Table 46 and the iteration history data given in Table 47 that the NEWSUMT version of ACCESS 1 converges more rapidly but to slightly higher weights when the control parameters are  $0.05 \times 1$  rather than  $0.5 \times 2$ . At the final design obtained for Problem 7A, using ACCESS 1 NEWSUMT ( $0.5 \times 2$ ), there are fifty six critical constraints, namely: minimum member size for 19, 20, 60, 61 and 62; tension stress load condition 1 for members 2, 4, 6, 8, 10, 12, 14, 16, 17, 23, 28, 29, 52, and 56; tension stress load condition 2 for members 27, 31, 32, 35, 36, 39, 40, 43, 44, 47, 48, and 55; compression stress load condition 1 for members 1, 3, 5, 7, 9, 11, 13, 15, 18, 24, 25, 50, and 51; and compression stress load condition 2 for members 26, 30, 33, 34, 37, 38, 41, 42, 45, 46, 49, and 54. The members that are not critical with respect to either minimum size or stress constraints are 22, 29, 53, 57, 58, 59 and 63. At the final design obtained for Problem 7A using ACCESS 1 NEWSUMT ( $0.05 \times 1$ ), the critical constraints follow substantially the same trend except for the following. Minimum member sizes for 20, 60, 61, 62 and stress constraints on 21, 25, 27, 31, 37, 38 and 39 are no longer critical and the member 29 becomes critical in tension for load condition 1. At the final design obtained for Problem 7B, using ACCESS 1 NEWSUMT ( $0.5 \times 2$ ), there are thirty three critical constraints, namely: relative displacement of nodes 1 and 2 in the x direction under load condition 2; minimum member size for 19, 20, 23, 24,

25, 29, 60, 61 and 62; tension stress load condition 1 for members 2, 4, 6, 8, 10, 12, 14, 16, 17, 21, 28 and 29; and compression stress load condition 1 for members 1, 3, 5, 7, 9, 11, 13, 15, 18, 50 and 51. At the final design obtained for Problem 7B using ACCESS 1 NEWSUMT ( $.05 \times 1$ ), the critical constraints follow essentially the same trend, except minimum size constraints on members 24, 25, 29, 60, 61 and 62, tensile stress constraints on members 21, 29, and compressive stress constraints on members 9 and 50 are no longer critical. It is interesting to note that for Problem 7B none of the members are found to be stress critical under load condition 2.

Iteration histories for the ACCESS 1 solutions of Problems 7A and 7B, and those reported in Ref. 83 are given numerically in Table 47 and presented graphically in Fig. 18. For Problems 7A and 7B it is seen that the ACCESS 1 NEWSUMT ( $.05 \times 1$ ) runs first achieve a lower weight than the method of Ref. 83 after 3 analyses. After eight analyses these two ACCESS 1 runs converge to weights that are 5.2% and 3.7% lighter than the weights reported in Ref. 83 after eight analyses. The final weights for Problems 7A and 7B reported in Ref. 83 after 50 analyses are still slightly higher than the best result obtained using ACCESS 1. It is also observed that the iteration histories obtained for Problems 7A and 7B using ACCESS 1 NEWSUMT ( $.5 \times 2$ ) exhibit somewhat slower convergence than those generated using the ( $.05 \times 1$ ) control parameter setting. Using the ( $.5 \times 2$ ) control parameter setting, the ACCESS 1 NEWSUMT runs for Problems 7A and 7B converge after 14 analyses to designs that are only slightly lighter than those obtained with the ( $0.05 \times 1$ ) parameter setting. The iteration history data given in Table 47 and plotted in Fig. 18 demonstrates that for this 63 design variable problem ACCESS 1 is competitive (measured in terms of the number of analyses needed to converge) with the automated redesign methods applied to this problem in Ref. 83. It is

perhaps noteworthy that imposing small tolerances on the permissible weight increase (the convergence criteria used in Ref. 83 on the 72 bar truss problem) would lead to premature termination in Problems 7A (i.e., after 8 analyses with  $W_7 = 5255$  lbs) and in Problem 7B (i.e., after 4 analyses with  $W_3 = 6884$  lbs).

#### 4.3 Idealized Wing Structures

In the previous section of this chapter it has been shown that ACCESS 1 offers a reliable and efficient means of obtaining minimum-weight designs for truss structures subject to static loadings with stress, displacement, and minimum size constraints. Attention is now focused on some idealized wing structures where the finite element model includes constant strain triangular (CST) elements and symmetric shear panel (SSP) elements. The first example problem to be discussed herein is a simple, 18 element wing box problem for which results have been previously reported in Refs. 34 and 21. The second example treated is an idealized representation of a swept wing subject to two distinct load conditions. This example is treated using CST elements to represent the wing skins, SSP elements for the shear webs, and TRUSS elements for the spar caps. The swept wing problem is initially studied omitting the spar caps. Subsequently leading and trailing edge spar caps are included. The third and final example problem involves an idealized thin delta wing, similar to the titanium alloy wing considered in Refs. 53 and 55. The upper half of this midsurface-symmetric wing is modeled using CST elements to represent the skin and SSP elements for the shear webs. The wing is subject to a single load condition and stress, displacement and minimum gage constraints are included. Using the delta-wing example, the influence of changing the number of independent design variables on the minimum weight achieved is explored.

##### 4.3.1 Eighteen Element Wing Box Beam (Problem 8)

Consider the idealized wing box beam shown in Fig. 2 that has been previously studied in Refs. 21 and 34. This example was also used to illustrate the data input requirements of ACCESS-1 in Section 3.3.3 of this report. The structure is symmetric with respect to the x-y plane which corresponds to

its middle surface. The upper half of the box beam is idealized using TRUSS, CST, and SSP elements.

#### 4.3.1.1 Detailed Problem Statement

The nodal coordinates describing the layout of the box beam were given previously in Table 2.

The truss element descriptors including design variable linking group number (same as truss member number because truss members are not linked in this example), initial cross sectional area ( $A_i^{(0)} = 0.98 \text{ in}^2$ ), configuration group number, and nodal connectivity were given previously in Table 3. The side constraint code -1 in the last column of Table 3 indicates that only lower limit side constraints ( $A_i^{(L)} = 0.10 \text{ in}^2$ ) are imposed on truss member sizes, even though upper limit values ( $A_i^{(U)} = 2.00 \text{ in}^2$ ) are included in Table 3 for the illustrative purposes of Section 3.3.3.

The box beam skin is modeled using five CST elements with appropriate linking so that the skin thickness is uniform in each of the two rectangular regions (1,2,4,3) and (3,4,6,5) (see Fig. 5). Table 4 specifies the design variable linking, the initial thickness ( $t_i^{(0)} = 0.1960 \text{ in}$ ), the minimum thickness ( $t_i^{(L)} = 0.020 \text{ in}$ ), the configuration number and the nodal connectivity of the CST elements for the first of two CST models. An alternative modeling of the box beam skin which also employs five CST elements is shown in Fig. 19, and the corresponding element descriptors are given in Table 48. The example with the CST modeling of Fig. 5 is designated Problem 8A; the example with the alternate modeling shown in Fig. 19 is designated Problem 8B. It should be noted that in Ref. 21 the box beam skin was modeled using two quadrilateral (1,2,4,3) and (3,4,6,5) and one triangular element (5,6,7).

The SSP element descriptors were previously specified and they are given in Table 5. The 18 element wing box example is seen to involve sixteen independent design variables; namely 5 for the bars, 3 for the skin and 8 for the shear webs. Referring to either Fig. 5 or Fig. 19, the displacements at nodes 1 and 2 are set to zero and it is apparent that the displacement method formulation involves fifteen independent displacement degrees of freedom. The TRUSS, CST and SSP element material properties were given previously in Tables 6, 7 and 8, respectively. The displacement boundary conditions were specified in Table 9 (nodes 1 and 2 are fixed). The two independent load conditions were given in Table 10, namely  $P_z = +5000$  lb at node 7 for load condition 1 and  $P_z = 10,000$  lb at node 5 for load condition 2. The displacement constraints previously given in Table 11 require the z deflection at the unsupported nodes to fall between -2 inches and +2 inches.

#### 4.3.1.2 Results and Discussion

Results for Problem 8 have been obtained using the NEWSUMI version of ACCESS 1 and they are presented in Table 49 along with the results reported in Refs. 34 and 21. In Table 49 the first column of ACCESS 1 results (Problem 8A) is based on the finite element model shown in Fig. 5 (Model 1) while the second column (Problem 8B) was obtained with the finite element model shown in Fig. 19 (Model 2). It is interesting to note that changing the idealization of the skin panel produces some moderate changes the final material distribution. Nevertheless, comparing the final weights obtained using models 1 and 2 (see Table 49), it is clear that they differ by less than 0.10%. It should be noted that all the weights shown in Tables 49 and 50 include the material above and below the x-y plane of symmetry (see Fig. 5 and/or Fig. 19).

The first two columns of ACCESS 1 results given in Table 49 exhibit final design weights that are approximately 3.7% heavier than those reported

in Refs. 34 and 21 (see the last two columns of results in Table 49). Examining Table 49 it is observed that the thicknesses of the SSP elements 1,2,3 and 4 (first two columns of ACCESS 1 results) are substantially higher than those reported in Refs. 34 and Ref. 21. This difference is attributed to the fact that in Refs. 34 and 21 pure shear webs are used (normal stresses  $\sigma_x$  and  $\sigma_y$  are assumed zero). Analyses of the final designs reported in Refs. 34 and 21 using SSP elements for the webs indicates violation of the combined stress constraints in SSP elements (i.e. in SSP elements 3,4 and 5 under load condition 1 and in SSP elements 1 and 2 under load condition 2). In an effort to obtain better agreement with the results reported in Refs. 34 and 21 a special modification of the NEWSUMT version of ACCESS 1 was made, adding a midplane-symmetric pure shear element. The third column of ACCESS 1 results (Problem 8C) shown in Table 49 (CST Model 1, pure shear webs) was obtained using this modified version of the program. It is noted that the weight of the final design achieved is approximately 7.7% lighter than the results previously reported in Refs. 34 and 21. The material distribution obtained using the modified version of ACCESS 1, while different from those reported in Refs. 34 and 21, exhibits a similar trend particularly in the shear webs.

The results for Problem 8 summarized in Table 49 point up the fact that optimum designs can be rather sensitive to changes in finite element idealization. If attention is focused on the three results obtained using ACCESS 1 it is seen that changing from CST Model 1 with SSP web elements (Problem 8A) to CST Model 1 with pure shear web elements (Problem 8C) produces an 11% difference in the minimum weight achieved. On the other hand, changing the CST skin modeling from Model 1 (Fig. 5) to Model 2 (Fig. 19), while using SSP elements for the webs in both cases, has almost no effect on the minimum weight achieved.

For the final designs obtained by applying the NEWSUMT version of ACCESS 1 to Problem 8 (see Table 49) the critical constraints are now identified. The final design obtained using CST Model 1 (see Fig. 5) with SSP web elements (Problem 8A) has the following critical constraints: minimum member size for TRUSS elements 2,3,5 and SSP elements 6,7; vertical (plus z direction in Fig. 5) displacement at node 7 under load condition 1; combined stress criteria in CST element number 5 under load condition 1; combined stress criteria in SSP elements 3,4,5,8 under load condition 1 and in SSP elements 1,2 under load condition 2. The final design obtained using CST Model 2 (see Fig. 19) with SSP web elements exhibits a collection of critical constraints which is the same as the foregoing set (for the CST Model 1 with SSP web elements) except for the addition of one constraint, namely combined stress criteria in CST element 4 under load condition 1. The final design obtained using CST Model 1 with pure shear web elements has the same minimum member size and displacement constraints as the two foregoing cases, however there are, strictly speaking, only two stress critical elements — namely combined stress criteria in CST element 2 under load condition 2 and compressive stress in TRUSS element 1 under load condition 2. When these three sets of critical constraints are qualitatively assessed it is gratifying to find that they are physically and intuitively reasonable.

Iteration histories for the ACCESS 1 (NEWSUMT version) solutions of problem 8 and the history reported in Ref. 34 are given numerically in Table 50 and illustrated graphically in Fig. 20. Iteration history data is not given in Ref. 21. However, the total number of analyses required to achieve convergence using the program reported in Ref. 21 has been reported in Ref. 34. The iteration histories for Problems 8A and 8B are rather similar and they converge (after 8 and 10 analyses, respectively) to final weights that differ by only 0.10%. Although the minimum weight achievable is apparently

insensitive to the change made in the cover skin modeling (see Figs. 5 and 19), it should be noted that the final material distributions found in Problems 8A and 8B are somewhat different.

Turning attention to the iteration history given for Problem 8C (see Table 50 and Fig. 20), it is seen that after only three analyses ACCESS 1 has achieved a weight that is lower than the best weight found in Ref. 34 after fifteen analyses. Since the finite element modeling used for Problem 8C is thought to be the same as that used in Ref. 34, the 7.8% difference in the minimum weights achieved must be attributed to some other cause. Comparison of the iteration history for Problem 8C with that reported in Ref. 34 indicates that ACCESS 1 is definitely competitive with the recursive redesign methods (based on stress ratio and optimality criteria concepts) used in Ref. 34.

#### 4.3.2 Swept Wing Example (Problem 9)

Consider the idealized swept wing structure shown in Fig. 21. The structure is taken to be symmetric with respect to the x-y plane which corresponds to the wing middle surface. The upper half of the swept wing is initially modeled using sixty CST elements to represent the skin and seventy SSP elements for the vertical webs. This problem, with no spar caps, is run starting from two different initial designs. Subsequently twenty TRUSS elements are added to represent forward and aft spar caps (see cross sectional view in Fig. 21). The swept wing problem, including spar caps, is also run starting from two distinct initial designs. Extensive, but plausible, design variable linking is employed. The number of independent design variables describing the skin, web and spar cap material distributions are 7, 11, and 14, respectively. Therefore when the wing is modeled using only CST and SSP elements the problem

involves a total of 18 design variables and when the spar caps are added the total number of independent design variables increases to 32. The wing is subject to two distinct static load conditions. In this example material properties representative of a typical aluminum alloy are used.

#### 4.3.2.1 Detailed Problem Statement

The nodal coordinates defining the layout of the idealized structure depicted in Fig. 21 are given in Table 51. The truss element descriptors including the design variable linking group number, the configuration group number, and the nodal connectivity are specified in Table 52. Truss elements appear only when spar caps are used. The side constraint code +2 in the last column of Table 52 indicates that both lower ( $A_i^{(L)} = 0.01 \text{ in}^2$ ) and upper ( $A_i^{(U)} = 1.50 \text{ in}^2$ ) limits are to be imposed on the TRUSS member sizes. The TRUSS member initial cross-sectional area is taken to be  $A_i^{(o)} = 0.02 \text{ in}^2$ .

The CST element descriptors are listed in Table 53. Note that for the CST elements only minimum thickness limits are specified (i.e.,  $t_i^{(L)} = 0.02 \text{ in.}$ ), which is why the side constraint code is -1 in the last column of Table 53. Initial thickness data is also given in Table 53 for two distinct starting points in the design space. For initial design I the 24 CST elements nearest the wing root are given a thickness of 0.20 inches (i.e.,  $t_i^{(o)} = 0.20$  inches for  $i = 1, 2, \dots, 24$ ) while the remaining 36 CST elements are assigned a thickness of 0.10 inches (i.e.,  $t_i^{(o)} = 0.10$  inches for  $i = 25, 26, \dots, 60$ ). For initial design II all of the CST elements are set equal to 0.30 inches (i.e.,  $t_i^{(o)} = 0.30$  inches for  $i = 1, 2, \dots, 60$ ).

The SSP element descriptors are enumerated in Table 54. Here again only minimum thickness limits are stipulated, namely  $\tau_i^{(L)} = 0.02$  inches.

Initial thicknesses for two distinct starting point designs are specified in Table 54. For initial design I all SSP elements are taken to have a thickness 0.20 inches (i.e.,  $\tau_i^{(0)} = 0.20$  inches for  $i = 1, 2, \dots, 70$ ) while for initial design II all SSP element thicknesses are set equal to 0.15 inches (i.e.,  $\tau_i^{(0)} = 0.15$  inches  $i = 1, 2, \dots, 70$ ).

The idealized swept wing depicted in Fig. 21 is supported at the root by setting all displacement components at nodes 1, 2, 3 and 4 to zero. These displacement boundary conditions are specified in Table 55 using the boundary condition code described in Section 3.3.3. When the spar caps are neglected, the swept wing is represented by a total of 130 finite elements (60 CST's and 70 SSP's). With the addition of 20 TRUSS elements to represent forward and aft spar caps, the total number of finite elements involved in the model become 150. That is the basis for the 150(130) notation in the tables. Referring to Fig. 21 it is apparent that, independent of whether or not spar caps are included, the number of displacement degrees of freedom involved in the structural analysis is 120.

The material properties used for all finite elements of all types are given in Table 56. The nodal load force components specifying the two independent load conditions are listed in Table 57. Note that only the  $P_z$  components are given since all of the x and y components are taken to be zero in both of the two independent loading conditions. Displacement constraints are imposed at nodes 41 and 44 only and they require that these two z displacement components fall between -60 and +60 inches.

#### 4.3.2.2 Results and Discussion

Results for Problem 9 have been obtained using the NEWSUMT version of ACCESS 1 and they are presented in Table 58. In Table 58 the first two columns of results are for the 130 element idealization (without spar caps) starting

from initial design I and II, respectively. These first two problems are denoted Problems 9A and 9B, respectively. Comparing these two results it is observed that the final skin material distributions (see CST elements Table 58) are quite similar and they are both represented by a single line in the skin thickness plot shown in Fig. 22. On the other hand it is seen (see SSP elements Table 58) that the final vertical web thickness distributions locally exhibit some substantial differences, particularly in the outboard portion of the wing (see Fig. 23 which schematically depicts the two web thickness distributions). It is noted that the web material accounts for less than 12% of the final wing weight in both cases. The differences in the web thickness distributions notwithstanding, it is gratifying to see that the final weights achieved (with no spar caps starting from initial designs I and II) are essentially the same (i.e., they differ by only 0.34%).

In Table 58 the third and fourth columns of results are for the 150 element idealization of the swept wing (with spar caps) starting from initial designs I and II, respectively. The third and fourth problems are denoted Problems 9C and 9D, respectively. Comparing these two results it is observed that the final skin material distributions (see CST elements Table 58) are quite similar and they are represented by a single line in the skin thickness plot shown in Fig. 22. It is seen (see TRUSS and SSP elements Table 58) that the spar cap and vertical web material distributions locally exhibit some substantial difference. The two vertical web material distributions are shown schematically in Fig. 24 and it is again observed that local differences in web thickness are more pronounced in the outboard portion of the wing. It is observed that the forward spar cap members (TRUSS elements 1-10 in Table 58) are near their minimum size ( $A_1^{(L)} = 0.01 \text{ in}^2$ ) while the aft spar cap members (TRUSS elements 11-20 in Table 58) are larger with the member at the root reaching the maximum size  $A_1^{(U)} = 1.50 \text{ in}^2$ . It is noted that the spar cap

material accounts for less than 0.5% of the final wing weight while the web material accounts for approximately 12.5% of the final wing weight in both cases. The local differences in spar cap and web material distributions aside, it is satisfying to see that the final weights achieved (with spar caps starting from initial designs I and II) are essentially the same (i.e., they differ by only 0.40%).

The results given in Table 58 and in Fig. 22 indicate that the addition of the twenty TRUSS elements to represent forward and aft spar caps does not have a significant influence on the minimum weight achieved. The skin thickness distribution (except for the panel nearest the root, i.e. CST elements 1 through 6) is not substantially changed by the addition of spar caps.

For the four final designs obtained by applying the NEWSUMT version of ACCESS 1 to Problem 9 (swept wing example) it is found that the set of critical constraints is the same. Thus while the material distributions for the four final designs (see Table 58) exhibit some local differences, the final weight and the critical constraint set are essentially unchanged. The critical constraints are depicted schematically in Fig. 25. The two final designs without spar caps have the following critical constraints: minimum member size for CST elements 49-60 and SSP elements 5-10, combined stress criteria in CST elements 8,14 and 20 under load condition 1; combined stress criteria in SSP elements 20,21,30,58 and 61 under load condition 1 and SSP elements 3,42 under load condition 2. In Fig. 25 both the critical finite elements and the linked design variable regions to which they belong are shown. The two final designs with spar caps exhibit the same set of critical constraints with the following additions: minimum area for TRUSS members 1,2,5,6,9,10,19 and 20. It is noted that none of the tip deflection constraints are found to be critical. The maximum tip deflection (approximately 45 inches) occurs at node 44 under load condition 1.

Since the tip deflection constraints are not critical it is reasonable to expect some stress critical elements at the wing root. In this connection it is noted that SSP element 21 (rear spar web element adjacent to the root) is strictly critical with respect to the combined stress criterion under load condition 1 while CST element 4 is nearly critical ( $\sigma_e/\sigma_a \approx 0.95$ ) under load condition 1. Since the SSP elements modeling the web includes bending as well as shear stress, it is reasonable to suppose that decreasing the root skin panel thickness will cause violation of the combined stress constraint by increasing the bending stress in SSP element 21. Furthermore, while increasing the thickness of the rear spar web would reduce the shear stress in SSP element 21, this would not be effective as a means of reducing the bending stress in SSP element 21. Thus it appears that the critical constraints are, on balance, physically and intuitively plausible when assessed qualitatively.

Iteration histories for the ACCESS 1 (NEWSUMT version) solutions of Problem 9 (swept wing example) are given numerically in Table 59 and illustrated graphically in Fig. 26. For Problem 9A (no spar caps initial design I) convergence occurs after 7 analyses and a design weight that is within 0.5% of the minimum weight achieved is obtained after only 4 analyses. In Problem 9B (no spar caps initial design II) convergence occurs after 7 analyses and a design weight within 0.5% of the minimum weight is obtained after 5 analyses. In Problem 9C (initial design I with spar caps) the design procedure is terminated after 8 analyses. After 4 analyses the design weight is within 0.5% of the minimum weight obtained. Finally, for Problem 9D (initial design II with spar caps) convergence occurs after 8 analyses and a design weight within 0.5% of the minimum weight achieved is obtained after 4 analyses.

It is emphasized that every weight, for all the iteration histories given in this report, is that of a feasible design. It should also be mentioned that all four swept wing runs (Problems 9A, 9B, 9C, and 9D) terminated automatically because the percentage change in the objective function value (prior to any scaling up) for two successive stages was less than 0.1%, as given by the input data. Note that since  $a' = 2$  for this example, each stage involves two unconstrained minimizations (in B dimensional space).

#### 4.3.3 Delta Wing Example (Problem 10)

Consider the idealized, thin, delta wing structure shown in Fig. 27. The structure is assumed to be symmetric with respect to its middle surface which corresponds to the x-y plane. The upper half of the wing is modeled using 63 CST elements to represent the skin and 70 SSP elements for the vertical webs. No TRUSS elements are used in the modeling. The wing is subject to a single static loading condition, the material properties used are representative of those for a typical titanium alloy and deflection constraints are specified at all free nodes. Five distinct runs are presented. They are denoted Problems 10A-10E. The runs differ in the design variable linking models and in the initial designs.

##### 4.3.3.1 Detailed Problem Statement

Various design variable linking models are employed. In the skin, three distinct linking arrangements designated I, II, and III leading to 10, 16, and 28 independent design variables, respectively, are employed (see Fig. 28). For the webs two alternative linking arrangements designated I and II involving 12 and 28 independent design variables, respectively, are employed (see Fig. 29). Results for five distinct runs will be presented (see Table 67). In Problems 10A and 10C skin linking arrangement II (i.e., 16 variables)

and web linking model I (i.e., 12 variables) are adopted. Problem 10A and 10C both involve a total of 28 independent design variables but Problem 10A starts from initial design II while Problem 10C starts with initial design I (see Tables 61 and 62). In Problem 10B skin linking arrangement I (i.e., 10 variables) and web linking model I (i.e., 12 variables) are employed. This 22 design variable problem is started from initial design I. In Problem 10D skin linking arrangement III (i.e., 28 variables) and web linking model I (i.e., 12 variables) are used. Thus Problem 10D involves 40 independent design variables and it is started from initial design I. Finally, Problem 10E employs skin linking model III (i.e., 28 variables) with web linking arrangement II (i.e., 28 variables). Thus Problem 10E, which starts from initial design I, involves a total of 56 independent design variables.

The nodal coordinates defining the layout of the idealized structure shown in Fig. 27 are specified in Table 60. The CST element descriptors are listed in Table 61. The three distinct skin design variable linking arrangements shown in Fig. 28 are specified in separate columns of Table 61. Note that only minimum thickness limits are specified (i.e.,  $t_1^{(L)} = 0.02$  in) for the CST elements. Furthermore, for initial design I all the CST elements are assigned a thickness of 0.10 inches and for initial design II they are set equal to 0.15 inches. It is interesting to observe that in this example the entire 63 element skin idealization involves only 5 configuration groups. The SSP element descriptors are enumerated in Table 62. The two alternative web design variable linking arrangements depicted schematically in Fig. 29 are stipulated in separate columns of Table 62. Here again only minimum thickness limits are specified, namely  $\tau_1^{(L)} = 0.02$  inches. Furthermore, for initial design I all the SSP element thicknesses are taken equal to 0.15 inches and for initial design II they are set equal to 0.12 inches.

The idealized delta wing shown in Fig. 27 is supported at the root by setting all displacement components at nodes 1 through 9 equal to zero. These displacement boundary conditions are specified in Table 63 using the boundary condition code described in Section 3.3.3. The remaining 35 nodes shown in Fig. 24 produce 105 degrees of freedom. Furthermore, the idealization employed involves a total of 133 finite elements (63 CST's and 70 SSP's). The material properties used for all finite elements of all types are given in Table 65. The nodal load force components specifying the single load condition are given in Table 64. Only  $P_z$  components are nonzero and the nodal loading given is roughly equivalent to a uniformly distributed load of  $144 \text{ lbs/ft}^2$ . In this connection it is noted that the delta wing examples dealt with here are roughly similar to those treated in Refs. 53 and 55.

Constraints are imposed on the vertical displacement components at all free nodes (i.e., 10 through 44). These displacement constraints are specified in Table 66 and it should be noted that they form a linear deflection constraint envelope varying from 100.8 inches at the wing tip to zero at the root. It is important to note that if only tip displacement constraints are specified, it is possible that the local displacements of nodes near the leading and trailing edges could become excessive (equal or exceed the tip deflection). Qualitatively this is attributed to the multiple load paths available in a delta wing. They offer the possibility of keeping the tip deflection within limits, while the structure in the neighborhood of the leading and trailing edges becomes rather flimsy, leading to excessive local deflections.

#### 4.3.3.2 Results and Discussion

Results for Problem 10 have been obtained using the NEWSUMT version of ACCESS 1 and they are presented in Table 67. The first and third columns of

results in Table 67 (Problems 10A and 10C) are based on skin linking arrangement II (16 design variables) and web linking arrangement I (12 design variables). Thus Problem 10A and 10C are the same except for the fact that 10A starts from initial design I (see Tables 61 and 62). Comparing these two results it is seen that both the skin and the web material distributions are almost identical to three decimal places. Furthermore, the final design weights achieved are identical to four significant figures.

The second column of results in Table 67 (Problem 10B) is based on skin linking arrangement I (10 design variables) and web linking arrangement I (12 design variables). In Problem 10B starting design I is employed. It is observed that reducing the number of independent design variables in the skin from 16 to 10 leads to a final design weight increase of less than 0.8%. The fourth and fifth columns of results in Table 67 (Problems 10D and 10E) are based on skin linking arrangement III (28 design variables) with web linking arrangement I (12 design variables) used in Problem 10D and web linking arrangement II (28 design variables) used in Problem 10E. In Problems 10D and 10E starting point I is employed. Comparing the final design weight achieved in Problem 10D with that obtained in Problems 10A and 10C it is seen the increasing the number of skin design variables from 16 to 28 produces a final design weight decrease of approximately 10%. Comparing the final design weight achieved in Problem 10E with that obtained in Problem 10D, shows that increasing the number of independent design variables in the web model from 12 to 28 while holding the number of skin design variables constant at 28, leads to a further reduction in the final design weight of 1.4%. As anticipated, increasing the number of skin design variables can lead to substantial final design weight reductions, while refining the web design variable model produces relatively small weight reductions. This was to be expected since

for each of the five final designs given in Table 67 the weight of the web material is less than 8% of the total weight.

The influence on skin thickness distribution of gradually refining the skin design variable model (from 10 to 16 to 28 variables), while holding the web linking arrangement fixed (at 12 design variables), is shown schematically in Fig. 30. It is apparent that changing the skin design variable linking arrangement can have significant influence on the final skin material distribution obtained. The influence on the web material distribution of increasing the number of web design variables from 12 to 28, while holding the skin linking arrangement fixed (at 28 variables) is depicted graphically in Fig. 31. Since much of the web material is minimum gage, it is observed that changing the web design variable linking arrangement has a relatively minor influence on the final web material distribution obtained.

It is found that the set of critical constraints at the final designs obtained in Problems 10A, B and C is essentially invariant. These critical constraints, shown schematically in Fig. 32, are: minimum member size for CST elements 1-8, 17-20 and 29-32; minimum member size for SSP elements 1-22, 29-38 and 64-70; combined stress criteria in SSP element 39 56, and vertical (z) deflection at node 44. These final designs are seen to be stress critical at the root, and deflection critical at the wing tip. They also exhibit substantial regions of skin and web where the material is minimum gage.

For Problems 10D and 10E, where the skin design variable linking arrangement involves 28 independent variables, the critical constraints at the final design are essentially the same, although they differ slightly from the critical set for Problems 10A, 10B and 10C. The following constraints are critical for the designs obtained in both Problem 10D and 10E: minimum member size for CST elements 1-8, 17-20, 29-32, 41-42, 49-52; minimum member

size for SSP elements 1-22, 29-38, and 64-70; combined stress criteria in SSP elements 39 and 44; and transverse (z) deflection at node 44. Furthermore, in Problem 10D CST elements 15, 16, 33, 34, 39, 40 become minimum member size critical while in Problem 10E combined stress criteria in SSP elements 41 and 46 are critical and SSP elements 23-25, 43, 48, 49 and 57-62 become minimum member size critical. It is observed that the mix of critical constraints at the final designs obtained in Problems 10D and 10E (see Fig. 33) is only slightly different than that obtained in Problems 10A, B, C; the main difference being that a larger portion of the skin reaches minimum gage. It is gratifying to note that qualitative assessment of the final material distributions (see Figs. 30 and 31), as well as the critical constraint sets (see Figs. 32 and 33), indicates that the results are physically plausible and intuitively reasonable.

Iteration histories for the ACCESS 1 (NEWSUMT version) solutions of Problem 10 (delta wing example) are given numerically in Table 68 and presented graphically in Fig. 34. For Problems 10A, B and C convergence occurs after 8 analyses and design weights that are within 1% of the minimum weight achieved are obtained after only 4 analyses. Note that the iteration histories for Problems 10A and 10C are very much alike and they appear as a single line in Fig. 34. Turning to Problem 10D (which involves a total of 40 independent design variables) it is seen that convergence occurs after 10 analyses to a weight that is approximately 10% lighter than that achieved in Problems 10A and C. In Problem 10D a design weight that is within 1% of the minimum weight achieved is obtained after 6 analyses and it is seen that increasing the number of skin design variables from 16 to 28 produces a significant decrease in the final design weight. Finally, in Problem 10E

(which involves a total of 56 design variables) convergence occurs after 11 analyses while a design weight within 0.6% of the minimum weight achieved is obtained after 7 analyses. Here it is seen that increasing the number of web design variables from 12 to 28 leads to a relatively small weight decrease, beyond that already achieved in Problem 10D.

#### 4.3.4 Additional Data on Example Problems

In this section additional data on the various examples treated in this report are presented. Tabular data pertinent to the swept and delta wing examples, previously presented in U.S. customary units, are also given in SI units. Furthermore, initial weight and CPU time data are given for all examples.

Results for example Problems 1 through 10 have been presented in U.S. customary units. Since example Problems 1 through 8 have been previously treated in the literature using U.S. customary units, comparison of the ACCESS 1 results with these available solutions is facilitated by using the same units system. On the other hand, the swept and delta wing examples (Problems 9 and 10) are new problems for which the results presented herein may become a base of comparison. Therefore it is appropriate to include, for the convenience of future investigators, problem statement data and results for the swept and delta wing examples in SI units as well as U.S. customary units.

The swept wing example (Problem 9) was previously discussed in Section 4.3.2. The detailed problem statement will be found in Tables 51 through 57 and the results are given in Tables 58 and 59. In Tables 52 through 56 information involving units is given in both U.S. customary and SI units. The nodal coordinate and load condition data previously presented in Tables 51 and 57 respectively (U.S. customary units) are also given in Tables 69 and 70 using

SI units. Final designs and iteration history data originally set forth in Tables 58 and 59 respectively (U.S. customary units) are also given in Tables 71 and 72 using SI units.

The delta wing example (Problem 10) was previously discussed in Section 4.3.3. The detailed problem statement is contained in Tables 60 through 66 and the results are presented in Tables 67 and 68. In Tables 61 through 65 information involving units is given in both U.S. customary and SI units. The nodal coordinate and displacement constraint data previously presented in Tables 60 and 66 respectively (U.S. customary units) are also given in Tables 73 and 74 using SI units. Furthermore, the final designs and iteration history data originally presented in Tables 67 and 68 respectively (U.S. customary units) are also given in Tables 75 and 76 using SI units.

It should be noted that all of the information presented in Tables 69 through 76 using SI units was obtained by converting the corresponding data expressed in U.S. customary units. While the ACCESS 1 program is in principle, independent of the units employed, the entire body of computational experience reported herein has been obtained using problem statements given in U.S. customary units.

Initial weight data (for each element type) for all example problems is given in Table 77. The information given in Table 77 provides an input data check for other investigators, who may wish to independently undertake solution of the example problems used in this report. It should be noted that the iteration history tables do not contain total initial weight data because they give the weight at the end of each iteration stage.

All the example problems reported here were executed on the IBM 360/91 at the UCLA Campus Computing Network using an object program compiled by the FORTRAN H compiler. Total CPU times as well as the CPU times spent in various major segments of the design process are given in Table 78 (for truss

problems discussed in Section 4.2) and Table 79 (for wing problems discussed in Section 4.3). This information is presented for completeness. Comparisons based on CPU time and run costs are avoided since they are only valid when the alternative programs are run on the same installation at nearly the same time (assuming a time shared operating environment).

Examining Tables 78 and 79 it is first observed that the total run times are modest. Secondly the distribution of effort between the approximate problem generator (APG) and the optimizer portions of the program is reasonably well balanced. It should be emphasized that the APG block in Fig. 1 includes structural analysis, constraint deletion, and generation of explicit approximations. The amount of time spent on gradient computation is almost always larger than that spent decomposing the system stiffness matrix, however it is certainly not prohibitively large in any of the examples. This can be attributed to the use of implicit differentiation, efficient computation of the pseudo load vectors  $\vec{V}_{bk}$  using Eq. (3.43) and the implementation of the selective sensitivity concept. It is interesting to note that in the optimizer portion of the program approximately 1/4 to 1/3 of the time is consumed by evaluation of the function  $\phi_e^{(p)}(\alpha, r_a)$  [see Eqs. (3.67) and (3.68)]. This is attributed to the constraint deletion feature and the fact that both the objective function  $W(\vec{\alpha})$  and the contributions to the penalty function  $F_e^{(p)}(\vec{\alpha})$  [see Eq. (3.68)] are explicit functions of the linked reciprocal design variables  $\vec{\alpha}$ .

In Problem 7 (the 63 bar wing carry through truss) the amount of CPU time spent on gradient computations is an order of magnitude higher than the amount of CPU times spent on decomposing the system stiffness matrix. This is due to the fact that this problem involves a small number of displacement degrees of freedom (42) and a relatively large number of independent design variables (63). Furthermore Problem 7 involves a large number of critical

stress constraints and therefore the selective sensitivity feature is not particularly effective in reducing the number of partial derivatives needed to construct explicit approximations.

In Problems 9 and 10 (the swept and delta wing examples), the amount of CPU time spent on gradient computations is of the same order of magnitude as the CPU time spent on decomposing the system stiffness matrix. This is attributed to the fact that these problems involve more displacement degrees of freedom (120 and 105) and relatively small numbers of design variables (ranging from 18 to 56). Also, Problems 9 and 10 involve a relatively small number of critical stress constraints and therefore the selective sensitivity feature is somewhat more effective.

Finally, it should be kept in mind that elapsed CPU time data tends to be rather sensitive to the convergence criteria control parameters employed. This is illustrated in Fig. 35 by plotting total weight versus elapsed CPU time for problem 10C (the delta wing example with 28 design variables from initial design I). The preassigned criterion that automatically terminated example 10C was that the percentage change in the objective function value (prior to any scaling up) for two successive stages was less than 0.1%, leading to the reported CPU time of 17.79 seconds. However, if this same diminishing returns criterion had been set at 0.5% termination would have occurred after 6 analyses giving a elapsed CPU time of 14.17 seconds and a final design weight that is only 0.070% heavier.



## 5. CONCLUSIONS AND RECOMMENDATIONS

It has been demonstrated that efficient structural synthesis capabilities based on combining finite element structural analysis methods and nonlinear mathematical programming techniques can be generated. The coordinated implementation of various approximation concepts has made it possible to achieve excellent efficiency while retaining the philosophically attractive generality inherent to the mathematical programming formulation of structural design optimization problems.

The ACCESS 1 computer program represents a new type of structural analysis/synthesis capability which may be viewed as a pilot program for a second generation of general purpose programs based on finite element analysis and mathematical programming algorithms. The scope of ACCESS 1 is such that it embraces a significant class of structural design optimization problems. For structural systems with fixed topology, material and layout -- that can be idealized using TRUSS, CST and SSP type elements -- subject to stress, displacement and member size constraints in each of several distinct loading conditions, the ACCESS 1 program automatically seeks a minimum weight design.

Based on the ACCESS 1 numerical results presented in this report two major conclusions are drawn:

- (1) The innovative use of approximation concepts has produced a dramatic reduction in the number of conventional structural analyses needed to obtain candidate optimum designs via the combined use of finite element and mathematical programming methods. Indeed, the numerical results reported herein indicate that ACCESS 1 is usually able to obtain a practical near optimum design within 5 to 10 analyses.

- (2) For structural synthesis problems of modest but useful size, approximation concepts have made possible the generation of an automated structural design capability, based on finite element analysis and mathematical programming algorithms, that is competitive with recursive redesign techniques based on fully stressed design and discretized optimality criteria concepts.

The basic ideas used in creating the ACCESS 1 program are rather general and therefore it may be argued that its successful development supports the contention that the introduction of approximation concepts will lead to the emergence of a new generation of practical and efficient large scale structural synthesis capabilities based on finite element analysis and mathematical programming algorithms. While the scope of ACCESS 1 is clearly limited, ideas such as:

- (1) design variable linking
- (2) dynamically updated constraint deletion via the regionalization and "throw away" concepts;
- (3) construction of high quality explicit approximations for constraints retained;
- (4) organization of the finite element structural analysis with the design optimization task in mind;

and

- (5) selective sensitive analysis, where in only those partial derivatives needed (to construct explicit approximations of retained constraints) are evaluated;

have marked promise for application to a much wider range of structural synthesis problems. Furthermore, the central notion of replacing the mathematical programming statement of the design optimization problem with a

sequence of small explicit approximate problems (see Fig. 4), that retain the essential features of the primary problem, should be widely applicable in structural synthesis.

Although a substantial body of computational experience is presented in this report, it is recommended that the ACCESS 1 computer program be further exercised. For example, it is suggested that:

- (1) the possibility of achieving additional gains in efficiency via systematic gradual refinement of design variable linking be explored;
- (2) a further assessment of the sensitivity of automated optimum design results to changes in modeling, loading conditions, allowable stresses and deflections be carried out;
- (3) parametric studies be conducted to evaluate the potential benefits expected to ensue from ultimately being able to treat configuration, material, and topological descriptors as design variables rather than as preassigned parameters.

It is also recommended that the efficiency gains obtained by implementing approximation concepts to create the ACCESS 1 program be extended to problems of significantly larger scale while at the same time introducing thermal effects and fiber composite materials. While these extensions are relatively straight forward in principle, their implementation will require substantial effort. It is anticipated that maximum problem size can be significantly increased by permitting some use of auxiliary storage (n.b. ACCESS 1 is an all core storage program). Thermal effects could be included by providing for uniform temperature change inputs (independent of the design variables) in each type of finite element. Limiting attention to balanced and symmetric laminates it should be possible to represent fiber composite skins

by stacking planform congruent orthotropic CST elements. It would also be useful to extend the finite element repertoire of ACCESS 1 (e.g., add pure shear, quadrilateral plane stress elements, etc.).

In the future, effort should also be directed toward applying approximation concepts to develop efficient structural synthesis capabilities that include consideration of more complex failure modes. Such capabilities could, for example, include consideration of buckling, natural frequency and dynamic stability constraints.

The regionalization and "throwaway" concepts (see Sections 2.4.1 and 2.4.2 respectively) used in ACCESS 1 are effective but relatively primitive methods for identifying and deleting redundant constraints. It is suggested that further study may lead to more refined methods for determining which of the many (Q) constraints in the basic problem statement (see Eqs. 2.1 and 2.2) are at least temporarily redundant and subject to deletion. Furthermore, the insightful selection of response quantities ( $\vec{Y}$ ) and intermediate variables ( $\vec{Z}$ ) can be expected to generally enhance the quality of explicit approximations obtainable (see Section 2.5.3) for a wide variety of constraint functions.

Efficient solution of large scale practical problems is likely to require the use of both design variable linking and basis reduction in design space (see Section 2.3.3). Therefore, it is recommended that effort be directed toward implementation of the generalized reduced basis concept. It is suggested that the reduced basis concept in design space (see Section 2.3.2) opens the way to development of hybrid methods of structural optimization. These hybrid methods are expected to have a major unifying influence leading to the coordinated use of stress ratio, optimality criteria, lower bound and mathematical programming methods in structural optimization. It is the earnest conviction

of the authors that approximation concepts make it possible to create philosophically sound, practical and efficient structural synthesis capabilities that could, by the end of this decade, come to enjoy a level of professional acceptance comparable to that currently commanded by finite element structural analysis methods.



## Appendix A

### Finite Elements Employed

#### Notation:

$x, y, z$	:	reference coordinate system
$\tilde{x}, \tilde{y}, \tilde{z}$	:	local coordinate system
$l_1, m_1, n_1$	:	direction cosines of the local $\tilde{x}$ axis in the reference coordinate system
$l_2, m_2, n_2$	:	direction cosines of the local $\tilde{y}$ axis in the reference coordinate system
$P, Q, R, S$	:	local node name
$\tilde{u}, \tilde{v}, \tilde{w}$	:	displacements in local coordinates
$u, v, w$	:	displacements in reference coordinates
$\epsilon_x, \epsilon_y, \epsilon_{xy}$	:	strain components in local coordinate system
$\sigma_x, \sigma_y, \tau_{xy}$	:	stress components in local coordinate system
$A$	:	cross sectional area of truss elements
$t$	:	thickness of CST elements
$\tau$	:	thickness of SSP elements
$E$	:	modulus of elasticity
$\nu$	:	Poisson's ratio
$\rho$	:	specific weight
$L$	:	length of truss elements
$S$	:	surface area of CST or SSP elements
$\theta = \frac{a}{b}$	:	aspect ratio of SSP elements
$a$	:	length of SSP elements (see Fig. A3)
$b$	:	base edge length of CST elements (see Fig. A2) height of SSP elements (see Fig. A3)
$h$	:	height of CST elements (see Fig. A2)
$s$	:	location of the point T of CST elements (see Fig A2)

- [ $\tilde{k}$ ]** : element stiffness matrix in local coordinates
- [k]** : element stiffness matrix in reference coordinates
- [B]** : strain-displacement relation matrix
- [D]** : stress-strain relation matrix
- [A]** : local to reference coordinate transformation matrix

**A.1 Truss Element with Uniform Cross Sectional Area.**

Let the node P be the origin of the local coordinate system.

Assume displacement state

$$\tilde{u}(\tilde{x}) = \tilde{u}_P + \frac{\tilde{x}}{L} (\tilde{u}_Q - \tilde{u}_P) \quad (\text{A.1})$$

Strain distribution

$$\epsilon_x(\tilde{x}) = \frac{1}{L} (\tilde{u}_Q - \tilde{u}_P) \quad (\text{A.2})$$

Strain displacement relation

$$\epsilon_x = \underbrace{\left[ -\frac{1}{L}, \frac{1}{L} \right]}_{[B]} \begin{Bmatrix} \tilde{u}_P \\ \tilde{u}_Q \end{Bmatrix} \quad (\text{A.3})$$

Displacement transformation law

$$\begin{Bmatrix} \tilde{u}_P \\ \tilde{u}_Q \end{Bmatrix} = \underbrace{\begin{bmatrix} l_1 & m_1 & n_1 & 0 & 0 & 0 \\ 0 & 0 & 0 & l_1 & m_1 & n_1 \end{bmatrix}}_{[A]} \begin{Bmatrix} u_P \\ v_P \\ w_P \\ u_Q \\ v_Q \\ w_Q \end{Bmatrix} \quad (\text{A.4})$$

Stress-strain relation

$$\sigma_x(\tilde{x}) = \underbrace{E}_{[D]} \epsilon_x(\tilde{x}) \quad (\text{A.5})$$

Stiffness matrix in the local coordinate system.

$$[\tilde{k}] = A \int_0^L B^T D B d\tilde{x} = A \int_0^L \frac{1}{L^2} \begin{bmatrix} -1 \\ 1 \end{bmatrix} E [-1, 1] d\tilde{x} = \frac{AE}{L} \begin{bmatrix} 1 & -1 \\ -1 & 1 \end{bmatrix} \quad (\text{A.6})$$

Stiffness matrix in the reference coordinate system

$$[k] = [\Lambda]^T [\tilde{k}] [\Lambda]$$

$$= \frac{AE}{L} \begin{bmatrix} l_1^2 & l_1 m_1 & l_1 n_1 & -l_1^2 & -l_1 m_1 & -l_1 n_1 \\ & m_1^2 & m_1 n_1 & -l_1 m_1 & -m_1^2 & -m_1 n_1 \\ & & n_1^2 & -l_1 n_1 & -m_1 n_1 & -n_1^2 \\ & & & l_1^2 & l_1 m_1 & l_1 n_1 \\ & & & & m_1^2 & m_1 n_1 \\ & & & & & n_1^2 \\ \text{symm.} & & & & & & n_1^2 \end{bmatrix}$$

(A.7)

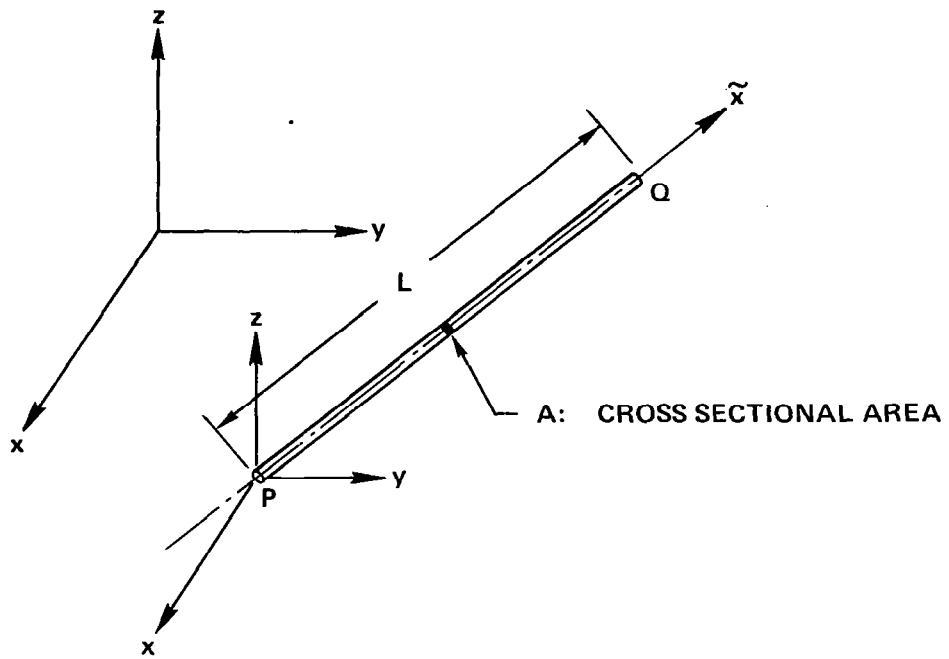


Figure A1. Truss Element.

## A.2 Constant Strain Triangular Element (CST)

Assumptions:

- Isotropic materials
- Uniform thickness
- Plane stress state
- Constant strain in the field

Displacement state

$$\begin{pmatrix} \tilde{u}(\tilde{x}, \tilde{y}) \\ \tilde{v}(\tilde{x}, \tilde{y}) \end{pmatrix} = \begin{bmatrix} (b-s)(b-\tilde{x})-h\tilde{y} & 0 & -s(\tilde{x}-s) - h(h-\tilde{y}) & 0 & b\tilde{x} & 0 \\ 0 & (b-s)(b-\tilde{x})-h\tilde{y} & 0 & -s(\tilde{x}-s)-h(h-\tilde{y}) & 0 & b\tilde{x} \end{bmatrix} \begin{pmatrix} \tilde{u}_1 \\ \tilde{v}_1 \\ \tilde{u}_2 \\ \tilde{v}_2 \\ \tilde{u}_3 \\ \tilde{v}_3 \end{pmatrix} \quad (\text{A.8})$$

Strain-displacement relation

$$\begin{pmatrix} \epsilon_x \\ \epsilon_y \\ \gamma_{xy} \end{pmatrix} = \frac{1}{bh} \underbrace{\begin{bmatrix} -(b-s) & 0 & -s & 0 & b & 0 \\ 0 & -h & 0 & h & 0 & 0 \\ -h & -(b-s) & h & -s & 0 & b \end{bmatrix}}_{[B]} \begin{pmatrix} \tilde{u}_1 \\ \tilde{v}_1 \\ \tilde{u}_2 \\ \tilde{v}_2 \\ \tilde{u}_3 \\ \tilde{v}_3 \end{pmatrix} \quad (\text{A.9})$$

Displacement transformation law

$$\begin{pmatrix} \tilde{u}_1 \\ \tilde{v}_1 \\ \tilde{u}_2 \\ \tilde{v}_2 \\ \tilde{u}_3 \\ \tilde{v}_3 \end{pmatrix} = \underbrace{\begin{bmatrix} [\lambda] & [0] & [0] \\ [0] & [\lambda] & [0] \\ [0] & [0] & [\lambda] \end{bmatrix}}_{[A]} \begin{pmatrix} u_P \\ v_P \\ u_Q \\ v_Q \\ u_R \\ v_R \end{pmatrix} \quad (\text{A.10})$$

$$[\lambda] = \begin{bmatrix} l_1 & m_1 & n_1 \\ l_2 & m_2 & n_2 \end{bmatrix} \quad (\text{A.11})$$

$$[0] = \begin{bmatrix} 0 & 0 & 0 \\ 0 & 0 & 0 \end{bmatrix} \quad (\text{A.12})$$

Stress-strain relation - Plane stress state

$$\begin{pmatrix} \sigma_x \\ \sigma_y \\ \tau_{xy} \end{pmatrix} = \frac{E}{1-\nu^2} \underbrace{\begin{bmatrix} 1 & \nu & 0 \\ \nu & 1 & 0 \\ 0 & 0 & \frac{1-\nu}{2} \end{bmatrix}}_{[D]} \begin{pmatrix} \epsilon_x \\ \epsilon_y \\ \gamma_{xy} \end{pmatrix} \quad (\text{A.13})$$

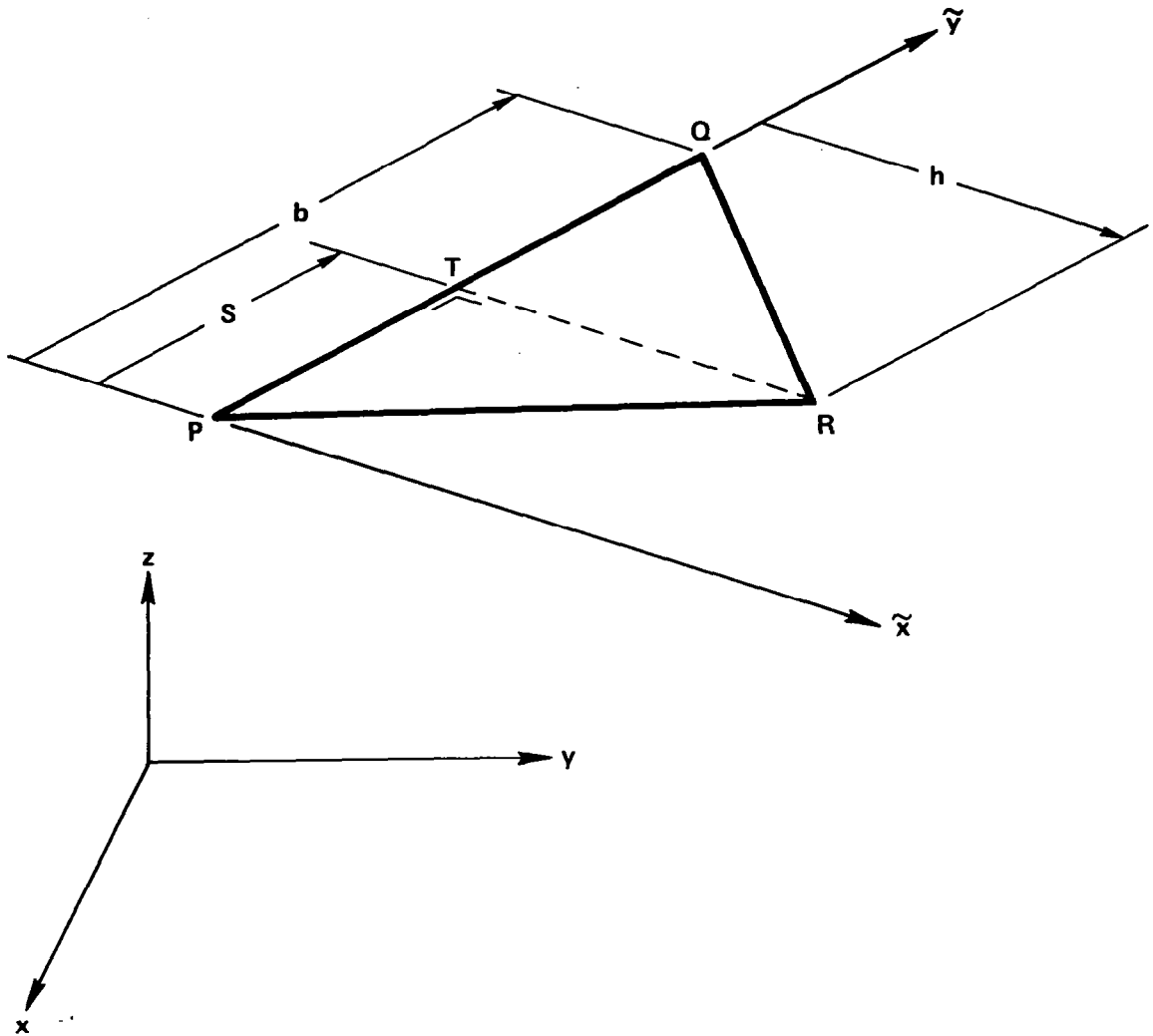
Element stiffness matrix in local coordinate system

$$[\tilde{k}] = \int_v [B]^T [D] [B] \alpha v = t \int_S [B]^T [D] [B] dA \quad (\text{A.14})$$

$$[\tilde{k}] = [\tilde{k}_n] + [\tilde{k}_s] \quad (\text{A.15})$$

$$[\tilde{k}_n] = \frac{Et}{4S(1-\nu^2)} \begin{bmatrix} (b-s)^2 & \nu(b-s)h & (b-s)s & -\nu(b-s)h & -(b-s)b & 0 \\ & h^2 & \nu hs & -h^2 & -\nu bh & 0 \\ & & s^2 & -\nu hs & -bs & 0 \\ & & & h^2 & \nu hb & 0 \\ \text{symm.} & & & & b^2 & 0 \\ & & & & & 0 \end{bmatrix} \quad (\text{A.16})$$

$$[\tilde{k}_s] = \frac{Et}{8S(1+\nu)} \begin{bmatrix} h^2 & (b-s)h & -h^2 & hs & 0 & -bh \\ & (b-s)^2 & -(b-s)h & (b-s)s & 0 & (b-s)h \\ & & h^2 & -hs & 0 & bh \\ & & & s^2 & 0 & -bs \\ \text{symm.} & & & & 0 & 0 \\ & & & & & b^2 \end{bmatrix} \quad (\text{A.17})$$



$$\begin{aligned}
 b &= x_q - x_p \\
 s &= x_r - x_p \\
 h &= y_r - y_p \\
 A &= 1/2 bh
 \end{aligned}$$

Figure A2. Constant Strain Triangular Element.

### A.3 Symmetric Shear Panel Element (SSP)

When carrying out the finite element analysis of thin wing structures that are symmetric with respect to their middle surface, it can often be important to separate the inplane deformation from the bending deformation. This approach circumvents possible numerical difficulties due to large differences in bending and inplane type stiffnesses. Referring to Fig. A3, the basic assumptions used in developing this element are summarized as follows:

- (1) isotropic materials;
- (2) uniform thickness;
- (3) rectangular configuration

If not rectangular, an equivalent rectangular plate of the same area is considered;

- (4) symmetric with respect to the middle surface;
- (5) plane stress state;
- (6) stress distribution in the field is assumed to have the form

$$\sigma_x(\tilde{x}, \tilde{y}) = D_1 \tilde{y} + D_2$$

$$\sigma_y(\tilde{x}, \tilde{y}) = 0.0$$

$$\tau_{xy}(\tilde{x}, \tilde{y}) = D_3$$

where  $D_1$ ,  $D_2$ ,  $D_3$  are constants;

- (7) Displacement boundary condition

$$u(\tilde{x}, 0) = 0.$$

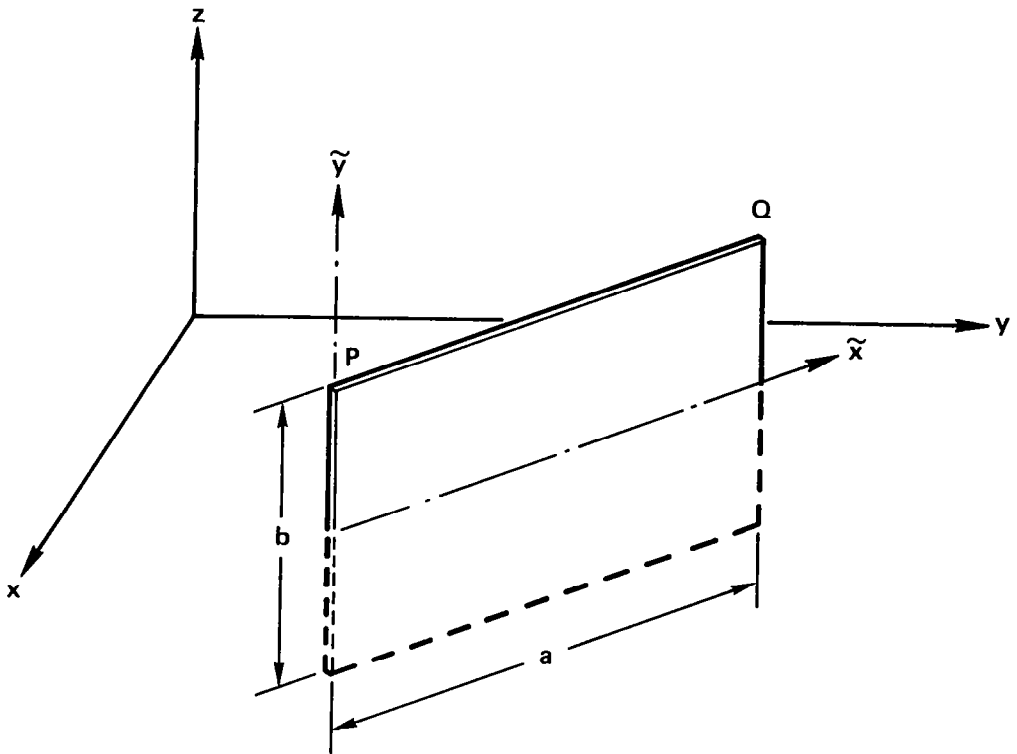


Figure A3. Symmetric Shear Panel.

The displacement state\* implied by the foregoing assumptions is now sought.

$$\frac{\partial u(x,y)}{\partial x} = \epsilon_x = \frac{1}{E} \sigma_x = \frac{1}{E} (D_1 y + D_2) \quad (\text{A.18})$$

$$\frac{\partial v(x,y)}{\partial y} = \epsilon_y = -\frac{\nu}{E} \sigma_x = -\frac{\nu}{E} (D_1 y + D_2) \quad (\text{A.19})$$

$$\frac{\partial u(x,y)}{\partial y} + \frac{\partial v(x,y)}{\partial x} = \gamma_{xy} = \frac{2(1+\nu)}{E} D_3 \quad (\text{A.20})$$

By integrating Eqs. (A.18) and (A.19),

$$u(x,y) = \frac{1}{E} (D_1 xy + D_2 x) + f(y) \quad (\text{A.21})$$

$$v(x,y) = -\frac{\nu}{E} \left( \frac{1}{2} D_1 y^2 + D_2 y \right) + g(x) \quad (\text{A.22})$$

and substitution of (A.21) and (A.22) into (A.20), yields

$$\frac{1}{E} D_1 x + f'(y) + g'(x) = \frac{2(1+\nu)}{E} D_3 \quad (\text{A.23})$$

where  $f(y)$ ,  $g(x)$  are arbitrary differentiable functions and  $f'(y)$ ,  $g'(x)$  are their first derivatives.

Since Eq. (A.23) must be satisfied for arbitrary  $x$  and  $y$ , it is necessary that

$$\frac{1}{E} D_1 x + g'(x) = -f'(y) + \frac{2(1+\nu)}{E} D_3 = D_4 \quad (\text{A.24})$$

where  $D_4$  is a constant.

---

\* Since the development in this subsection is carried out exclusively in the local coordinate systems, tildas over  $u, v, x, y$  etc. are omitted except for the final result (see Eq. (A.41)) as a matter of convenience.

Upon integration Eq. (A.24) yields

$$f(y) = - D_4 - \left[ \frac{2(1+\nu)}{E} \right] D_3 y + D_5 \quad (\text{A.25})$$

$$g(x) = - \frac{1}{2E} D_1 x^2 + D_4 x + D_6 \quad (\text{A.26})$$

where  $D_5, D_6$  are constants.

Equations (A.25) and (A.26) are introduced into Eqs. (A.21) and (A.22)

giving

$$u(x,y) = \frac{1}{E} (D_1 xy + D_2 x) - \left[ D_4 - \frac{2(1+\nu)}{E} D_3 \right] y + D_5 \quad (\text{A.27})$$

$$v(x,y) = - \frac{\nu}{E} \left( \frac{1}{2} D_1 y^2 + D_2 y \right) - \frac{1}{2E} D_1 x^2 + D_4 x + D_6 \quad (\text{A.28})$$

Recalling the displacement boundary condition,

$$u(x,0) = \frac{1}{E} D_2 x + D_5 \equiv 0 \quad (\text{A.29})$$

and therefore

$$D_2 = 0 \quad , \quad D_5 = 0 \quad . \quad (\text{A.30})$$

Now it follows that Eqs. (A.27) and (A.28) may be rewritten as

$$u(x,y) = 2 c_1 xy + (c_2 - c_3) y \quad (\text{A.31})$$

$$v(x,y) = -c_1 (x^2 + \nu y^2) + c_3 x + c_4 \quad (\text{A.32})$$

These four constants may be expressed in terms of the node displacement components,  $u_R, v_R, u_Q$  and  $v_Q$ .

$$u_P = u(0, \frac{1}{2} b) = \frac{1}{2} (c_2 - c_3) b \quad (\text{A.33})$$

$$u_Q = u(a, \frac{1}{2} b) = c_1 ab + \frac{1}{2} (c_2 - c_3) b \quad (\text{A.34})$$

$$v_P = v(0, \frac{1}{2} b) = -c_1 \frac{\nu b^2}{4} + c_4 \quad (\text{A.35})$$

$$v_Q = v(a, \frac{1}{2} b) = -c_1 \left( a^2 + \frac{\nu b^2}{4} \right) + c_3 a + c_4 \quad (\text{A.36})$$

then solving for  $c_1, c_2, c_3$  and  $c_4$ , gives

$$c_1 = \frac{u_Q - u_P}{ab} \quad (\text{A.37})$$

$$c_2 = \frac{u_Q + u_P}{b} + \frac{v_Q - v_P}{a} \quad (\text{A.38})$$

$$c_3 = \frac{u_Q - u_P}{b} + \frac{v_Q - v_P}{a} \quad (\text{A.39})$$

$$c_4 = v_P + \frac{vb}{4a} (u_Q - u_P) \quad (\text{A.40})$$

Finally the displacement state in the field may be expressed in matrix form as follows

$$\begin{pmatrix} \tilde{u}(\tilde{x}, \tilde{y}) \\ \tilde{v}(\tilde{x}, \tilde{y}) \end{pmatrix} = \begin{bmatrix} \frac{2}{b} (1 - \frac{\tilde{x}}{a}) \tilde{y} & 0 & \frac{2\tilde{x}\tilde{y}}{ab} & 0 \\ \left( -\frac{\tilde{x}}{b} + \frac{\tilde{x}^2 + v\tilde{y}^2}{ab} - \frac{vb}{4a} \right) \left( 1 - \frac{\tilde{x}}{a} \right) \left( \frac{\tilde{x}}{b} - \frac{\tilde{s}^2 + v\tilde{y}^2}{ab} + \frac{vb}{4a} \right) \frac{\tilde{x}}{a} \end{bmatrix} \begin{pmatrix} \tilde{u}_P \\ \tilde{v}_P \\ \tilde{u}_Q \\ \tilde{v}_Q \end{pmatrix} \quad (\text{A.41})$$

The strain displacement relations are obtained by differentiating

Eq. (A.41)

$$\begin{pmatrix} \epsilon_x \\ \epsilon_y \\ \gamma_{xy} \end{pmatrix} = \underbrace{\begin{bmatrix} -\frac{2\tilde{y}}{ab} & 0 & \frac{2\tilde{y}}{ab} & 0 \\ \frac{2v\tilde{y}}{ab} & 0 & -\frac{2v\tilde{y}}{ab} & 0 \\ \frac{1}{b} & -\frac{1}{a} & \frac{1}{b} & \frac{1}{a} \end{bmatrix}}_{[B]} \begin{pmatrix} \tilde{u}_P \\ \tilde{v}_P \\ \tilde{u}_Q \\ \tilde{v}_Q \end{pmatrix} \quad (\text{A.42})$$

Stress-strain relation — plane stress state

$$\begin{pmatrix} \sigma_x \\ \sigma_y \\ \tau_{xy} \end{pmatrix} = \frac{E}{1-\nu^2} \underbrace{\begin{bmatrix} 1 & \nu & 0 \\ \nu & 1 & 0 \\ 0 & 0 & \frac{1-\nu}{2} \end{bmatrix}}_{[D]} \begin{pmatrix} \epsilon_x \\ \epsilon_y \\ \epsilon_{xy} \end{pmatrix} \quad (\text{A.43})$$

Stress displacement relation

Substitution of (A.42) into (A.43) yields

$$\begin{pmatrix} \sigma_x \\ \sigma_y \\ \tau_{xy} \end{pmatrix} = E \begin{bmatrix} -\frac{2\tilde{y}}{ab} & 0 & \frac{2\tilde{y}}{ab} & 0 \\ 0 & 0 & 0 & 0 \\ \frac{1}{2(1+\nu)b} & -\frac{1}{2(1+\nu)a} & \frac{1}{2(1+\nu)b} & \frac{1}{2(1+\nu)a} \end{bmatrix} \begin{pmatrix} \tilde{u}_P \\ \tilde{v}_P \\ \tilde{u}_Q \\ \tilde{v}_Q \end{pmatrix} \quad (\text{A.44})$$

Element stiffness matrix in the local coordinate system

$$[\tilde{k}] = \int_V [B]^T [D] [B] dV = \tau \int_S [B]^T [D] [B] dA \quad (\text{A.45})$$

$$[\tilde{k}] = \frac{E\tau}{12(1+\nu)} \begin{bmatrix} \frac{2(1+\nu)}{\theta} + 3\theta & -3 & -\frac{2(1+\nu)}{\theta} + 3\theta & 3 \\ -3 & \frac{3}{\theta} & -3 & -\frac{3}{\theta} \\ -\frac{2(1+\nu)}{\theta} + 3\theta & -3 & \frac{2(1+\nu)}{\theta} + 3\theta & 3 \\ 3 & -\frac{3}{\theta} & 3 & \frac{3}{\theta} \end{bmatrix} \quad (\text{A.46})$$

where  $\theta = \frac{a}{b}$  . (A.47)

Displacement transformation law

$$\begin{pmatrix} \tilde{u}_P \\ \tilde{v}_P \\ \tilde{u}_Q \\ \tilde{v}_Q \end{pmatrix} = \underbrace{\begin{bmatrix} l_1 & m_1 & 0 & 0 \\ 0 & 0 & 1 & 0 \\ 0 & 0 & l_1 & m_1 \\ 0 & 0 & 0 & 1 \end{bmatrix}}_{[\Lambda]} \begin{pmatrix} u_P \\ v_P \\ w_P \\ u_Q \\ v_Q \\ w_Q \end{pmatrix} \quad (\text{A.48})$$

Element stiffness matrix in the reference coordinate system

$$[k] = [\Lambda]^T [\tilde{k}] [\Lambda] \quad (\text{A.49})$$

## Appendix B

### Relationship Between "Throw Away" Concept (Section 2.4.2) and Detailed Implementation (Section 3.3.6.2)

Deletion of constraints that are neither critical nor potentially critical can be achieved by ignoring all constraints for which the response ratio ( $R_q$ ) is less than a specified value such as 0.5. Alternatively constraint deletion can be accomplished by dropping all constraints for which

$$R_q < R_1 f_{tr} \quad (B.1)$$

where  $f_{tr}$  is called the truncation factor and  $R_1$  is the largest response ratio, that is

$$R_1 = \text{Max}_q [R_q] = \text{Max}_q [1 - h_q] \quad (B.2)$$

Substituting Eq. (B.2) into Eq. (B.1) and replacing  $R_q$  by  $1 - h_q$  it follows that

$$(1 - h_q) < f_{tr} \left\{ \text{Max}_q [1 - h_q] \right\} \quad (B.3)$$

or equivalently

$$-h_q < f_{tr} \left\{ \text{Max}_q [1 - h_q] \right\} - 1 \quad (B.4)$$

Now recalling that  $-h_q = h_q^-$  (see Eq. 3.34) it follows that Eq. (B.4) can be written as

$$h_q^- < f_{tr} \left\{ \text{Max}_q [1 + h_q^-] \right\} - 1 \quad (B.5)$$

Comparing the right hand side of Eq. (B.5) to Eq. (3.35) with  $c$  set equal to 1 it follows that Eq. (B.5) reduces to

$$h_q^- < TBV \quad (B.6)$$

Hence it is seen that the simple constraint deletion procedure described in Section 2.4.2 is essentially a special case of the dynamic constraint deletion process implemented by ACCESS 1. Specifically, all constraints with values  $h_q^-(\vec{\alpha})$  less than the current TBV are deleted from consideration during the upcoming design stage.

## Appendix C

### Derivation of Pseudo Load Vector Formula (see Eq. 3.43)

Referring to Eq. (3.42), the pseudo load vectors  $\vec{V}_{bk}$  are defined as

$$\vec{V}_{bk} = - \left[ \frac{\partial K}{\partial \alpha_b} \right] \vec{u}_k \quad (C.1)$$

The system stiffness matrix is given by the expression

$$[K] = \sum_{i=1}^I [k_i] = \sum_{i=1}^I [\Lambda_i]^T [\tilde{k}_i] [\Lambda_i] \quad (C.2)$$

but

$$[\tilde{k}_i] = D_i [k_{\ell(i)}] \quad (C.3)$$

Substituting Eq. (C.3) into Eq. (C.2) gives

$$[K] = \sum_{i=1}^I D_i [\Lambda_i]^T [k_{\ell(i)}] [\Lambda_i] \quad (C.4)$$

and noting that  $D_i = T_{ib(i)} / \alpha_{b(i)}$  yields

$$[K] = \sum_{i=1}^I \frac{T_{ib(i)}}{\alpha_{b(i)}} [\Lambda_i]^T [k_{\ell(i)}] [\Lambda_i] \quad (C.5)$$

Taking the partial derivative with respect to  $\alpha_b$  leads to the following expression

$$\left[ \frac{\partial K}{\partial \alpha_b} \right] = - \sum_{i \in b} \frac{T_{ib(i)}}{2 \alpha_{b(i)}} [\Lambda_i]^T [k_{\ell(i)}] [\Lambda_i] \quad (C.6)$$

and substituting Eq. (C.6) into Eq. (C.1) gives

$$\vec{V}_{bk} = \sum_{i \in b} \frac{T_{ib(i)}}{2 \alpha_{b(i)}} [\Lambda_i]^T [k_{\ell(i)}] [\Lambda_i] \vec{u}_{ik} \quad (C.7)$$

where  $\vec{u}_{ik}$  denotes the displacement degrees of freedom (in the reference coordinate system) associated with the  $i^{\text{th}}$  finite element in the  $k^{\text{th}}$  load condition.

## REFERENCES

1. Heyman, J.: Plastic Design of Beams and Frames for Minimum Material Consumption. Quart. Appl. Math., vol. 8, 1951, pp. 373-381.
2. Foulkes, J.: The Minimum Weight Design of Structural Frames. Proc. of the Royal Society (London), vol. A223, no. 1155, 1954, pp. 482-494.
3. Livesley, R.K.: The Automated Design of Structural Frames. Quart. J. Mech. Appl. Math., vol. 9, 1956, pp. 257-278.
4. Heyman, J.; and Prager, W.: Automatic Minimum Weight Design of Steel Frames. J. Franklin Inst., vol. 266, 1958, pp. 339-364.
5. Livesley, R.K.: Optimum Design of Structural Frames for Alternative Systems of Loading. Civil Engr. and Public Works Review, vol. 54, no. 636, June 1959, pp. 737-740.
6. Pearson, C.W.: Structural Design by High Speed Computing Machines. Proc. 1st Conf. on Electronic Computation ASCE, New York, 1958, pp. 417-436.
7. Klein, B.: Direct Use of Extremal Principles in Solving Certain Optimization Problems Involving Inequalities. Operations Research, vol. 3, 1955, pp. 168-175.
8. Schmit, L.A.: Structural Design by Systematic Synthesis. Proc. 2nd Conf. on Electronic Computation ASCE, New York, 1960, pp. 105-122.
9. Schmit, L.A.; Kicher, T.P.; and Morrow, W.M.: Structural Synthesis Capability for Integrally Stiffened Waffle Plates. AIAA J., vol. 1, no. 12, 1963, pp. 2820-2836.
10. Schmit, L.A.; and Thornton, W.A.: Synthesis of an Airfoil at Supersonic Mach Number. NASA CR-144, 1965.
11. Kicher, T.P.: Structural Synthesis of Integrally Stiffened Cylinders. J. of Spacecraft and Rockets, vol. 5, no. 1, 1968, pp. 62-67.
12. Morrow, W.M.; and Schmit, L.A.: Structural Synthesis of a Stiffened Cylinder. NASA CR-1217, 1968.
13. Stroud, W.J.; and Sykes, N.P.: Minimum Weight Stiffened Shells with Slight Meridional Curvature Designed to Support Axial Compressive Loads. AIAA J., vol. 7, no. 8, 1969, pp. 1599-1601.
14. Chao, T.L.: Minimum Weight Design of Stiffened Fiber Composite Cylinders. AFML-TR-69-251, 1969.
15. Kicher, T.P.; and Chao, T.L.: Minimum Weight Design of Stiffened Fiber Composition Cylinders. J. of Aircraft, vol. 8, no. 7, 1971, pp. 562-568.
16. Thornton, W.A.; and Schmit, L.A.: The Structural Synthesis of an Ablating Thermostructural Panel. NASA CR-1215, 1968.

## References (Cont'd)

17. Fox, R.L.; and Kapoor, M.P.: Structural Optimization in the Dynamic Response Regime. AIAA J., vol. 8, no. 10, 1970, pp. 1798-1804.
18. Waddoups, M.E.; McCullers, L.A.; Olsen, F.O.; and Ashton, J.E.: Structural Synthesis of Anisotropic Plates. Paper presented at the AIAA/ASME 11th Structures, Structural Dynamics and Materials Conf., Denver, Colorado, April 1970.
19. Gellatly, R.A.; Gallagher, R.H.; and Lubracki, W.A.: Development of a Procedure for Automated Synthesis of Minimum Weight Structures. AFFDL-TDR-64-141, 1964.
20. Gellatly, R.A.; and Gallagher, R.H.: A Procedure for Automated Minimum Weight Structural Design, Part I - Theoretical Basis, Part II - Applications. Aero. Quart., vol. 17, no. 3, 1966, pp. 216-230 and no. 4, 1966, pp. 332-342.
21. Gellatly, R.A.: Development of Procedures for Large Scale Automated Minimum Weight Structural Design. AFFDL - TR-66-180, 1966.
22. Karnes, R.N.; and Tocher, J.L.: Automatic Design of Optimum Hole Reinforcement. Boeing Report D6-23359, 1968.
23. Tocher, J.L.; and Karnes, R.N.: The Impact of Automated Structural Optimization on Actual Design. AIAA Paper No. 73-361, April 1971.
24. Pope, G.G.; and Schmit, L.A.; (Editors): Structural Design Applications of Mathematical Programming Techniques. AGARDograph No. 149, 1971.
25. Schmit, L.A.: Structural Synthesis 1959-1969 A Decade of Progress. Proc. Japan-U.S. Seminar on Matrix Methods of Structural Analysis and Design. Univ. of Alabama Press, 1971.
26. Schmit, L.A.; and Fox, R.L.: Structural Synthesis Notebook. AIAA Educational Programs, New York, 1970.
27. Fox, R.L.: Optimization Methods for Engineering Design. Addison-Wesley, 1971.
28. Venkayya, V.B.; Khot, N.S.; and Reddy, V.S.: Optimization of Structures based on the Study of Strain Energy Distribution. Proc. 2nd Conf. on Matrix Methods in Structural Mech; WPAFB, AFFDL-TR-68-150, 1968, pp. 111-153.
29. Dwyer, W.; Rosenbaum, J.; Shulman, M.; and Pardo, H.: Fully-Stressed Design of Airframe Redundant Structures. Proc. 2nd Conf. on Matrix Methods in Structural Mech., WPAFB, AFFDL-TR-68-150, 1968, pp. 155-181.

## References (Cont'd)

30. Lansing, W.; Dwyer, W.; Emerton, R.; and Ranalli, E.: Application of Fully-Stressed Design Procedures to Wing and Empennage Structures. *J. of Aircraft*, vol. 8, no. 9, 1971, pp. 683-688.
31. Venkayya, V.B.: Design of Optimum Structures. *J. of Computers and Structures*, vol. 1, no. 1-2, 1971, pp. 265-309.
32. Gellatly, R.A.; Berke, L.; and Gibson, W.: The Use of Optimality Criteria in Automated Structural Design. Paper presented at the 3rd Conf. on Matrix Methods in Structural Mech., WPAFB, Ohio, October 1971.
33. Dwyer, W.J.; Emerton, R.K.; and Ojalvo, I.U.: An Automated Procedure for the Optimization of Practical Aerospace Structures. AFFDL-TR-70-118, 1971.
34. Gellatly, R.A.; and Berke, L.: Optimal Structural Design. AFFDL-TR-70-165, 1971.
35. Taig, I.C.; and Kerr, R.I.: Optimization of Aircraft Structures with Multiple Stiffness Requirements. AGARD Conf. Proc. No. 123, 2nd Symposium on Structural Optimization, Milan, Italy, April 1973.
36. Venkayya, V.B.; Khot, N.S.; and Berke, L.: Application of Optimality Criteria Approaches to Automated Design of Large Practical Structures. AGARD Conf. Proc. No. 123, 2nd Symposium on Structural Optimization, Milan, Italy, April 1973.
37. Giles, G.L.: Procedure for Automating Aircraft Wing Structural Design. *J. of the Structural Div., ASCE*, vol. 97, no. ST1, 1971, pp. 99-113.
38. Fulton, R.E.; and McComb, H.G.: Automated Design of Aerospace Structures. *Transactions of ASME, J. of Engr. for Industry*, vol. 96, no. 1, 1974, pp. 217-225.
39. Giles, G.L.; Blackburn, C.L.; and Dixon, S.C.: Automated Procedures for Sizing Aerospace Vehicle Structures (SAVES). *J. of Aircraft*, vol. 9, no. 12, 1972, pp. 812-819.
40. Sobieszczanski, J.; and Loendorf, D.: A Mixed Optimization Method for Automated Design of Fuselage Structures. *J. of Aircraft*, vol. 9, no. 12, 1972, pp. 805-811.
41. Fulton, R.E.; Sobieszczanski, J.; and Landrum, E.J.: An Integrated Computer System for Preliminary Design of Advanced Aircraft. AIAA Paper No. 72-796, August 1972.
42. Fulton, R.E.; Sobieszczanski, J.; Storaasli, O.; Landrum, E.J.; and Loendorf, D.: Application of Computer-Aided Aircraft Design in a Multi-disciplinary Environment. AIAA Paper No. 73-353, March 1973.

### References (Cont'd)

43. Heldenfels, R.R.: Automating the Design Process: Progress, Problems, Prospects, Potential. AIAA Paper No. 73-410, March 1973.
44. Melosh, R.J.; and Luik, R.: Approximate Multiple Configuration Analysis and Allocation for Least Weight Structural Design. AFFDL-TR-67-59, 1967.
45. Fox, R.L.: Constraint Surface Normals for Structural Synthesis Techniques. AIAA J., vol. 3, no. 8, 1965, pp. 1516-1517.
46. Fox, R.L.; and Kapoor, M.P.: Rates of Change of Eigenvalues and Eigenvectors. AIAA J. vol. 6, no. 12, 1968, pp. 2426-2429.
47. Storaasli, O.O.; and Sobieszczanski, J.: On the Accuracy of the Taylor - Approximation for Structural Resizing. AIAA J., vol. 12, no. 2, 1974, pp. 231-233.
48. Fox, R.L.; and Miura, H.: An Approximate Analysis Technique for Design Calculations. AIAA J., vol. 9, no. 1, 1971, pp. 177-179.
49. Noor, A.K.; and Lowder, H.E.: Approximate Techniques of Structural Reanalysis. J. of Computers and Structures, vol. 4, no. 4, 1974, pp. 801-812.
50. Noor, A.K.; and Lowder, H.E.: Structural Reanalysis via a Mixed Method. Int. J. of Computers and Structures, Vol. 5, No. 1, 1975, pp. 9-12.
51. Noor, A.K.: Multiple Configuration Analysis via Mixed Method. J. of the Structural Div. ASCE, vol. 100, no. ST9, 1974, pp. 1991-1997.
52. Bhatia, K.G.: Rapid Iterative Reanalysis for Automated Design. NASA TN D-6534, 1971.
53. Haftka, R.: Automated Procedure for Design of Wing Structures to Satisfy Strength and Flutter Requirements. NASA TN D-7264, 1973.
54. Rudisill, C.S.; and Bhatia, K.G.: Optimization of Complex Structures to Satisfy Flutter Requirements. AIAA J., vol. 9, no. 8, 1971, pp. 1487-1491.
55. Stroud, W.J.; Dexter, C.B.; and Stein, M.: Automated Preliminary Design of Simplified Wing Structures to Satisfy Strength and Flutter Requirements. NASA TN D-6534, 1971.
56. Miura, H.: An Optimal Configuration Design of Lifting Surface Type Structure under Dynamic Constraints. Ph.D. Dissertation, CWRU, Cleveland, Ohio, 1971.
57. Rao, S.S.: Automated Optimum Design of Aircraft Wings to Satisfy Strength, Stability, Frequency and Flutter Requirements. Ph.D. Dissertation, CWRU, Cleveland, Ohio, 1971.

58. Fox, R.L.; Miura, H.; and Rao, S.S.: Automated Design Optimization of Supersonic Airplane Wing Structures under Dynamic Constraints. AIAA Paper No. 72-333, April 1972.
59. Gwinn, L.B.; and Taylor, R.F.: A General Method for Flutter Optimization. AIAA J., vol. 11, no. 12, 1973, pp. 1613-1617.
60. Schmit, L.A., and Tung, T.K.: Optimum Design. Advanced Composites Design Guide, 3rd Edition, vol. 2, section 2.3, January 1973.
61. Schmit, L.A.: and Farshi, B.: Optimum Laminate Design for Strength and Stiffness. Int. J. for Numerical Methods in Engineering, vol. 7, no. 4, 1973.
62. Laakso, J.H.: Design Synthesis of a Boron/Epoxy Reinforced Metal Shear Web. AIAA Paper No. 72-395, April 1972.
63. Laakso, J.H. and Zimmerman, D.K.: Synthesis of Compression Panels Having Nonuniform Stiffener Sections. AIAA Paper No. 73-347, March 1973.
64. McCullers, L.A.; and Lynch, R.W.: Dynamic Characteristics of Advanced Filamentary Composite Structures, vol. II, Aeroelastic Synthesis Procedure Development, AFFDL-TR-73-111, August 1973.
65. Pope, G.G.: Optimum Design of Stressed Skin Structures. AIAA J., vol. 11, no. 11, 1973, pp. 1545-1552.
66. Smith, G.K.; and Woodhead, R.G.: A Design Scheme for Ship Structures. The Royal Institution of Naval Architects Paper No. 5, Spring Meeting, April 1973.
67. Vanderplaats, G.N.; and Moses, F.: Structural Optimization by Methods of Feasible Directions. J. of Computers and Structures, vol. 3, no. 4, 1973, pp. 739-755.
68. Vanderplaats, G.N.: CONMIN - A Fortran Program for Constrained Function Minimization - User's Manual. NASA TMX-62-282, August 1973.
69. Pickett, R.M.: Automated Structural Synthesis using a Reduced Number of Design Coordinates. Ph.D. Dissertation, UCLA, Los Angeles, California, 1971.
70. Pickett, R.M.; Rubinstein, M.F.; and Nelson, R.B.: Automated Structural Synthesis using a Reduced Number of Design Coordinates. AIAA J., vol. 11, no. 4, 1973, pp. 489-494.

71. Farshi, B.: Approximation Concepts for Efficient Design Synthesis of Structures. Ph.D. Dissertation, UCLA, Los Angeles, California, 1973.
72. Schmit, L.A.; and Farshi, B.: Some Approximation Concepts for Structural Synthesis. AIAA J., vol. 12, no. 5, 1974, pp. 692-699.
73. Baldur, R.: Structural Optimization by Inscribed Hyperspheres. J. of the Engr. Mech. Div., ASCE, vol. 98, no. EM3, 1972, pp. 503-508.
74. Terai, K.: Application of Optimality Criteria in Structural Synthesis. M.S. Thesis, UCLA, Los Angeles, California, 1974.
75. Kavlie, D.; and Moe, J.: Automated Design of Frame Structures. J. of the Structural Div., ASCE, vol. 97, no. ST1, 1971, pp. 33-62.
76. Miura, H. and Schmit, L.A.: ACCESS 1 Program Documentation and User's Guide, NASA CR-144905, 1976.
77. Melosh, R.J.; and Bamford, R.M.: Efficient Solution of Load-Deflection Equations. J. of the Structural Div., ASCE, vol. 95, no. ST 4, 1969, pp. 661-676.
78. Rosen, J.B.: The Gradient Projection Method for Nonlinear Programming, Part I, Linear Constraints. Journal SIAM, vol. 8, 1960, pp. 181-217.
79. Fiacco, A.; and McCormick, G.P.: The Sequential Unconstrained Minimization Technique for Nonlinear Programming, A Primal-Dual Method. Manag. Sci., vol. 10, 1964, pp. 360-365.
80. Fletcher, R.; and Reeves, C.M.: Function Minimization by Conjugate Gradients. Computer Journal (British), vol. 7, 1964, pp. 149-154.
81. Fletcher, R.; and Powell, M.J.D.: A Rapidly Convergent Descent Method for Minimization. Computer Journal (British), vol. 6, 1963, pp. 163-168.
82. Wilde, D.J.: Optimum Seeking Methods. Prentice Hall, 1964.
83. Berke, L.; and Khot, N.S.: Use of Optimality Criteria Methods for Large Scale Systems. AGARD Lecture Series No. 70 on Structural Optimization, AGARD-LS-70, 1974, pp. 1-29.
84. Farshi, B.; and Schmit, L.A.: Minimum Weight Design of Stress Limited Trusses. J. of the Structural Div., ASCE, vol. 100, no. ST1, 1974, pp. 97-107.

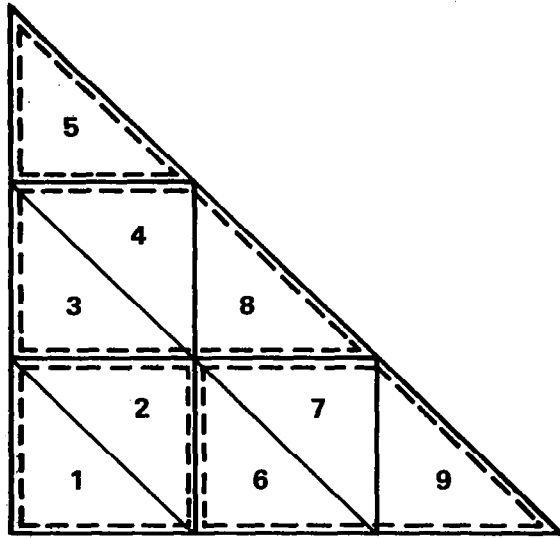


**Figure 1. Design Variable Linking. Simple Example.**

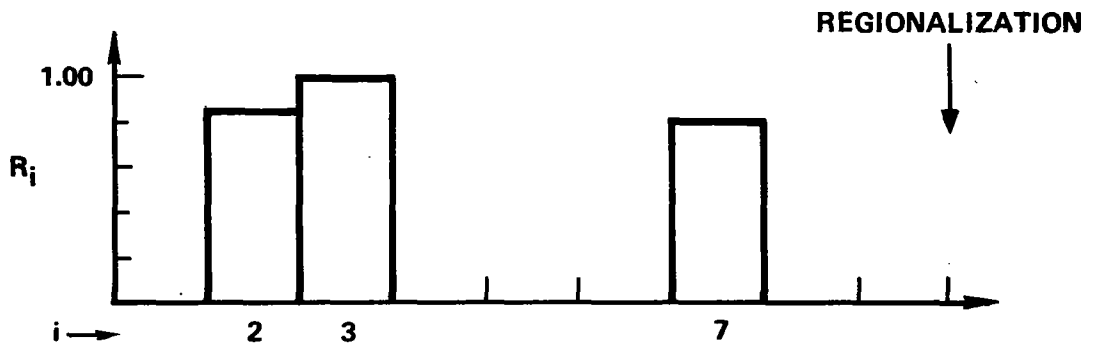
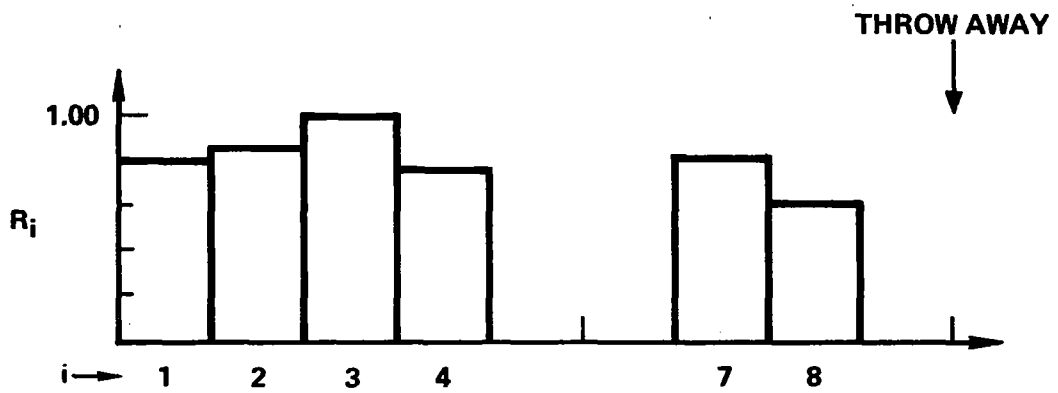
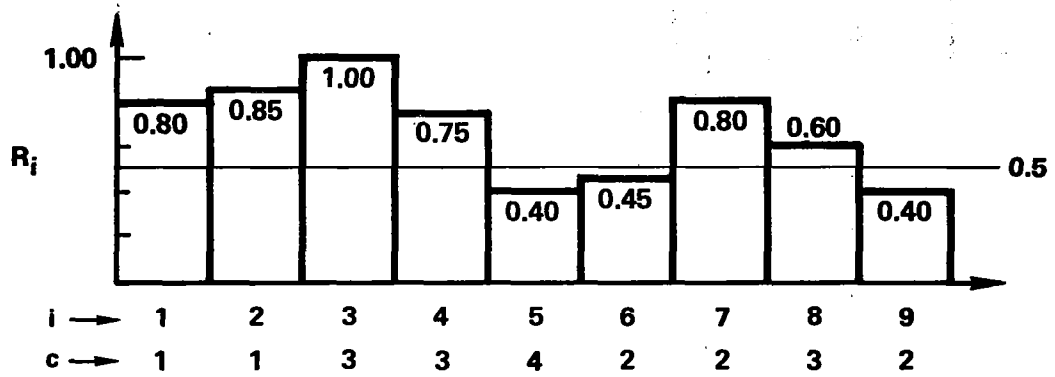


**Figure 2. Throw Away Followed by Regionalization.**

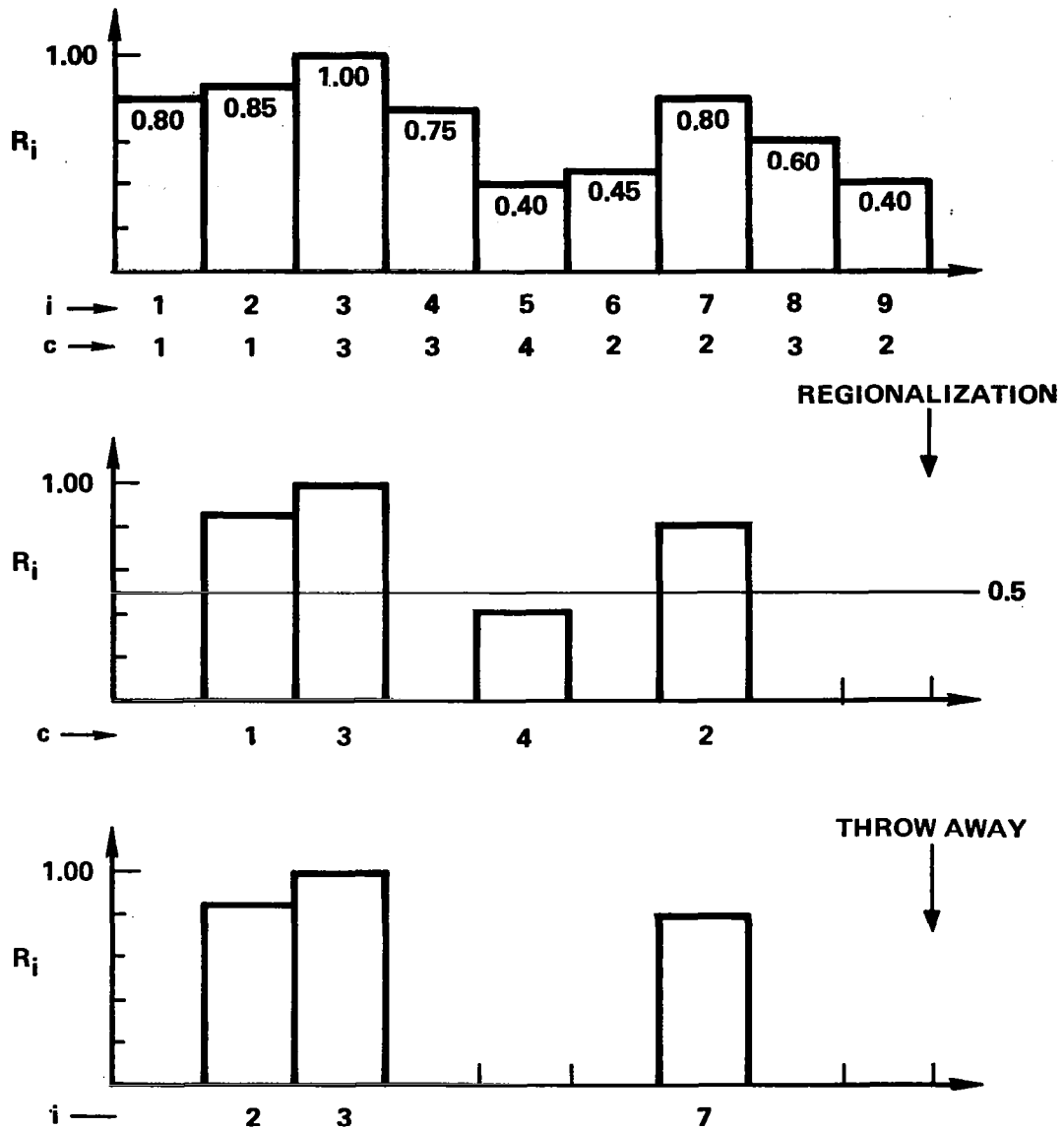


Figure 3. Regionalization Followed by Throw Away.

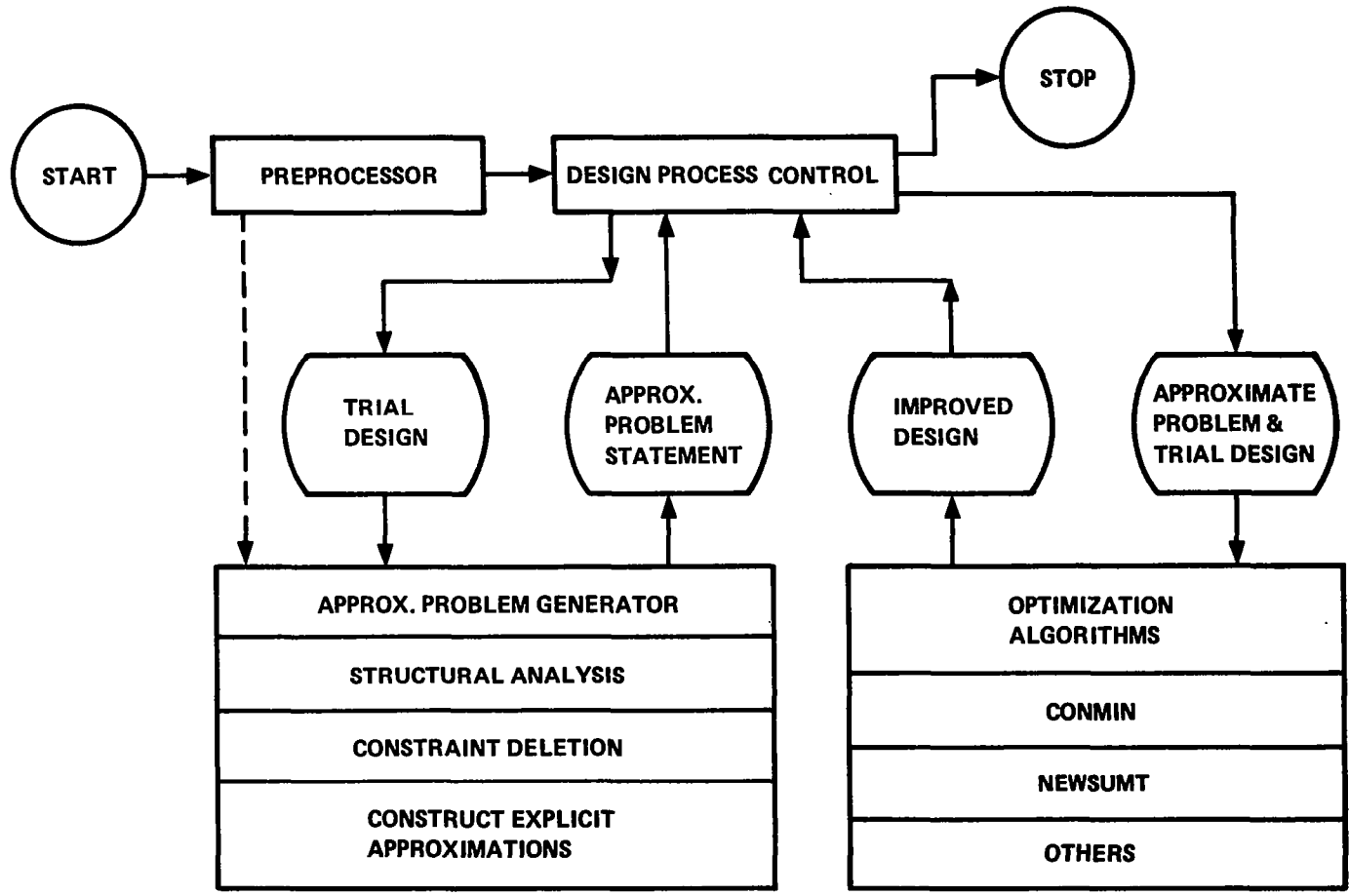


Figure 4. ACCESS 1 Basic Organization.

- TRUSS
- △ CST
- SSP

NUMBERS WITHIN SYMBOLS INDICATE ELEMENT NO.  
 NUMBERS AT ELEMENT JUNCTIONS INDICATE NODE NO.

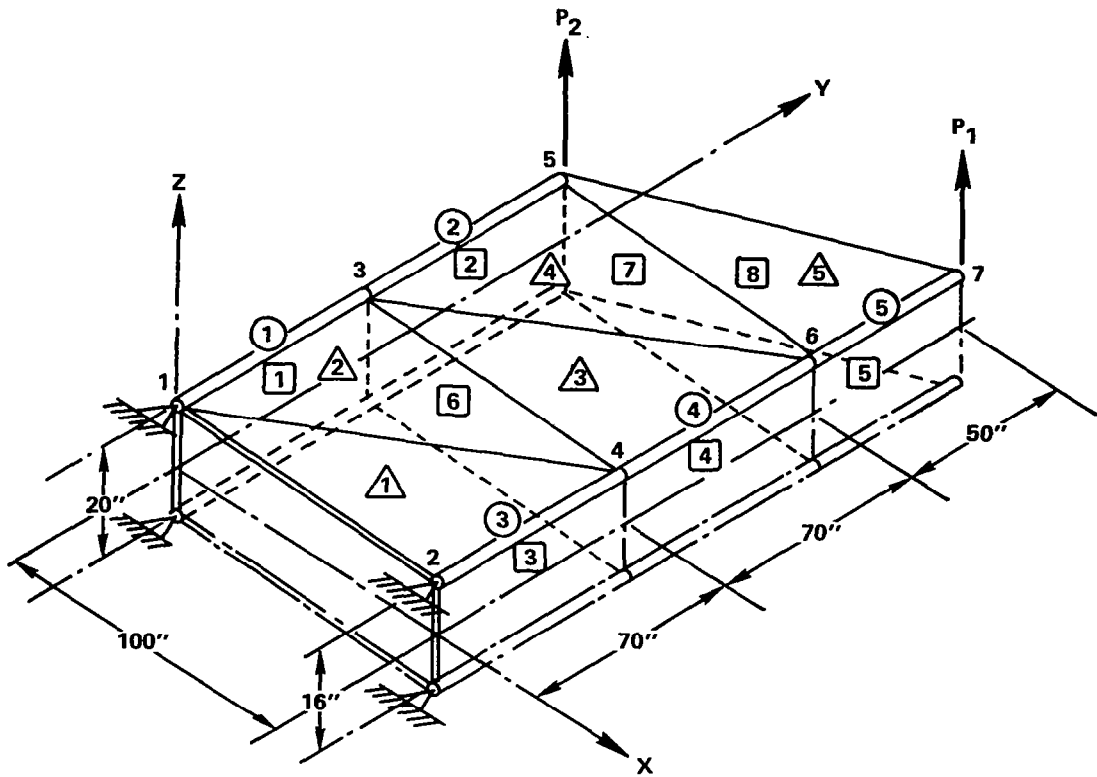


Figure 5. Finite Element Model for Eighteen Element Wing Box (Model 1).

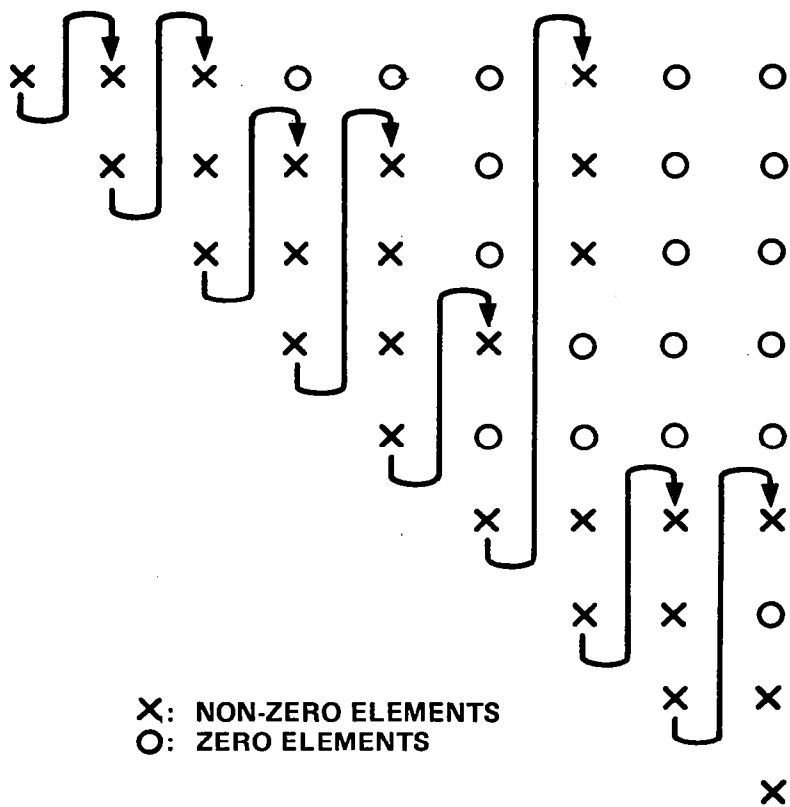


Figure 6. Compact Vector Form of System Stiffness Matrix [K] Used to Reduce Storage Requirements for ACCESS 1.

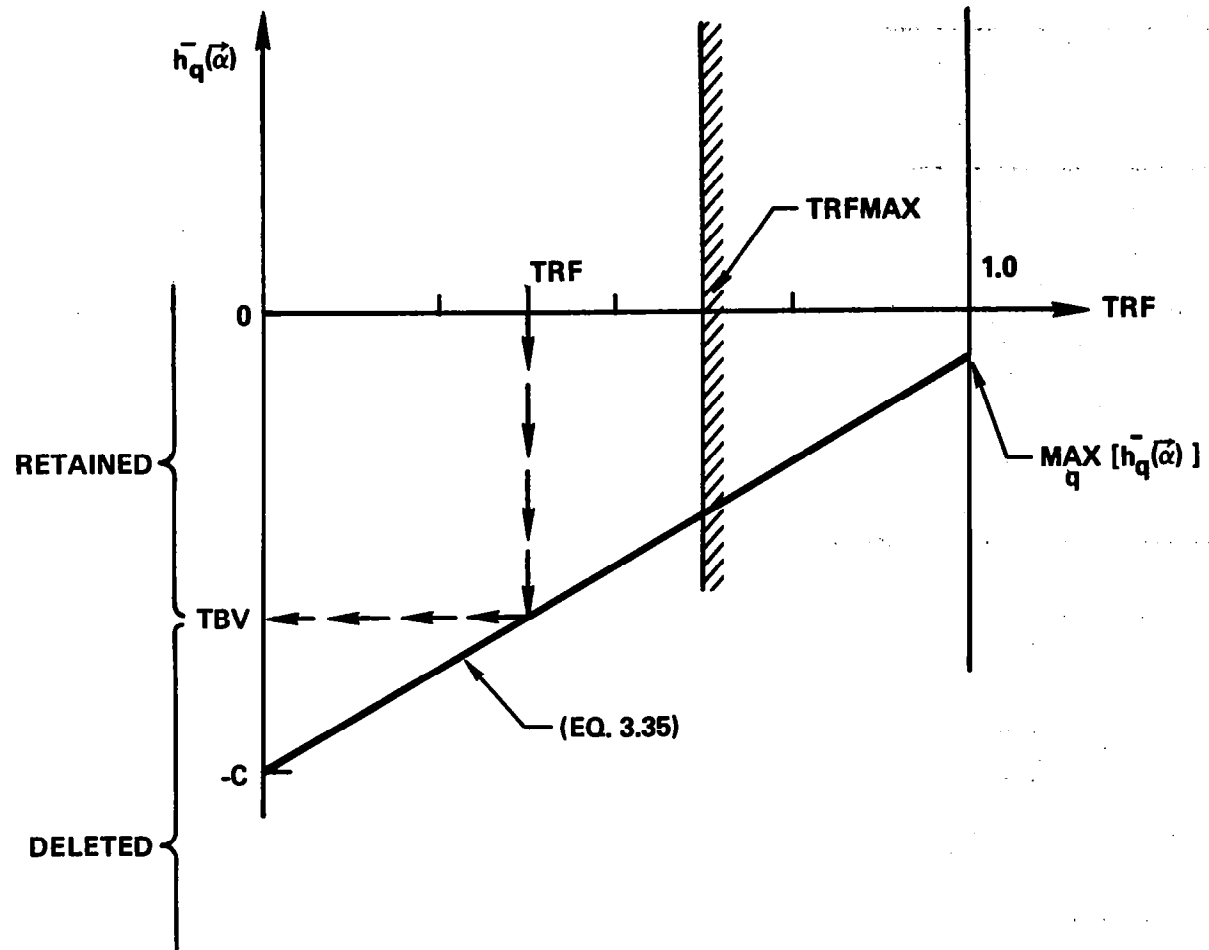


Figure 7. Truncation Boundary Value (TBV) versus Truncation Factor (TRF).

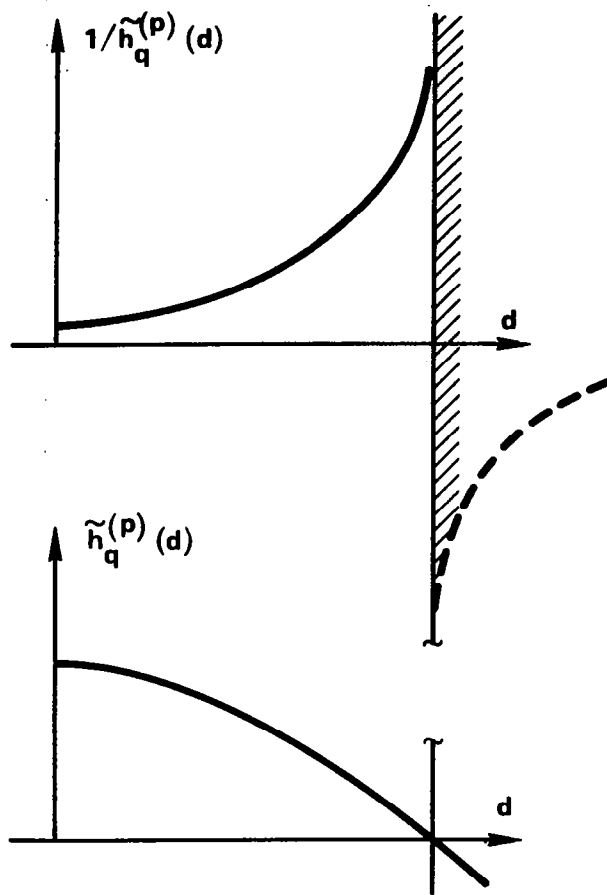
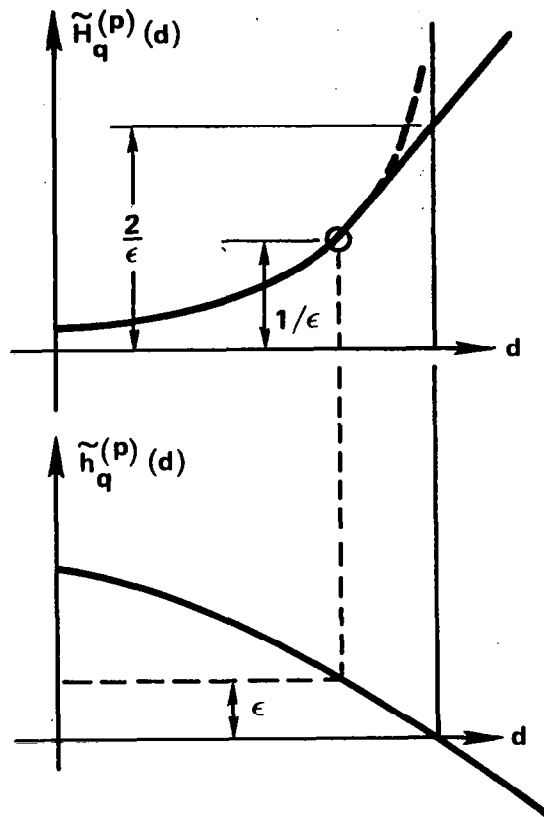


Figure 8. Interior Penalty Function (Fiacco and McCormick, Ref. 79).



**Figure 9.** Extended Interior Penalty Function (Kavlie and Moe, Ref. 75).  
 (SEE Eg. 3.66)

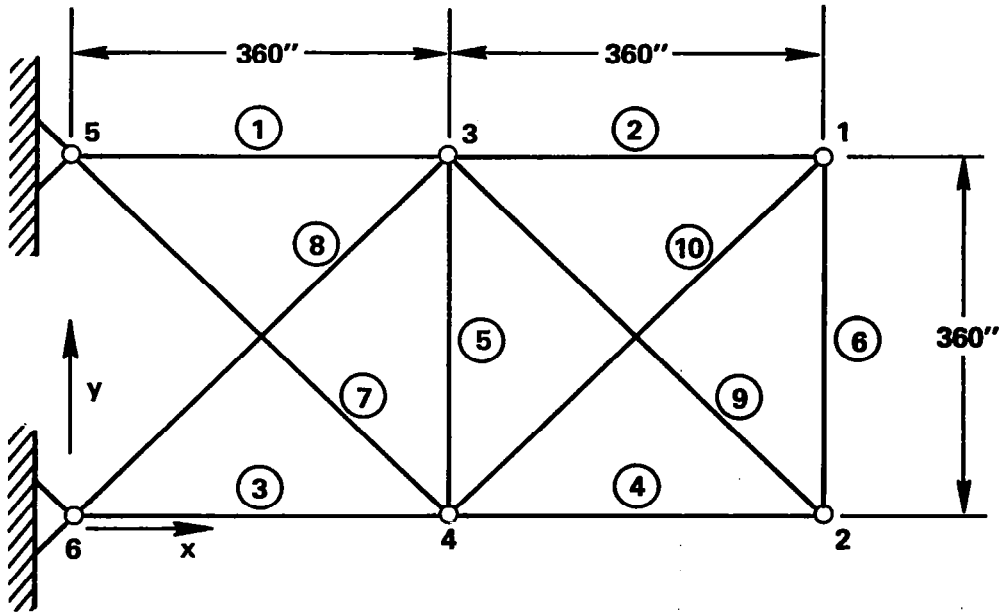


Figure 10. Planar Ten Bar Cantilever Truss.

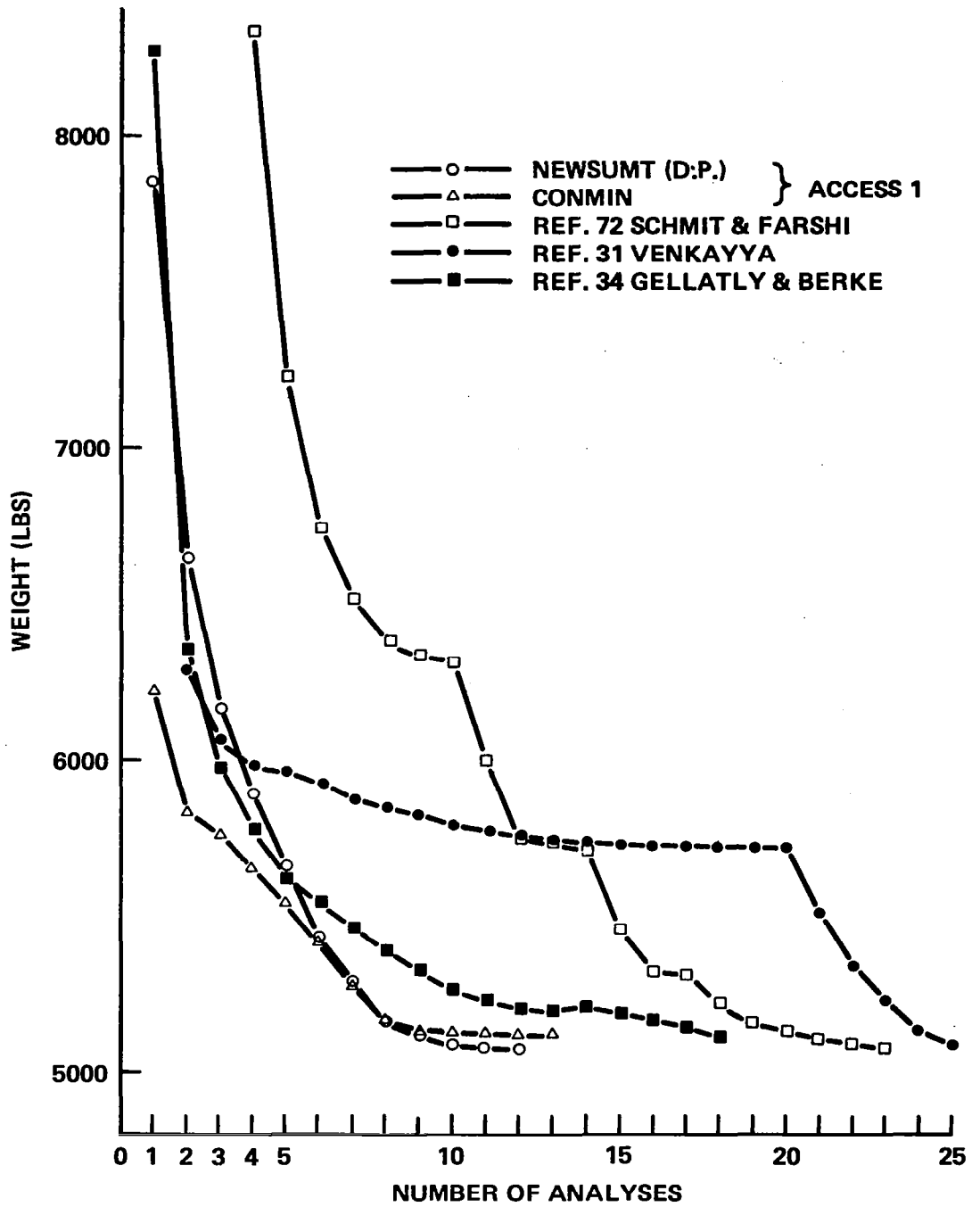


Figure 11. Iteration Histories for Problem 3, Planar Ten Bar Cantilever Truss (See Table 25).

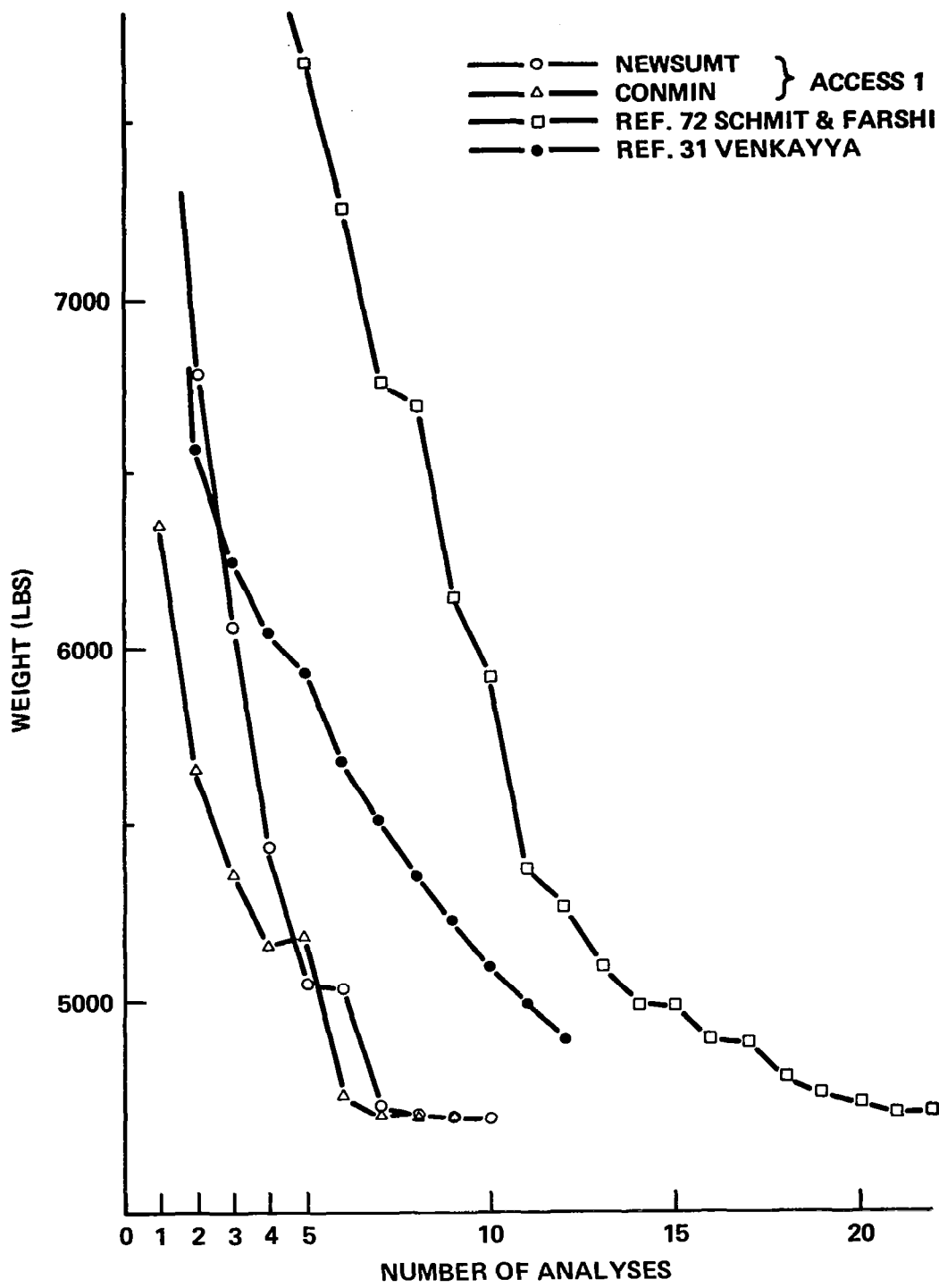


Figure 12. Iteration Histories for Problem 4, Planar Ten Bar Cantilever Truss (See Table 27).

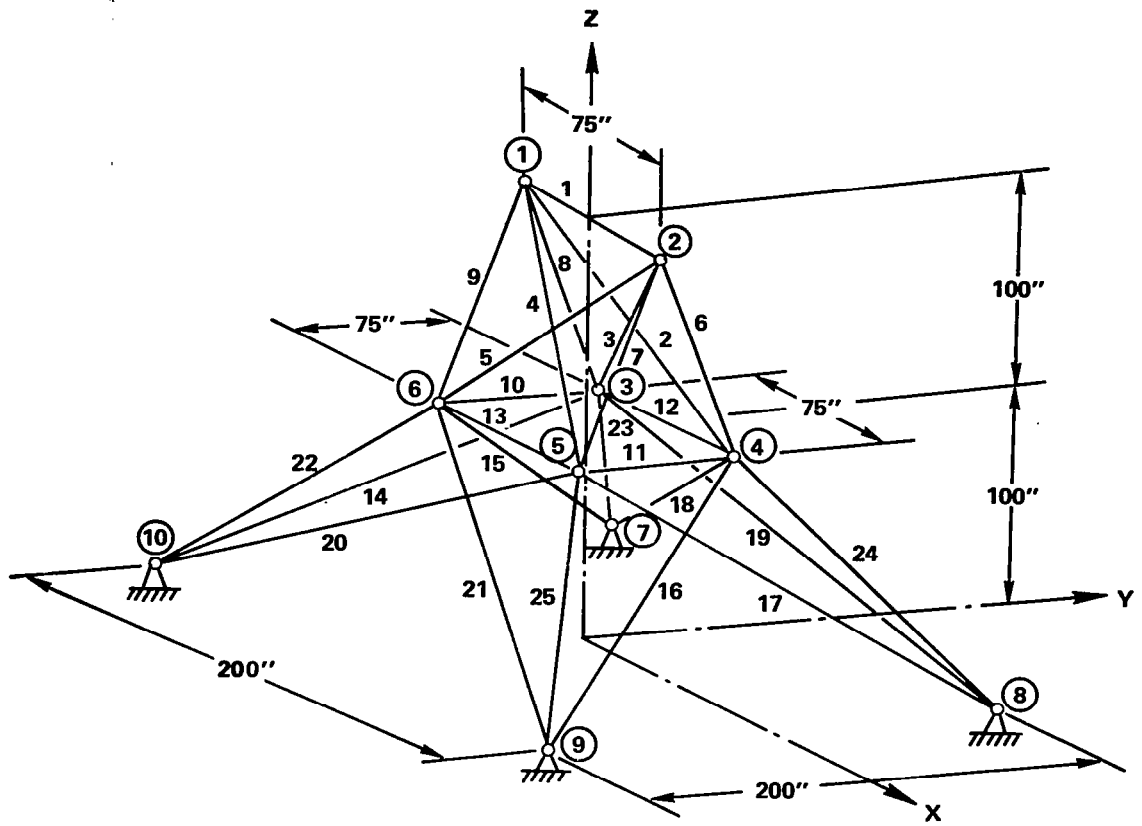


Figure 13. 25 Bar Space Truss.

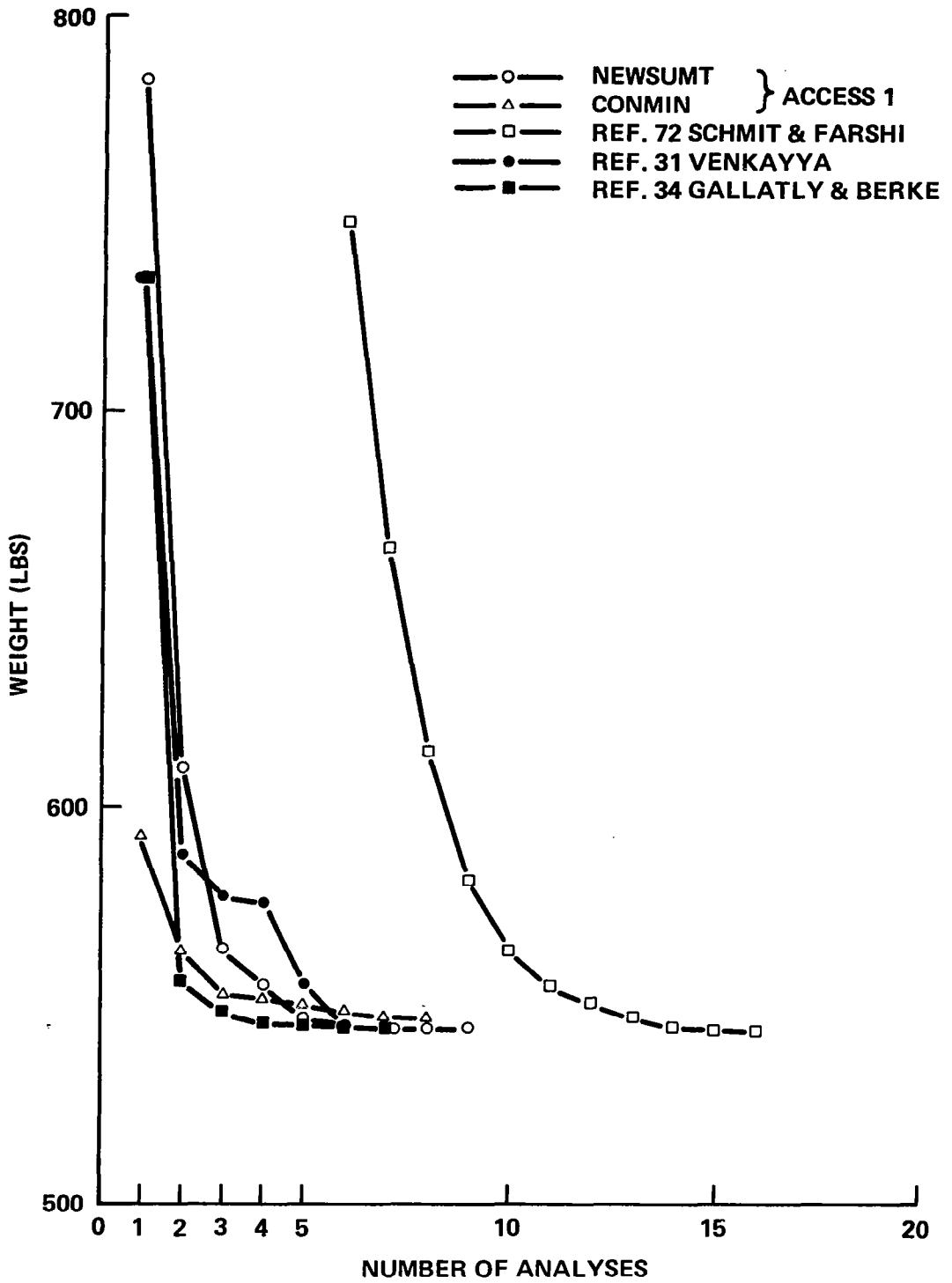
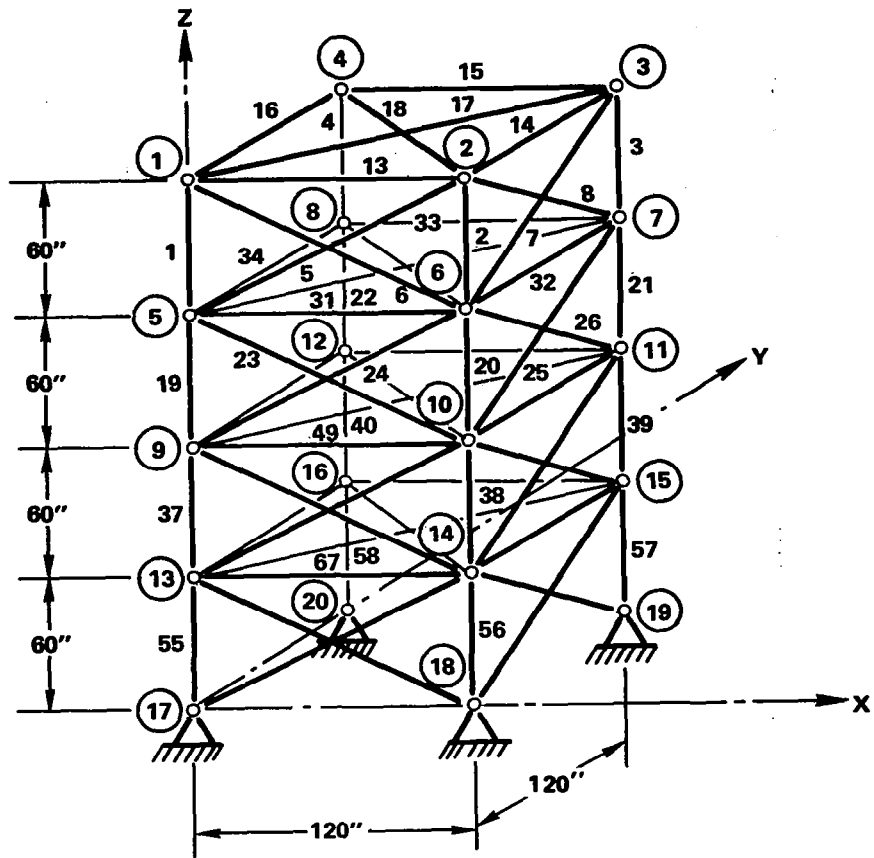


Figure 14. Iteration Histories for Problem 5, 25 Bar Space Truss (See Table 34).



**Note:** For the sake of clarity, not all elements are drawn in this figure.

**Figure 15. 72 Bar Space Truss.**

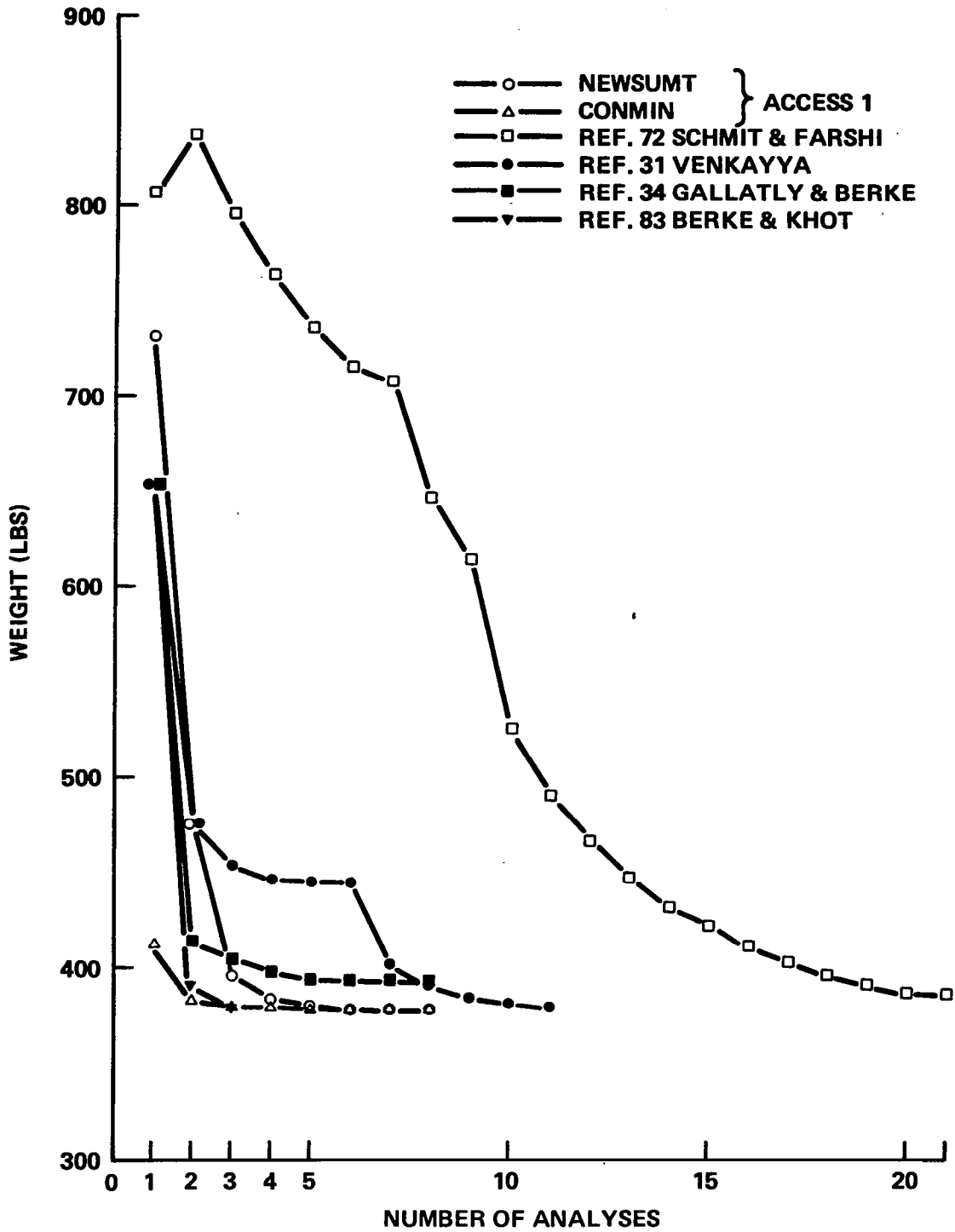
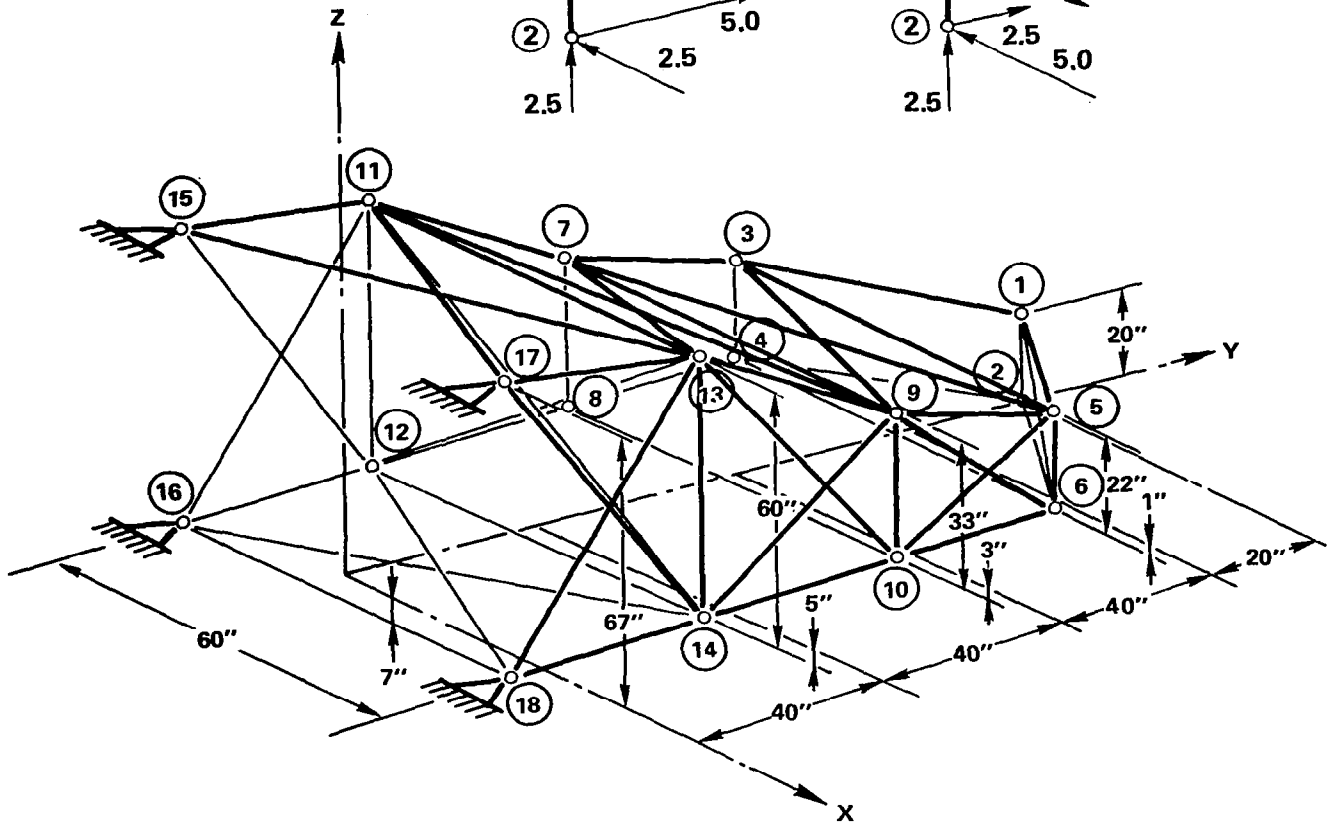
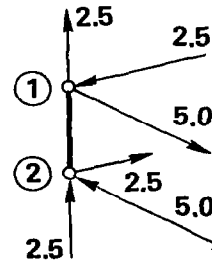
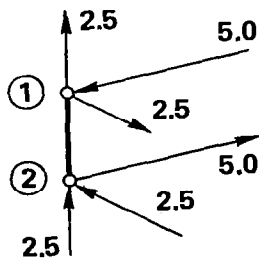


Figure 16. Iteration Histories for Problem 6, 72 Bar Space Truss (See Table 41).

LOAD CONDITION 1  
( $10^6$  LBS)

LOAD CONDITION 2  
( $10^6$  LBS)



Note: For the sake of clarity, not all elements are drawn in this figure.

Figure 17. Truss Idealization of Wing Carry Through Structure.

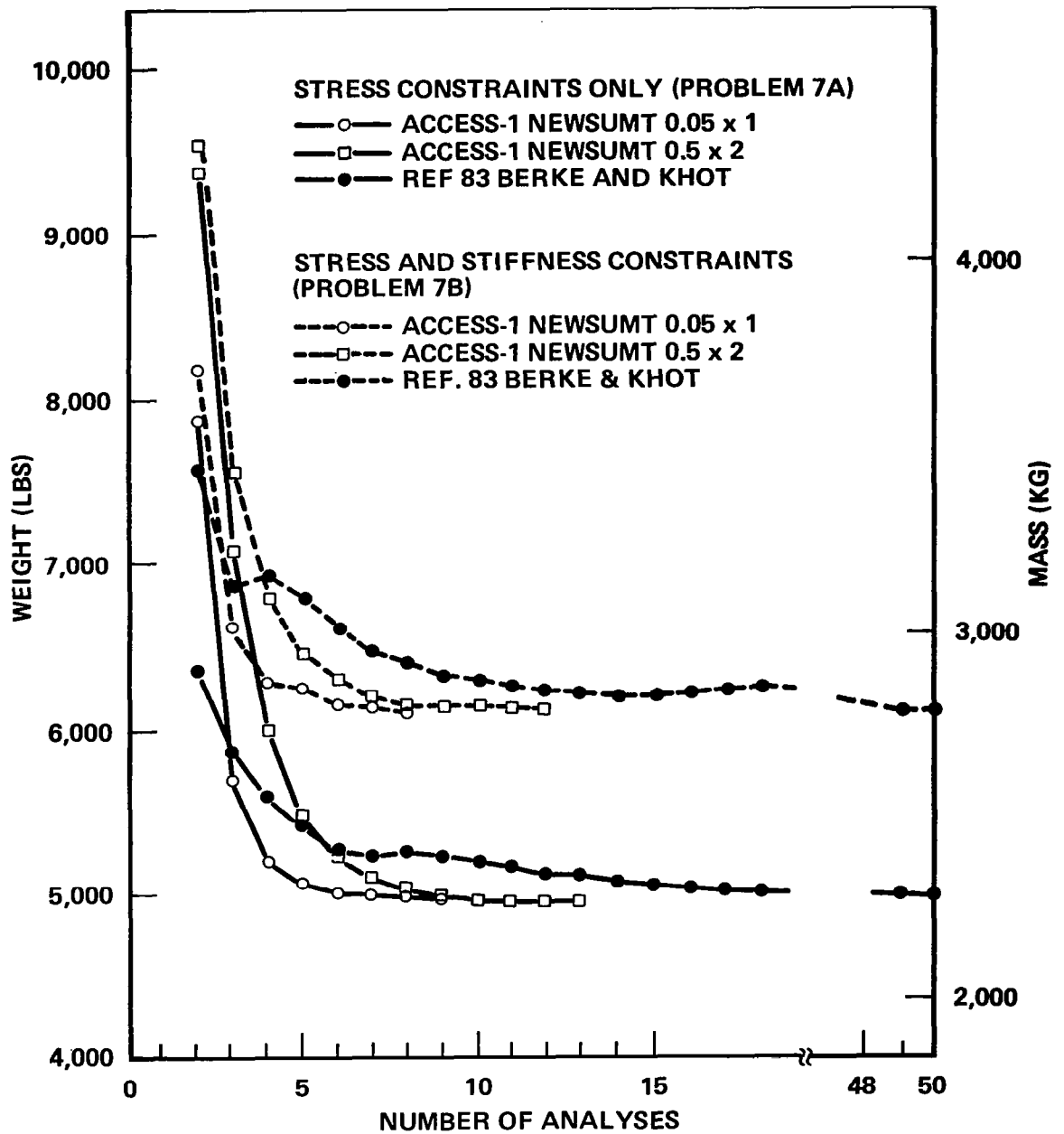


Figure 18. Iteration Histories for Problem 7 Wing Carry-Through Structure Truss Model (From Ref. 83) (See Section 4.2.4 and Table 47).

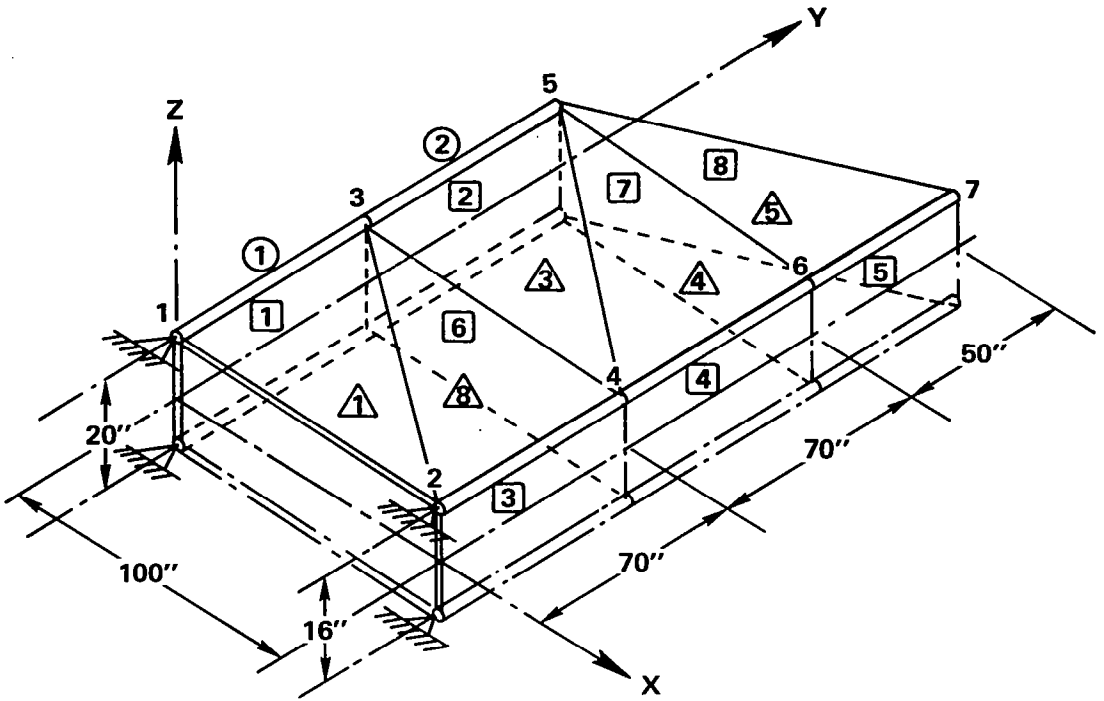


Fig. 19 Eighteen Element Wing Box (Model 2)

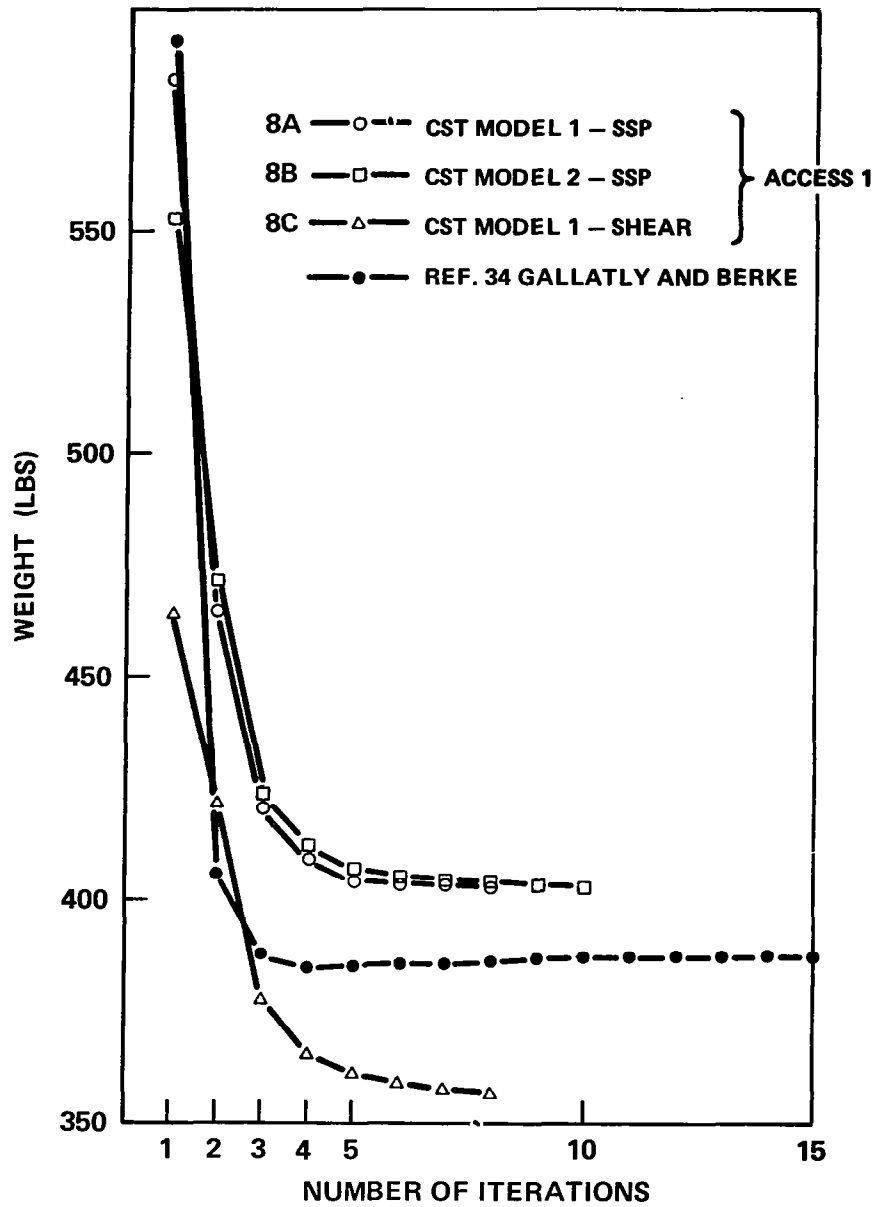


Figure 20. Iteration History for Problem 8  
18 Element Wing Box

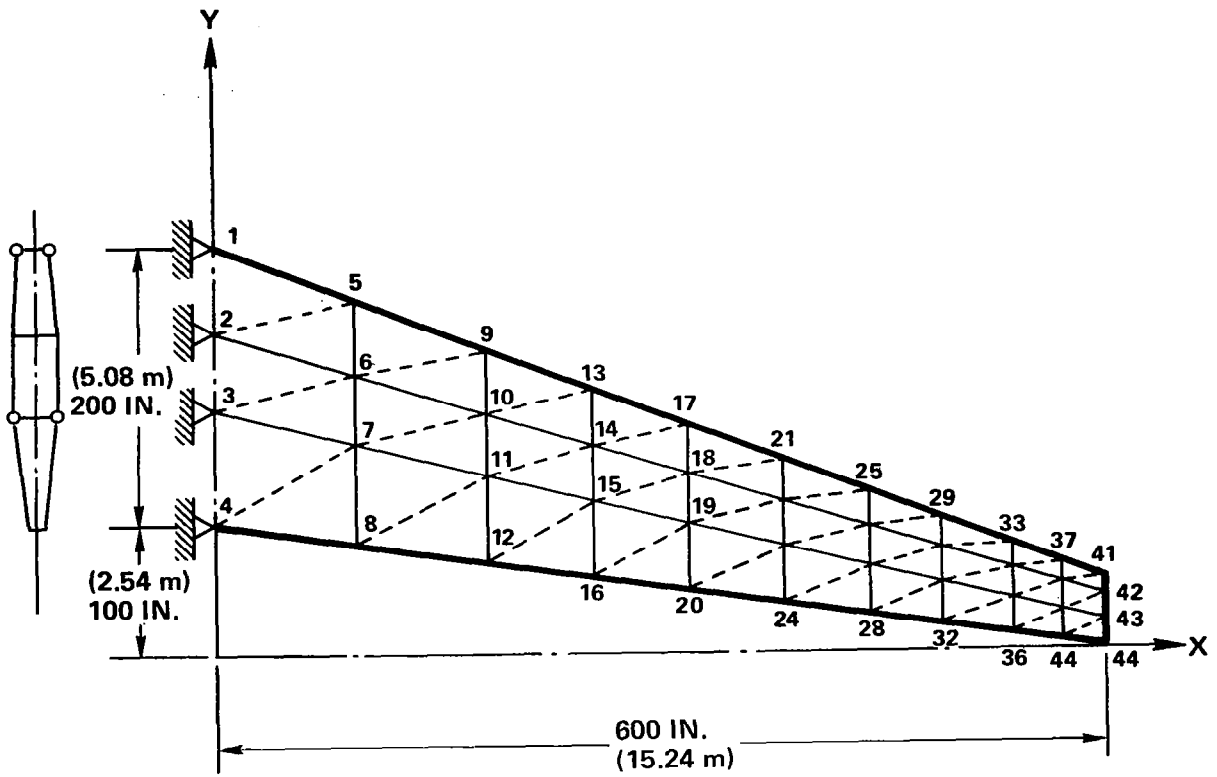
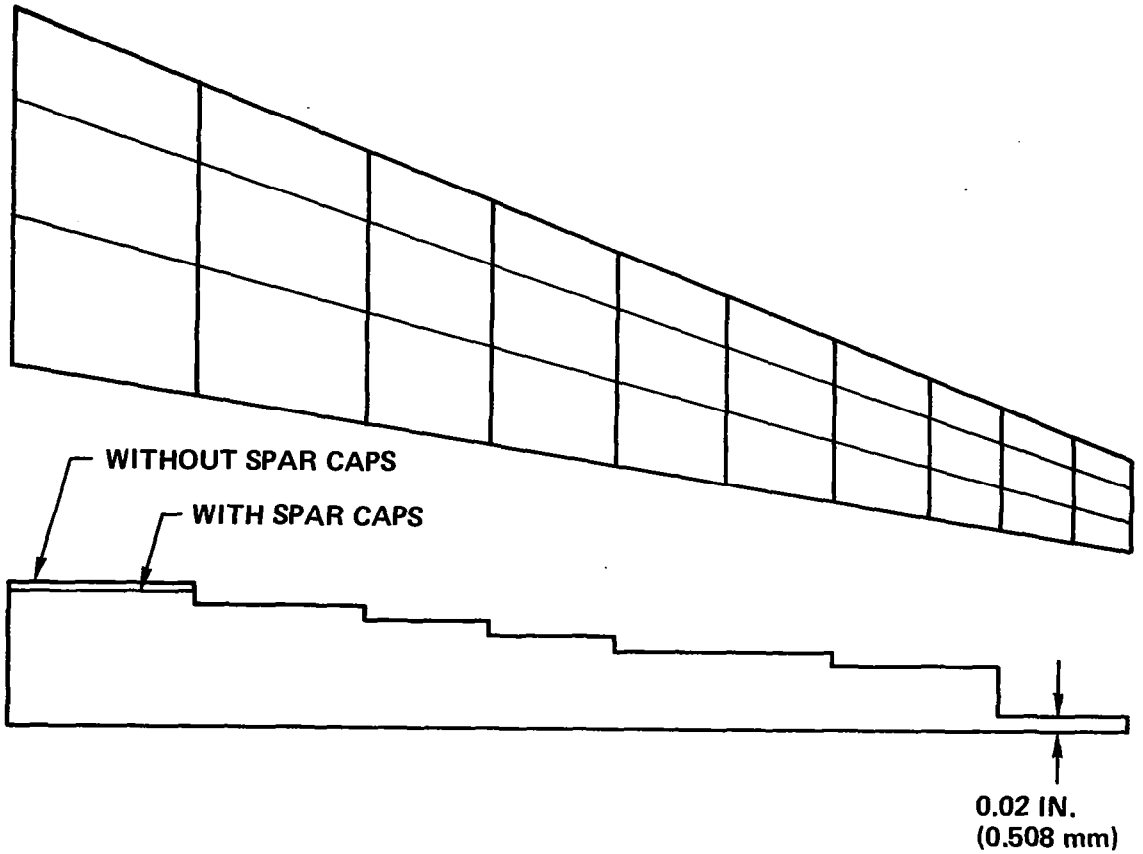
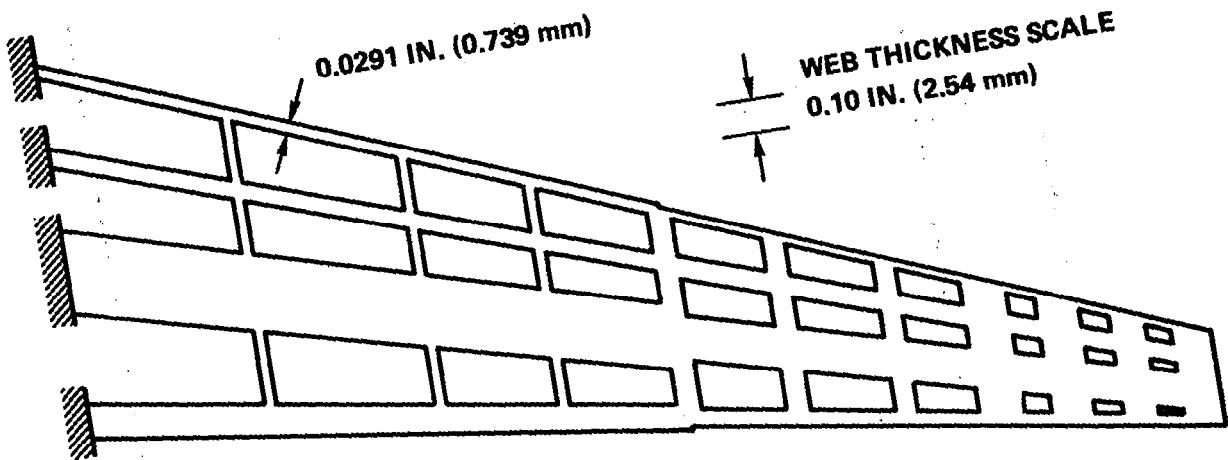


Figure 21. Finite Element Model for Swept Wing Example (Problem 9).

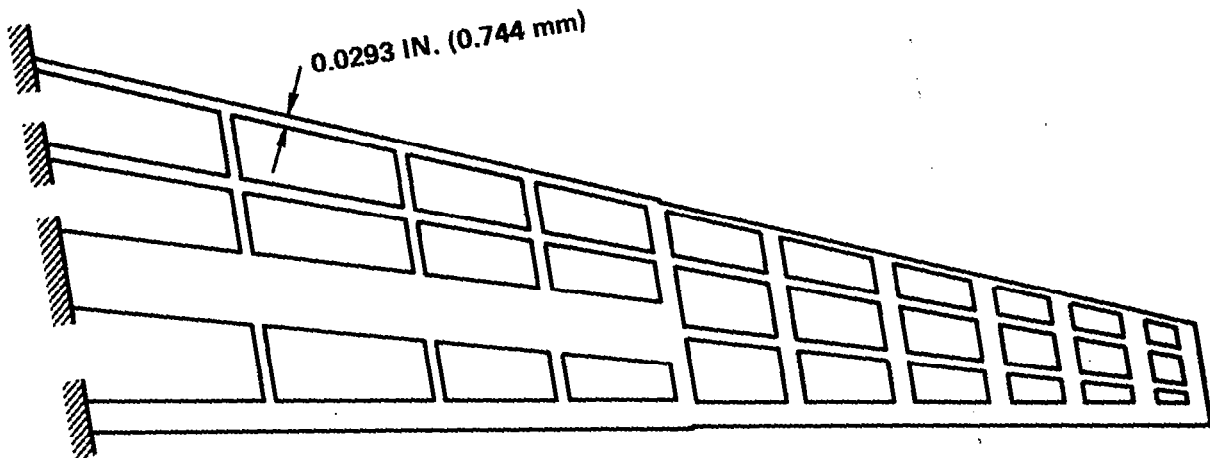


**NOTE: SKIN PANEL THICKNESSES ARE UNIFORM CHORD WISE**

**Figure 22. Final Skin Panel Thickness Distribution. 150 (130) Element Swept Wing.**

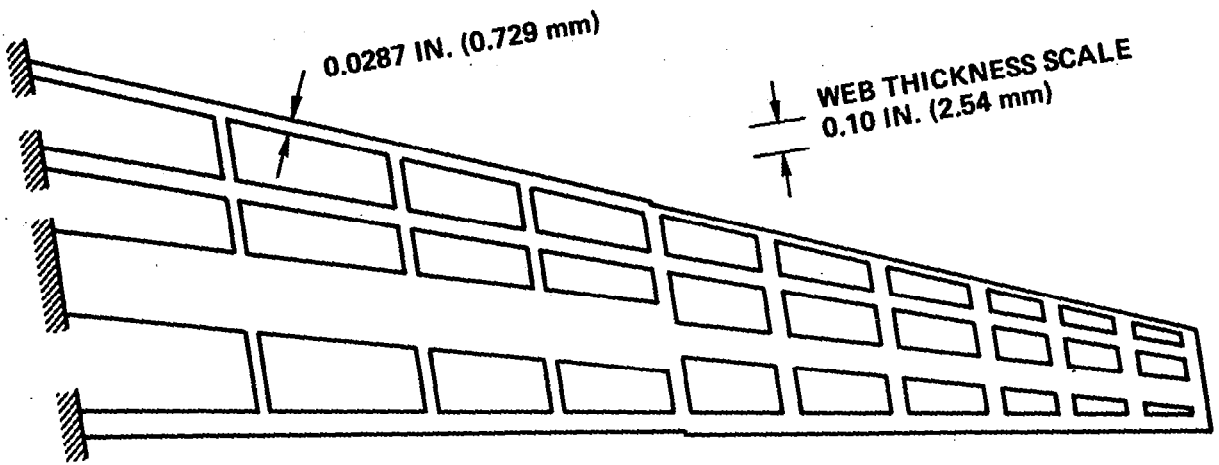


INITIAL DESIGN I  
9A

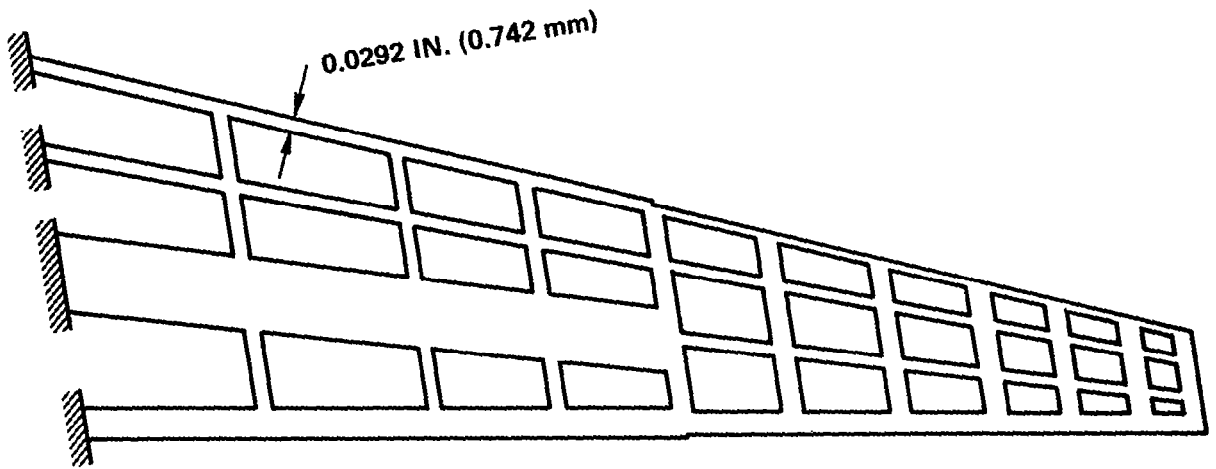


INITIAL DESIGN II  
9B

Figure 23. Final Web Thickness Distribution for Swept Wing Example. Cases Without Spar Caps.



INITIAL DESIGN I  
9C



INITIAL DESIGN II  
9D

Figure 24. Final Web Thickness Distribution for Swept Wing Example Cases with Spar Caps.

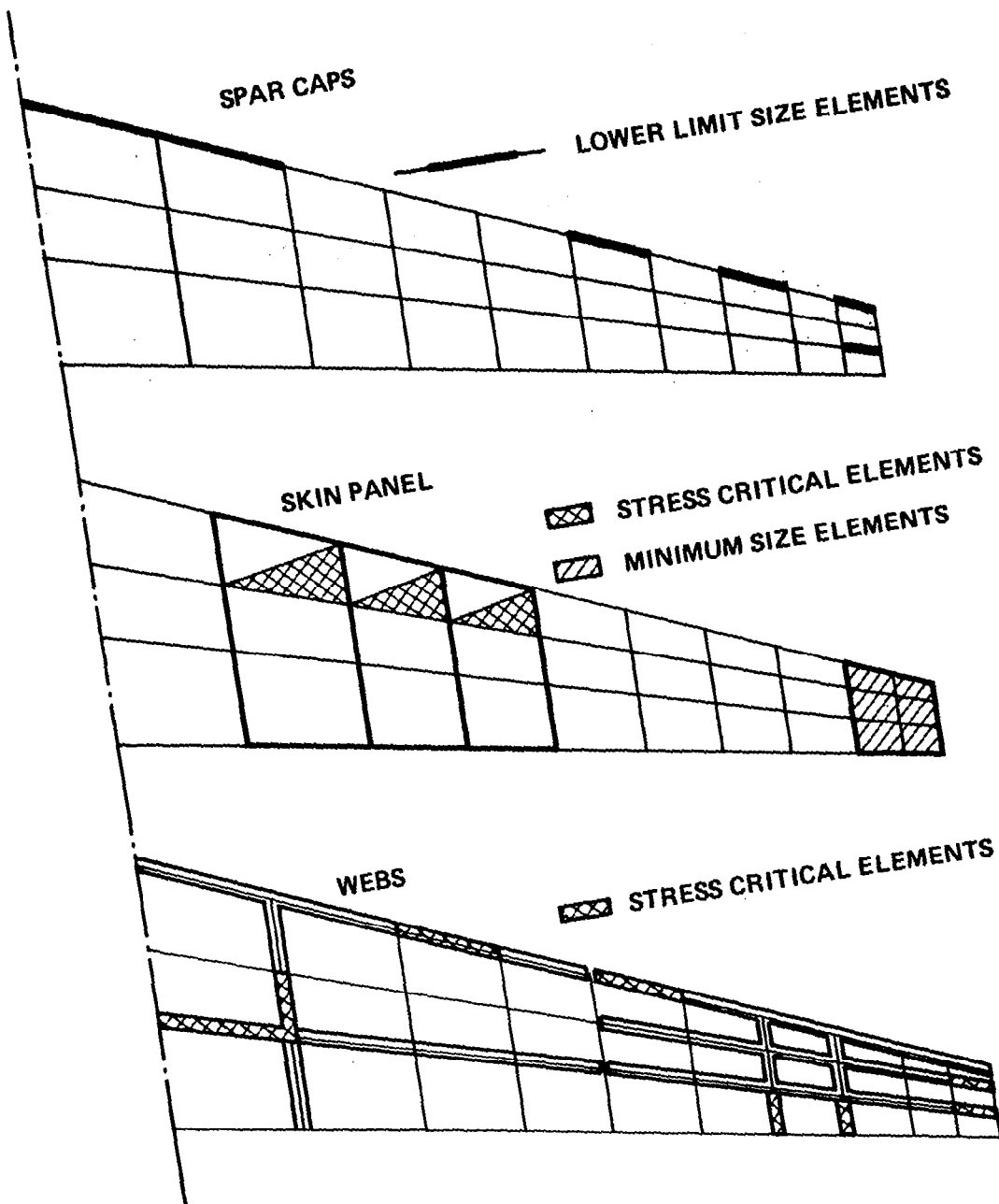


Figure 25. Critical Constraints for Final Designs  
150(130)-Element Swept Wing.

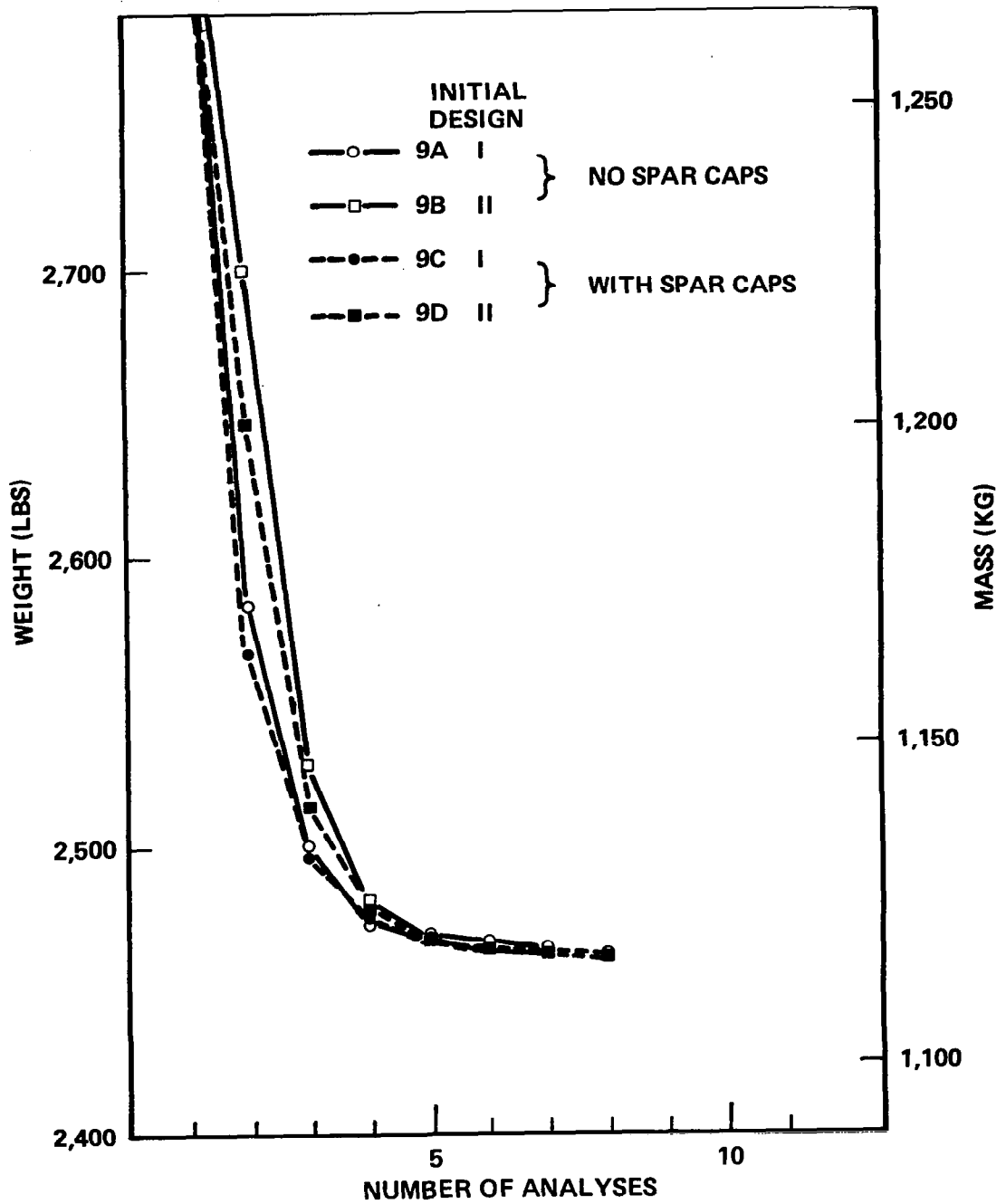


Figure 26. Iteration Histories for Problem 9 150, (130) Element Swept Wing.

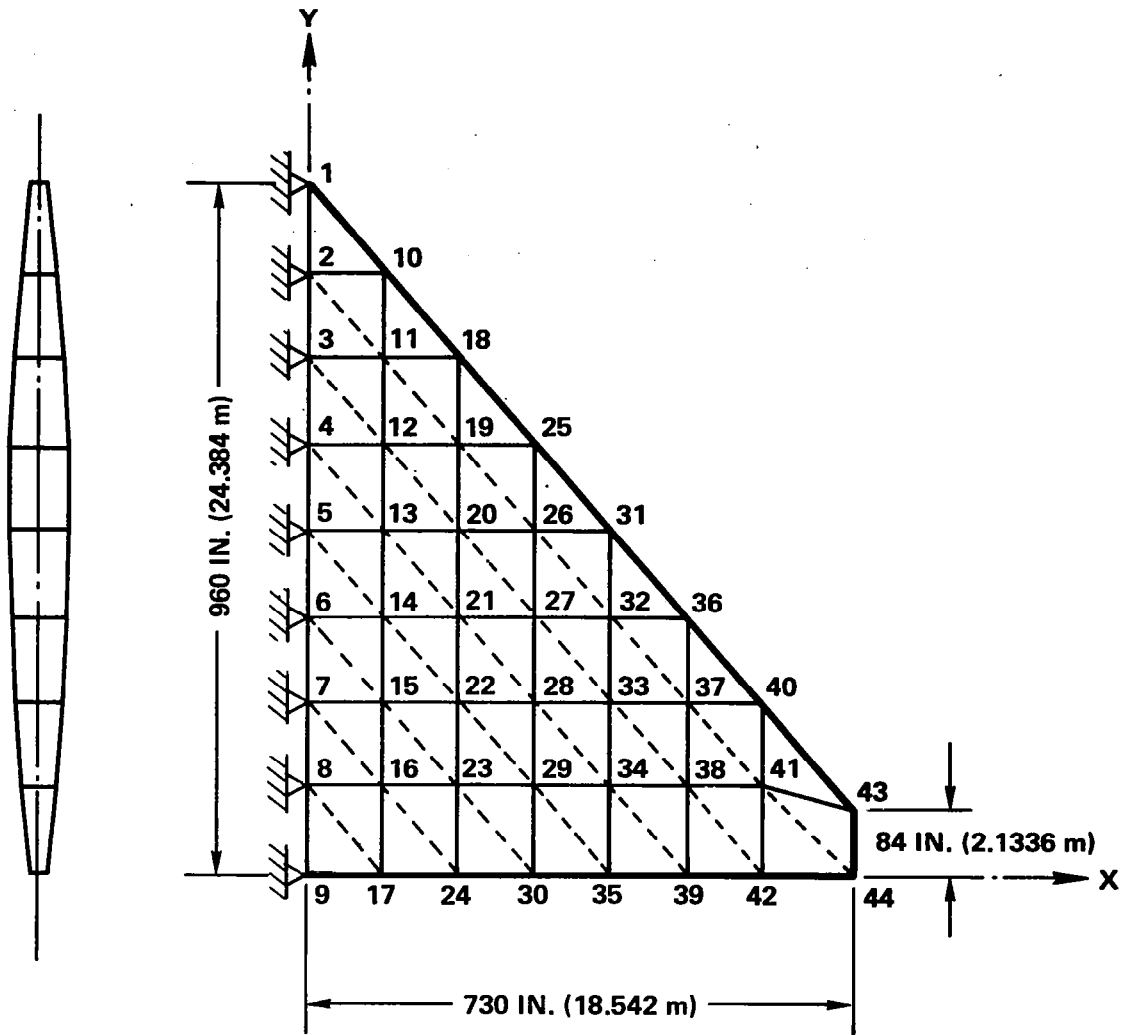
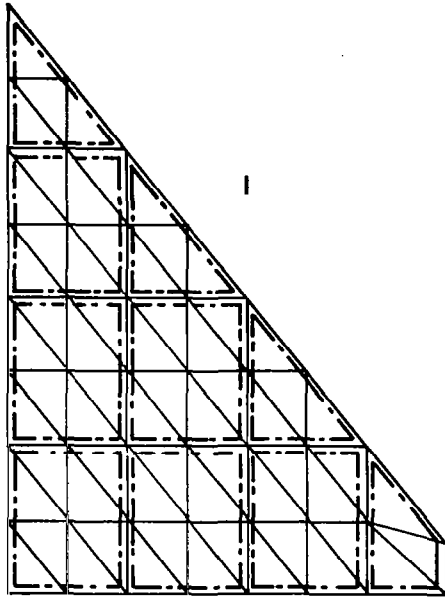
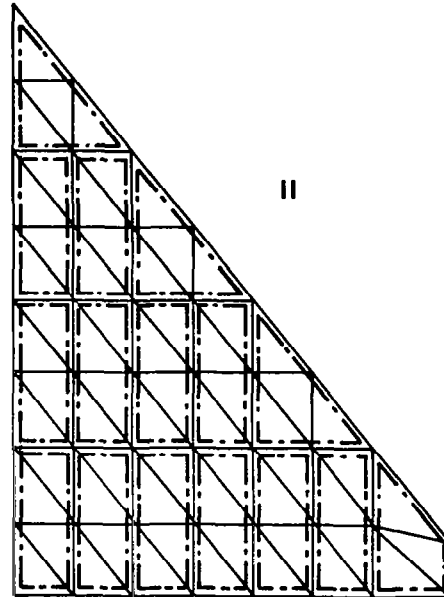


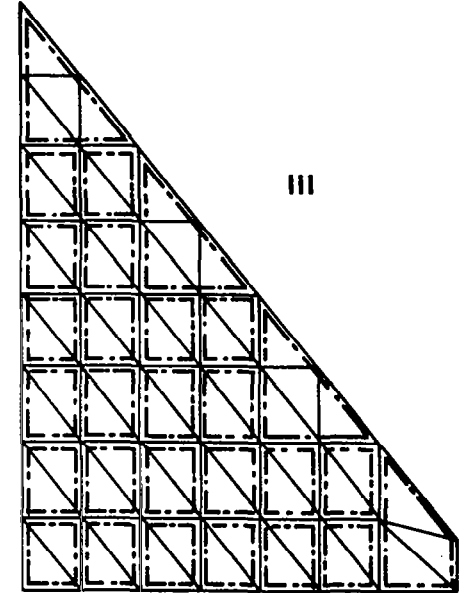
Figure 27. Delta Wing Example (Problem 10).



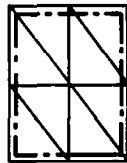
10 LINKED DESIGN VARIABLES



16 LINKED DESIGN VARIABLES

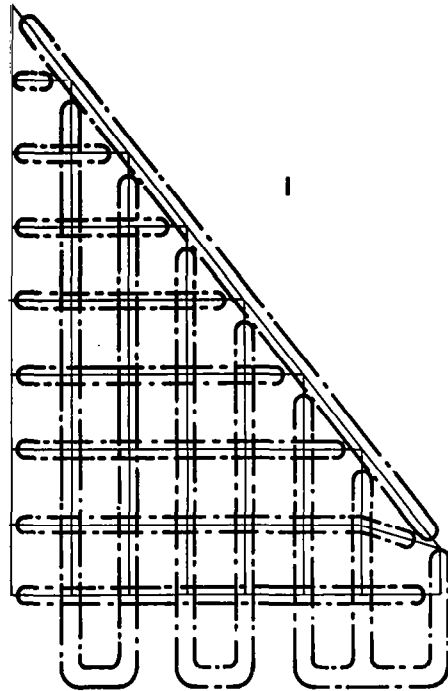


28 LINKED DESIGN VARIABLES

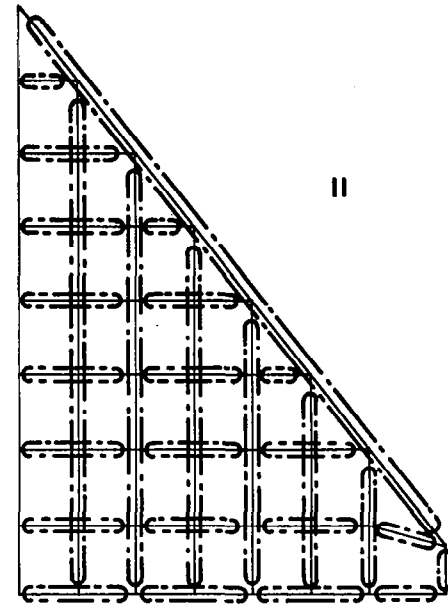


INDICATES THAT THE THICKNESSES OF THESE 8 TRIANGULAR MEMBRANE ELEMENTS ARE "LINKED" AND CONTROLLED BY A SINGLE DESIGN VARIABLE

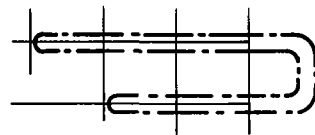
Figure 28. Alternate Linking Arrangements for the Skin (CST Elements) of Delta Wing Examples (Problem 10).



12 LINKED DESIGN VARIABLES



28 LINKED DESIGN VARIABLES



INDICATES THAT THE THICKNESSES OF THESE 5 SHEAR PANELS ARE LINKED AND CONTROLLED BY A SINGLE DESIGN VARIABLE

Figure 29. Alternate Linking Arrangements for the Webs (SSP Elements) of Delta Wing Examples (Problem 10).

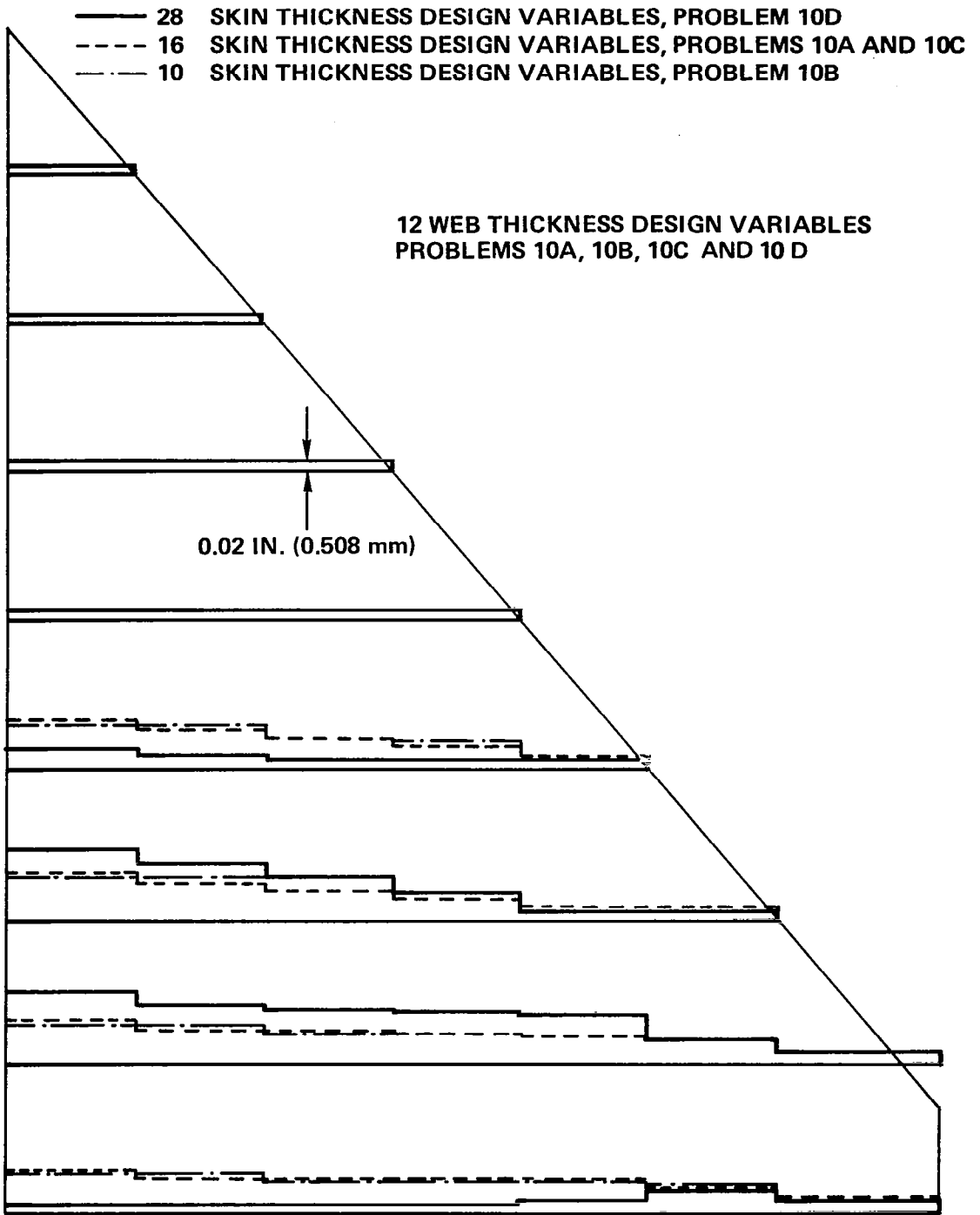


Figure 30. Final Skin Panel Thickness Distributions for Four Delta Wing Examples (Problem 10).

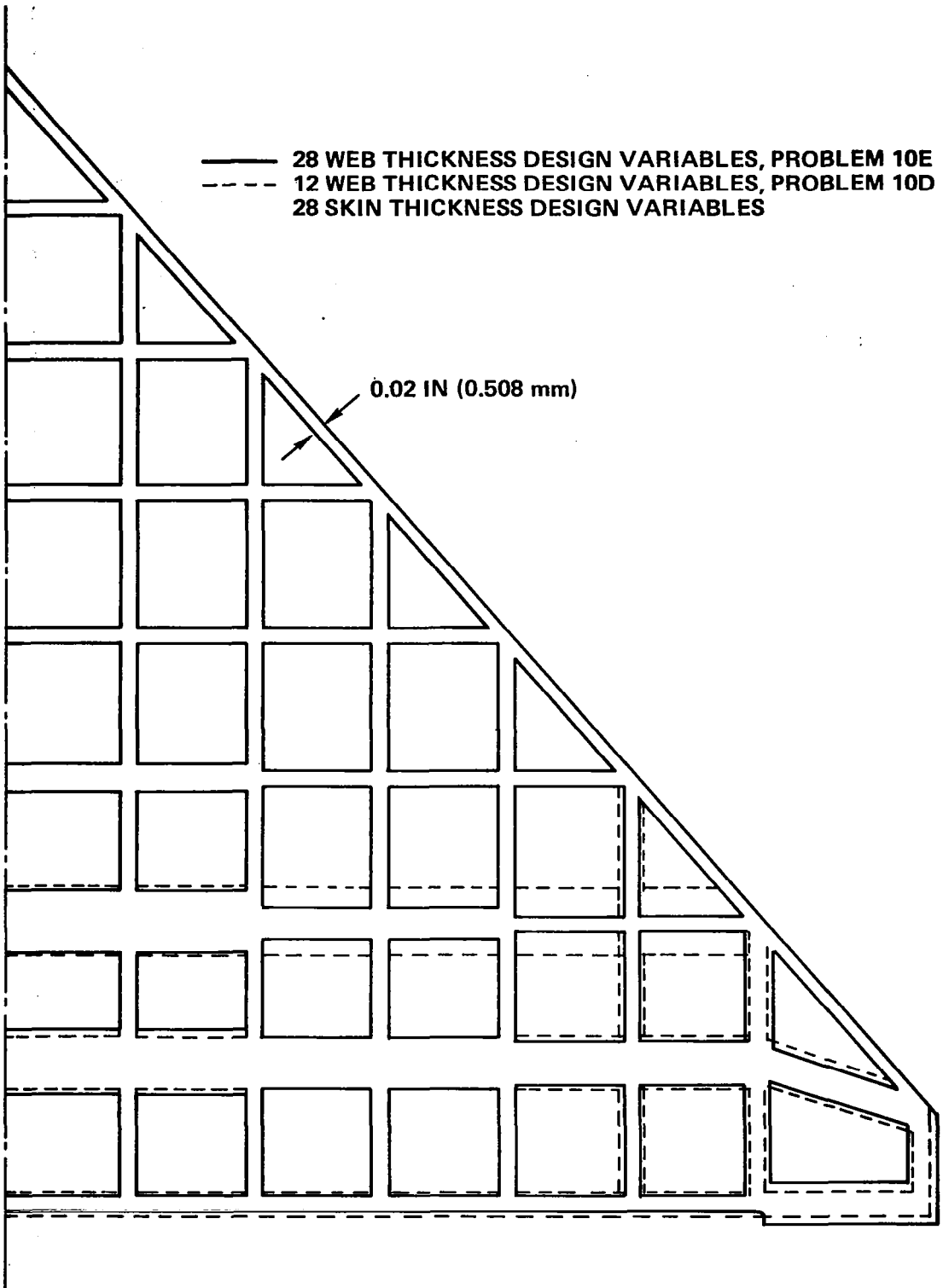
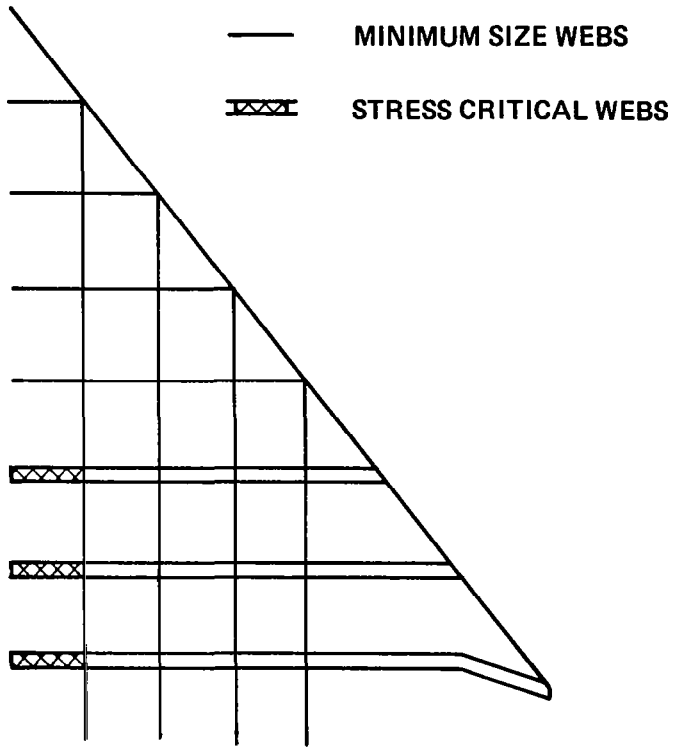
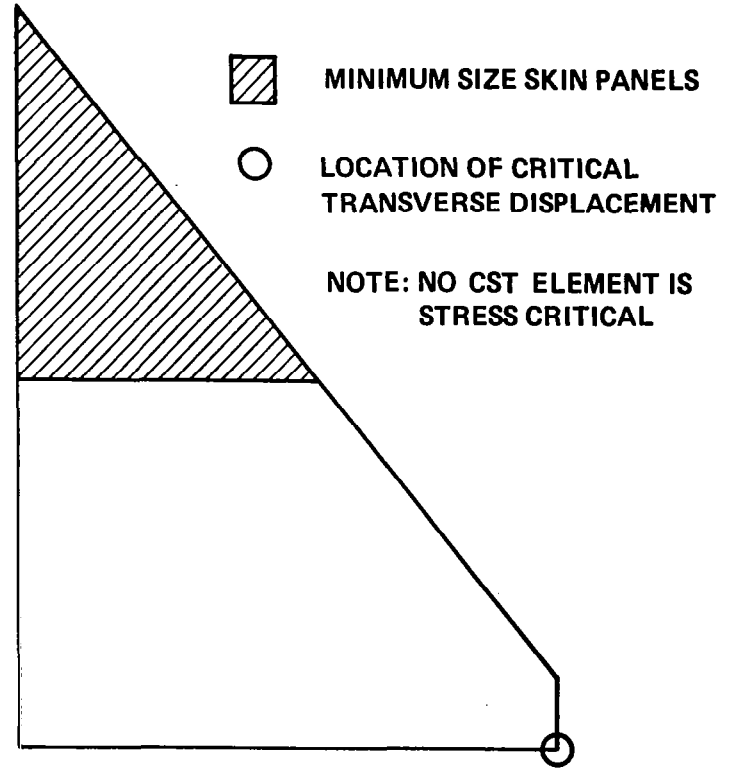


Figure 31. Final Web Thickness Distribution for Two Delta Wing Examples (Problem 10).



(a) CRITICAL CONSTRAINTS FOR WEBS (SSP ELEMENTS)



(b) CRITICAL CONSTRAINTS FOR SKIN PANELS (CST ELEMENTS)

Figure 32. Critical Constraints for Final Designs of Delta Wing Examples; Problems 10A, 10B and 10C.

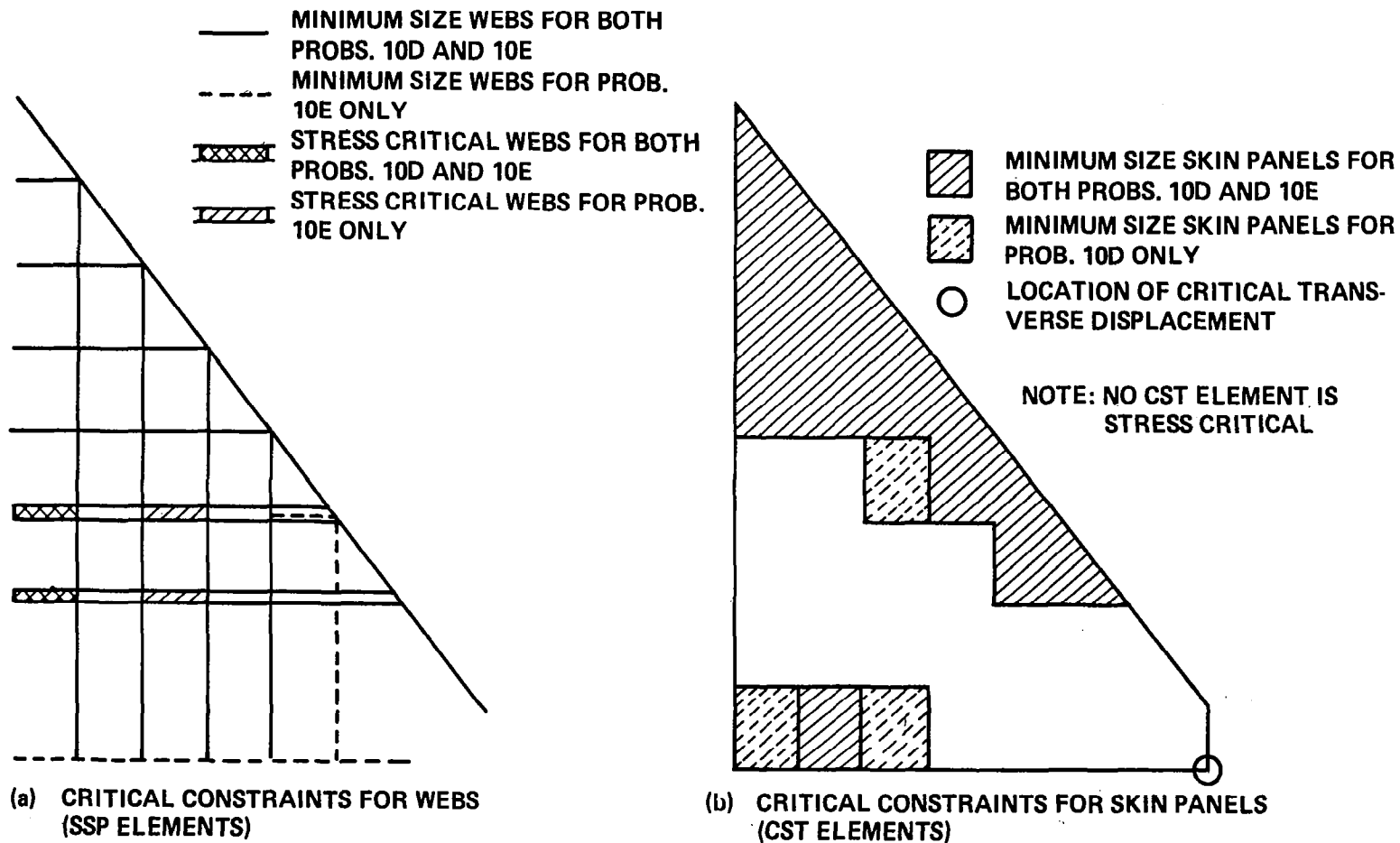


Figure 33. Critical Constraints for Final Designs of Delta Wing Examples; Problems 10D and 10E.

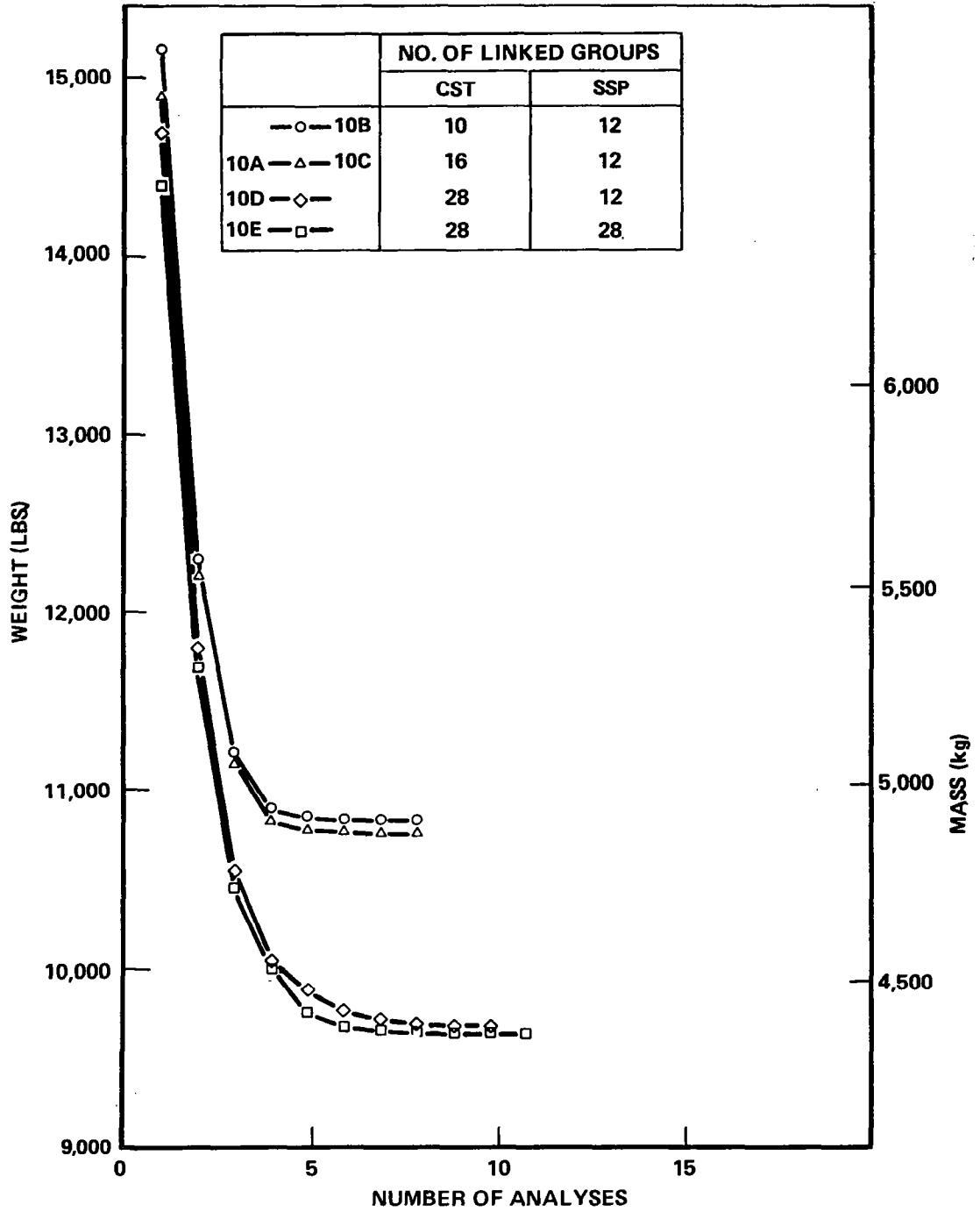


Figure 34. Iteration History for Delta Wing Examples; Problems 10A – 10E.

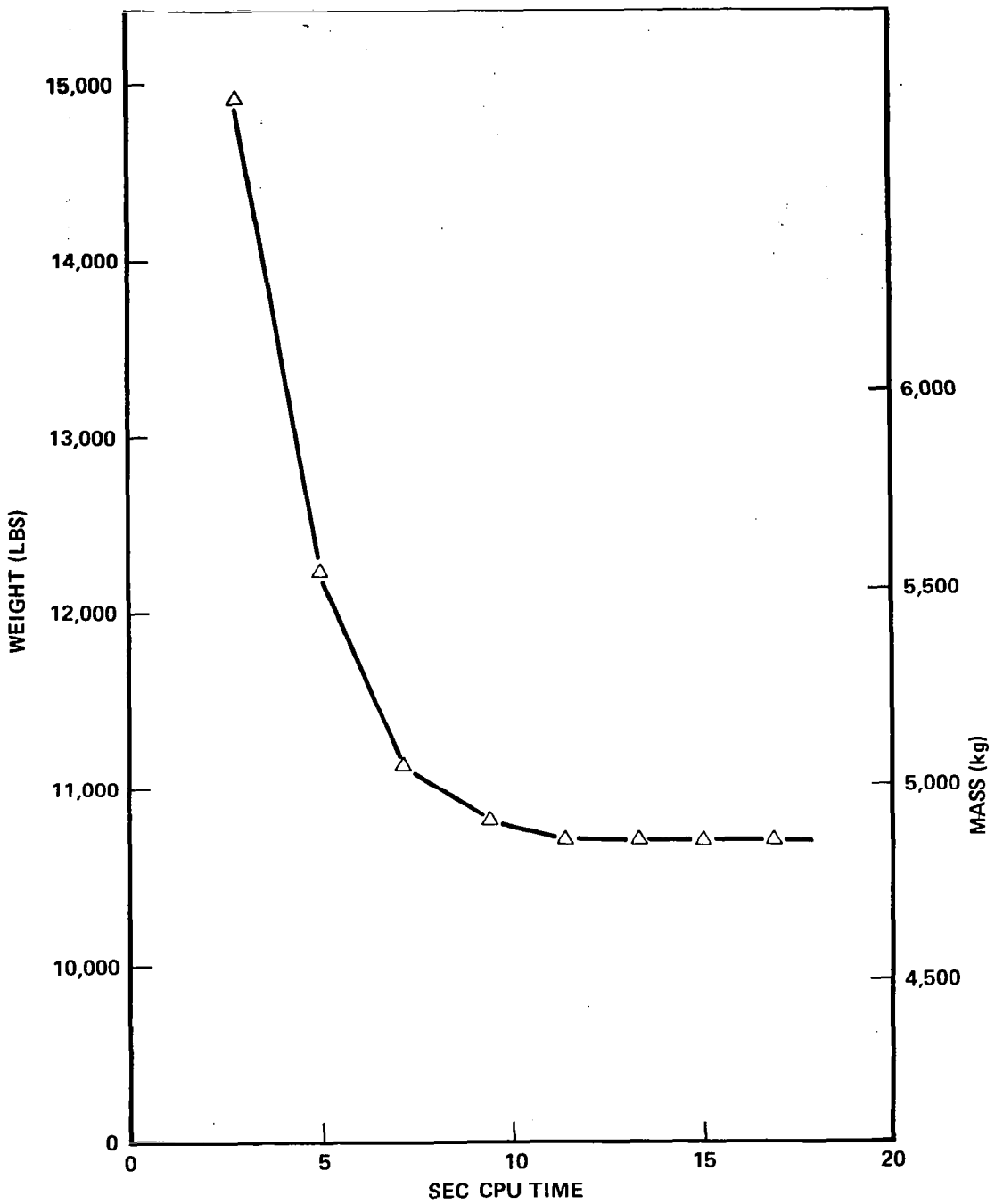


Figure 35. Weight versus Elapsed CPU Time for Delta Wing Example Problem 10C, 16 CST Design Variables, 12 SSP Design Variables.



Table 1

ACCESS 1 - Main Storage Requirements

I. IBM 360/91 at UCLA FORTRAN-H

	NEWSUMT-version	CONMIN-version
70-70-40-2 <sup>+</sup>	364 <sup>K*</sup> (91 <sup>K</sup> )	434 <sup>K*</sup> (109 <sup>K</sup> )
100-100-120-5	778 <sup>K</sup> (195 <sup>K</sup> )	904 <sup>K</sup> (226 <sup>K</sup> )

II. CDC 6600 Lawrence, Berkeley Laboratory

	NEWSUMT-version	CONMIN-version
70-70-40-2 <sup>+</sup>		
Load	244 <sup>K**</sup> (82 <sup>K</sup> )	305 <sup>K**</sup> (101 <sup>K</sup> )
Execution	228 <sup>K</sup> (84 <sup>K</sup> )	270 <sup>K</sup> (95 <sup>K</sup> )

<sup>+</sup>Four numbers stand for the following in order

- Maximum number of elements in one type
- Maximum number of nodes
- Maximum number of independent design variables
- Maximum number of load conditions

\*Decimal bytes

\*\*Octal words

( )Equivalent decimal words

Table 2

Nodal Coordinates for  
18 Element Wing Box Example  
(see Fig. 5)

Node No.	x inches	y inches	z inches
1	0	0	10
2	100	0	8
3	0	70	10
4	100	70	8
5	0	140	10
6	100	140	8
7	100	190	8

Table 3

TRUSS Element Descriptions for  
18 Element Wing Box Example

TRUSS Member No. i	DV Linking Group b(i)	Initial Area $A_i^{(0)}$ $\text{in}^2$	Area Upper limit $A_i^{(U)}$ $\text{in}^2$	Area Lower limit $A_i^{(L)}$ $\text{in}^2$	Config./Mat. Group No. l(i)	P <sup>th</sup> mode No.	Q <sup>th</sup> mode No.	Side Constraint Code *
1	1	0.9800	2.00	0.10	1	1	3	-1
2	2	0.9800	2.00	0.10	1	3	5	-1
3	3	0.9800	2.00	0.10	1	2	4	-1
4	4	0.9800	2.00	0.10	1	4	6	-1
5	5	0.9800	2.00	0.10	2	6	7	-1

- \*  
 -1 : Area lower limit only  
 0 : Area nonnegativity only  
 +1 : Area upper limit and nonnegativity  
 +2 : Area upper and lower limits

Note: Because there is no design variable linking of truss elements in this example, the DV Linking Group "b(i)" and the TRUSS Member No. "i" are the same.

Table 4

CST Element Descriptions for  
18 Element Wing Box Example

CST Member No. i	DV Linking Group b(i)	Initial Thickness $t_i^{(0)}$ in.	Thickness Upper Limit $t_i^{(U)}$ in.	Thickness Lower Limit $t_i^{(L)}$ in.	Config. Group No. $g(i)$	P <sup>th</sup> Node No.	Q <sup>th</sup> Node No.	R <sup>th</sup> Node No.	Side Constraint Code *
1	1	0.1960	1.00	0.020	1	1	2	4	-1
2	1	0.1960	1.00	0.020	1	4	3	1	-1
3	2	0.1960	1.00	0.020	1	3	4	6	-1
4	2	0.1960	1.00	0.020	1	6	5	3	-1
5	3	0.1960	1.00	0.020	2	5	6	7	-1

- \* -1 : Area lower limit only  
 0 : Area nonnegativity only  
 +1 : Area upper limit and nonnegativity  
 +2 : Area upper and lower limits

Table 5

SSP Element Descriptions for  
18 Element Wing Box Example

SSP Member No. i	DV Linking Group b(i)	Initial Thickness $\tau_i^{(0)}$ in.	Thickness Upper Limit $\tau_i^{(U)}$ in.	Thickness Lower Limit $\tau_i^{(L)}$ in.	Config. Group No. $\ell(i)$	P <sup>th</sup> Node No.	Q <sup>th</sup> Node No.	Side Constraint Code *
1	1	0.1960	1.00	0.020	1	1	3	-1
2	2	0.1960	1.00	0.020	1	3	5	-1
3	3	0.1960	1.00	0.020	2	2	4	-1
4	4	0.1960	1.00	0.020	2	4	6	-1
5	5	0.1960	1.00	0.020	3	6	7	-1
6	6	0.1960	1.00	0.020	4	3	4	-1
7	7	0.1960	1.00	0.020	4	5	6	-1
8	8	0.1960	1.00	0.020	5	5	7	-1

- \*  
 -1 : Area lower limit only  
 0 : Area nonnegativity only  
 +1 : Area upper limit and nonnegativity  
 +2 : Area upper and lower limits

Table 6

TRUSS Element Material Properties for  
18 Element Wing Box Example

Config. Group No.	Stress Upper Limit $\sigma_{\ell}^{(U)}$ lb/in <sup>2</sup>	Stress Lower Limit $\sigma_{\ell}^{(L)}$ lb/in <sup>2</sup>	Specific Weight $\rho_{\ell}$ lb/in <sup>3</sup>	Modulus of Elasticity $E_{\ell}$ lb/in <sup>2</sup>
1	+10,000	-10,000	0.100	$10 \times 10^6$
2	+10,000	-10,000	0.100	$10 \times 10^6$

Table 7

CST Element Material Properties for  
18 Element Wing Box Example

Config. Group No.	Equivalent Stress Upper Limit	Specific Weight	Modulus of Elasticity	Poisson's Ratio
$l$	$\sigma_{al}$ lb/in <sup>2</sup>	$\rho_l$ lb/in <sup>3</sup>	$E_l$ lb/in <sup>2</sup>	$\nu_l$
1	+10,000	0.100	$10 \times 10^6$	0.300
2	+10,000	0.100	$10 \times 10^6$	0.300

Table 8

SSP Element Material Properties for  
18 Element Wing Box Example

Config. Group No.	Equivalent Stress Upper Limit	Specific Weight	Modulus of Elasticity	Poisson's Ratio
$\ell$	$\sigma_{a\ell}$ lb/in <sup>2</sup>	$\rho_{\ell}$ lb/in <sup>3</sup>	$E_{\ell}$ lb/in <sup>2</sup>	$\nu_{\ell}$
1	+10,000	0.100	$10 \times 10^6$	0.300
2	+10,000	0.100	$10 \times 10^6$	0.300
3	+10,000	0.100	$10 \times 10^6$	0.300
4	+10,000	0.100	$10 \times 10^6$	0.300
5	+10,000	0.100	$10 \times 10^6$	0.300

Table 9

Displacement Boundary Conditions for  
18 Element Wing Box Example

Boundary Node No.	b. c. Code for $u_x$	b. c. Code for $u_y$	b. c. Code for $y_z$
1	+ 1	+ 1	+ 1
2	+ 1	+ 1	+ 1

Table 10

Load Condition Data for  
18 Element Wing Box Example

Load Condition No. k	No. of Loaded Nodes	Node No.	Load Component  $P_x$ lbs.	Load Component  $P_y$ lbs.	Load Component  $P_z$ lbs.
1	1	7	0	0	+ 5,000
2	1	5	0	0	+10,000

Table 11

Displacement Constraints for  
18 Element Wing Box Example

No. of d.o.f.'s Constrained	Node No.	Direction x,y,z	Displ. Constr. Code *	Displ. Upper Limit in.	Displ. Lower Limit in.
5	3	3	2	2.00	-2.00
	4	3	2	2.00	-2.00
	5	3	2	2.00	-2.00
	6	3	2	2.00	-2.00
	7	3	2	2.00	-2.00

- \*  
 -1 : Lower limit only  
 0 : Neglect this constraint  
 +1 : Upper limit only  
 +2 : Both lower and upper limits

Table 12

Truncation Factors for Delta Wing Example  
(see Section 3.3.6.2)

Stage	TRF	TRF <sub>displacement</sub>
1	0.1	0.3
2	0.12	0.32
3	0.144	0.344
4	0.1728	0.3728
5	0.20736	0.40736
6	0.248832	0.448832
7	0.2985984	0.4985984
8	0.35831808	0.55831808

Table 13

Nodal Coordinates for  
Planar Ten Bar Cantilever Truss  
(see Fig. 10)

Node No.	x inches	y inches	z inches
1	720	360	0
2	720	0	0
3	360	360	0
4	360	0	0
5	0	360	0
6	0	0	0

Table 14

TRUSS Element Descriptions for  
Planar Ten-Bar Cantilever Truss  
(see Fig. 10)

TRUSS Member No. <i>i</i>	DV Linking Group <i>b(i)</i>	Initial Area $A_i^{(0)}$ in <sup>2</sup>	Area Upper Limit $A_i^{(U)}$ in <sup>2</sup>	Area Lower Limit $A_i^{(L)}$ in <sup>2</sup>	Config. Group No. $\ell(i)$	P <sup>th</sup> Node No.	Q <sup>th</sup> Node No.	Side Constraint Code
1	1	*	N/A	0.100	1	5	3	-1
2	2	*	↓	↓	1	3	1	↓
3	3	*	↓	↓	1	6	4	↓
4	4	*	↓	↓	1	4	2	↓
5	5	*	↓	↓	1	3	4	↓
6	6	*	↓	↓	1	1	2	↓
7	7	*	↓	↓	2	5	4	↓
8	8	*	↓	↓	2	6	3	↓
9	9	*	↓	↓	2	3	2	↓
10	10	*	N/A	0.100	2	4	1	-1

\* Initial Areas for All Members

10.0 for Problems 1A, 1B, 1C, 1D and 2

30.0 for Problems 3 and 4

Table 15

Displacement Boundary Conditions for  
Planar Ten Bar Cantilever Truss  
(see Fig. 10)

Boundary Node No.	b.c. Code for $u_x$	b.c. Code for $u_y$	b.c. Code for $u_z$
5	+1	+1	+1
6	+1	+1	+1

Table 16

Load Condition Data (Problems 1A,1B,1C,1D,3)  
for Planar Ten Bar Cantilever Truss

Load Condition No.	No. of Loaded Nodes	Node No.	Load Component $P_x$ lbs.	Load Component $P_y$ lbs.	Load Component $P_z$ lbs.
1	2	2	0	-100,000	0
		4	0	-100,000	0

Table 17

TRUSS Element Material Properties for  
Planar Ten Bar Cantilever Truss  
(Problems 1A,2,3 and 4)

Config. Group No.	Stress Upper Limit $\sigma_{\ell}^{(U)}$ lb/in <sup>2</sup>	Stress Lower Limit $\sigma_{\ell}^{(L)}$ lb/in <sup>2</sup>	Specific Weight $\rho_{\ell}$ lb/in <sup>3</sup>	Modulus of Elasticity $E_{\ell}$ lb/in <sup>2</sup>
1	+25,000	-25,000	0.100	$10 \times 10^6$
2	+25,000	-25,000	0.100	$10 \times 10^6$

Table 18

Final Designs\* for Problems 1A,1B,1C,1D for  
Planar Ten Bar Cantilever Truss

TRUSS Member No. 1	Final Cross Sectional Areas (in <sup>2</sup> )			
	1A ±25,000	1B ±30,000	1C ±50,000	1D ±70,000
1	7.938	7.930	7.900	7.900
2	0.1000	0.1000	0.1000	0.1000
3	8.062	8.071	8.100	8.100
4	3.938	3.930	3.900	3.900
5	0.1000	0.1000	0.1000	0.1000
6	0.1000	0.1000	0.1000	0.1000
7	5.745	5.757	5.798	5.798
8	5.569	5.557	5.516	5.516
9	5.569	4.631	3.677	3.677
10	0.1000	0.1000	0.1415	0.1415
Final Weight (lb)	1593.23	1545.17	1497.65	1497.65
Analyses Needed	16	16	16	16

\*These results were obtained using  $c_p = 0.5$  and 2 unconstrained minimizations per analysis.

Table 19

Comparison of Minimum Weights Achieved and  
Number of Analysis Required  
for Planar Ten-Bar Cantilever Truss

Problem Method	1A Weight (lbs) No. of Anal.	1B Weight (lbs) No. of Anal.	1C Weight (lbs) No. of Anal.	1D Weight (lbs) No. of Anal.
FSD Ref. 83	1593.18 16	1545.13 23	1725.24 14	1725.24 29
MIH Ref. 72	1593.18 21	1545.21 19	1497.61 21	1497.61 21
ACCESS 1 NEWSUMT	1593.23 16	1545.17 16	1497.65 16	1497.65 16

Table 20

Final Designs for Problems 1A', 1B', 1C', 1D' for  
Planar Ten-Bar Cantilever Truss  
(using method of Ref. 84)

TRUSS Member No. i	Final Cross Sectional Areas (in <sup>2</sup> )			
	1A' ±25,000	1B' ±30,000	1C' ±50,000	1D' ±70,000
1	8.000	8.000	8.000	8.000
2	0	0	0	0
3	8.000	8.000	8.000	8.000
4	4.000	4.000	4.000	4.000
5	0	0	0	0
6	0	0	0	0
7	5.657	5.657	5.657	5.657
8	5.657	5.657	5.657	5.657
9	5.657	4.714	2.828	2.020
10	0	0	0	0
Final Weight (lbs)	1584.0	1536.0	1440.0	1398.86
Analyses Needed	2	2	2	2

Table 21

Load Condition Data (Problems 2 and 4) for  
Planar Ten-Bar Cantilever Truss

Load Condition No. k	No. of Loaded Nodes	Node No.	Load Component $P_x$ lbs	Load Component $P_y$ lbs	Load Component $P_z$ lbs
1	4	1	0	+50,000	0
		2	0	-150,000	0
		3	0	+50,000	0
		4	0	-150,000	0

Table 22

Final Designs for Problem 2 for  
Planar Ten-Bar Cantilever Truss  
(see Section 4.2.1.1)

TRUSS Member No.  i	Final Cross Sectional Areas (in <sup>2</sup> )			
	ACCESS 1		Ref. 31 Vankayya	Ref. 72 Schmit & Farshi
	NEWSUMT	CONMIN		
1	5.948	5.953	5.948	5.948
2	0.100	0.105	0.100	0.100
3	10.05	10.07	10.053	10.052
4	3.948	3.952	3.948	3.948
5	0.100	0.100	0.100	0.100
6	2.052	2.059	2.052	2.052
7	8.559	8.597	8.559	8.559
8	2.755	2.752	2.755	2.754
9	5.583	5.588	5.583	5.583
10	0.100	0.114	0.100	0.100
Final Weight (lb)	1664.55	1667.92	1664.6	1664.5
Analyses Needed	11	9	11	20

Table 23

Displacement Constraints for  
Planar Ten-Bar Cantilever Truss  
(Problems 3 and 4, Section 4.2.1.2)

No. of Displacements Constrained	Node No.	Direction x,y,z	Displ. Constr. Code	Displ. Upper Limit in.	Displ. Lower Limit in.
4	1	2	2	2.00	-2.00
	2	2	2	2.00	-2.00
	3	2	2	2.00	-2.00
	4	2	2	2.00	-2.00

Table 24

Final Designs for Problem 3  
Planar Ten-Bar Cantilever Truss  
(see Section 4.2.1.2)

TRUSS Member  No.  i	Final Cross Sectional Areas (in <sup>2</sup> )					
	ACCESS 1			Ref.	Ref.	Ref.
	NEWSUMT		CONMIN	72	31	34
	Single Precision	Double Precision	Single Precision	Schmit, Farshi	Venkayya	Gellatly
1	30.23	30.67	30.57	33.432	30.416	31.35
2	0.179	0.100	0.369	0.100	0.128	0.100
3	23.94	23.76	23.97	24.260	23.408	20.03
4	13.48	14.59	14.73	14.26	14.904	15.60
5	0.100	0.100	0.100	0.100	0.101	0.140
6	0.180	0.100	0.364	0.100	0.101	0.240
7	8.565	8.578	8.547	8.338	8.696	8.350
8	21.95	21.07	21.11	20.740	21.084	22.21
9	21.19	20.96	20.77	19.690	21.077	22.06
10	0.241	0.100	0.320	0.100	0.186	0.100
Final Weight (lb)	5096.7	5076.85	5107.3	5089.0	5084.9	5112
Analyses Needed	13	13	14	24	26	19

Table 25

Iteration History Data for Problem 3  
Planar Ten-Bar Cantilever Truss  
(see Section 4.2.1.2)

No. of Analyses	Weight (lbs)					
	ACCESS 1			Ref. 72 Schmit & Farshi	Ref. 31 Venkayya	Ref. 34 Gellatly & Berke
	NEWSUMT		CONMIN			
Single Precision	Double Precision	Single Precision				
1	7853.1	7852.9	6234.1	12846.7	8266.1	8266
2	6650.7	6650.8	5835.1	8733.4	6281.7	6356
3	6161.4	6161.4	5771.9	9144.6	6065.7	5980
4	5892.6	5892.6	5657.0	8332.5	5984.5	5779
5	5656.4	5656.3	5541.4	7243.0	5963.1	5625
6	5427.4	5426.8	5416.3	6749.6	5920.1	5547
7	5291.3	5790.8	5281.1	6507.9	5881.6	5470
8	5154.2	5153.8	5158.4	6384.3	5848.1	5392
9	5107.6	5110.3	5133.9	6339.8	5819.7	5323
10	5096.7	5087.2	5124.8	6314.9	5795.9	5266
11	5096.7	5081.1	5116.7	5998.7	5776.4	5225
12	<u>5096.7</u>	<u>5076.9</u>	5111.7	5750.1	5760.7	5200
13			<u>5107.3</u>	5734.6	5748.2	5195
14				5705.6	5738.3	5206
15				5468.8	5730.7	5191
16				5315.8	5724.7	5169
17				5306.2	5720.2	5147
18				5215.8	5716.7	5112
19				5162.9	5713.7	<u>5112</u>
20				5135.8	5712.2	
21				5107.0	5502.9	
22				5094.1	5343.8	
23				5089.0	5221.5	
24				<u>5089.0</u>	5127.0	
25					<u>5084.9</u>	

Table 26

Final Designs for Problem 4  
Planar Ten-Bar Cantilever Truss  
(see Section 4.2.1.2)

TRUSS Member  No. 1	Final Cross Sectional Area (in <sup>2</sup> )				
	ACCESS 1			Ref. 72 Schmit & Farshi	Ref. 31 Venkayya
	NEWSUM1		CONMIN		
	Single Precision	Double Precision	Single Precision		
1	23.52	23.55	23.55	24.289	25.190
2	0.100	0.100	0.176	0.100	.363
3	25.28	25.29	25.20	23.346	25.419
4	14.38	14.36	14.39	13.654	14.327
5	0.100	0.100	0.100	0.100	.417
6	1.97	1.97	1.967	1.969	3.144
7	12.39	12.39	12.40	12.670	12.083
8	12.83	12.81	12.86	12.544	14.612
9	20.32	20.34	20.41	21.971	20.261
10	0.100	0.100	0.100	0.100	.513
Final Weight (lb)	4676.93	4676.96	4684.11	4691.84	4895.6
Analyses Needed	11	11	10	23	13

Table 27

Iteration History Data for Problem 4  
 Planar Ten-Bar Cantilever Truss  
 (see Section 4.2.1.2)

No. of Analyses	Weight (lbs)				
	ACCESS 1			Ref. 72 Schmit & Farshi	Ref. 31 Venkayya
	NEWSUMT		CONMIN		
	Single Precision	Double Precision	Single Precision		
1	7988.5	7988.3	6355.6	13315.7	8417.7
2	6782.7	6782.8	5666.0	9204.9	6565.2
3	6061.7	6061.7	5376.8	9455.0	6242.8
4	5427.1	5427.2	5159.8	8009.2	6031.6
5	5055.3	5054.8	5193.9	7665.2	5935.4
6	5031.6	5034.7	4736.2	7240.9	5686.3
7	4700.5	4700.1	4684.6	6755.6	5505.2
8	4680.8	4680.8	4684.1	6694.1	5354.9
9	4677.1	4677.1	4684.1	6143.7	5220.2
10	4676.9	4677.0	<u>4684.1</u>	5915.3	5099.0
11				5377.8	4991.4
12				5269.7	4895.6
13				5096.7	<u>4895.6</u>
14				4986.3	
15				4964.1	
16				4882.1	
17				4826.8	
18				4786.6	
19				4722.8	
20				4706.1	
21				4686.5	
22				4691.8	

Table 28

Nodal Coordinates for  
 25-Bar Space Truss  
 see (Fig. 13)

Node No.	X inches	Y inches	Z inches
1	-37.5	0.0	200.0
2	37.5	0.0	200.0
3	-37.5	37.5	100.0
4	37.5	37.5	100.0
5	37.5	-37.5	100.0
6	-37.5	-37.5	100.0
7	-100.0	100.0	0.0
8	100.0	100.0	0.0
9	100.0	-100.0	0.0
10	-100.0	-100.0	0.0

Table 29

TRUSS Element Descriptions for  
25-Bar Space Truss

Member No. i	D.V. Linking Group b(i)	Initial Area $A_i^{(0)}$ in <sup>2</sup>	Area Upper Limit $A_i^{(U)}$ in <sup>2</sup>	Area Lower Limit $A_i^{(L)}$ in <sup>2</sup>	Config./Material Group.No. $\ell(i)$	P <sup>th</sup> Node No.	Q <sup>th</sup> Node No.	Side Constraint Code
1	1	2.0	N/A	0.01	1	1	2	-1
2	2	↓	↓	↓	2	1	4	↓
3	2	↓	↓	↓	2	2	3	↓
4	2	↓	↓	↓	2	1	5	↓
5	2	↓	↓	↓	2	2	6	↓
6	3	↓	↓	↓	3	2	4	↓
7	3	↓	↓	↓	3	2	5	↓
8	3	↓	↓	↓	3	1	3	↓
9	3	↓	↓	↓	3	1	6	↓
10	4	↓	↓	↓	4	3	6	↓
11	4	↓	↓	↓	4	4	5	↓
12	5	↓	↓	↓	5	3	4	↓
13	5	↓	↓	↓	5	5	6	↓
14	6	↓	↓	↓	6	3	10	↓
15	6	↓	↓	↓	6	6	7	↓
16	6	↓	↓	↓	6	4	9	↓
17	6	↓	↓	↓	6	5	8	↓
18	7	↓	↓	↓	7	4	7	↓
19	7	↓	↓	↓	7	3	8	↓
20	7	↓	↓	↓	7	5	10	↓
21	7	↓	↓	↓	7	6	9	↓
22	8	↓	↓	↓	8	6	10	↓
23	8	↓	↓	↓	8	3	7	↓
24	8	↓	↓	↓	8	5	9	↓
25	8	2.0	N/A	0.01	8	4	8	-1

Table 30

Displacement Boundary Conditions for  
25-Bar Space Truss  
(see Fig. 13)

Boundary Node No.	b.c. Code for $u_x$	b.c. Code for $u_y$	b.c. Code for $u_z$
7	+1	+1	+1
8	+1	+1	+1
9	+1	+1	+1
10	+1	+1	+1

Table 31

Load Condition Data for  
25-Bar Space Truss

Load Condition No.	No. of Loaded Nodes	Node No.	Load Components		
			$P_x$ lbs	$P_y$ lbs	$P_z$ lbs
1	4	1	1000.0	10000.0	-5000.0
		2	0.0	10000.0	-5000.0
		3	500.0	0.0	0.0
		6	500.0	0.0	0.0
2	2	1	0.0	20000.0	-5000.0
		2	0.0	-20000.0	-5000.0

Table 32

Element Material Properties for  
25-Bar Space Truss

Config. Group No. $\ell$	Stress Upper Limit $\sigma_{\ell}^{(U)}$ lb/in <sup>2</sup>	Stress Lower Limit $\sigma_{\ell}^{(L)}$ lb/in <sup>2</sup>	Specific Weight $\rho_{\ell}$ lb/in <sup>3</sup>	Modulus of Elasticity $E_{\ell}$ lb/in <sup>2</sup>
1	40000.0	-35092.0	0.1	$10 \times 10^6$
2	↓	-11590.0	↓	↓
3	↓	-17305.0	↓	↓
4	↓	-35092.0	↓	↓
5	↓	-35092.0	↓	↓
6	↓	- 6759.0	↓	↓
7	↓	- 6959.0	↓	↓
8	40000.0	-11082.0	0.1	$10 \times 10^6$

Table 33

Final Designs for Problem 5  
25-Bar Space Truss

Members in D.V. Group b(i)	Final Cross Sectional Areas (in <sup>2</sup> )				
	ACCESS 1		Ref. 72	Ref. 31	Ref. 34
	NEWSUMI	CONMIN	MIH	Venkayya	Gallatly & Berke
1	0.010	0.166	0.010	0.028	0.0100
2	1.985	2.017	1.964	1.942	2.0069
3	2.996	3.026	3.033	3.081	2.9631
4	0.010	0.087	0.010	0.010	0.0100
5	0.010	0.097	0.010	0.010	0.0100
6	0.684	0.675	0.670	0.693	0.6876
7	1.677	1.636	1.680	1.678	1.6784
8	2.662	2.669	2.670	2.627	2.6638
Final Weight (lb)	545.172	548.475	545.225	545.49	545.36
Analyses Needed	10	9	17	7	8

Table 34

Iteration History Data for Problem 5  
 72-Bar Space Truss  
 (see Section 4.2.3)

No. of Analyses	Weight (lbs)				
	ACCESS 1		Ref 72 Schmit & Farshi	Ref. 31 Venkayya	Ref. 34 Gallatly & Berke
	NEWSUMT	CONMIN			
1	783.70	593.59	1060.9	734.4	734.38
2	609.72	565.46	1073.1	589.2	555.72
3	564.42	552.91	1019.0	578.3	549.08
4	552.07	552.05	906.58	577.3	546.54
5	547.36	550.99	864.06	555.6	545.92
6	546.02	549.17	748.64	545.5	545.45
7	545.39	548.48	666.68		<u>545.36</u>
8	545.22	<u>548.48</u>	614.49		
9	545.17		581.75		
10			564.95		
11			556.13		
12			551.07		
13			548.39		
14			545.22		
15			545.23		
16			545.23		

Table 35

Nodal Coordinates for  
72-Bar Space Truss  
(see Fig. 15)

Node No.	X inches	Y inches	Z inches
1	0.0	0.0	240.0
2	120.0	0.0	240.0
3	120.0	120.0	240.0
4	0.0	120.0	240.0
5	0.0	0.0	180.0
6	120.0	0.0	180.0
7	120.0	120.0	180.0
8	0.0	120.0	180.0
9	0.0	0.0	120.0
10	120.0	0.0	120.0
11	120.0	120.0	120.0
12	0.0	120.0	120.0
13	0.0	0.0	60.0
14	120.0	0.0	60.0
15	120.0	120.0	60.0
16	0.0	120.0	60.0
17	0.0	0.0	0.0
18	120.0	0.0	0.0
19	120.0	120.0	0.0
20	0.0	120.0	0.0

Table 36 .

Truss Element Descriptions for  
72-Bar Space Truss

Member No. i	DV Linking Group b(i)	Cross Sect. Area (in <sup>2</sup> )			Config. Group No. ℓ(i)	Pth Node No.	Qth Node No.	Side Const. Code
		Initial A <sub>i</sub> <sup>(O)</sup>	Upper Limit A <sub>i</sub> <sup>(U)</sup>	Lower Limit A <sub>i</sub> <sup>(L)</sup>				
1	1	1.0	N/A	0.1	1	1	5	-1
2	1	↓	↓	↓	1	2	6	↓
3	1	↓	↓	↓	1	3	7	↓
4	1	↓	↓	↓	1	4	8	↓
5	2	↓	↓	↓	2	2	5	↓
6	2	↓	↓	↓	2	1	6	↓
7	2	↓	↓	↓	2	3	6	↓
8	2	↓	↓	↓	2	2	7	↓
9	2	↓	↓	↓	2	4	7	↓
10	2	↓	↓	↓	2	3	8	↓
11	2	↓	↓	↓	2	1	8	↓
12	2	↓	↓	↓	2	4	5	↓
13	3	↓	↓	↓	3	1	2	↓
14	3	↓	↓	↓	3	2	3	↓
15	3	↓	↓	↓	3	3	4	↓
16	3	↓	↓	↓	3	4	1	↓
17	4	↓	↓	↓	4	1	3	↓
18	4	↓	↓	↓	4	2	4	↓
19	5	↓	↓	↓	1	5	9	↓
20	5	↓	↓	↓	1	6	10	↓
21	5	↓	↓	↓	1	7	11	↓
22	5	↓	↓	↓	1	8	12	↓
23	6	↓	↓	↓	2	6	9	↓
24	6	↓	↓	↓	2	5	10	↓
25	6	↓	↓	↓	2	7	10	↓
26	6	↓	↓	↓	2	6	11	↓
27	6	↓	↓	↓	2	8	11	↓
28	6	↓	↓	↓	2	7	12	↓
39	6	↓	↓	↓	2	5	12	↓
30	6	↓	↓	↓	2	8	9	↓
31	7	1.0	N/A	0.1	3	5	6	-1

Table 36 (Cont'd)

Member No. i	DV Linking Group b(i)	Cross Sect. Area (in <sup>2</sup> )			Config. Group No. ℓ(i)	Pth Node No.	Qth Node No.	Side Const. Code
		Initial A <sub>i</sub> <sup>(O)</sup>	Upper Limit A <sub>i</sub> <sup>(U)</sup>	Lower Limit A <sub>i</sub> <sup>(L)</sup>				
32	7	1.0	N/A	0.1	3	6	7	-1
33	7				3	7	8	
34	7				3	8	5	
35	8				4	5	7	
36	8				4	6	8	
37	9				1	9	13	
38	9				1	10	14	
39	9				1	11	15	
40	9				1	12	16	
41	10				2	10	13	
42	10				2	9	14	
43	10				2	11	14	
44	10				2	10	15	
45	10				2	12	15	
46	10				2	11	16	
47	10				2	9	16	
48	10				2	12	13	
49	11				3	9	10	
50	11				3	10	11	
51	11				3	11	12	
52	11				3	12	9	
53	12				4	9	11	
54	12				4	10	12	
55	13				1	13	17	
56	13				1	14	18	
57	13				1	15	19	
58	13				1	16	20	
59	14				2	14	17	
60	14				2	13	18	
61	14				2	15	18	
62	14				2	14	19	
63	14				2	16	19	
64	14				2	15	20	
65	14				2	13	20	
66	14				2	16	17	
67	15				3	13	14	
68	15				3	14	15	
69	15				3	15	16	
70	15				3	16	13	
71	16				4	13	15	
72	16	1.0	N/A	0.1	4	14	16	

Table 37

Displacement Boundary Conditions  
for 72-Bar Space Truss  
(see Fig. 15)

Boundary Node No.	b.c. Code for $u_x$	b.c. Code for $u_y$	b.c. Code for $u_z$
17	+1	+1	+1
18	+1	+1	+1
19	+1	+1	+1
20	+1	+1	+1

Table 38

Load Condition Data for  
72-Bar Space Truss

Load Condition No. k	No. of Loaded Nodes	Node No.	Load Components		
			$P_x$ (lbs)	$P_y$ (lbs)	$P_z$ (lbs)
1	1	1	5000.0	5000.0	-5000.0
2	4	1	0.0	0.0	-5000.0
		2	0.0	0.0	-5000.0
		3	0.0	0.0	-5000.0
		4	0.0	0.0	-5000.0

Table 39

Element Material Properties for  
72-Bar Space Truss

Config. Group No. $l(i)$	Stress Upper Limit $\sigma_l^{(U)}$ lb/in <sup>2</sup>	Stress Lower Limit $\sigma_l^{(L)}$ lb/in <sup>2</sup>	Specific Weight $\rho_l$ lb/in <sup>3</sup>	Modulus of Elasticity $E_l$ lb/in <sup>2</sup>
1	25000.0	-25000.0	0.1	$10 \times 10^6$
2	25000.0	-25000.0	0.1	$10 \times 10^6$
3	25000.0	-25000.0	0.1	$10 \times 10^6$
4	25000.0	-25000.0	0.1	$10 \times 10^6$

Table 40

Final Designs for Problem 6  
72-Bar Space Truss  
(see Section 4.2.3)

Members in D.V. Group  b(i)	Final Cross Sectional Areas (in <sup>2</sup> )					
	ACCESS 1		Ref. 72 MIH	Ref. 31 Venkayya	Ref. 34 Gallatly & Berke	Ref. 83 Berke & Knot
	NEWSUMT	CONMIN				
1	0.1565	0.1558	0.1585	0.161	0.1492	0.1571
2	0.5458	0.5484	0.5936	0.557	0.7733	0.5385
3	0.4105	0.4105	0.3414	0.377	0.4534	0.4156
4	0.5699	0.5614	0.6076	0.506	0.3417	0.5510
5	0.5233	0.5228	0.2643	0.611	0.5521	0.5082
6	0.5173	0.5161	0.5480	0.532	0.6084	0.5196
7	0.1000	0.1000	0.1000	0.100	0.1000	0.1000
8	0.1000	0.1133	0.1509	0.100	0.1000	0.1000
9	1.267	1.268	1.1067	1.246	1.0235	1.2793
10	0.5118	0.5111	0.5792	0.524	0.5421	0.5149
11	0.1000	0.1000	0.1000	0.100	0.1000	0.1000
12	0.1000	0.1000	0.1000	0.100	0.1000	0.1000
13	1.885	1.885	2.0784	1.818	1.4636	1.8931
14	0.5125	0.5118	0.5034	0.524	0.5207	0.5171
15	0.1000	0.1000	0.1000	0.100	0.1000	0.1000
16	0.1000	0.1000	0.1000	0.100	0.1000	0.0000
Final Weight (1b)	379.640	379.792	388.63	381.2	395.97	379.67
Analyses Needed	9	8	22	12	9	5

Table 41

Iteration History Data for Problem 6  
72-Bar Space Truss  
(see Section 4.2.3)

No. of Analyses	Weight (lbs)					
	ACCESS 1		Ref. 72 Schmit & Farshi	Ref. 31 Venkayya	Ref. 34 Gallatly & Berke	Ref. 83 Berke & Knot
	NEWSUMT	CONMIN				
1	731.15	415.15	809.12	656.8	656.77	656.77
2	477.95	383.79	838.09	478.6	416.07	387.01
3	397.43	380.63	796.16	455.0	406.21	379.67
4	383.27	380.42	763.61	446.9	399.06	<u>379.87</u>
5	380.47	379.91	736.69	445.5	396.82	
6	379.86	379.79	716.63	445.4	396.25	
7	379.68	<u>379.79</u>	708.77	401.7	396.02	
8	<u>379.64</u>		645.07	391.5	<u>395.97</u>	
9			616.97	383.6		
10			525.29	381.6		
11			491.96	<u>381.2</u>		
12			468.69			
13			450.22			
14			433.77			
15			423.94			
16			413.65			
17			404.08			
18			397.43			
19			393.88			
20			388.14			
21			388.63			

Table 42

Nodal Coordinates for  
63-Bar Truss Wing Carry-Through Structure  
(see Fig. 17).

Node No.	X inches	Y inches	Z inches
1	0.0	140.0	20.0
2	0.0	140.0	0.0
3	-30.0	120.0	21.0
4	-30.0	120.0	-1.0
5	30.0	120.0	21.0
6	30.0	120.0	-1.0
7	-30.0	80.0	30.0
8	-30.0	80.0	-3.0
9	30.0	80.0	30.0
10	30.0	80.0	-3.0
11	-30.0	40.0	55.0
12	-30.0	40.0	-5.0
13	30.0	40.0	55.0
14	30.0	40.0	-5.0
15	-30.0	0.0	60.0
16	-30.0	0.0	-7.0
17	30.0	0.0	60.0
18	30.0	0.0	-7.0

Table 43

Truss Element Descriptions for  
63-Bar Truss Wing Carry-Through Structure

Member No. <i>i</i>	DV Linking Group <i>b(i)</i>	Cross Sect. Area (in <sup>2</sup> )			Config. Group No. <i>ℓ(i)</i>	pth Node No.	Qth Node No.	Side Const. Code
		Initial <i>A<sub>i</sub><sup>(O)</sup></i>	Upper Limit <i>A<sub>i</sub><sup>(U)</sup></i>	Lower Limit <i>A<sub>i</sub><sup>(L)</sup></i>				
1	1	20.0	N/A	0.01	1	1	3	-1
2	2	↓	↓	↓	2	2	4	↓
3	3	↓	↓	↓	1	1	5	↓
4	4	↓	↓	↓	2	2	6	↓
5	5	↓	↓	↓	3	7	3	↓
6	6	↓	↓	↓	4	8	4	↓
7	7	↓	↓	↓	3	9	5	↓
8	8	↓	↓	↓	4	10	6	↓
9	9	↓	↓	↓	5	11	7	↓
10	10	↓	↓	↓	6	12	8	↓
11	11	↓	↓	↓	5	13	9	↓
12	12	↓	↓	↓	6	14	10	↓
13	13	↓	↓	↓	7	15	11	↓
14	14	↓	↓	↓	8	16	12	↓
15	15	↓	↓	↓	7	17	13	↓
16	16	↓	↓	↓	8	18	14	↓
17	17	↓	↓	↓	9	3	5	↓
18	18	↓	↓	↓	9	4	6	↓
19	19	↓	↓	↓	9	7	9	↓
20	20	↓	↓	↓	9	8	10	↓
21	21	↓	↓	↓	9	11	13	↓
22	22	↓	↓	↓	9	12	14	↓
23	23	↓	↓	↓	10	1	2	↓
24	24	↓	↓	↓	11	3	4	↓
25	25	↓	↓	↓	11	5	6	↓
26	26	↓	↓	↓	12	7	8	↓
27	27	↓	↓	↓	12	9	10	↓
28	28	↓	↓	↓	13	11	12	↓
29	29	↓	↓	↓	13	13	14	↓
30	30	↓	↓	↓	14	3	9	↓
31	31	↓	↓	↓	15	4	10	↓
32	32	↓	↓	↓	14	5	7	↓
33	33	↓	↓	↓	15	6	8	↓
34	34	↓	↓	↓	16	7	13	↓
35	35	↓	↓	↓	17	8	14	↓
36	36	↓	↓	↓	16	9	11	↓
37	37	↓	↓	↓	17	10	12	↓
38	38	↓	↓	↓	18	11	17	↓
39	39	↓	↓	↓	19	12	18	↓
40	40	↓	↓	↓	18	13	15	↓
41	41	↓	↓	↓	19	14	16	↓
42	42	20.0	N/A	0.01	20	1	6	-1

Table 43 (Cont'd)

Member No. i	DV Linking Group b(i)	Cross Sect. Area (in <sup>2</sup> )			Config. Group No. ℓ(i)	pth Node No.	Q <sup>th</sup> Node No.	Side Const. Code
		Initial A <sub>i</sub> <sup>(O)</sup>	Upper Limit A <sub>i</sub> <sup>(L)</sup>	Lower Limit A <sub>i</sub> <sup>(U)</sup>				
43	43	20.0	N/A	0.01	20	1	4	-1
44	44	↓	↓	↓	21	5	2	
45	45	↓	↓	↓	21	3	2	
46	46	↓	↓	↓	22	5	10	
47	47	↓	↓	↓	22	3	8	
48	48	↓	↓	↓	23	9	6	
49	49	↓	↓	↓	23	7	4	
50	50	↓	↓	↓	24	9	14	
51	51	↓	↓	↓	24	7	12	
52	52	↓	↓	↓	25	13	10	
53	53	↓	↓	↓	25	11	8	
54	54	↓	↓	↓	26	13	18	
55	55	↓	↓	↓	26	11	16	
56	56	↓	↓	↓	27	17	14	
57	57	↓	↓	↓	27	15	12	
58	58	↓	↓	↓	28	5	4	
59	59	↓	↓	↓	28	3	6	
60	60	↓	↓	↓	29	9	8	
61	61	↓	↓	↓	29	7	10	
62	62	↓	↓	↓	30	13	12	
63	63	20.0	N/A	0.01	30	11	14	

Table 44

Displacement Boundary Conditions for  
63-Bar Truss Wing Carry-Through Structure  
(see Fig. 17)

Boundary Node No.	b.c. Code for $u_x$	b.c. Code for $u_y$	b.c. Code for $u_z$
15	+1	+1	+1
16	+1	+1	+1
17	+1	+1	+1
18	+1	+1	+1

Table 45

Load Condition Data for  
63-Bar Truss Wing Carry-Through Structure

Load Condition No. $k$	No. of Loaded Nodes	Node No.	Load Components		
			$P_x$ (lbs)	$P_y$ (lbs)	$P_z$ (lbs)
1	2	1	$2.5 \times 10^6$	$-5.0 \times 10^6$	$2.5 \times 10^5$
		2	$-2.5 \times 10^6$	$5.0 \times 10^6$	$2.5 \times 10^5$
2	2	1	$5.0 \times 10^6$	$-2.5 \times 10^6$	$2.5 \times 10^5$
		2	$-5.0 \times 10^6$	$2.5 \times 10^6$	$2.5 \times 10^5$

Table 46

Final Designs for  
63-Bar Truss Wing Carry-Through Structure  
(Problem 7, Section 4.2.4)

Truss Member No.	Final Cross Sectional Area (in <sup>2</sup> )					
	(A) Stress Constraints Only			(B) Stress & Stiffness Constraints		
	ACCESS 1 0.5 × 2	NEWSUMT 0.05 × 1	Ref. 83 Berke-Khot	ACCESS 1 0.5 × 2	NEWSUMT 0.05 × 1	Ref. 83 Berke-Khot
1	38.28	38.01	38.78	37.55	37.42	36.86
2	35.93	35.90	36.40	36.49	36.40	36.90
3	51.69	52.03	52.38	52.66	52.75	53.33
4	54.49	54.40	55.04	53.76	53.80	53.31
5	24.98	24.77	25.44	23.79	24.00	24.13
6	28.46	28.40	28.69	28.95	28.87	27.82
7	17.64	17.95	17.73	17.26	17.74	17.35
8	20.52	20.90	20.75	21.40	21.81	22.00
9	25.21	24.94	25.32	26.06	25.29	23.42
10	26.82	26.14	27.49	25.15	24.67	25.95
11	7.535	7.666	7.62	8.784	8.701	9.44
12	8.801	9.128	8.82	8.966	9.105	9.82
13	24.21	23.20	24.62	23.43	22.34	22.37
14	20.63	19.83	20.98	19.57	18.72	18.59
15	4.123	4.169	4.16	5.165	5.064	5.79
16	2.495	3.201	2.38	2.956	3.132	4.47
17	37.07	36.90	37.53	37.07	36.64	36.89
18	37.14	36.97	36.65	37.30	36.93	37.52
19	0.010	0.010	.01	0.010	0.011	0.01
20	0.010	0.013	.01	0.010	0.010	0.01
21	0.151	1.565	.07	0.218	1.957	0.15
22	0.067	1.231	.01	0.170	1.616	0.01
23	0.137	0.0797	.08	0.010	0.011	0.01
24	1.085	0.904	1.22	0.010	0.084	0.18
25	0.065	0.132	.07	0.010	0.026	0.01
26	2.574	2.488	2.83	4.191	4.291	0.11
27	0.804	1.077	.81	0.985	1.314	0.01
28	4.582	4.300	4.87	3.285	3.239	4.43
29	0.670	0.895	.51	0.010	0.205	1.15
30	2.651	2.819	2.69	7.861	6.985	6.94
31	2.580	3.126	2.70	7.799	7.235	9.76
32	5.829	5.783	5.89	9.300	10.53	11.03
33	5.839	5.439	5.82	9.229	10.12	8.09
34	6.122	6.073	6.19	9.769	11.07	11.59
35	5.839	5.439	5.82	9.230	10.13	8.09
36	2.783	2.961	2.82	8.257	7.356	7.30
37	2.579	3.123	2.70	7.801	7.259	9.77
38	2.705	3.698	2.71	7.883	8.834	6.98
39	2.603	3.629	2.70	7.852	8.615	9.77
40	5.736	5.025	5.83	9.184	8.762	10.92
41	5.821	5.065	5.80	9.181	8.915	8.09

Table 46 (Cont'd)

Truss Member No.	Final Cross Sectional Area (in <sup>2</sup> )					
	(A) Stress Constraints Only			(B) Stress & Stiffness Constraints		
	ACCESS 1 0.5 × 2	NEWSUMT 0.05 × 1	Ref. 83 Berke-Khot	ACCESS 1 0.5 × 2	NEWSUMT 0.05 × 1	Ref. 83 Berke-Khot
42	16.45	15.96	16.60	25.23	24.67	24.61
43	18.80	18.33	18.99	27.07	26.54	24.54
44	11.01	11.02	11.25	19.35	19.39	19.78
45	13.40	13.40	13.66	21.18	21.23	21.63
46	11.42	11.63	11.60	16.81	17.13	17.19
47	5.961	6.158	6.03	12.65	12.76	12.98
48	12.16	11.97	12.24	18.55	18.31	18.09
49	14.25	14.07	14.40	19.91	19.98	19.67
50	7.240	7.389	7.26	6.650	6.772	6.73
51	7.416	7.024	7.85	5.758	5.797	7.49
52	5.501	5.423	5.62	8.128	7.812	9.50
53	0.566	1.127	.01	3.642	3.354	0.01
54	3.639	3.548	3.69	5.986	5.621	6.79
55	9.631	8.982	9.97	11.93	11.02	8.90
56	4.375	4.053	4.54	5.848	5.569	3.80
57	0.310	0.985	.03	1.691	2.316	3.38
58	0.051	0.498	.01	0.010	0.397	.01
59	0.125	0.543	.01	0.010	0.344	.01
60	0.010	0.013	.01	0.010	0.036	.01
61	0.010	0.018	.01	0.010	0.057	.01
62	0.010	0.068	.01	0.010	0.069	.01
63	0.015	0.246	.01	0.010	0.231	.01
Final Weight (lb)	4976.0	5007.8	5034.5	6120.9	6152.8	6159.3
Analyses Needed	14	10	50	13	9	50

Table 47

Iteration History Data for Problem 7  
 63-Bar Truss Wing Carry-Through Structure  
 (see Section 4.2.4 and Fig. 18)

No. of Analyses	Weight (lb)					
	(A) Stress Constraints Only			(B) Stress & Stiffness Constraints		
	ACCESS 1	NEWSUMT	Ref. 83	ACCESS 1	NEWSUMT	Ref. 83
	0.5 × 2	0.05 × 1	Berke-Khot	0.5 × 2	0.05 × 1	Berke-Khot
1	14264.3	15868.2	30214.0	13022.8	15868.2	30214.0
2	9352.6	7864.1	6360.0	9550.6	8172.5	7577.0
3	7079.7	5706.2	5886.0	7544.2	6633.4	6884.0
4	5997.6	5205.4	5615.0	6806.8	6287.1	6928.0
5	5483.4	5083.7	5385.0	6456.7	6251.4	6801.0
6	5230.2	5025.4	5262.0	6284.9	6158.4	6609.0
7	5104.6	5010.7	5255.0	6201.5	6154.6	6473.0
8	5042.2	5008.8	5284.0	6160.4	6152.8	6388.0
9	5009.8	<u>5007.8</u>	5272.0	6159.9	—	6333.0
10	4992.5		5239.0	6140.6		6292.5
11	4983.1		5201.0	6123.8		6262.6
12	4982.2		5164.1	<u>6120.9</u>		6240.5
13	<u>4978.4</u>		5131.8			6230.7
14			5104.6			6215.7
15			5082.3			6220.1
16			5064.1			6258.7
17			5049.3			6286.3
18			5049.7			6300.4
19			5051.5			6301.7
20			5053.2			6296.0
⋮			⋮			⋮
48			5037.9			6159.8
49			5036.2			6159.6
50			5034.5			6159.3

Table 48

CST Element Descriptions (Model 2) for  
18-Element Wing Box Example

CST Member No. $i$	D.V. Linking Group No. $b(i)$	Initial Thickness $t_i^{(0)}$ (in.)	Thickness Upper Limit $t_i^{(U)}$ (in.)	Thickness Lower Limit $t_i^{(L)}$ (in.)	Config. Group No. $g(i)$	pth Node No.	Qth Node No.	Rth Node No.	Side Constraint Code
1	1	0.1960	1.00	0.020	1	1	2	3	-1
2	1	0.1960	1.00	0.020	1	4	3	2	-1
3	2	0.1960	1.00	0.020	1	3	4	5	-1
4	2	0.1960	1.00	0.020	1	6	5	4	-1
5	3	0.1960	1.00	0.020	2	5	6	7	-1

Table 49

Final Designs for Problem 8  
18-Element Wing Box  
(see Section 4.3.1)

Member No.  i	Final Designs				
	ACCESS 1			Ref. 34 Gallatly & Berke	Ref. 21 Gallatly*
	8A CST Model 1 SSP	8B CST Model 2 SSP	8C CST Model 1 Shear Webs		
TRUSS	$A_i$ (in <sup>2</sup> )	$A_i$ (in <sup>2</sup> )	$A_i$ (in <sup>2</sup> )	$A_i$ (in <sup>2</sup> )	$A_i$ (in <sup>2</sup> )
1	4.045	3.151	2.229	0.6505	1.0431
2	0.1001	0.1000	0.0001	0.1001	0.1036
3	0.1001	0.1000	0.1001	0.2366	0.3508
4	0.1330	0.2324	0.3202	0.2352	0.3315
5	0.1002	0.1000	0.1001	0.1001	0.1035
CST	$t_i$ (in)	$t_i$ (in)	$t_i$ (in)	$t_i$ (in)	$t_i$ (in)
1,2	0.08286	0.08641	0.1093	0.1328	**0.1441
3,4	0.05363	0.05733	0.05911	0.0702	**0.0599
5	0.03786	0.03932	0.04098	0.0449	0.0435
SSP	$\tau_i$ (in)	$\tau_i$ (in)	$\tau_i$ (in)	$\tau_i$ (in)	$\tau_i$ (in)
1	0.3636	0.3851	0.09345	0.0876	0.0876
2	0.2236	0.2152	0.09437	0.0889	0.0895
3	0.1310	0.1361	0.07687	0.0808	0.0664
4	0.1156	0.1004	0.07293	0.0768	0.0553
5	0.09166	0.09113	0.07570	0.0815	0.0537
6	0.02000	0.02000	0.02001	0.0200	0.0219
7	0.02000	0.02000	0.02001	0.0200	0.0215
8	0.03096	0.03090	0.02804	0.0337	0.0256
Final Weight (lbs)	402.97	403.35	357.82	387.67	389.8
Analyses Needed	9	11	9	4***	193

\*The original design obtained by Gallatly was scaled up so that the triangular idealization of the cover plates satisfies stress constraints.

\*\*Each portion was modelled by a quadrilateral element in the original work by Gallatly.

\*\*\*Subsequent iterations give heavier designs as shown in Table 50.

Table 50

Iteration History for Problem 8  
18-Element Wing Box

No. of Analyses	Weight (lbs)				
	ACCESS 1			Ref. 34 Gallytly & Berke	Ref. 21 Gallytly
	8A CST Model 1 SSP	8B CST Model 2 SSP	8C CST Model 1 Shear Webs		
1	585.066	553.876	565.344	593.44	NOT AVAILABLE
2	466.410	472.150	422.770	407.09	
3	422.779	424.312	378.480	388.95	
4	408.848	412.152	366.354	387.67	
5	404.744	407.856	361.926	387.90	
6	403.516	405.716	359.776	387.91	
7	403.118	404.608	358.546	387.68	
8	<u>402.966</u>	403.822	<u>357.824</u>	387.85	
9		403.542		387.97	
10		<u>403.354</u>		388.07	
11				388.15	
12				388.14	
13				388.23	
14				388.26	
15				388.28	

Table 51

Nodal Coordinates for  
150(130)—Element Swept Wing  
(see Fig. 21)

Node No.	X (inches)	Y (inches)	Z (inches)
1	0.0	300.0	10.00
2	0.0	250.0	15.00
3	0.0	185.0	13.00
4	0.0	100.0	5.0000
5	100.0	258.3	8.58333
6	100.0	214.2	12.8333
7	100.0	157.2	11.0833
8	100.0	83.33	4.33333
9	190.0	220.8	7.30833
10	190.0	181.9	10.8833
11	190.0	132.1	9.35833
12	190.0	68.33	3.73333
13	260.0	191.7	6.31667
14	260.0	156.8	9.36667
15	260.0	112.6	8.01667
16	260.0	56.67	3.26667
17	325.0	164.6	5.396
18	325.0	133.5	7.958
19	325.0	94.54	6.771
20	325.0	45.83	2.833
21	385.0	139.6	4.546
22	385.0	112.0	6.658
23	385.0	77.84	5.621
24	385.0	35.83	2.433
25	440.0	116.7	3.767
26	440.0	92.33	5.467
27	440.0	62.53	4.567
28	440.0	26.67	2.067
29	490.0	95.83	3.058
30	490.0	74.42	4.383
31	490.0	48.62	3.608
32	490.0	18.33	1.733
33	535.0	77.08	2.421
34	535.0	58.29	3.408
35	535.0	36.09	2.746
36	535.0	10.83	1.433
37	570.0	62.50	1.925
38	570.0	45.75	2.650
39	570.0	26.35	2.075
40	570.0	5.00	1.200
41	600.0	50.00	1.500
42	600.0	35.00	2.000
43	600.0	18.00	1.500
44	600.0	0.00	1.000

Table 52

Truss Element Description for  
150(130)—Element Swept Wing

Cross Sectional Area Data for All Elements	
Initial Design	$A_i^{(0)} = 0.02 \text{ in}^2 \text{ (0.1292 cm}^2\text{)}$
Upper Limit	$A_i^{(U)} = 1.50 \text{ in}^2 \text{ (9.6774 cm}^2\text{)}$
Lower Limit	$A_i^{(L)} = 0.01 \text{ in}^2 \text{ (0.0645 cm}^2\text{)}$

Member No. <i>i</i>	DV Linking Group No. <i>b(i)</i>	Config. Group No. <i>ℓ(i)</i>	<i>p</i> th Node No.	<i>Q</i> <sup>th</sup> Node No.	Side Constraint Code
1	1	1	1	5	+2
2	2	2	5	9	
3	3	3	9	13	
4	4	4	13	17	
5	5	5	17	21	
6	5	6	21	25	
7	6	7	25	29	
8	6	8	29	33	
9	7	9	33	37	
10	7	10	37	41	
11	8	11	3	7	
12	9	12	7	11	
13	10	13	11	15	
14	11	14	15	19	
15	12	15	19	23	
16	12	16	23	27	
17	13	17	27	31	
18	13	18	31	35	
19	14	19	35	39	
20	14	20	39	43	+2



Table 53 (Cont'd)

Member No. i	DV Linking Group No. b(i)	Config. Group No. ℓ(i)	Connectivity Data			Side Constraint Code
			P <sup>th</sup> Node No.	Q <sup>th</sup> Node No.	R <sup>th</sup> Node No.	
22	4	22	19	18	15	-1
23	4	23	15	16	19	
24	4	24	20	19	16	
25	5	25	17	18	21	
26	5	26	22	21	18	
27	5	27	18	19	22	
28	5	28	23	22	19	
29	5	29	19	20	23	
30	5	30	24	23	20	
31	5	31	21	22	25	
32	5	32	26	25	22	
33	5	33	22	23	26	
34	5	34	27	26	23	
35	5	35	23	24	27	
36	5	36	28	27	24	
37	6	37	25	26	29	
38	6	38	30	29	26	
39	6	39	26	27	30	
40	6	40	31	30	27	
41	6	41	27	28	31	
42	6	42	32	31	28	
43	6	43	29	30	33	
44	6	44	34	33	30	
45	6	45	30	31	34	
46	6	46	35	34	31	
47	6	47	31	32	35	
48	6	48	36	35	32	
49	7	49	33	34	37	
50	7	50	38	37	34	
51	7	51	34	35	38	
52	7	52	39	38	35	
53	7	53	35	36	39	-1

Table 53 (Cont'd)

Member No. i	DV Linking Group No. b(i)	Config. Group No. l(i)	Connectivity Data			Side Constraint Code
			pth Node No.	Qth Node No.	Rth Node No.	
54	7	54	40	39	36	-1
55	7	55	37	38	41	
56	7	56	42	41	38	
57	7	57	38	39	42	
58	7	58	43	42	39	
59	7	59	39	40	43	
60	7	60	44	43	40	-1

Table 54

SSP Element Description for  
150(130) Element Swept Wing

Thickness Limits for All SSP Elements  
 Upper Limit  $\tau_i^{(U)}$  = Not Assigned  
 Lower Limit  $\tau_i^{(L)}$  = 0.02 in. (0.508mm)  
 Initial Thickness Data for All SSP Elements  
 Design I  $\tau_i^{(O)}$  = 0.20 in. (5.08mm)  
 Design II  $\tau_i^{(O)}$  = 0.15 in. (3.81mm)

Member No. i	DV Linking Group No. b(i)	Configuration Group No. l(i)	Connectivity Data		Side Constraint Code
			Pth Node No.	Qth Node No.	
1	1	1	1	5	-1
2	1	2	5	9	
3	1	3	9	13	
4	1	4	13	17	
5	2	5	17	21	
6	2	6	21	25	
7	2	7	25	29	
8	2	8	29	33	
9	2	9	33	37	
10	2	10	37	41	
11	3	11	2	6	
12	3	12	6	10	
13	3	13	10	14	
14	3	14	14	18	
15	4	15	18	22	
16	4	16	22	26	
17	4	17	26	30	
18	4	18	30	34	
19	4	19	34	38	
20	4	20	38	42	
21	5	21	3	7	
22	5	22	7	11	-1



Table 54 (Cont'd)

Member No. 1	DV Linking Group No. b(i)	Configuration Group No. l(i)	Connectivity Data		Side Constraint Code
			P <sup>th</sup> Node No.	Q <sup>th</sup> Node No.	
55	10	55	23	24	-1 ----- ↓ -1
56	10	56	25	26	
57	10	57	26	27	
58	10	58	27	28	
59	11	59	29	30	
60	11	60	30	31	
61	11	61	31	32	
62	11	62	33	34	
63	11	63	34	35	
64	11	64	35	36	
65	11	65	37	38	
66	11	66	38	39	
67	11	67	39	40	
68	11	68	41	42	
69	11	69	42	43	
70	11	70	43	44	

Table 55

Displacement Boundary Conditions for  
 150(130)-Element Swept Wing  
 (see Fig. 21)

Boundary Node No.	b.c. Code for $U_x$	b.c. Code for $U_y$	b.c. Code for $U_z$
1	+1	+1	+1
2	+1	+1	+1
3	+1	+1	+1
4	+1	+1	+1

Table 56

Element Material Properties for  
150(130)--Element Swept Wing

For All Elements of All Element Types;

Stress Upper Limit	$\sigma_{\ell}^{(U)}$	= 25000	psi (17237 N/cm <sup>2</sup> )
Stress Lower Limit	$\sigma_{\ell}^{(L)}$	= -25000	psi (-17237 N/cm <sup>2</sup> )
Specific Weight	$\rho_{\ell}$	= 0.096	lbs/in <sup>3</sup> (2.6573 g/cm <sup>3</sup> )
Modulus of Elasticity	$E_{\ell}$	= $10.6 \times 10^6$	psi ( $7.3084 \times 10^6$ N/cm <sup>2</sup> )
Poisson's Ratio	$\nu_{\ell}$	= 0.3	

Table 57

Load Condition Data for  
150(130)-Element Swept WingFor all nodes,  $P_x = 0.0$  and  $P_y = 0.0$ 

Node No.	$P_z$ (lbs)	Node No.	$P_z$ (lbs)	Node No.	$P_z$ (lbs)
Load Condition 1					
5	1282.0	19	1453.0	33	206.0
6	2581.0	20	1057.0	34	431.0
7	3398.0	21	459.0	35	563.0
8	2380.0	22	958.0	36	383.0
9	978.0	23	1251.0	37	144.0
10	2013.0	24	852.0	38	302.0
11	2593.0	25	362.0	39	395.0
12	1764.0	26	756.0	40	269.0
13	727.0	27	986.0	41	62.0
14	1386.0	28	671.0	42	129.0
15	1906.0	29	282.0	43	169.0
16	1297.0	30	589.0	44	116.0
17	570.0	31	768.0		
18	1190.0	32	522.0		
Load Condition 2					
5	2361.0	19	1025.0	33	402.0
6	3876.0	20	355.0	34	646.0
7	2308.0	21	843.0	35	398.0
8	793.0	22	1374.0	36	154.0
9	1772.0	23	825.0	37	311.0
10	2895.0	24	284.0	38	482.0
11	1705.0	25	665.0	39	306.0
12	582.0	26	1092.0	40	135.0
13	1310.0	27	651.0	41	133.0
14	2135.0	28	224.0	42	206.0
15	1258.0	29	518.0	43	131.0
16	433.0	30	851.0	44	58.0
17	1047.0	31	508.0		
18	1719.0	32	175.0		

Table 58

Final Designs for Problem 9  
150(130)-Element Swept Wing  
(see Section 4.3.2 )

Problem	9A	9B	9C	9D
Initial Design	I No Spar Caps	II No Spar Caps	I	II
<b>Truss</b>			in. <sup>2</sup>	in. <sup>2</sup>
1	-	-	0.01001	0.01002
2	-	-	0.01001	0.01002
3	-	-	0.02421	0.02559
4	-	-	0.02868	0.01485
5,6	-	-	0.01000	0.01585
7,8	-	-	0.02004	0.01725
9,10	-	-	0.01004	0.01002
11	-	-	0.2918	0.2727
12	-	-	0.06336	0.09786
13	-	-	0.05966	0.08638
14	-	-	0.07223	0.1102
15,16	-	-	0.07242	0.08050
17,18	-	-	0.03183	0.06264
19,20	-	-	0.01000	0.01001
<b>CST</b>	in.	in.	in.	in.
1 ~ 6	0.2033	0.2039	0.2013	0.2020
7 ~ 12	0.1773	0.1777	0.1765	0.1766
13 ~ 18	0.1562	0.1569	0.1556	0.1561
19 ~ 24	0.1288	0.1296	0.1281	0.1288
25 ~ 36	0.1096	0.1153	0.1098	0.1146
37 ~ 48	0.09276	0.1027	0.09352	0.1023
49 ~ 60	0.02000	0.02000	0.02000	0.0200
<b>SSP</b>	in.	in.	in.	in.
1 ~ 4	0.02912	0.02932	0.02870	0.02921
5 ~ 10	0.02001	0.02177	0.02000	0.02171
11 ~ 14	0.04795	0.04439	0.04850	0.04425
15 ~ 20	0.05293	0.03531	0.05080	0.03587
21 ~ 24	0.2074	0.2089	0.2076	0.2092
25 ~ 30	0.1122	0.03732	0.1043	0.03300
31 ~ 34	0.09017	0.09038	0.08992	0.08976
35 ~ 40	0.05539	0.07999	0.05634	0.07837
41 ~ 49	0.03194	0.03255	0.03186	0.03257
50 ~ 58	0.07131	0.04911	0.06871	0.04759
59 ~ 70	0.1279	0.06435	0.1179	0.06160
<b>Final Weight (lbs)</b>	2464.20 <sup>lbs</sup>	2462.82 <sup>lbs</sup>	2463.12 <sup>lbs</sup>	2460.84 <sup>lbs</sup>
<b>Analyses Needed</b>	8	8	9	9

Table 59

Iteration History for Problem 9  
150(130)- Element Swept Wing

Problem	9A	9B	9C	9D
Initial Design	I No Spar Caps	II No Spar Caps	I	II
1	2992.18 <sup>lbs</sup>	3381.40 <sup>lbs</sup>	2968.12 <sup>lbs</sup>	3351.28 <sup>lbs</sup>
2	2584.38	2701.50	2567.02	2647.94
3	2499.98	2528.02	2496.10	2514.66
4	2473.40	2480.20	2474.08	2478.78
5	2469.12	2468.81	2467.74	2467.94
6	2466.50	2463.46	2465.04	2463.92
7	<u>2464.20</u>	<u>2462.81</u>	2463.64	2462.06
8			<u>2463.12</u>	<u>2460.84</u>
9				
10				

Table 60

Nodal Coordinates for  
133-Element Delta Wing  
(see Fig. 27)

Node No.	X inches	Y inches	Z inches
1	0.0	960.0	6.468
2	0.0	840.0	11.47
3	0.0	720.0	15.01
4	0.0	600.0	17.08
5	0.0	480.0	17.69
6	0.0	360.0	16.84
7	0.0	240.0	14.52
8	0.0	120.0	10.74
9	0.0	0.0	5.492
10	100.0	840.0	6.385
11	100.0	720.0	11.14
12	100.0	600.0	14.26
13	100.0	480.0	15.76
14	100.0	360.0	15.62
15	100.0	240.0	13.86
16	100.0	120.0	10.46
17	100.0	0.0	5.434
18	200.0	720.0	6.281
19	200.0	600.0	10.72
20	200.0	480.0	13.33
21	200.0	360.0	14.09
22	200.0	240.0	13.02
23	200.0	120.0	10.11
24	200.0	0.0	5.362
25	300.0	600.0	6.146
26	300.0	480.0	10.19
27	300.0	360.0	12.12
28	300.0	240.0	11.94
29	300.0	120.0	9.660
30	300.0	0.0	5.268
31	400.0	480.0	5.966
32	400.0	360.0	9.463
33	400.0	240.0	10.49
34	400.0	120.0	9.051
35	400.0	0.0	5.143
36	500.0	360.0	5.710
37	500.0	240.0	8.441
38	500.0	120.0	8.193
39	500.0	0.0	4.966
40	600.0	240.0	5.322
41	600.0	120.0	6.887
42	600.0	0.0	4.696
43	730.0	84.0	4.360
44	730.0	0.0	3.959

Table 61

CST Element Description for  
133-Element Delta Wing

Thickness Data for All Elements		
Initial Design	I	$t_i^{(0)} = 0.10 \text{ in. (2.54mm)}$
	II	$t_i^{(0)} = 0.15 \text{ in. (3.81mm)}$
Upper Limit		$t_i^{(U)} = \text{Not assigned}$
Lower Limit		$t_i^{(L)} = 0.02 \text{ in. (0.508mm)}$

Member No. i	Design Variable Linking Data			Config. Group No. $\ell(i)$	Node Numbers			Side Constr. Code
	I	II	III		pth	qth	rth	
	$b^{(I)}(i)$	$b^{(I)}(i)$	$b^{(I)}(i)$		Node	Node	Node	
1	1	1	1	1	1	2	10	-1
2	1	1	1	2	2	11	10	
3	1	1	1	1	2	3	11	
4	1	1	1	1	10	11	18	
5	2	2	2	2	3	12	11	
6	2	2	2	1	3	4	12	
7	2	2	3	2	4	13	12	
8	2	2	3	1	4	5	13	
9	3	3	4	2	5	14	13	
10	3	3	4	1	5	6	14	
11	3	3	5	2	6	15	14	
12	3	3	5	1	6	7	15	
13	4	4	6	2	7	16	15	
14	4	4	6	1	7	8	16	
15	4	4	7	2	8	17	16	
16	4	4	7	1	8	9	17	
17	2	5	8	2	11	19	18	
18	2	5	8	1	11	12	19	
19	2	5	9	2	12	20	19	
20	2	5	9	1	12	13	20	
21	3	6	10	2	13	21	20	
22	3	6	10	1	13	14	21	
23	3	6	11	2	14	22	21	
24	3	6	11	1	14	15	22	
25	4	7	12	2	15	23	22	
26	4	7	12	1	15	16	23	
27	4	7	13	2	16	24	23	
28	4	7	13	1	16	17	24	
29	5	8	14	1	18	19	25	
30	5	8	14	2	19	26	25	
31	5	8	14	1	19	20	26	
32	5	8	14	1	25	26	31	
33	6	9	15	2	20	27	26	-1



Table 62

SSP Element Description for  
133-Element Delta Wing

Thickness Data for All Elements		
Initial Design	I	$t_i^{(0)} = 0.15 \text{ in. (3.810mm)}$
	II	$t_i^{(0)} = 0.12 \text{ in. (3.302mm)}$
Upper Limit		$t_i^{(U)} = \text{not assigned}$
Lower Limit		$t_i^{(L)} = 0.02 \text{ in. (0.508mm)}$

Member No. i	Design Variable Linking Data		Config. Group No.	Node Number		Side Constr. Code
	I $b^{(I)}(i)$	II $b^{(II)}(i)$		P <sup>th</sup> Node	Q <sup>th</sup> Node	
1	1	1	1	10	11	-1   -1
2	1	1	2	11	12	
3	1	1	3	12	13	
4	1	1	4	13	14	
5	1	1	5	14	15	
6	1	1	6	15	16	
7	1	1	7	16	17	
8	1	2	8	18	19	
9	1	2	9	19	20	
10	1	2	10	20	21	
11	1	2	11	21	22	
12	1	2	12	22	23	
13	1	2	13	23	24	
14	2	3	14	25	26	
15	2	3	15	26	27	
16	2	3	16	27	28	
17	2	3	17	28	29	
18	2	3	18	29	30	
19	2	4	19	31	32	
20	2	4	20	32	33	
21	2	4	21	33	34	
22	2	4	22	34	35	
23	3	5	23	36	37	
24	3	5	24	37	38	
25	3	5	25	38	39	
26	3	6	26	40	41	
27	3	6	27	41	42	
28	3	7	28	43	44	
29	4	8	29	2	10	
30	5	9	30	3	11	
31	5	9	31	11	18	

Table 62 (Cont'd)

Member No. i	Design Variable Linking Data		Config. Group No.	Node Number		Side Constr. Code
	I $b^{(I)}(i)$	II $b^{(II)}(i)$		Pth Node	Qth Node	
32	6	10	32	4	12	-1 ↓ -1
33	6	10	33	12	19	
34	6	11	34	19	25	
35	7	12	35	5	13	
36	7	12	36	13	20	
37	7	13	37	20	26	
38	7	13	38	26	31	
39	8	14	39	6	14	
40	8	14	40	14	21	
41	8	15	41	21	27	
42	8	15	42	27	32	
43	8	16	43	32	36	
44	9	17	44	7	15	
45	9	17	45	15	22	
46	9	18	46	22	28	
47	9	18	47	28	33	
48	9	19	48	33	37	
49	9	19	49	37	40	
50	10	20	50	8	16	
51	10	20	51	16	23	
52	10	21	52	23	29	
53	10	21	53	29	34	
54	10	22	54	34	38	
55	10	22	55	38	41	
56	10	23	56	41	43	
57	11	24	57	9	17	
58	11	24	58	17	24	
59	11	25	59	24	30	
60	11	25	60	30	35	
61	11	26	61	35	39	
62	11	26	62	39	42	
63	11	27	63	42	44	
64	12	28	64	1	10	
65	12	28	65	10	18	
66	12	28	66	18	25	
67	12	28	67	25	31	
68	12	28	68	31	36	
69	12	28	69	36	40	
70	12	28	70	40	43	

Table 63

Displacement Boundary Conditions for  
133-Element Delta Wing  
(see Fig. 27)

Boundary Node No.	b.c. Code for $U_x$	b.c. Code for $U_y$	b.c. Code for $U_z$
1	+1	+1	+1
2	+1	+1	+1
3	+1	+1	+1
4	+1	+1	+1
5	+1	+1	+1
6	+1	+1	+1
7	+1	+1	+1
8	+1	+1	+1
9	+1	+1	+1

Table 64

Load Condition Data for  
133-Element Delta Wing

No. of Load Conditions	1
No. of Loaded Nodes	35 (all free nodes)
Loaded Node Numbers	10,11,12,...43,44
Load Components	
for all Loaded Nodes	$P_x = 0.0$ lbs. $P_y = 0.0$ lbs. $P_z = 8075.0$ lbs. (35919.2 N)

Table 65

Element Material Properties for  
133-Element Delta Wing

For all elements in all element types;

Stress Upper Limit	$\sigma_{\ell}^{(U)}$	= 125,000 psi (86,184 N/cm <sup>2</sup> )
Stress Lower Limit	$\sigma_{\ell}^{(L)}$	= -125,000 psi (-86,184 N/cm <sup>2</sup> )
Specific Weight	$\rho_{\ell}$	= 0.16 lb/in <sup>3</sup> (0.004429 kg/cm <sup>3</sup> )
Modulus of Elasticity	$E_{\ell}$	= $16.4 \times 10^6$ psi ( $1.1307 \times 10^9$ N/cm <sup>2</sup> )
Poisson's Ratio	$\nu_{\ell}$	= 0.3

Table 66

Displacement Constraints for 133-Element Delta Wing

No. of d.o.f.'s Constrained	Node No.	Direction x,y,z	Displ. Constraint Code	Displ. Upper Limit in.	Displ. Lower Limit in.
35	10	3	2	14.0	-14.0
	11			↓	↓
	12			↓	↓
	13			↓	↓
	14			↓	↓
	15			↓	↓
	16			↓	↓
	17			↓	↓
	18			14.0	-14.0
	19			28.0	-28.0
	20			↓	↓
	21			↓	↓
	22			↓	↓
	23			↓	↓
	24			28.0	-28.0
	25			42.0	-42.0
	26			↓	↓
	27			↓	↓
	28			↓	↓
	29			↓	↓
	30			30.0	-30.0
	31			56.0	-56.0
	32			↓	↓
	33			↓	↓
	34			↓	↓
	35			56.0	-56.0
	36			70.0	-70.0
	37			↓	↓
	38			↓	↓
	39			70.0	-70.0
	40			84.0	-84.0
	41			84.0	-84.0
	42			84.0	-84.0
	43			100.8	-100.8
	44	100.8	-100.8		
	3	2			

Table 67

Final Designs for  
133-Element Delta Wing

Problem		Thicknesses (in)				
		10A	10B	10C	10D	10E
CST Model		II	I	II	III	III
SSP Model		I	I	I	I	II
Initial Design		II	I	I	I	I
CST Elements	1 ~ 4	0.02000	0.02000	0.02000	0.02000	0.02000
	5 , 6	0.02000	0.02000	0.02000	0.02000	0.02000
	7 , 8	0.02000	0.02000	0.02000	0.02001	0.02000
	9 , 10	0.1498	0.1368	0.1494	0.05171	0.05037
	11 , 12	0.1498	0.1368	0.1494	0.2361	0.2233
	13 , 14	0.1450	0.1353	0.1457	0.2134	0.2148
	15 , 16	0.1450	0.1353	0.1457	0.02000	0.02104
	17 , 18	0.02000	0.02000	0.02000	0.02000	0.02000
	19 , 20	0.02000	0.02000	0.02000	0.02000	0.02000
	21 , 22	0.1164	0.1368	0.1159	0.02888	0.03322
	23 , 24	0.1164	0.1368	0.1159	0.1853	0.1776
	25 , 26	0.1289	0.1353	0.1297	0.1943	0.1959
	27 , 28	0.1289	0.1353	0.1297	0.02000	0.02000
	29 ~ 32	0.02000	0.02000	0.02000	0.02000	0.02000
	33 , 34	0.09088	0.08104	0.09022	0.02000	0.02266
	35 , 36	0.09088	0.08104	0.09022	0.1364	0.1381
	37 , 38	0.1223	0.1174	0.1232	0.1902	0.1874
	39 , 40	0.1223	0.1174	0.1232	0.02000	0.02150
	41 , 42	0.06518	0.08104	0.06431	0.02000	0.02000
	43 , 44	0.06518	0.08104	0.06431	0.08141	0.08606
	45 , 46	0.1172	0.1174	0.1181	0.1885	0.1858
	47 , 48	0.1172	0.1174	0.1181	0.02521	0.02710
	49 ~ 52	0.03628	0.03961	0.03488	0.02000	0.02000
53 , 54	0.1074	0.09565	0.1081	0.1691	0.1714	
55 , 56	0.1074	0.09565	0.1081	0.04288	0.04176	
57 , 58	0.08406	0.09565	0.08406	0.08617	0.08820	
59 , 60	0.08406	0.09565	0.08406	0.07335	0.07484	
61 ~ 63	0.05036	0.04990	0.05028	0.04511	0.04519	

Continued to the next page

Table 67 (Cont'd)

		Thickness (in)				
Problem		10A	10B	10C	10D	10E
CST Model		II	I	II	III	III
SSP Model		I	I	I	I	II
Initial Design		II	I	I	I	I
SSP Elements	1 ~ 7	0.02000	0.02000	0.02000	0.02000	0.02000
	8 13	0.02000	0.02000	0.02000	0.02000	0.02000
	14 ~ 18	0.02000	0.02000	0.02000	0.02000	0.02000
	19 ~ 22	0.02000	0.02000	0.02000	0.02000	0.02000
	23 ~ 25	0.02172	0.02219	0.02161	0.02391	0.02000
	26 ~ 27	0.02172	0.02219	0.02161	0.02391	0.03555
	28	0.02172	0.02219	0.02161	0.02391	0.04184
	29	0.02001	0.02001	0.02001	0.02000	0.02000
	30 , 31	0.02001	0.02001	0.02001	0.02000	0.02000
	32 , 33	0.02001	0.02000	0.02001	0.02000	0.02000
	34	0.02001	0.02000	0.02001	0.02000	0.02000
	35 , 36	0.02000	0.02000	0.02001	0.02000	0.02000
	37 , 38	0.02000	0.02000	0.02001	0.02000	0.02000
	39 , 40	0.05958	0.06159	0.05960	0.03702	0.03903
	41 , 42	0.05958	0.06159	0.05960	0.03702	0.03116
	43	0.05958	0.06159	0.05960	0.03702	0.02000
	44 , 45	0.07531	0.08104	0.07506	0.1049	0.1012
	46 , 47	0.07531	0.08104	0.07506	0.1049	0.04810
	48 , 49	0.07531	0.08104	0.07506	0.1049	0.02000
	50 , 51	0.07347	0.07546	0.07366	0.08940	0.1056
	52 , 53	0.07347	0.07546	0.07366	0.08940	0.08814
	54 , 55	0.07347	0.07546	0.07366	0.08940	0.07648
	56	0.07347	0.07546	0.07366	0.08940	0.05479
	57 , 58	0.05702	0.05678	0.05714	0.03033	0.02000
	59 , 60	0.05702	0.05678	0.05714	0.03033	0.02000
	61 , 62	0.05702	0.05678	0.05714	0.03033	0.02000
63	0.05702	0.05678	0.05714	0.03033	0.07340	
64 ~ 70	0.02000	0.02000	0.02000	0.02000	0.02000	
Final Weight (lb)		10742.24	10824.14	10741.50	9636.31	9521.22
Analyses Needed		9	9	9	11	12

Table 68

Iteration History for Problem 10  
133-Element Delta Wing

Problem No.	Weight (lbs)				
	10A	10B	10C	10D	10E
CST Model	II(16)*	I(10)	II(16)	III(28)	III(28)
SSP Model	I(12)	I(12)	I(12)	I(12)	II(28)
Initial Design	II	I	I	I	I
No. of Analyses					
1	14871.40	15207.54	14946.32	14689.76	14424.34
2	12061.76	12309.34	12210.22	11827.41	11693.76
3	11169.82	11199.10	11153.64	10545.80	10433.40
4	10848.26	10882.88	10812.32	10082.38	9907.82
5	10774.66	10842.60	10764.38	9851.14	9745.98
6	10754.16	10830.14	10749.08	9694.20	9648.46
7	10747.34	10826.48	10743.14	9658.88	9586.08
8	<u>10742.24</u>	<u>10824.14</u>	<u>10741.50</u>	9640.82	9541.12
9				9637.64	9533.94
10				9636.18	9526.32
11					9521.22

\*Numbers in ( ) indicate the numbers of linked design variable groups.

Table 69

Nodal Coordinates for  
150(130) Element Swept Wing  
(see Fig. 21)

Node No.	X (meters)	Y (meters)	Z (meters)
1	0.0	7.6200	0.2540
2	0.0	6.3500	0.3810
3	0.0	4.6990	0.3302
4	0.0	2.5400	0.1270
5	2.5400	6.5608	0.2180
6	2.5400	5.4407	0.3259
7	2.5400	3.9923	0.2815
8	2.5400	2.1166	0.1101
9	4.8260	5.6083	0.1856
10	4.8260	4.6203	0.2764
11	4.8260	3.3553	0.2377
12	4.8260	1.7356	0.0948
13	6.6040	4.8692	0.1604
14	6.6040	3.9827	0.2379
15	6.6040	2.8600	0.2036
16	6.6040	1.4394	0.0830
17	8.2550	4.1808	0.1371
18	8.2550	3.3909	0.2021
19	8.2550	2.4013	0.1720
20	8.2550	1.1641	0.0720
21	9.7790	3.5458	0.1155
22	9.7790	2.8448	0.1691
23	9.7790	1.9771	0.1428
24	9.7790	0.9101	0.0618
25	11.1760	2.9642	0.0957
26	11.1760	2.3452	0.1389
27	11.1760	1.5883	0.1160
28	11.1760	0.6774	0.0525
29	12.4460	2.4341	0.0777
30	12.4460	1.8903	0.1113
31	12.4460	1.2350	0.0916
32	12.4460	0.4656	0.0440
33	13.5890	1.9578	0.0615
34	13.5890	1.4806	0.0866
35	13.5890	0.9167	0.0697
36	13.5890	0.2751	0.0364
37	14.4780	1.5875	0.0489
38	14.4780	1.1621	0.0673
39	14.4780	0.6693	0.0527
40	14.4780	0.1270	0.0305
41	15.2400	1.2700	0.0381
42	15.2400	0.8890	0.0508
43	15.2400	0.4572	0.0381
44	15.2400	0.0000	0.0254

Table 70

Load Condition Data for  
150(130) Element Swept Wing

For all nodes  $P_x = 0.0$  and  $P_y = 0.0$

Node No.	$P_z$ (N)	Node No.	$P_z$ (N)	Node No.	$P_z$ (N)
Load Condition 1					
5	5702.62	19	6463.27	33	916.33
6	11480.9	20	4701.77	34	1917.18
7	15115.1	21	2041.73	35	2504.35
8	10586.8	22	4261.39	36	1703.67
9	4350.36	23	5564.72	37	6405.44
10	8954.27	24	3789.89	38	1345.14
11	11534.2	25	1610.26	39	1757.05
12	7846.66	26	3362.86	40	1196.57
13	3233.86	27	4385.95	41	2757.90
14	6165.23	28	2984.76	42	5738.21
15	8478.31	29	1254.40	43	7517.50
16	5769.34	30	2620.00	44	5159.94
17	2535.49	31	3416.23		
18	5293.38	32	2321.97		
Load Condition 2					
5	10502.3	19	4559.43	33	1788.19
6	17241.3	20	1579.12	34	2873.55
7	10266.5	21	3749.85	35	1770.39
8	3527.44	22	6111.86	36	685.03
9	7882.25	23	3669.78	37	1383.40
10	12877.6	24	1263.29	38	2144.04
11	7584.22	25	2958.07	39	1361.16
12	2588.87	26	4857.46	40	600.51
13	5827.17	27	2895.79	41	591.61
14	9496.95	28	996.40	42	916.33
15	5595.86	29	2304.18	43	582.72
16	1926.08	30	3785.44	44	258.00
17	4657.29	31	2259.70		
18	7646.49	32	778.44		

Table 71

Final Designs for Problem 9  
150(130) Element Swept Wing  
(see Section 4.3.2)

Problem No.	9A	9B	9C	9D
Initial Design	I No Spar Caps	II No Spar Caps	I	II
<b>Truss</b>			$A_i$ (cm <sup>2</sup> )	$A_i$ (cm <sup>2</sup> )
1	-	-	0.06458	0.06465
2	-	-	0.06458	0.06465
3	-	-	0.15619	0.16510
4	-	-	0.18503	0.09581
5,6	-	-	0.06452	0.10226
7,8	-	-	0.12429	0.11129
9,10	-	-	0.06477	0.06465
11	-	-	1.88258	1.75935
12	-	-	0.40877	0.63135
13	-	-	0.38490	0.55729
14	-	-	0.46600	0.71097
15,16	-	-	0.46725	0.51935
17,18	-	-	0.20535	0.40413
19,20	-	-	0.06452	0.06458
<b>CST</b>	$t_i$ (mm)	$t_i$ (mm)	$t_i$ (mm)	$t_i$ (mm)
1 ~ 6	5.1638	5.1791	5.1587	5.1308
7 ~ 12	4.5034	4.5136	4.4831	4.4856
13 ~ 18	3.9675	3.9853	3.9522	3.9649
19 ~ 24	3.2715	3.2918	3.2537	3.2715
25 ~ 36	2.7838	2.9286	2.7889	2.9108
37 ~ 48	2.3561	2.6086	2.3754	2.5984
49 ~ 60	0.5080	0.5080	0.5080	0.5080
<b>SSP</b>	$\tau_i$ (mm)	$\tau_i$ (mm)	$\tau_i$ (mm)	$\tau_i$ (mm)
1 ~ 4	0.7396	0.7447	0.7290	0.7419
5 ~ 10	0.5083	0.5530	0.5080	0.5514
11 ~ 14	1.2179	1.1275	1.2319	1.1240
15 ~ 20	1.3444	0.8969	1.2903	0.9111
21 ~ 24	5.2680	5.3061	5.2730	5.3137
25 ~ 30	2.8499	0.9479	2.6492	0.8382
31 ~ 34	2.2903	2.2957	2.2840	2.2799
35 ~ 40	1.4069	2.0318	1.4310	1.9906
41 ~ 49	0.8113	0.8268	0.8092	0.8273
50 ~ 58	1.8113	1.2474	1.7452	1.2088
59 ~ 70	3.2487	1.6345	2.9947	1.5646
<b>Final Mass (KG)</b>	1117.74	1117.11	1117.25	1116.22
<b>Analyses Needed</b>	8	8	9	9

Table 72

Iteration History for Problem 9  
150(130) Element Swept Wing

Problem	Mass (KG)			
	9A	9B	9C	9D
Initial Design	I	II	I	II
	No Spar Caps	No Spar Caps		
	KG	KG	KG	KG
1	1357.23	1533.78	1346.32	1520.11
2	1172.25	1225.38	1164.38	1201.08
3	1133.97	1146.69	1132.21	1140.63
4	1121.98	1125.00	1122.22	1124.35
5	1119.97	1119.83	1119.35	1119.44
6	1118.79	1117.41	1118.12	1117.61
7	<u>1117.74</u>	<u>1117.11</u>	1117.49	1116.77
8			<u>1117.25</u>	<u>1116.72</u>
9				
10				

Table 73

Nodal Coordinates for  
133-Element Delta Wing  
(see Fig. 27)

Node No.	X (meters)	Y (meters)	Z (meters)
1	0.0	24.3840	0.1643
2		21.3360	0.2913
3		18.2880	0.3813
4		15.2400	0.4338
5		12.1920	0.4493
6		9.1440	0.4277
7		6.0960	0.3688
8		3.0480	0.2728
9	0.0	0.0	0.1395
10	2.5400	21.3360	0.1622
11		18.2880	0.2830
12		15.2400	0.3622
13		12.1920	0.4003
14		9.1440	0.3967
15		6.0960	0.3520
16		3.0480	0.2657
17	2.5400	0.0	0.1380
18	5.0800	18.2880	0.1595
19		15.2400	0.2723
20		12.1920	0.3386
21		9.1440	0.3579
22		6.0960	0.3307
23		3.0480	0.2568
24	5.0800	0.0	0.1362
25	7.6200	15.2400	0.1561
26		12.1920	0.2588
27		9.1440	0.3078
28		6.0960	0.3033
29		3.0480	0.2454
30	7.6200	0.0	0.1338
31	10.1600	12.1920	0.1515
32		9.1440	0.2404
33		6.0960	0.2664
34		3.0480	0.2299
35	10.1600	0.0	0.1306
36	12.7000	9.1440	0.1451
37		6.0960	0.2144
38		3.0480	0.2081
39	12.7000	0.0	0.1261
40	15.2400	6.0960	0.1352
41		3.0480	0.1749
42	15.2400	0.0	0.1193
43	18.5420	3.0480	0.1107
44	18.5420	0.0	0.1006

Table 74

## Displacement Constraints for 133 Element Delta Wing

No. of d.o.f.'s Constrained	Node No.	Direction x,y,z	Displ. Constraint Code	Displ. Upper Limit (m)	Displ. Lower Limit (m)
35	10	3	2	0.3556	-0.3556
	11			↓	↓
	12			↓	↓
	13			↓	↓
	14			↓	↓
	15			↓	↓
	16			↓	↓
	17			↓	↓
	18			↓	↓
	19			↓	↓
	20			↓	↓
	21			↓	↓
	22			↓	↓
	23			↓	↓
	24			↓	↓
	25			↓	↓
	26			↓	↓
	27			↓	↓
	28			↓	↓
	29			↓	↓
	30			↓	↓
	31			↓	↓
	32			↓	↓
	33			↓	↓
	34			↓	↓
	35			↓	↓
	36			↓	↓
	37			↓	↓
	38			↓	↓
	39			↓	↓
	40			↓	↓
	41			↓	↓
	42			↓	↓
	43			↓	↓
	44			↓	↓
		3	2	0.3556	-0.3556
				0.3556	-0.3556
				0.7112	-0.7112
				0.7112	-0.7112
				1.0668	-1.0668
				1.0668	-1.0668
				1.4224	-1.4224
				1.4224	-1.4224
				1.7780	-1.7780
				1.7780	-1.7780
				2.1336	-2.1336
				2.1336	-2.1336
				2.5603	-2.5603
				2.5603	-2.5603

Table 75

Final Designs for  
133-Element Delta Wing

Problem No.		Thickness $t_1$ (mm)				
		10A	10B	10C	10D	10E
CST Model		II	I	II	III	III
SSP Model		I	I	I	I	II
Initial Design		II	I	I	I	I
CST Elements	1 ~ 4	0.508	0.508	0.508	0.508	0.508
	5 , 6	0.508	0.508	0.508	0.508	0.508
	7 , 8	0.508	0.508	0.508	0.508	0.508
	9 , 10	3.805	3.475	3.795	1.313	1.279
	11 , 12	3.805	3.475	3.795	5.994	5.672
	13 , 14	3.683	3.437	3.701	5.420	5.456
	15 , 16	3.683	3.437	3.701	0.508	5.344
	17 , 18	0.508	0.508	0.508	0.508	0.508
	19 , 20	0.508	0.508	0.508	0.508	0.508
	21 , 22	2.957	3.475	2.944	0.734	0.844
	23 , 24	2.957	3.475	2.944	4.707	4.511
	25 , 26	3.274	3.437	3.294	4.935	4.976
	27 , 28	3.274	3.437	3.294	0.508	0.508
	29 ~ 32	0.508	0.508	0.508	0.508	0.508
	33 , 34	2.308	2.058	2.292	0.508	0.576
	35 , 36	2.308	2.058	2.292	3.464	3.508
	37 , 38	3.106	2.982	3.129	4.831	4.760
	39 , 40	3.106	2.982	3.129	0.508	5.461
	41 , 42	1.656	2.058	1.633	0.508	0.508
	43 , 44	1.656	2.058	1.633	2.068	2.186
	45 , 46	2.977	2.982	3.000	4.788	4.719
	47 , 48	2.977	2.982	3.000	0.640	0.688
	49 ~ 52	0.922	1.006	0.886	0.508	0.508
	53 , 54	2.728	2.430	2.746	4.295	4.354
55 , 56	2.728	2.430	2.746	1.089	1.061	
57 , 58	2.135	2.430	2.135	2.189	2.240	
59 , 60	2.135	2.430	2.135	1.863	1.901	
61 ~ 63	1.279	1.267	1.277	1.146	1.148	

Continued to the next page

Table 75 (Cont'd)

Problem No.		Thickness $\tau_1$ (mm)				
		10A	10B	10C	10D	10E
CST Model		II	I	II	III	III
SSP Model		I	I	I	I	II
Initial Design		II	I	I	I	I
SSP Elements	1 ~ 7	0.508	0.508	0.508	0.508	0.508
	8 ~ 13	↓	↓	↓	↓	↓
	14 ~ 18	↓	↓	↓	↓	↓
	19 ~ 22	0.508	0.508	0.508	0.508	↓
	23 ~ 25	0.552	0.564	5.489	0.607	0.508
	26 ~ 27	↓	↓	↓	↓	0.903
	28	0.552	0.564	5.489	0.607	1.063
	29	0.508	0.508	0.508	0.508	0.508
	30 , 31	↓	↓	↓	↓	↓
	32 , 33	↓	↓	↓	↓	↓
	34	↓	↓	↓	↓	↓
	35 , 36	↓	↓	↓	↓	↓
	37 , 38	0.508	0.508	0.508	0.508	0.508
	39 , 40	1.513	1.564	1.514	0.940	0.991
	41 , 42	↓	↓	↓	↓	0.791
	43	1.513	1.564	1.514	0.940	0.508
	44 , 45	1.913	2.058	1.907	2.664	2.570
46 , 47	↓	↓	↓	↓	1.222	
48 , 49	1.913	2.058	1.907	2.664	0.508	
50 , 51	1.866	1.917	1.871	2.271	2.682	
52 , 53	↓	↓	↓	↓	2.239	
54 , 55	↓	↓	↓	↓	1.943	
56	1.866	1.917	1.871	2.271	1.392	
57 , 58	1.448	1.442	1.451	0.770	0.508	
59 , 60	↓	↓	↓	↓	↓	
61 , 62	↓	↓	↓	↓	0.508	
63	1.448	1.442	1.451	0.770	1.864	
64 ~ 70	0.508	0.508	0.508	0.508	0.508	
Final Mass (KG)		4872.59	4909.74	4872.26	4370.89	4318.75
Analyses Needed		9	9	9	11	12

Table 76

Iteration History for Problem 10  
133-Element Delta Wing

Problem No.	Mass (KG)				
	10A	10B	10C	10D	10E
CST Model	II(16)*	I(10)	II(16)	III(28)	III(28)
SSP Model	I(12)	I(12)	I(12)	I(12)	II(28)
Initial Design	II	I	I	I	I
No. of Analyses					
1	6745.55	6898.02	6779.53	6663.16	6542.77
2	5471.12	5583.42	5538.46	5364.82	5304.20
3	5066.54	5079.82	5059.20	4783.49	4732.51
4	4420.68	4936.39	4904.38	4573.29	4494.11
5	4887.30	4918.12	4882.64	4468.40	4420.70
6	4878.00	4912.46	4875.70	4397.21	4376.46
7	4874.91	4910.80	4873.00	4381.19	4348.17
8	4872.59	4909.74	4872.26	4373.00	4327.78
9				4371.56	4324.52
10				4370.89	4321.06
11					4318.75

\*Numbers in ( ) indicate the numbers of linked design variable groups.

Table 77

## Initial Weights of All Example Problems

Problem No.	Description	Weight* (lbs)			
		TRUSS	GST	SSP	Total
1	10 Bar Truss without Displacement Constraints	4196.46	-	-	4196.46
2					
3	10 Bar Truss with Displacement Constraints	12589.4	-	-	12589.4
4					
5	25 Bar Truss	661.440 <sup>†</sup> (1468.77)	- -	- -	661.440 <sup>†</sup> (1468.77)
6	72 Bar Truss	853.087	-	-	853.087
7	63 Bar Wing Carry-Through	11104.7 <sup>†</sup> (60432.1)	- -	- -	11104.7 <sup>†</sup> (60432.1)
8	18 Element Wing Box	64.6800	646.930	224.468	936.078
9	Swept Wing Design I with Spar Caps	4.888	2442.00	835.092	3281.98
	Design I without Spar Caps	-	2442.00	835.092	3277.08
	Design II with Spar Caps	4.888	4332.56	626.318	4963.78
	Design II without Spar Caps	-	4332.56	626.318	4958.88
10	Delta Wing Design I	-	12218.50	3581.58	15800.08
	Design II		18327.76	2865.26	21193.00

\*Weights for problems 8 through 10 are for one wing.

<sup>†</sup>Initial designs are infeasible and scaled up to the weight indicated in ( ).

Table 78  
CPU Times for Truss Examples  
(see Section 4.2)

Problem Description			Pre-Processor	Analyses			Optimizer		Gross Total
Struc.	No.			Decompose K	Gradient	Analyses Total	Function Evaluations	Total	
10 Bar	1A	NEWSUMT	0.1176	0.0149	0.3497	0.9972	0.6348	1.6241	2.8604
	1B	NEWSUMT	0.1023	0.0161	0.3564	1.0279	0.6478	1.6849	2.9296
	1C	NEWSUMT	0.1057	0.0174	0.3688	1.0471	0.6745	1.7276	3.0028
	1D	NEWSUMT	0.1061	0.0149	0.3582	1.0374	0.6608	1.6941	2.9567
	2	NEWSUMT	0.0985	0.0151	0.2354	0.6809	0.4719	1.3745	2.2783
	2	CONMIN	0.0962	0.0134	0.1965	0.6012	0.2093	0.7308	1.5964
	3	NEWSUMT	0.1163	0.0219	0.2580	0.8425	0.5237	1.4893	2.5253
	3	D.P. NEWSUMT	0.1476	0.0122	0.2575	0.7845	0.5604	1.3451	2.3537
	3	CONMIN	0.1115	0.0211	0.2562	0.8303	0.8939	2.1371	3.2304
	4	NEWSUMT	0.1211	0.0156	0.2311	0.7360	0.4822	1.3203	2.2968
4	D.P. NEWSUMT	0.1082	0.0101	0.2093	0.6706	0.4867	1.1432	2.0383	
4	CONMIN	0.1126	0.0143	0.1980	0.6146	0.9457	2.2541	3.1651	
25 Bar	5	NEWSUMT	0.2119	0.0865	0.5199	1.8697	0.3887	1.0175	3.1689
25 Bar	5	CONMIN	0.2043	0.0781	0.4720	1.6808	0.1355	0.4827	2.4663
72 Bar	6	NEWSUMT	0.3587	0.6475	1.7268	7.3587	0.6979	1.9648	9.7358
72 Bar	6	CONMIN	0.4503	0.6481	1.7209	7.3171	0.4446	1.0586	8.9272
63 Bar	7A	.5x2 NEWSUMT	0.4887	0.7216	13.8404	22.3682	19.5635	67.1472	90.4671
63 Bar	7B	0.05x1 NEWSMI	0.4646	0.5231	10.3327	16.0890	11.6198	35.1771	52.0825
WCTS	7C	.5x2 NEWSUMT	0.4780	0.6467	12.1667	19.8499	20.0149	66.7336	87.5114
WCTS	7D	0.05x1 NEWSMT	0.4634	0.4474	8.9331	13.9237	10.0092	30.3099	44.9616

Table 79

CPU Times for Wing Examples (seconds)  
(See Section 4.3)

Problem Description			Pre-Processor	Analyses			Optimizer		Gross Total
Struc.	No.			Decompose K	Gradient	Analyses Total	Function Evaluations	Total	
18E. Wing Box	8A	NEWSUMT	0.1934	0.0388	0.7914	1.4944	0.6629	1.8016	3.3663
	8B	NEWSUMT	0.2050	0.0474	0.9748	1.8893	0.8155	2.2993	4.2747
	8C	NEWSUMT	0.1907	0.0394	0.6807	1.4567	0.6265	1.7328	3.4273
Swept Wing	9A	NEWSUMT	1.2604	3.2957	4.7495	15.0074	1.1711	2.7007	19.0559
	9B	NEWSUMT	1.2804	3.7126	5.3579	16.9855	1.3509	3.1303	21.4959
	9C	NEWSUMT	1.5008	3.8625	9.0155	23.5768	4.3269	10.8091	35.9675
	9D	NEWSUMT	1.4164	3.7216	8.7616	22.9311	4.2720	10.2195	34.6471
Delta Wing	10A	NEWSUMT	0.8833	4.1195	4.4148	11.6084	1.6869	5.3825	17.9467
	10B	NEWSUMT	0.8739	4.0156	3.4463	10.4747	1.1611	3.0374	14.7252
	10C	NEWSUMT	0.8955	4.0711	4.3311	11.4568	1.7297	5.3993	17.8281
	10D	NEWSUMT	0.8956	4.9267	7.1228	15.8396	4.3581	15.4182	32.2925
	10E	NEWSUMT	0.9442	6.0469	12.6151	24.7358	9.6434	41.4708	67.7864